




1983

**Analysis of clay minerals, other silicate and nonsilicate minerals,
and the grading of chrysotile asbestos by attenuated total
reflection infrared spectrophotometry (with atlas)**

Ashraf Muhammad Chaudhry
University of the Pacific

Follow this and additional works at: https://scholarlycommons.pacific.edu/uop_etds

 Part of the [Chemistry Commons](#), and the [Earth Sciences Commons](#)

Recommended Citation

Chaudhry, Ashraf Muhammad. (1983). *Analysis of clay minerals, other silicate and nonsilicate minerals, and the grading of chrysotile asbestos by attenuated total reflection infrared spectrophotometry (with atlas)*. University of the Pacific, Thesis. https://scholarlycommons.pacific.edu/uop_etds/2094

This Thesis is brought to you for free and open access by the University Libraries at Scholarly Commons. It has been accepted for inclusion in University of the Pacific Theses and Dissertations by an authorized administrator of Scholarly Commons. For more information, please contact mgibney@pacific.edu.

ANALYSIS OF CLAY MINERALS, OTHER SILICATE AND
NONSILICATE MINERALS, AND THE GRADING OF CHRYSOTILE
ASBESTOS BY ATTENUATED TOTAL REFLECTION INFRARED
SPECTROPHOTOMETRY (WITH ATLAS)

A Dissertation
Presented to
the Graduate Faculty of the
University of the Pacific

In Partial Fulfillment
of the Requirements for the Degree
Master of Science

by
Ashraf M. Chaudhry

August 1982

ACKNOWLEDGMENTS

The author acknowledges, with gratitude, the guidance of Dr. Herschel Frye, the support of the University of the Pacific Chemistry Department, the encouragement of Dr. D. K. Wedegaertner and Dean Reuben Smith. The author wishes to thank Dr. J. Kramer of the University of the Pacific Geology Department and S. Pottratz of the S. J. Delta College Geology Department for the donation of part of the samples used in this study.

TABLE OF CONTENTS

	Page
ACKNOWLEDGMENTS	iii
LIST OF FIGURES	v
LIST OF TABLES	vi
CHAPTER	
1. INTRODUCTION	1
2. CLAYS, CLAY MINERALS AND CHRYSOTILE	
A. CLAYS AND CLAY MINERALS	4
B. CHRYSOTILE ASBESTOS	11
3. METHODS OF MINERAL ANALYSIS	
A. INFRARED SPECTROPHOTOMETRY	16
B. ATTENUATED TOTAL REFLECTION	20
C. OTHER ANALYTICAL METHODS OF ANALYSIS	28
4. EXPERIMENTAL	
A. INSTRUMENTATION	40
B. PROCEDURE	45
5. RESULTS AND DISCUSSION	50
6. CONCLUSION	82
BIBLIOGRAPHY	86
APPENDICES	
A. LIST AND ATR-IR SPECTRA OF MINERALS	90
B. MASTER TABLE OF ATR-IR SPECTRAL POSITIONS IN MINERALS	205
C-O. CERTIFICATES OF ANALYSIS	213
P. LIST OF ABBREVIATIONS USED	234
Q. NAMES AND FORMULAS OF VARIOUS MINERALS	235

LIST OF FIGURES

Figure	Page
1. Diagrammatic Representation of the Succession of Layers in Some Clay Minerals	8
2. Fundamental Sheet of a Chrysotile Structure	13
3. Internal Reflection	22
4. Diffraction of X-rays by a Set of Planes	33
5. Optical Schematic of Perkin-Elmer IR Model 283	41
6. Model 12 Working Diagram and Optical Schematic [Wilks 1965]	43
7. Internal Reflection Element	44

LIST OF TABLES

Table	Page
1. Properties of Chrysotile	14
2. Characteristic Group Frequencies in Minerals	29
3. Some Infrared IRE Materials	45
4. Names and Sources of Mineralogical Samples	48
5. Characteristic Absorptions in Kaolinites	53
6. Characteristic Absorptions in Bentonites	54
7. Characteristic Absorptions in Halloysites	55
8. Characteristic Absorptions in Bauxites	56
9. Characteristic Absorptions in Flint Clay	57
10. Characteristic Absorptions in Plastic Clay	59
11. Characteristic Absorptions in Muscovite	60
12. Characteristic Absorptions in Biotite	61
13. Characteristic Absorptions in Sodium Feldspar	63
14. Characteristic Absorptions in Potassium Feldspar, SRM # 70a	64
15. Characteristic Absorptions in Potassium Feldspar, SRM # 607	65
16. Characteristic Absorptions in Talcs	66
17. Characteristic Absorptions in High Iron Glass Sand	67
18. Characteristic Absorptions in Low Iron Glass Sand	67
19. Characteristic Absorptions in Pumice	68

LIST OF TABLES [CONTINUED]

20.	Characteristic Absorptions in Petalite	70
21.	Characteristic Absorptions in Spodumene	71
22.	Characteristic Absorptions in Lepidolites	71
23.	Characteristic Absorptions in Dolomitic Limestone	72
24.	Characteristic Absorptions in Argillaceous Limestone	73
25.	Characteristic Absorptions in Phosphate Rock	73
26.	Various Absorptions in Chrysotiles	76
27.	Absorptions in Various Chrysotile Grades	77
28.	Various Absorptions in Grade 7 Chrysotile	79
29.	Various Absorptions in Chrysotile Grades	80
30.	Absorptions of Chrysotile Grade 10	81

CHAPTER ONE

INTRODUCTION

Attenuated Total Reflection Infrared [ATR-IR] Spectrophotometry is an excellent nondestructive method for the study of minerals, including identification and their placement in their respective groups. It is free from the interference and dispersion effects which make IR unsuccessful in some cases.

To a certain extent this project is a continuation of Anderson's work (2), since one purpose of the project was to devise a new technique or use one of the existing techniques to overcome the difficulty of contact problem between the sample and the reflector plate, a major problem he faced in his work and a critically important factor in taking good ATR-IR spectra. The main emphasis of this project has been not only in preparing an Atlas of spectra but also in identifying various absorption bands in different groups of silicates such as clay minerals, micas, feldspars, talc, high silica materials, lithium ores and various rocks. Chrysotile samples of various grades have been studied and an effort has been made to answer the question: "Is it possible to use ATR-IR as a tool to place chrysotile fibers of variable size and length in their proper class based on their ATR-IR spectra? "

Though IR and ATR-IR spectra under some conditions provide absorption bands which occur at the same wavenumbers, a direct comparison of ATR-IR spectra taken in this study to IR spectra in the literature has been avoided because the underlying principles in both techniques are different.

ATR-IR is still in its developmental phases especially as an instrumental method in studying minerals. No ATR-IR references were found in the literature. Incidentally, ATR-IR has been used recently in the textile industry for quality control of cloth fibers (13).

Various research groups have been using IR to study crystal structure and bonding in minerals and to use this information for identification. Lyon [1962] has compiled a list of 440 papers which represents world-wide IR mineral-related studies up to September, 1962. Gadsden [1975] listed 685 references of IR mineral-related papers and books, most of them for silicate minerals. Nyquist [1971] listed 900 IR spectra of Inorganic compounds, including 9 minerals but none by ATR-IR.

ATR-IR spectrophotometry is a modification of simple IR spectrophotometry. It was first introduced by Fahrenfort in 1961 as an application of IR. Harrick [1967] reported 450 references on internal reflection spectroscopy but none on ATR of minerals. Anderson [1975] did not find any ATR-IR work on minerals up to the end of 1974. A search of Chemical Abstracts up to July, 1981 did not reveal any article in

the area of ATR-IR of minerals.

ATR-IR was chosen rather than transmission IR for the study of silicate minerals, chrysotile grading and a few other minerals for the following reasons:

1. It is a simple and convenient method of analysis;
2. It can be applied to both opaque and transparent materials;
3. It can be used for both powder samples and thin sections;
4. It often requires little sample preparation; and
5. It is superior to "simple" IR in providing better resolved spectra, especially in the low wavenumber range.

This study of ATR-IR involved taking spectra of various silicate minerals in powder samples, finding similarities and differences in nature, and locating various bands and intensities of absorption bands for identification and classification purposes. This study is limited to 4000-300 cm^{-1} with major emphasis on absorptions in the 2000-300 cm^{-1} region.

CHAPTER TWO

CLAYS, CLAY MINERALS AND CHRYSOTILE

A. CLAYS AND CLAY MINERALS

A chemist's standard definition of clay is "an earthy or stony mineral aggregate consisting essentially of hydrous silicates and alumina, plastic when sufficiently pulverized and vitreous when fired at a sufficiently high temperature" (21).

There are several processes through which clays may originate: (1) hydrolysis and hydration of a silicate, i.e. $\text{alkali silicate} + \text{water} \rightarrow \text{hydrated aluminosilicate clay} + \text{alkali hydroxide}$; (2) solution of a limestone or other soluble rock containing relatively insoluble clay impurities that are left behind; (3) slaking and weathering of shales (clay-rich sedimentary rocks); (4) replacement of a pre-existing host rock by invading guest clay whose constituents are carried in part or wholly in solution; (5) deposition of clay in cavities or veins from solution; (6) bacterial or other organic activity, including the extraction of metal cations as nutrients by plants; (7) action of acid clays, humus and inorganic acids on primary silicates; (8) alteration of parent material or diagenetic processes following sedimentation in marine and freshwater environments and

resilication of high alumina minerals; (9) the action of surface water charged with carbon dioxide; (10) the action of water draining from peat bogs containing organic acids in solution; and (11) the action of volcanic gases and vapours (pneumatolytic action).

A number of things need to be considered in the study and classification of clays; these include: (1) the dominant clay-mineral type; (2) the ion exchange capacity; (3) the exchangeable ions present in the clay; (4) the prevalence of an expanding or nonexpanding lattice mineral; (5) the electrolytes and the solutions in association with the clay deposit; (6) the necessary minerals or mineral impurities; (7) the organic matter content; (8) the size and discreteness of particles; (9) the hydrated alumina and/or silica content; and (10) the structure and texture of the clay deposit.

Clays have many uses in everyday life; these depend on the physical and chemical properties of clays and these properties in turn are dependent on the type and amount of clay minerals which form the major part of that clay.

A clay mineral is a hydrous aluminum silicate, somewhat variable in chemical and physical properties. Its two- or three-layer crystal lattice permits the replacement of aluminous ions by nonaluminous ions to form nonaluminous clays. Exchangeable cations may be on the surface of silicate layers, and their amounts determined by the excess negative charge within the layer; these cations are usually

Ca(II) and Na(I) but K(I), Mg(II), H(I) and Al(III) are also exchangeable. A brief description of the clay mineral groups follows.

KAOLINITE GROUP

A group of hydrous aluminum silicates are the chief constituents of the white clay kaolin including kaolinite, dickite, nacrite and anauxite. The kaolinite lattice consists of one set of tetrahedrally coordinated Si(IV) (with O(II)) and one set of octahedrally coordinated Al(III) (with O(II) and OH(I)), hence a 1:1 or a two-layer structure (Fig 1). A layer of OH(I) completes the charge requirements of the octahedral sheet. The so-called fire clay mineral is a b-axis disordered kaolinite; halloysite and endellite are disordered along both the 'a' and 'b' axes. Indeed, most variations in the kaolin group originate as structural polymorphs.

Analysis of various kaolins show that SiO_2 is the major constituent ranging from 42-53%; Al_2O_3 is the next, ranging from 32-39%, followed by water (removable above 110°C) at 12-15%. Other components present are Fe_2O_3 , FeO , MgO , CaO , K_2O , Na_2O , TiO_2 and H_2O (removable at 105°C).

SMECTITE (MONTMORILLONITE) GROUP

This is a group of complex 2:1 (three-layer crystal lattice) clay minerals that carry a lattice charge and characteristically expand when solvated with water and alcohols, notably ethylene glycol and glycerol. With beidellite and

nontronite as end members, this group of minerals forms a continuous series of solid solutions with Fe(III) and Al(III) proxying for one another in all proportions in the lattice structure. Al(III) also proxies for Si(IV) not exceeding one ion in four. Clay minerals which belong to this group are montmorillonite, beidellite, nontronite, hectrite, bentonite (a mixture of montmorillonite and beidellite), saponite and many more.

Smectites are derived from pyrophyllite or talc by substitutions mainly in the octahedral layers. Some substitutions may occur for Si(IV) in the tetrahedral layer, and by F(I) for OH(I) in the structure. In montmorillonite Mg(II) is a significant substituent for Al(III) in the tetrahedral layer (Fig 1). When substitutions occur between ions of unlike charge, deficit or excess charge develops on corresponding parts of the structure. Deficit charges are compensated by cations (usually Na(I), Ca(II), K(I)) sorbed between the three-layer (two tetrahedral and one octahedral) "sandwiches".

The major constituents of montmorillonite minerals are SiO_2 (42-56%), Al_2O_3 (0-21%), Fe_2O_3 (0-29%), MgO (0-26%), F(I) (up to 6%), water removable at 105°C (9-15%) and water removable at higher temperatures (2-8%). Other compounds present in montmorillonites are FeO, MnO, ZnO, CaO, K_2O , Na_2O , Li_2O , TiO_2 and P_2O_5 . The quantities of various compounds in these clay minerals vary from one mine to another, even for the same mineral species.

HALLOYSITE GROUP

This is a group of porcelain-like minerals of general formula $\text{Al}_2\text{Si}_2\text{O}_5(\text{OH})_4$ which under the electron microscope, show crystallinity in the form of minute, slender and hollow tubes. On dehydration these tubes split and "unroll". They may also form tube-within-tube arrangements. Examples include allophane, endellite (Fig 1) and metahalloysite (hydrous forms of halloysite), indianite (a white porcelain-like mixture of halloysite and kaolinite) and halloysite.

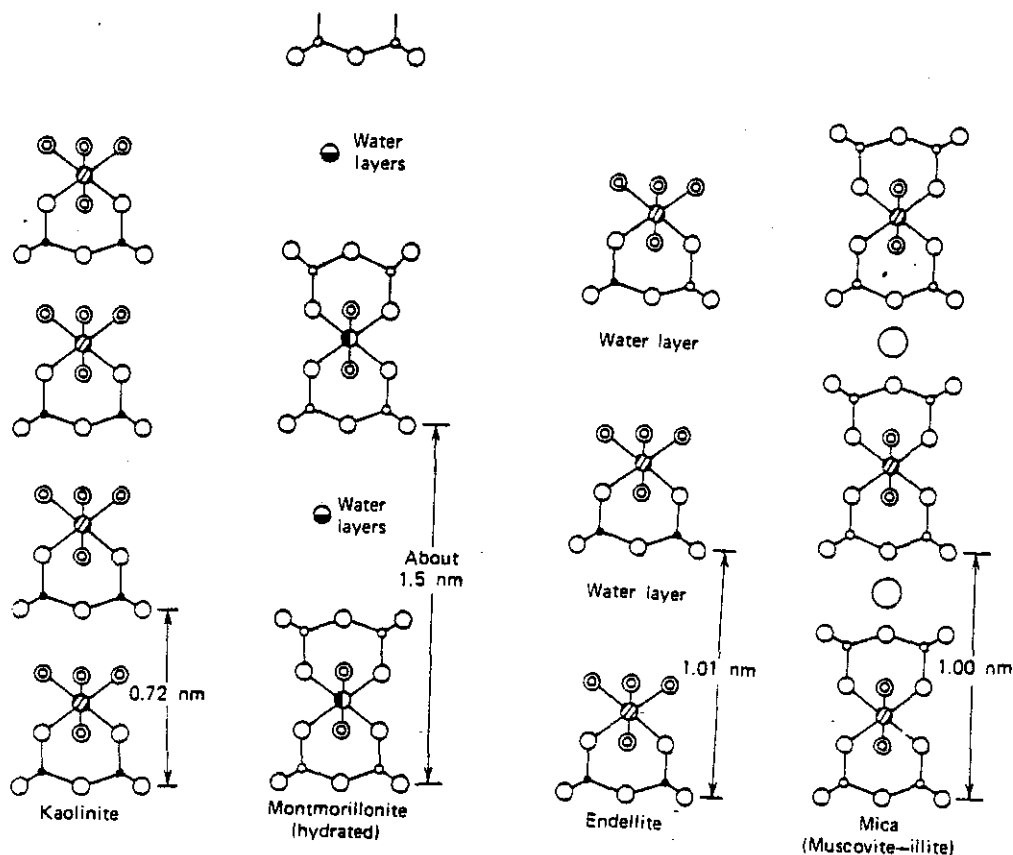


Figure 1. Diagrammatic Representation of the Succession of Layers in some Clay Minerals

○, oxygen; ⊙, (OH); ●, silicon; ○, Si-Al; ⊕, aluminum; ⊙, Al-Mg; ○, potassium; ⊙, Na-Ca.

Allophane is essentially an amorphous solid solution of silica, alumina and water. It may be associated with halloysite or it may occur as a homogenous mixture with evansite, an isomorphous solid solution of phosphorous, alumina and water.

A chemical analysis of two samples of allophane obtained from different locations is reported to have 4.34% and 32.30% of SiO₂, 41.42% and 30.41% of Al₂O₃, 4.30% and 4.06% ZnO, 9.23% and 0.02% of P₂O₅, 2.07% and 0.65% CO₂, 20.92% and 16.38% water removable at 105°C and 14.43% and 14.43% water removable above 110°C. Compounds present in small quantities were Fe₂O₃, MgO, CaO, K₂O, Na₂O, CuO and SO₃.

ILLITE GROUP

Illite is a general term for a group of mica-like minerals which are common in argillaceous sediments. They are not specific mineral species and have the general formula $K_y(Al_4 \cdot Fe_4 \cdot Mg_4 \cdot Mg_6)(Si_{8-y}Al_y)O_{20}(OH)_4$, where y refers to the K(I) ions that satisfy the excess charges that result from replacement of about 15% of the Si(IV) positions by Al(III). This group embraces the most common and widespread of the clay minerals and shales. Examples are illite, bravaisite, sericite, brammallite and hydromica.

Mica minerals possess a 2:1 sheet structure similar to montmorillonite except that the maximum charge deficit in mica is typically in the tetrahedral layers which contain K(I) held in the inter-layer space which contributes to a

1.0 nm basal spacing(Fig 1). Since the micas in argillaceous sediments may be widely diverse in origin, considerable variation exists in the composition and polymorphism of the illite minerals. A representative chemical analysis of illite is: 51.22% SiO₂, 25.91% Al₂O₃, 4.59% Fe₂O₃, 1.70% FeO, 2.84% MgO, 0.16% CaO, 0.17% Na₂O, 6.09% K₂O, 0.53% TiO₂, 7.49% ignition loss above 110°C and 100.70% total.

BAUXITE GROUP

This group consists of hydrous or colloidal oxides of aluminum. These oxides are secondary in origin and are formed from the decomposition of various minerals through weathering, leaching or by the action of volcanic gas. It is generally believed that a very humid, subtropical climate is required for such a weathering. Kaolins may be formed from bauxites by silicification. Examples are boehmite, cliachite, diaspore, sporogelite, bauxite and gibbsite.

Typical percentages of alumina and water in diaspore, bauxite and gibbsite are 85% and 15%, 75% and 25% and 65.4% and 34.6%, respectively.

ATTAPULGITE AND SEPIOLITE GROUP

Important members of this group include attapulgite, named from its occurrence at Attapulgius, Georgia, and sepiolite (meerchaum), named from the Greek word for cuttle fish; these possess chain-like structures, or combination chain-sheet structures. Approximate composition is SiO₂ = 55.05%, Al₂O₃ = 10.24%, Fe₂O₃ = 3.53%, MgO = 10.49%, K₂O = 0.47%,

water removable at 150°C = 9.73% and water removable at temperatures higher than 150°C = 10.13%. Sepiolite is used in drilling muds where resistance to flocculation in briny water is required. Alygorskite, α -palygorskite, β -palygorskite, paramontmorillonite, parasepiolite and floridin-floridine are other members of this group.

UNCLASSIFIED GROUP

Any mineral difficult to place in any of the classes listed above becomes a member of this group. An example is glauconite, a green, dioctahedral, micaceous clay rich in Fe (III) and K(I). It has many characteristics common to illite but may contain randomly mixed expanding layers, a property found in montmorillonites. It has been used as an ion exchanger for water softening and a source of slowly released potassium for soil amendments. Other members of the group are parakaolinite, ptilolite (an orthorhombic, zeolite-like clay mineral), pyrophyllite (a mineral resembling talc), evansite (a hydrous aluminum phosphate), faratsihite (a mixture of kaolinite and nontronite), leverrierite (a mixture of muscovite and kaolinite), porcellana (a mixture of kaolinite and halloysite), potash bentonite and potash montmorillonite and many more.

B. CHRYSOTILE ASBESTOS

Asbestos is a generic term describing a variety of naturally formed fibrous hydrated mineral silicates that

are incombustible, can be separated into filaments and differ in chemical composition. Asbestos appears in many forms and types varying from long, soft, silky fiber with a definite orientation of the crystals to a short, harsh, brittle mass fiber with a random orientation of crystals. It may be divided into two large groups; serpentine or chrysotile and the amphiboles.

The chemical composition of asbestos varies from a simple magnesium silicate, i.e. chrysotile, to complex iron silicates such as anthophyllite and amosite.

Asbestos fibers are unique minerals, combining unusual physical and chemical properties which make them useful in the manufacture of a wide variety of residential and industrial products. When processed into long, thin fibers, asbestos is sufficiently soft and flexible to be woven into fire resistant fabrics. Its usefulness is based on its non-flammable nature together with flexing strength, good tensile strength, great surface area, low density, good absorption, fair resistance to heat and to acids and to alkalies, high electrical resistivity and low magnetic permeability. The chrysotile variety of fiber is used in about 90% of all products requiring asbestos.

The current opinion is that chrysotile fiber resulted from two separate metamorphic reactions in ultrabasic rocks of igneous origin(22). The initial hydrothermal reaction altered the olivines and pyroxenes to serpentine. At a subsequent point the serpentine was redissolved and mineral-rich

solutions flowed into the cracks and crevices in the host rock where the chrysotile fiber was reprecipitated.

The empirical composition of chrysotile is $3\text{MgO} \cdot 2\text{SiO}_2 \cdot 2\text{H}_2\text{O}$; however the unit cell may be represented as $\text{Mg}_6 (\text{OH})_8 \text{Si}_4 \text{O}_{10}$.

The crystal structure of chrysotile is layered or sheeted like the kaolinite group. It is based on an infinite silica sheet $(\text{Si}_2\text{O}_5)_n$ in which all the silica tetrahedra point one way. One side of the sheet structure, joining the silica tetrahedra, is a layer of brucite, $\text{Mg}(\text{OH})_2$, in which two out of every three hydroxyl groups are replaced by oxygen at the apices of the tetrahedra. The result is a layered structure as shown in Fig 2.

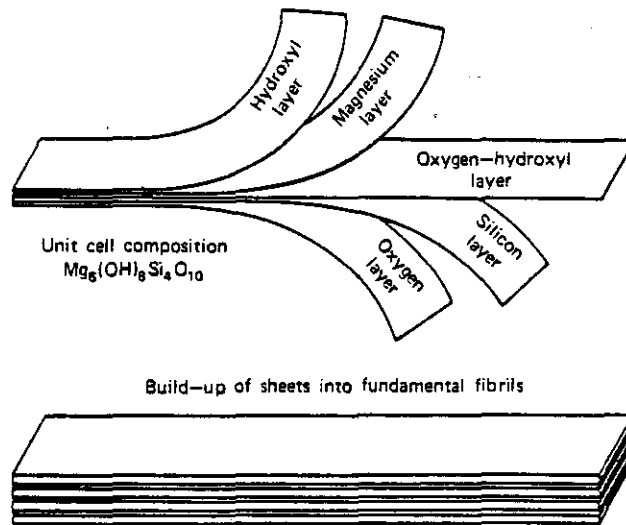


Figure 2. Fundamental Sheet of a Chrysotile structure

A chemical analysis of chrysotile will typically have $\text{SiO}_2 = 37-44\%$, $\text{MgO} = 39-44\%$, $\text{FeO} = 0-6\%$, $\text{Fe}_2\text{O}_3 = 0.1-5\%$, $\text{H}_2\text{O} = 12-15\%$ and $\text{CaO} = \text{trace}-5\%$ as constituents. The varia-

tions in analyses are due to impurities, some of which are part of the crystal structure, and/or isomorphic substitutions in the crystal lattice.

Properties of chrysotile are given in Table 1.

Table 1. Properties of Chrysotile

occurrence	in veins of serpentine, etc.
mineral associations	in altered peridotite adjacent to serpentine and limestone near contact with basic igneous rocks
origin	alteration and metamorphism of basic igneous rocks rich in magnesium silicates
veining	cross and slip fibers
essential composition	hydrous silicates of magnesia
crystal structure	fibrous and asbestiform
crystal system	monoclinic (pseudoorthorhombic)
color	white, gray, green, yellowish
luster	silky
hardness, Mohs	2.5-4.0
specific gravity	2.53-2.58
cleavage	010 perfect
optical properties	biaxial positive extinction parallel
refractive index	1.50-1.55
fusibility, Seger cones	fusible at 6, 1190-1230°C
flexibility	very flexible
diameter of fibers	0.02-0.03 micro meter
length	short to long
texture	soft to hard, also silky
acid resistance	soluble up to approximately 57%
spinnability	best
tensile strength	100,000-400,000 psi
Young modulus	23.1×10^6 lb/in ²
specific heat, Btu/(lb) (F°)	0.266

CLASSIFICATION AND GRADING

Most American and all Canadian asbestos producers use the method formulated by Quebec Asbestos Producers Association (Q.A.P.A.) for classifying and grading chrysotile fibers which utilize a mesh of three sieves and a pan. Various grades available are

Crude # 1 fiber : 3/4 in. (1.9 cm) staple and longer
Crude # 2 fiber : 3/8-3/4 in. (0.95-1.9 cm) staple
Crude run of mine : unsorted crudes
Crudes, sundry : crudes other than above

Group 3-10, with letter designations within each group, are milled fibers of increasing fineness down to floats. For example, group 3 grades are 3F, 3K, 3R, 3T and 3Z.

Asbestos fiber grading and classification in Australia, Cyprus, Russia and South Africa does not conform with Q.A.P.A. but is based on local decisions for hand cobbing and extent of milling and different grades are given numbers and letters corresponding to the length of fiber.

CHAPTER THREE

METHODS OF MINERAL ANALYSIS

A. INFRARED SPECTROPHOTOMETRY

Although the region of the electromagnetic spectrum between $10,000 \text{ cm}^{-1}$ and 10 cm^{-1} is designated as the infrared [IR], most clay minerals and other materials described in this study absorb in the range from 4000 cm^{-1} to 200 cm^{-1} , and only this range will be described.

Vibrational and rotational energies are important in IR studies. In solids rotational energies are negligible, so vibrational energies are our only concern here. To describe activity in the infrared, the selection rule must be applied to every normal vibration. From a quantum mechanical point of view, a vibration is active in the IR if the dipole moment of the molecule is changed during the vibration. Homonuclear diatomic molecules are not IR active.

If there is an oscillating electric dipole associated with a particular vibratory mode, then there will occur an interaction with the electrical vector of electromagnetic radiation of this same frequency, leading to the absorption of energy which appears as an increased amplitude of vibration. The frequency of vibration is given by

$$\nu = \frac{1}{2\pi} \left(\frac{k}{\mu} \right)^{1/2} \quad \text{or} \quad \bar{\nu} = \frac{1}{2\pi c} \left(\frac{k}{\mu} \right)^{1/2} \quad \dots (1)$$

where ν is the frequency of vibration, $\bar{\nu}$ is the wavenumber, μ is the reduced mass and is given by $m_1 m_2 / m_1 + m_2$ and k is the force constant for the vibration.

The force constant is a measure of the curvature of the potential well near the equilibrium position:

$$k = (d^2V/dq^2)_{q \rightarrow 0} \quad \dots \dots \dots (2)$$

where V is the potential energy and q is the change of internuclear distance. Thus a large force constant means sharp curvature of the potential well near the bottom but does not necessarily indicate a deep potential well. Usually however, a large force constant is an indication of a stronger bond in a series of molecules of the same type. The value of the force constant can be approximated by the empirical equation:

$$k = aN X_A X_B / d^{3/4} + b \quad \dots \dots \dots (3)$$

where k = force constant in dynes/cm;

a = a constant of value 1.67;

N = bond order;

b = a constant of value 0.30;

d = internuclear distance in angstroms and

X_A and X_B are the Pauling electronegativities of atoms A and B, respectively.

According to equation (1), the frequency of vibration in a diatomic molecule is proportional to the square root of k/μ . If k is approximately the same for a series of diatom-

ic molecules, the frequency is inversely proportional to the square root of μ . If μ is the same for a series of diatomic molecules, the frequency is proportional to the square root of k .

Linear molecules have $3N - 5$ independent vibrations. Nonlinear molecules can be resolved into a set of $3N - 6$ normal vibrations each of which is simple in the sense that all atoms in the molecule vibrate with one and the same frequency and maintain phase relationships. Moreover, individual normal vibrations are independent of each other; that is they can be excited one at a time without coupling with any other.

According to the selection rule for the harmonic oscillator, any transitions corresponding to $v = \pm 1$ are allowed. The intensity of an IR absorption band is proportional to the square of the rate of change of dipole moment with respect to the displacement of atoms. Weak polar molecules yield weak absorption bands, and partially ionic bonds result in strong absorption bands. The intensity of all bands is proportional to the amount of sample in the path of IR radiation.

In general, the motions of the atomic nuclei in crystals can be divided into two types of vibrations: (1) Lattice vibrations between the molecules considered as rigid entities and (2) Molecular vibrations within the individual molecules. The latter correspond, at least approximately, to those of the free molecules, but more or less modified by

the intermolecular forces.

To analyze the spectra of crystals, it is necessary to carry out site group or factor group analysis.

The introduction of IR spectroscopy into the field of clay mineral analysis has been limited due to the excellence of X-ray diffraction techniques. However, the IR technique is quick, simple, relatively inexpensive and serves as a useful supplement in the identification of clay minerals.

The IR spectra derived from inorganic compounds usually have absorption bands that are broad and overlapping making assignment and specific identification of cation-anion pair difficult.

The frequencies at which a substance absorbs IR energy depend upon the internal vibrations of the molecule and hence upon its composition. Polyatomic anions absorb IR energy of different wavelengths and can be distinguished one from the other. Different minerals can be identified by IR but caution is vital as the position of maximum absorption in the IR spectrum is sensitive to certain impurity minerals and to changes in mass and charge of the constituent ions; however, the experienced spectroscopist can place an unknown within a fairly narrow composition range.

For the identification of a clay mineral or other silicate and nonsilicate mineral, the spectrum of an unknown mineral should be compared with the spectrum of a well-characterized specimen of the reference mineral. Extreme care in the selection of both sample and reference must be

exercised to ensure authenticity, as the amounts of material examined are very small (0.1-10 mg depending upon the method of sample preparation).

B. ATTENUATED TOTAL REFLECTION

The following terms dealing with internal reflection spectroscopy have been approved by the sponsoring committee and accepted by the American Society for Testing Materials (ASTM) and published in the 1971 ASTM Book of Standards.

1. Internal Reflection Spectroscopy (IRS): The technique of recording optical spectra by placing a sample material in contact with a transparent medium of greater refractive index and measuring the reflectance from interface, generally at angles of incidence greater than the critical angle.

2. Spectrum, Internal Reflection: The spectrum obtained by the technique of internal reflection spectroscopy. Note: Depending on the angle of incidence the spectrum recorded may qualitatively resemble that obtained by conventional transmission measurements, may resemble the mirror image of the dispersion in the index of refraction or may resemble some composite of the two.

3. Attenuated Total Reflection (ATR): Reflection which occurs when an absorbing coupling mechanism acts in the process of total internal reflection to make the reflectance less than unity.

Note: In this process, if an absorbing sample is placed in contact with the reflecting surface, the reflectance for total internal reflection will be attenuated to some value between greater than zero and unity in regions of the spectrum where absorption of the radiant power can take place.

4. Frustrated Total Reflection (FTR): Reflection which occurs when a nonabsorbing coupling mechanism acts in the process of total internal reflection to make the reflectance less than unity.

Note: In this process, the reflectance can vary continuously between zero and unity if: (a) An optically transparent medium is within a fraction of a wavelength of the reflecting surface and its distance from the reflecting surface is changed and (b) Both the angle of incidence and refractive index of one of the media vary in an appropriate manner.

In these cases part of the radiant power may be

transmitted through the interface into the second medium without loss at the reflecting surface in such a way that transmittance plus reflectance equals unity. It is possible to have this process take place in some spectral regions even when a sample having absorption bands is placed in contact with the reflecting surface.

5. Internal Reflection Element (IRE): The transparent optical element used in internal reflection spectroscopy for establishing the conditions necessary to obtain the internal reflection spectra of materials.

Note: Radiant power is propagated through it by means of internal reflection. The sample material is placed in contact with the reflecting surface or it may be the reflecting surface itself. If only a single reflection takes place, the element is said to be a single-reflection element; if more than one reflection takes place, the element is said to be a multiple reflection element. When the element has a recognized shape, it is recognized according to each shape, for example, internal reflection prism, internal reflection hemicylinder, internal reflection plate, internal reflection rod, internal reflection fiber, etc.

6. Single-Pass Internal Reflection Element: An internal reflection element in which the radiant power transverses the length of the element only once; that is, the radiant power enters at one end of the optical element and leaves via the other end.

7. Double-Pass Internal Reflection Element: An internal reflection element in which the radiant power transverses the length of the optical element twice, entering and leaving via the same end.

8. Fixed-Angle Internal Reflection Element: An internal reflection element which is designed to be operated at a fixed angle of incidence.

9. Variable-Angle Internal Reflection Element: An internal reflection element which can be operated over a range of angles of incidence.

Total internal reflection is a familiar phenomenon.

Newton observed that the rays of light in going out of glass into a vacuum, if they fall too obliquely on the vacuum, are bent backwards into the glass, and totally reflected. He attributed this to the power of glass to attract the rays going out of it into the vacuum, and bringing them back. If the farther surface of glass is moistened with water or clear oil, the rays which otherwise will be reflected go

into the water or clear oil and are not reflected.

Newton's explanation to this phenomenon is very convenient but not correct since there is no propagation of light perpendicular to the surface except very near to the edges of the beam. In fact, a standing wave normal to the reflecting surface is established in the denser medium and there is an evanescent, nonpropagating field in the rarer medium whose electric field amplitude decays exponentially with distance from the surface.

Internal reflection is the technique of recording the optical spectrum of a sample material that is in contact with an optically denser but transparent medium and then measuring the wavelength dependence of the reflectivity of this interface by introducing light into the denser medium, as shown in Fig 3.

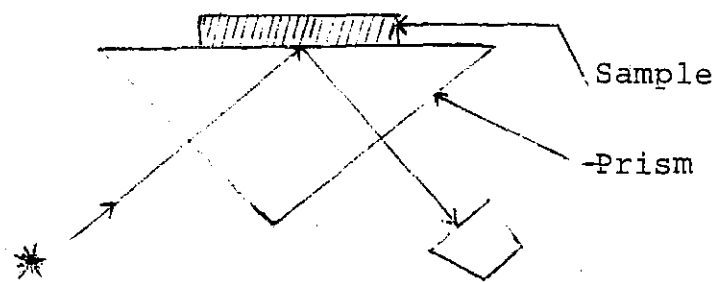


Figure 3. Internal Reflection

In this technique, reflectivity is a measure of the interaction of the evanescent wave with the sample material, and the resulting spectrum is characteristic of the sample

material. For most angles of incidence above the critical angle, the reflection spectra resemble transmission spectra fairly closely; however, for angles of incidence just below the critical angle, the spectra may resemble the mirror image of the dispersion in the index of refraction. The angle of incidence which controls the nature of spectrum in IRS can be a powerful tool if used properly.

Light striking an interface between two transparent semiinfinite media of different refractive indices will be partially reflected and partially transmitted. The transmitted beam is refracted according to Snell's Law:

$$n_1 \sin \theta = n_2 \sin \phi \dots\dots\dots (4)$$

where n_1 and n_2 are refractive indices of denser and rarer medium, respectively, θ is angle of incidence and ϕ is angle at which the radiation is refracted. θ , ϕ and interfacial angles are in the same plane called the plane of incidence. Light is refracted at the interface when $n_1 \neq n_2$. When $n_1 > n_2$ then $\theta < \phi$. There is a value of θ less than 90° at which ϕ is 90° or parallel to the interface. This value of θ is called critical angle (θ_c). Mathematically:

$$\theta_c = \sin^{-1} n_{21} \dots\dots\dots (5)$$

where $n_{21} = n_2/n_1$. All values of θ larger than θ_c result in total reflection.

For the reflected beam, the angle of reflection is equal to the angle of incidence. It is known that all reflected light is partially polarized and that there is an angle of incidence for the interface between any two media

in which the reflected light is completely polarized. This angle is known as Brewster's angle and is given by

$$\theta_B = \tan^{-1} n_{12} \dots\dots\dots(6)$$

The value of Brewster's angle is characteristic of the two media. For nonabsorbing media polarized radiation with an arbitrary angle of incidence, the reflectivity is determined from Fresnel's formulas;

$$R_{\perp} = -\sin(\phi - \theta) / \sin(\phi + \theta) \dots\dots\dots(7)$$

$$R_{\parallel} = \tan(\phi - \theta) / \tan(\phi + \theta) \dots\dots\dots(8)$$

Here R_{\perp} refers to the wave with the electric vector perpendicular to the plane of incidence and R_{\parallel} refers to the wave with the electric vector parallel to the plane of incidence.

When radiation is incident normally (i.e. when $\theta = 0$) at a plane boundary between two transparent media of different refractive indices, the reflectivity $[R]$ which is the fraction of radiation reflected, is identical for both components and is given by

$$R = \frac{(n_1 - n_2)^2}{(n_1 + n_2)^2} \dots\dots\dots(9)$$

It is known that for propagating waves, the electric field vector vibrates perpendicular to the direction of propagation. The electric field vector lies parallel to the plane of incidence for parallel polarization. Since the refracted and reflected beams are 90° apart, the electric field oscillates in the direction of R_{\parallel} for the refracted beam and therefore there can be no propagation in the

reflected beam. All the power therefore is transmitted into medium 1.

When the light approaches the interface from the denser medium, the reflectivities R_{\perp} and R_{\parallel} become 100% and are calculated by equations (7) and (8). For angles larger than θ_c , θ becomes imaginary. This is apparent from equation (4), where $\sin^2 \theta > n_{21}^2$ and the refracted angle may be obtained from

$$\cos \theta = (1 - \sin^2 \theta)^{1/2} \dots\dots\dots (10)$$

$$= i \frac{(\sin^2 \theta - n_{21}^2)^{1/2}}{n_{21}} \quad \text{Here } i = (-1)^{1/2} \dots (11)$$

θ can be eliminated by the use of equations (4) and (11), and Fresnel's reflection equations become

$$r_{\perp} = \frac{\cos \theta - i(\sin^2 \theta - n_{21}^2)^{1/2}}{\cos \theta + i(\sin^2 \theta - n_{21}^2)^{1/2}} \dots\dots\dots (12)$$

$$r_{\parallel} = \frac{n_{21}^2 \cos \theta - i(\sin^2 \theta - n_{21}^2)^{1/2}}{n_{21}^2 \cos \theta + i(\sin^2 \theta - n_{21}^2)^{1/2}} \dots\dots\dots (13)$$

It is evident that $|r_{\perp}| = |r_{\parallel}| = 1$, which means reflection is total when n_{21} is real. In total internal reflection, the reflectivity associated with total internal reflection is indeed very high. In many cases, the largest attenuation comes from absorption losses in the bulk rather than reflection losses.

Fresnel's equations can be modified for absorbing rare medium by replacing n_2 by the complex refractive index, \bar{n}_2 ,

$$\bar{n}_2 = n_2(1 - ik_2) \dots\dots\dots (14)$$

where k_2 , the attenuation index is related to absorption

coefficient, α , via

$$nk = \alpha c / 4\pi\nu \dots\dots\dots(15)$$

where c is the velocity of light and ν is the frequency of radiant beam.

The reflectivity at normal incidence for the absorbing rarer medium is given by

$$R = \frac{(n_2 - n_1)^2 + n_2^2 k_2^2}{(n_2 + n_1)^2 + n_2^2 k_2^2} \dots\dots\dots(16)$$

Dependence of reflectivity on angle of incidence for the absorbing rarer medium is complicated. The simple Fresnel's equations become complex. Calculations can be very time consuming unless done with electronic computers.

The reflectivity is strongly affected by the absorbing medium, and this is particularly true closer to the critical angle. The critical angle loses its significance when the rarer medium is absorbing and becomes a range of angles rather than a sharp angle as it is for nonabsorbing cases. Reflectivity does not follow Beer's Law but at first decreases, then reaches a minimum and finally increases as the absorption coefficient increases. The depth of penetration, d_p increases with increasing wavelength of radiation and is given by

$$d_p = \frac{\lambda_1}{2(\sin^2 \theta - n_{21}^2)^{1/2}} \dots\dots\dots(17)$$

where $\lambda_1 = \lambda/n_1 =$ wavelength in the denser medium.

Because of this direct dependence of penetration depth on wavelength, the absorption bands are stronger towards

higher wavelengths in total internal reflection spectra contributing to band distortion. A sample should absorb the evanescent ray strongly in order to produce strong absorption bands. This is achieved when the angle of incidence is very close to the critical angle due to the greatest depth of penetration near the critical angle. However, this deeper penetration of the evanescent ray is accompanied by lag of the subsequent reflection of that part of the evanescent ray.

Attenuated total reflection achieves the combination of both strong absorption and relatively undisplaced sharp spectra when the incident angle is much larger than the critical angle and the multiple reflection element is used. A larger angle of incidence results in weak absorption of the evanescent ray per reflection and multiple reflection results in multiplication of these small absorptions. The multiple reflection approach can thus produce undistorted spectra of any desired intensity provided there are enough reflections.

To obtain good ATR-IR spectra, very good contact between the sample and the reflector plate is required. Solid powder samples often have surfaces irregular enough to require them to be pressed against the reflector plate to improve contact by deformation. This approach was used in this work to obtain reproducible spectra of minerals. A contact fluid can be used between the samples and prism; soft thin samples give better spectra because of better

contact. The contact fluid must be transparent and should have higher refractive index than the sample; use of the liquids with lower refractive index degrades sensitivity.

C. OTHER ANALYTICAL METHODS OF ANALYSIS

Every successful analytical method has its benefits and pitfalls. In ATR-IR 0.10 microgram quantities can be studied because of developments in the area of total internal spectroscopy. It is a convenient and easily applicable technique both qualitatively and quantitatively. But it requires a lot of practice in order to be able to properly use the factors, such as incident angle, refractive index, thickness of the sample and absorption coefficient, which affect the spectra appreciably. Wainerdi and Uken [1971] in their monograph, "Modern Methods of Geochemical Analysis" (36), and Nicol [1975] in his book, "Physicochemical Methods of Mineral Analysis" have discussed different methods of mineral analysis in detail. Brief descriptions of principles, advantages and limitations of these methods follow.

INFRARED TRANSMISSION

IR spectroscopy provides spectra of compounds which are characteristic of various groups. Voluminous literature in this area has made transmission spectra very useful for identification purposes and it finds use both as a qualitative and a quantitative tool. In many cases it works in noncrystalline solids where X-ray techniques do not. IR can

also provide information on the presence and nature of water in clay minerals and can provide clues to the nature of the silicate anions in the mineral structure.

Some characteristic vibrational group frequencies in the minerals are given in Table 2.

Table 2. Characteristic Group Frequencies in Minerals

Wavenumber (cm^{-1})	Description of Absorption
3704-3195	Strong sharp band for O-H of hydroxyl group and H_2O
3597	Strong sharp band for O-H stretching of water of hydration
3407-3195	Strong broad band for O-H stretching of free water
3401	One or more strong sharp bands for O-H stretching of water of hydration
3401-2000	Strong to medium-strong multipeaked O-H stretching for acidic salts as HCO_3^- , HPO_4^{2-} and HSO_4^-
3330-2800	N-H stretch in NH_4^+
1650	H-O-H bending
1650-1590	H-O-H bending, medium, for water of hydration
1650-1300	C-O stretching in carbonates and bicarbonates
1500-1390	N-H bending in ammonium ions
1499-300	Stretching and bending of polyatomic ions
1460-1200	B-O stretch of $(\text{BO}_3)_n$
1250-900	Si-O stretching in $(\text{SiO}_4)_n$
1200-1100	S-O stretch of sulfates
1200-900	P-O stretching in $(\text{PO}_4)_n$
1100-850	B-O stretching in $(\text{BO}_4)_n$
1000-750	Mo-O stretch of molybdates
950-600	Si-O stretching in $(\text{SiO}_6)_n$
915-730	V-O stretch of VO_4
900-700	W-O stretching in $(\text{WO}_6)_n$
890-700	C-O bending in carbonates and bicarbonates
870-700	Cr-O stretch of CrO_4
850-730	As-O stretching in arsenates
800-600	B-O bending in $(\text{BO}_3)_n$ and $(\text{BO}_4)_n$
700-600	S-O bending in sulfates
600-500	P-O bending in $(\text{PO}_4)_n$
<500	Si-O bending in silicates
<500	V-O bending in VO_4 , Cr-O bending in CrO_4 , W-O bending in WO_4 and $(\text{WO}_6)_n$, Mo-O bending in MoO_4 and $(\text{MoO}_6)_n$ and As-O bending in arsenates
400-10	Lattice modes between metal and nonmetal in a lattice

IR spectroscopy provides a rapid, simple and

convenient nondestructive means of characterizing and identifying some minerals. Limitations are primarily associated with sample preparation. For example, the higher temperatures resulting from fine grinding will cause loss of volatile component of the mineral. The high pressures (130,000 psi) required to make clear discs may change the mineral. Windows of KBr, NaCl and CsBr cannot be used with mulls as they cause ion exchange.

WET CHEMICAL ANALYSIS

The study of minerals by wet chemical analysis requires grinding to a fine size and solution in an appropriate acid. In some cases fusing in a platinum crucible may be required before solution. The chemical species to be determined are separated from interfering substances by group precipitation, controlled precipitation, electrodeposition, or solvent extraction. The constituents are then determined by fire assay or by gravimetric or volumetric methods.

Conventional wet chemical analyses are laborious, time consuming and thus expensive, especially if many samples are to be analyzed. Detection limits are usually poor compared to instrumental procedures, so these methods are not suitable for trace constituent analyses. In spite of these drawbacks, wet chemical methods are still most valuable and are commonly used for routine analyses.

ION EXCHANGE CHROMATOGRAPHY

This is a commonly used technique for the analysis of silicate rocks and minerals, especially for components in low concentration. Using ion exchange, these components can be separated and concentrated; further analysis can be done spectrographically or by other suitable methods. Ion exchange chromatography is used as a step in analysis; the experimental technique is simple and in most cases fairly rapid.

COLORIMETRY

The determination of elements in geological samples based on the intensity of colored solutions obtained by appropriate chemical treatment of these materials is a well-established quantitative method that is often used in mineral analysis. In many cases, the color intensities follow Beer's Law.

Colorimetric methods are accurate and sensitive, and provide reliable and precise results. Detection limits often fall in the parts per million range. However, the accuracy and precision of a colorimetric analysis diminishes when measurements are made outside the optimum absorbance and concentration limits. Obviously colored systems which decompose or which do not obey Beer's Law cannot be studied.

MICROSCOPIC METHODS

A good petrographic microscope with accessories is

essential for mineral analysis. Minerals are most conveniently examined microscopically either in the form of fragments or thin sections. The important properties of minerals include crystal form, twinning, inclusions, alterations, cleavage, color, refractive index, optical anomalies, associated minerals, texture relations, axial angles in biaxial species, mode of occurrence and diagnostics.

Refractive index measurements have been used for identification and approximate composition determination purposes. An accuracy of 0.01 for the former and 0.005 for the latter is required in measurements(2).

In the immersion method, the refractive index of the clay mineral is determined by suspending its grains in liquids of various refractive indices as determined by the normal illumination; the grains are transparent in the liquid having the same refractive index.

Factors which affect the refractive index measurements by immersion methods are the design of the microscope, the skill and acuity of the worker, the particle size, the shape and refractive index of particles and their visibility, the uniformity of refractive index throughout the specimen, the precision with which the reference liquids are calibrated and the refractive index intervals between adjacent members of a standard series.

X-RAY TECHNIQUES

X-ray methods utilize the fact that X-rays have wave-

lengths of the order of distance between lattice planes containing atoms in a crystal lattice and these planes act as a diffraction grating as shown in Fig 4.

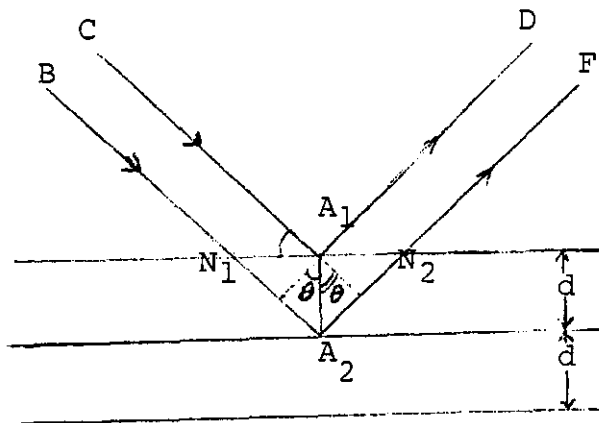


Figure 4. Diffraction of X-rays by a Set of Planes

The path difference between CA_1D and BA_2F rays is equal to $2d\sin \theta$ and in order for two beams to reinforce, the path difference has to be an integral multiple of wavelength of X-ray. This information led to what is known as Bragg's equation;

$$n = 2d\sin \theta \dots\dots\dots(18)$$

Every clay mineral scatters the X-rays in its own distinct diffraction pattern giving rise to a "fingerprint" of its atomic and molecular structure. This diffraction pattern can be photographed and kept for future comparative work.

Advantages of X-ray diffraction are the relative simplicity of spectra, almost complete freedom from chemical influences, predictability of behavior, and nondestructive nature. The greatest disadvantage is that X-rays are

dangerous and safety precautions must be observed. Expense is also a factor.

THERMAL ANALYSIS

Thermal analysis covers "a group of related techniques whereby the dependence of the parameters of a physical property of a substance on temperature is measured"(30). Differential thermal analysis (DTA), thermogravimetry (TG), derivative thermogravimetry (DTG) and evolved gas analysis (EGA) are included under thermal analysis methods and are being used extensively in clay mineralogy.

In DTA the difference in temperature between a substance and a reference material is recorded against either time or temperature as the two specimens are subjected to identical temperature regimes in an environment heated or cooled at a controlled rate.

In TG the mass of a clay mineral heated or cooled at a controlled rate is recorded as a function of temperature or time. DTG provides the first derivative of TG curve with respect to temperature or time.

EGA is defined as a technique to determine the nature and amounts of volatile components formed during thermal analysis.

DTA has definite advantages over TG and EGA since it enables phase changes and solid state reactions to be detected as well as decomposition or oxidation reactions. A comparison of DTA and DTG shows which reactions are

associated with mass changes and which are not.

None of these techniques is truly diagnostic by itself but they have value when they are combined with others. Thermoanalytical results combined with X-ray diffraction and IR can provide reasonably complete information on a mineral.

ELECTRON MICROSCOPY

Electron microscopy uses the resolving power of a beam of electrons to investigate the shapes and sizes of a crystal at a finer level. An important feature of an electron microscope is its ability to form diffraction patterns from very small regions of a sample (typically 1 micrometer in diameter). This information combined with other morphological evidence can be very useful in mineral studies. In spite of the thinness of the specimen one is constrained to use, electron microscopy is a useful technique but its applications in mineralogical chemistry still need to be exploited.

SCANNING ELECTRON MICROSCOPY AND MICROANALYSIS

The techniques normally studied under this topic are scanning electron microscopy (SEM), electron probe microanalysis (EPMA), ion probe microanalysis and the surface and near-surface techniques as Augur Electron Spectroscopy (AES), low energy electron diffraction (LEED) and electron spectroscopy for chemical analysis (ESCA). Of these, SEM

and EPMA are commonly used for qualitative and quantitative studies of minerals.

These techniques use very small amounts of the sample for analytical work. Electron beams are normally used as excitation radiation, and also as the detected radiation in some cases. These techniques use novel ways of imaging the specimen and, to a large extent, are complementary to one another. Their major application in geochemistry is on elemental, microstructural and crystallographic analysis of minerals.

A better depth of resolution is obtained going from the EPMA to the ion microprobe, to ESCA and to AES. However, for maximum sensitivity in measurements optical spectroscopy and X-ray fluorescence rate better than SEM and EPMA but both SEM and EPMA provide 'in situ' analysis on the micro-scale.

ELEMENTAL ANALYSIS USING MASS SPECTROGRAPHIC TECHNIQUES

The determination of elemental compositions of rocks, minerals and allied materials by using mass spectrographic procedures is a new development in analytical geochemistry and one can obtain data on about 70 elements in a single run of a given sample.

The spectrographic method involves incorporation of the sample into a pair of electrodes, dispersing of the resulting ion beam into separate component beams, each consisting of particles with the same mass/charge ratio, and

finally measurement of the number of particles in the individual dispersed beams.

Features of spectrographic techniques which interest geochemists are the very wide range of elements that can be detected in a single analytical run, the low probability of missing any element present in the analyzed material and the high sensitivity of the method for almost all elements.

EMISSION SPECTROSCOPY

Emission spectroscopy was the first direct instrumental technique to be widely used in geochemical investigations and in spite of development of new methods, it remains today as an indispensable tool for the geochemist. It is advantageous to the spectrochemist to use emission spectrography together with one or more other techniques such as IR, X-ray diffraction, atomic absorption, flame photometry and colorimetry; however, this may not be necessary in every analysis.

Emission spectroscopy can be used for qualitative, semiquantitative or quantitative analyses. Its major applications are in element abundance and distribution studies, environmental studies and mineral exploration. The major advantages of the technique are rapidity and simplicity when a large number of determinations are to be made on a sample. A semiquantitative analysis can be performed for 30-40 elements with a 1 mg sample in one run. On the negative side, spectrochemistry is a destructive process. Equipment and

techniques are complex and require trained personnel, especially with respect to method development and spectrum interpretation.

ATOMIC ABSORPTION

Atomic absorption is a simple, sensitive and relatively inexpensive technique whereby a wide range of elements can be determined accurately and precisely. It is mostly used for the determination of trace and minor elements because of its high sensitivity but it is equally good for major elemental determinations.

Most geochemical laboratories use atomic absorption for mineral analyses. A one percent absorption or 0.004 absorbance units is normally accepted as the detection limit, and atomic absorption results are reproducible within 0.5 to 2.5%. When the precision is poorer than this, it is usually due to bad technique or instrumental disfunction. Interferences which may be chemical, molecular and spectral should be accounted for in order to obtain accurate results.

Among the limitations of atomic absorption is the requirement of bringing the sample in solution and the fact that only one element can be determined at a time in many applications.

RADIOCHEMICAL ANALYSIS

Radioisotopes and general radiochemical techniques are widely used for mineral detection and processing studies and

in metallurgical industries. Activation analysis, one of the most commonly used radiochemical methods, is based on the principle that when a material is irradiated by nuclear particles such as neutrons, protons, alpha particles, and high energy photons, some of the atoms of that material will be transformed into radioactive isotopes of the same or different atoms.

Neutron activation analysis is automated and computer-based. However, there are certain requirements for the automated methods: (1) the elements to be studied should have the required activation cross sections; (2) the element should produce at least one gamma-ray emitting isotope on neutron activation; (3) the half lives of the resulting radioisotopes should be within the desired range; (4) the element to be studied should be present in sufficient amounts; and (5) the nuclear properties of both the nonradioactive and the activation products should be known.

The detection limit falls in the $>1000-10^{-5}$ parts per million depending on what element is to be analyzed in a sample. In most cases data can be reproduced with 5% accuracy. In spite of its excellence, neutron activation analysis is not widely used in geochemical analyses due to high cost of equipment.

CHAPTER FOUR

EXPERIMENTAL

A. INSTRUMENTATION

The instrument used in this project was a Perkin-Elmer Model 283 Double Beam Infrared Spectrophotometer equipped with a Wilks Model 12 Double Beam Internal Reflection Attachment.

The design features of the spectrophotometer enable it to provide high performance and wide choice of operation parameters. The optical unit houses the sample area, the grating monochromator, the thermocouple detector, the slit program and baseline controls. The display panel of the control unit indicates digitally the control settings while in use. Optical schematic of spectrophotometer is shown in Fig 5.

The Wilks Model 12 Attachment is designed so that KRS-5 reflector plates can be used in both sample and reference beams. The attachment consists of an anodized aluminum optical bench with two track mounted platforms. After some grinding and polishing of one end of one of the platforms, the attachment was adapted to fit the spectrophotometer between the IR source and the chopper. Each platform has four rotatable mirrors, a trimmer comb, and anchor pins to

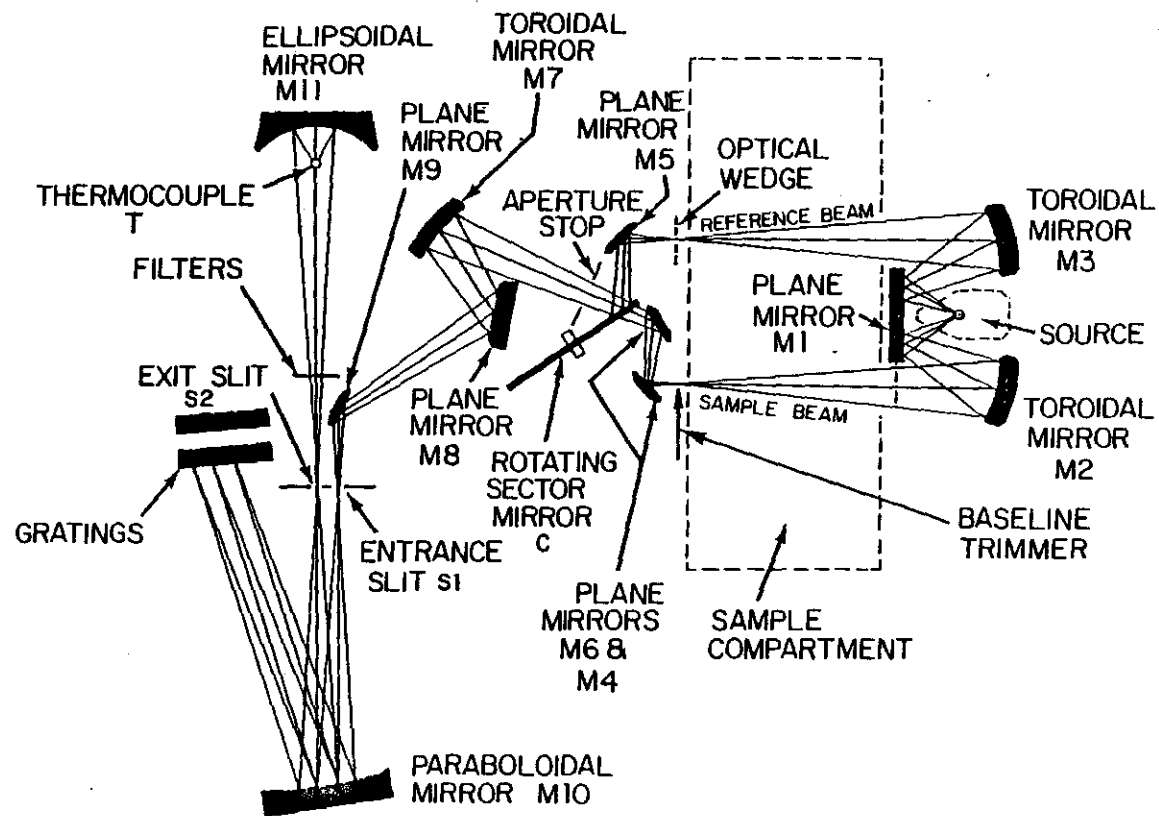


Figure 5. Optical Schematic of Perkin-Elmer IR Model 283

position the reflector plate holders. The sample reflector plate holder is a part of the stainless steel solid sample holder. The ATR solid steel sample holder is comprised of two interlocking steel sections which can be connected; pressure is applied via a thumbscrew. A flat section holds the sample against one face of the plate. The other section has a rectangular projection from a flat steel base which ensures good contact with the sample on the second face of the reflector plate. A working diagram and optical schematics of Wilks Model 12 Attachment are shown in Fig 6.

The sample holder is designed to hold a sandwich of solid powder or slab or fibrous samples in contact with the reflector plate to give maximum transmission of IR radiation. A multiple reflection element multiplies small absorptions by many-fold to provide stronger absorptions. This condition is achieved by mounting the steel pressure plate and tightening the retaining screws to bring the pressure plate into firm contact with the sandwich. With samples in which absorption bands bottom out because of high absorptivities of the sample, less reflector plate was covered with sample, but if the absorption is very low, the opposite is done. If weak absorption results because of poor contact between the sample and the reflector plate, more pressure is applied on the sample. This problem can be overcome by the use of thinner reflector plates also.

A trapezoid-shaped KRS-5 multiple reflection element roughly 50 X 20 X 2 millimeters thick giving approximately

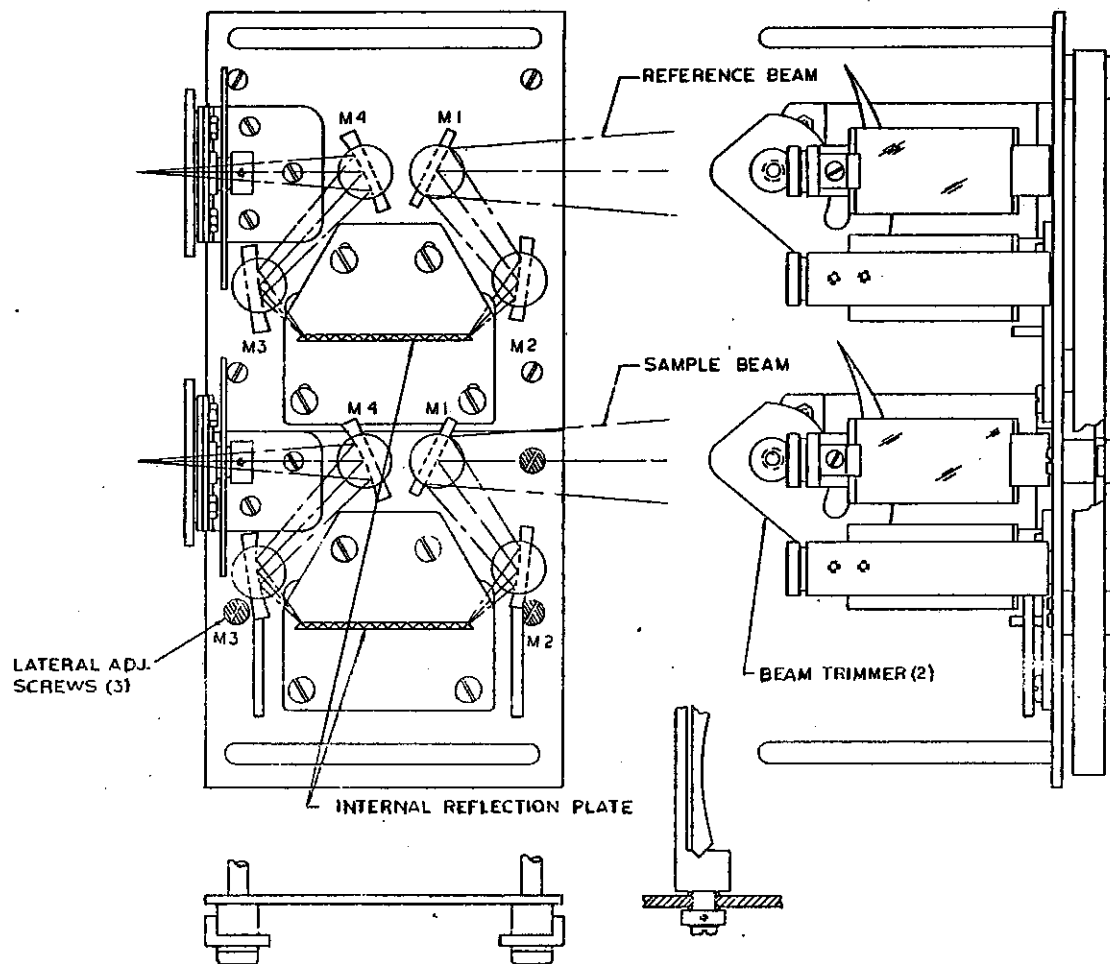


Figure 6. Model 12 Working Diagram and Optical Schematic [Wilks 1965]

25 reflections was used (Fig 7). The ratio of the length to thickness of the IRE is decisive and is chosen so that the IR beam enters the reflection plate through the center of the plate at an angle normal to the edge and leaves through the opposite edge and normal to it. The length of the IRE cannot be more than a certain value because of radiation losses due to diffusion with each reflection.

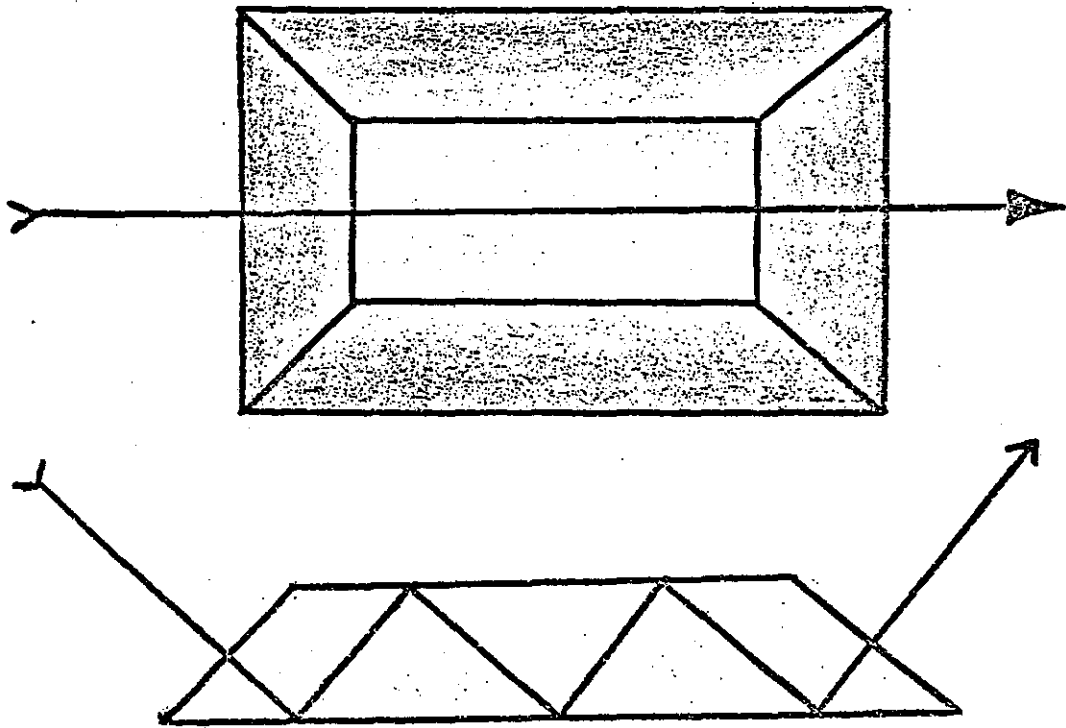


Figure 7. Internal Reflection Element

To ensure high transmission of the reflected beam and higher life of the IRE, the IRE material should be tough and hard, should keep a high surface polish on both sides, should have a higher refractive index than the sample,

should be IR transparent with no important absorption within the spectral range of study, and should be reasonably inexpensive. Some of the commonly used materials are listed in Table 3.

Table 3. Some Infrared IRE Materials

Material	Useful range (cm^{-1})	Refractive index	Comments
AgCl	25,000-500	2.5	Spectral range not useful and too soft to work with mineral samples.
AgBr	22,000-333	2.2	Maintains finish but soft, excellent spectral range.
KRS-5	16,000-250	2.4	Good over wide range but relatively soft and toxic. Proved excellent for this study.
GaAs	10,000-588	3.3	Very expensive and does not cover the range of interest to geochemical spectroscopist.
Ge	5,000-833	4.0	Relatively inexpensive but may not be good for inorganic studies.

B. PROCEDURE

The experimental procedure involves four steps: beam balancing, sampling, spectrum recording and reflector plate reconditioning.

Balancing the signal from the IR source using a double beam spectrophotometer requires balancing the spectrophotometer, rough adjustment of the attachment and fine adjustment of the attachment.

Balance control of the instrument is checked by blocking both beams simultaneously with a thick opaque object

such as a book. While blocking the sample beam, partially unblock the reference beam until the pen is in between 30% to 50% T. Block the reference beam gain and adjust the balance knob until the pen very slowly drifts upscale. If the balance knob requires significant adjustment, the gain control must be rechecked.

In order to roughly align the optics of ATR accessory, the unit is held up at eye level and the two mirrors are adjusted until the image of the face of the reflector plate appears centered in the mirror nearest the eye. Turn the unit around to adjust the other two mirrors in the same way. In order to accomplish the fine adjustment follow the instructions in Wilks "Internal Reflection Spectroscopy"(15).

Sampling is done in three steps; i.e. sample collection, preparation and application.

As far as sample selection and preparation is concerned, all the samples obtained from National Bureau of standards (NBS) were in powder form. Milled chrysotile samples were soft and uniform. Both of these categories did not require any selection and preparation. The samples donated by UOP Geology Department and Delta College Geology Department were solid and had to be ground using a Plattner mortar and pestle. Final grinding followed sieving through a 88 micron sieve to obtain a fine homogenous powder.

Very small amounts of samples were used to prepare a thin covering on the reflector plate; a depth of only five microns is required. Powdered samples were spread on the

reflector plate with paper or simply from the slowly shaken sieve. Thumbscrew pressure was applied in all cases before mounting the sample holder on the accessory.

Various control settings used for taking spectra are: Response = 1; Scan time = 12 minutes; Slit program = 6; Ordinate expansion = 1 and Abscissa expansion = 1. Previously balanced instrument was set at 4000 cm^{-1} and the pen was allowed to stabilize before every scan. Each spectrum was so run as to not miss any important absorption band and also not top-out or bottom-out. Feathering the trimmer combs was a requisite for almost all spectra because internal reflection decreases the energy throughput in the sample beam.

Reconditioning the sample reflector plate required removing the sample holder from the ATR attachment and dismantling it, cleaning with acetone and drying the reflector plate, the holder and the pressure plates. The reflector plate did not need repolishing during the course of this study. The reflector plates required considerable care in cleaning to ensure a smooth regular surface. Most of the spectra were taken during the time nobody else was using the instrument, so rebalancing was not often needed.

The names and sources of various mineral samples studied in this project are given in Table 4 on the following page.

All spectra were satisfactory and reproducible within $\pm 2\text{ cm}^{-1}$. Spectra were run from $4000\text{-}200\text{ cm}^{-1}$ but the 2000-

Table 4. Names and Sources of Mineralogical Samples

Name of sample	Source
Kaolinite	Langley, South Carolina
Kaolinite	Bath, South Carolina
Kaolinite	Delta College Geology Department
Kaolinite	UOP Geology Department
Bentonite	Rock River, Wyoming
Bentonite	Osage, Wyoming
Halloysite	Eureka, Utah
Halloysite	Bedford, Indiana
Bauxite (Dominican), SRM # 697	NBS
Bauxite (Jamaican), SRM # 698	NBS
Bauxite (Arkansas), SRM # 69b	NBS
Bauxite (Surinam), SRM # 696	NBS
Flint Clay, SRM # 97a	NBS
Plastic Clay, SRM # 98a	NBS
Muscovite (Potassium mica)	Delta College Geology Department
Biotite (Iron mica)	Delta College Geology Department
Sodium feldspar, SRM # 70a	NBS
Potassium feldspar, SRM # 70a	NBS
Potassium feldspar, SRM # 607	NBS
Talc (Low-Vis)	John K. Bice Company
Talc	Delta College Geology Department
Talc	UOP Chemistry Department
Glass sand (High iron), SRM # 81a	NBS
Glass sand (Low iron), SRM # 165a	NBS
Pumice	Rabia Winters Corporation
Lithium ore (Petalite), SRM # 182	NBS
Lithium ore (Spodumene), SRM # 181	NBS
Lithium ore (Lepidolite), SRM # 183	NBS
Lithium ore (Lepidolite)	Delta College Geology Department
Dolomitic limestone, SRM # 88a	NBS
Argillaceous limestone, SRM # 1b	NBS
Phosphate rock, SRM # 120b	NBS
Serpentine	Delta College Geology Department
Asbestos	S. W. Corner Company
Remping fiber asbestos	UOP Chemistry Department
Chrysotile, 4K, 4T, 4T-2	UOP Chemistry Department
Chrysotile, 5RNS, 6DN, 7EK-3	Pacific Asbestos Corporation
Chrysotile, 7EX-3	S. W. Corner Company
Chrysotile, 7EX-3, 7EX-3A	UOP Chemistry Department
Chrysotile, 7MS-1	Carey Company
Chrysotile, KB-753, JM-7M02, JM-7M05, 10A, 10B, 10C	UOP Chemistry Department

300 cm^{-1} portion will be discussed in detail and the region 4000-2000 cm^{-1} will be described briefly due to the fact that ATR-IR spectra are not very informative at higher wavenumbers, and KRS-5 absorbs in the 300-200 cm^{-1} range.

A transmission spectrum of the reflector plate showed complete transparency in the 4000-300 cm^{-1} range (Spectrum # 1A, 1B) but it did absorb at 1025 cm^{-1} in its ATR-IR spectrum against reference KRS-5 plate (Spectrum # 2B) due to either surface irregularities or trapped siliceous impurities within irregular surfaces of the plate. Spectra with absorptions in the vicinity of 1025 cm^{-1} will have some contribution from the reflection element.

Various slit program settings were tried on a sample of talc to find the optimal control which provides reasonably detailed ATR-IR spectra of mineral samples and minimal noise level. The slit program selected based on this run was six, which is normal (Spectrum # 3A, 3B).

Carbon dioxide and moisture present in the laboratory atmosphere were not problems and no remedial procedure was deemed necessary.

CHAPTER FIVE

RESULTS AND DISCUSSION

ATR-IR spectrum of each mineral (Appendix A) has two parts. Part A covers region 4000-1400 cm^{-1} and part B that between 2000 and 300 cm^{-1} .

This chapter briefly discusses spectral studies of mineral groups, lists absorption bands for each mineral, and describes spectra of individual minerals.

The ATR-IR spectra of minerals containing the same structural groups were found to have absorption bands of the same general shape differing slightly in their relative intensities. In some cases, these absorption bands were slightly shifted from one mineral to another in the same group. By comparing the spectra of different minerals in the same group and due to the resemblances of the ATR-IR spectra to transmission spectra it was possible to assign some of these absorption bands to specific groups but most of the work done is comparative.

Various abbreviations used to describe band intensities are: b = broad; d = doublet; m = medium; mp = multiplet; s = strong; sh = sharp; v = very and w = weak.

CLAY MINERALS

Clay minerals absorbed strongly in the region 1100-900 cm^{-1} (Spectra 4A-15B). All clay minerals except bauxites gave an absorption band of medium intensity in the range 770 to 760 cm^{-1} and 550 to 500 cm^{-1} . None of the minerals but kaolinites, plastic clay and flint clay, the latter two mainly kaolinites, gave absorption bands in the range 1022 to 1018, 932 to 922 and 680 to 678 cm^{-1} . All clay mineral samples gave a weak absorption band at 600 cm^{-1} . Bauxite spectra showed stronger absorptions for the hydroxyl groups as compared to the rest of the clay minerals. The intensities and relative positions of bands due to hydroxyl groups can also be used to identify various minerals, but they have not been emphasized in this work due to some band distortions in the 4000-3000 cm^{-1} range.

The various mineral samples studied were of siliceous origin or had silica in them in one form or another except two samples of limestone and one sample of phosphate rock. The absorptions in the 1100-900 cm^{-1} are due to stretching of the Si-O bands and the ones in the 500 cm^{-1} are due to Si-O bending.

KAOLINITE

ATR-IR spectra of the various kaolinite samples are shown in Spectra 4A-7B. A number of hydroxyl absorption bands appear in the region 3600-3300 cm^{-1} . One weak but broad band appears due to free water around 1600 cm^{-1} in

each kaolinite sample. One absorption of medium intensity at 1100 cm^{-1} and a strong absorption band at 1000 cm^{-1} are probably due to Si-O bond stretchings. The absorption at 927 cm^{-1} and 900 cm^{-1} are due to Al-O-H bonding like those appearing in transmission spectra. Though it is difficult to assign exactly various bands, it appears that the absorption peaks at 778 cm^{-1} and 676 cm^{-1} may be due to a silica structure. Other bands appearing in kaolinites are one at 766 cm^{-1} , a broad band at $740\text{-}32\text{ cm}^{-1}$, bands of medium intensity at 650 and 600 cm^{-1} , and one strong band at 520 , 450 and 315 cm^{-1} . Some of the absorption bands in the 450 to 300 cm^{-1} region may be due to lattice vibrations. Absorption bands in various kaolinites are given in Table 5 on the following page.

The spectrum of kaolinite from the UOP Geology Department showed a very different pattern as compared to the rest of the samples, and Dr. Kramer of that Department expressed doubt concerning the validity of the sample. After comparison, it was felt that the specimen is not a kaolinite but resembled bentonite more closely than either kaolinite or halloysite.

Apparently in all three samples of kaolinite studied, isomorphous substitutions had taken place to nearly the same extent because all absorption bands were almost superimposable.

Table 5. Characteristic Absorptions in Kaolinities

Kaolinite (Langley, SC)							
3955w	3000w	1600-1500b,mp,w	1018s	760w	650m	453m	
3880w	2905w	1100m	1000d,s	742-35m		310w	
3720w	2798w		930w		600m		
3660w	2700w		902s,sh		520s		
3630w	2522-12w						
3616w	2103w						
3602w							
3442w							
3318-3260w							
3127-20w							
Kaolinite (Bath, SC)							
3918w	3000w	1615-1589b,mp,w	1022s	770w	650w	442w	
3770w	2782w	1099w	1000d,s	740-32w		412w	
3660w	2580w		932w		600w	400w	
3630w	2100w		903s		518s	315w	
3608w							
3520-3492w							
3400w							
3350w							
3278w							
3160w							
3130w							
Kaolinite (DCG, Unk)							
3900w	3000w	1611-1580b,mp,w	1019s	766w	650w	448w	
3808w	2982w	1098m	1009s	750-32b,w		415w	
3724w	2950w		928w		600w	315w	
3662w	2808w		906s		525s		
3632w	2712-2690w						
3620w	2602w						
3540w	2555w						
3415w	2460w						
3360w	2345w						
3278w							
Kaolinite (UOP, Unk)							
3850w	3020w	2060w	1010s	760w	660w	422w	
3810w	2890w	1602-1560b,mp,w			600w	415s	
3634w	2806w				518m		
3476w	2778w						
3403w	2600w						
3300w	2355-14w						
	2240-00w						

BENTONITE

The montmorillonite group is represented by two samples of bentonite whose spectra are given in Spectrum 8A-9B and characteristic absorptions in Table 6.

Table 6. Characteristic Absorptions in Bentonites

Bentonite (Rock River, WY)							
3720w	2920w	2005w	1570w	1000s	790w	682-68w	
3630-10w		1620-1478w		998s	780w	600w	435w
3500w	2780w				770w	505-495m	
3160w	2630w						420s
3072w	2540-24w						
	2360w						
Bentonite (Osage, WY)							
3840w	2740w	1620-1590b,mp,w	1010s	880m	675w	410-00	
3800w	2560-20w	1450w	1000s	790w	600w	m,mp	
3690-50w			953m	780w	510w	330w	
3468-3378w			910m	770w			
3180-30w				749w			
	2410-2280w			719w			

Both the spectra give distortions above 2500 cm^{-1} . Many bands appear in this range; some are probably due to hydroxyl O-H stretch. Both spectra have common absorption bands at 905, 860, 805, 790, 780, 770, 680, 600, 502 and 440 cm^{-1} . The slight differences between the two spectra are indicated below.

The absorption bands at 1450, 958, 910 and 510 cm^{-1} are stronger in the Osage sample spectrum while a band at 1570 cm^{-1} for the Rock River is stronger than its counterpart. The Si-O absorption band at 1000 cm^{-1} in the case of Rock River spectrum has shifted to 1010 cm^{-1} for Osage spectrum, probably due to more substitutions of Si by Al in the second case.

HALLOYSITE

Both samples of halloysite (Spectrum 10A-11B) absorb at $1600-1450\text{ cm}^{-1}$ due to O-H bending. This band is slightly different in shape and position in the two samples. There

is also a weak absorption band at 1200 cm^{-1} . Halloysite spectra have other bands at 900, 745, 645, 520, 450 and 400 cm^{-1} similar to those observed in kaolinite. One halloysite sample shows hydroxyl stretch between 3580 and 3300 cm^{-1} ; the other between 3380 and 3240 cm^{-1} . The Si-O stretching absorption in halloysite has shifted to higher wavenumbers by 15 cm^{-1} compared to kaolinite. The ratio of height of this peak to the one at 900 cm^{-1} is greater in halloysite than in kaolinite.

The absorption bands for two samples of halloysite are given in Table 7.

Table 7. Characteristic Absorptions in Halloysites

Halloysite (Eureka, UT)						
3540-3310w	1786w	1590-50b,w	882w	642w	450m	
2740-24w		1510w	1032s	868w	600w	438w
2476-62w			1012s	740w	560m	415w
2250-2178w			992s		529-19m	
	1770-64mp,w		928w		515w	392w
			904m			355w
						335w
Halloysite (Bedford, IN)						
3580-3455w	1858w	1508w	1010d,s	669w	448-38	
3380-3260w	1812w	1235w	900m	770w	600w	d,w
	2920-2740w	1160-50mp,w		745w	580w	360w
	2440-2280w			738w	520m	330w
	1806w					
	1772w					
	1750w					
	1657w					
	1600-1570b,w					

BAUXITE

Bauxite ATR-IR spectra were taken of four samples of bauxite (Spectra 12A-15B). All four spectra are much alike; they show a broad absorption band at $1600-1400\text{ cm}^{-1}$

due to O-H bending of water; both these bands are missing from the spectrum of the Surinam bauxite. Like other silicate minerals, there is strong absorption in the region 1100 to 900 cm^{-1} with maxima at 995 cm^{-1} in the case of bauxite from Surinam and Arkansas and at 1005 cm^{-1} for Dominican and Jamaican bauxite. There are also other bands in the 1000 cm^{-1} range in all four spectra. Various absorption bands in bauxites are given in Table 8.

Table 8. Characteristic Absorptions in Bauxites

Bauxite (Dominican), SRM # 697 (NBS)						
3900w	1150w	1046m	790w	655w	462w	
3362-40d,w		1034s	732-26w		450-10	
3200w		1005s	700w	600w	mp,w	
		1000s		558w	340w	
		990s		504w		
		930s				
		910w				
Bauxite (Jamaican), SRM # 698 (NBS)						
3900w	1150w	1078w	790w	600w	496w	
3366-40w		1046m	732-24w		478w	
		1014m		570w	460w	
		1005s			448w	
		990m			330w	
		930w				
		910w				
		900w				
Bauxite (Arkansas), SRM # 69b (NBS)						
3895w	2550w	1170w	1090w	790w	600w	450w
3378-65w			1042m	750-01w		
3267-00w			1008s		540-480w	
	2500w		1001s			
			995s			
			930w			
			910w			
Bauxite (Surinam), SRM # 696 (NBS)						
3880-65w	1150w	1090w	790w	600w	492-34	
3424-3360w		1027m	730-678w		mp,w	
3300w	2525w	1006s		553w	355w	
		992s			329w	
		930w				
		910w				

The Si-O bond stretching absorption for the Jamaican

bauxite is least strong among various samples. This is probably due to the low percentage of SiO_2 in the sample as shown by the NBS Certificate of Analyses. The Dominican bauxite absorbed more compared to rest of the samples in the $790\text{-}300\text{ cm}^{-1}$ range and the absorption bands are also somewhat better resolved in this case.

FLINT CLAY

The spectrum of flint clay is given in Spectrum 16A-B. It has a broad absorption band at $3630\text{-}3385\text{ cm}^{-1}$ characteristic of O-H stretching; more O-H stretching absorptions occur at 3684 , 2992 and $2924\text{-}08\text{ cm}^{-1}$. Hydroxyl group bending occurs at 1650 , 1594 and 1576 cm^{-1} . There is an absorption band at $1450\text{-}20\text{ cm}^{-1}$ due to C-O stretch of carbonate ions or N-H stretch of ammonium ions. The Si-O stretching maximum occurs at $1023\text{-}00\text{ cm}^{-1}$ and is somewhat broad and is a multiplet rather than a single absorption. This may be the result of more than one type of molecular environment around Si-O bonds.

Various absorption bands in flint clay are given in Table 9.

Table 9. Characteristic Absorptions in Flint Clay
SRM # 97a (NBS)

3684w	2992w	1595w	1022-01mp,s	669m	450w
3630-3386w		1586w	933w	770w	652w
	2924-08w	1448w	910m	739w	600w
		1430w			529m
		1152w			304w

Some absorptions in the $850\text{-}300\text{ cm}^{-1}$ range which

showed poor resolution in kaolinite were better resolved in the flint clay spectrum. From the similarity of peaks and intensity and location of absorption bands in the spectra of kaolinite and flint clay, it is concluded that kaolinite forms the major part of its composition; but the differences in hydroxyl band stretching and bending absorptions and the better resolution of peaks (some even different from kaolinite bands) show that they are different in chemical composition.

PLASTIC CLAY

The plastic clay spectrum (Spectrum 17A-B) shows water absorption bands at 3880, 3680, 3595, 3400 and 2920 cm^{-1} due to O-H stretch and at 1652-1540 cm^{-1} due to bending of O-H. It has a band at 1436 cm^{-1} due to C-O stretch in carbonates or N-H stretch in ammonium ions. This band is sharp in contrast to its counterpart in flint clay. The Si-O absorption band located at 1003 cm^{-1} is sharper than that for flint clay and appears at a lower wavenumber. This can be explained by the fact that plastic clay has a higher percentage of SiO_2 and Fe_2O_3 compared to flint clay, which means that in crystal lattice of plastic clay more sites are occupied by Si(IV) and Fe(III) thereby moving the position of Si-O band towards lower wavenumbers.

The band at 902 cm^{-1} is a doublet; this is probably due to Al-O-H bonding of the crystal lattice. A band located at 348 cm^{-1} in flint clay is very weak in the spectrum of

plastic clay, while the bands at 450 and 410 cm^{-1} are better resolved in plastic clay as compared to flint clay but are still better resolved than those in kaolinities.

Table 10. Characteristic Absorptions in Plastic Clay, SRM # 98a (NBS)

3880w	3090w	1600w	1580w	1088m	778w	660m	450w
3700w	2920-2880w		1518w	1036s	749w	600w	412w
3660w	2738w		1435w	1010s	740w	532-18m,mp	
3590w	2640w		1150w	1003s			328w
3410-3380w			1132w	908w			
3330-20w				902m			
	2512w						

OTHER SILICATE MINERALS

All silicates absorb strongly in the region 1100-800 cm^{-1} . The environment of SiO_4^{-4} changes from one silicate mineral to another which is used to place minerals in their correct classes. Minerals of the same class sometimes differ enough in their chemical composition to enable identification by looking at their ATR-IR spectra.

ATR-IR spectra of eight silicates (two micas-muscovite and biotite, three feldspars-sodium feldspar, SRM # 99a, NBS, potassium feldspars, SRM # 70a and SRM # 607, NBS and three samples of talc) were taken (Spectrum 18A-25B).

MICAS

Muscovite (Potassium mica) has only two marked bands, one at 1008 cm^{-1} and the other at 440 cm^{-1} . However, it has a very distinct absorption at 3630-3500 cm^{-1} due to O-H stretch. In the biotite (Iron mica) spectrum the same bands

occur as in muscovite spectrum but somewhat broadened due to replacement of potassium and calcium by iron.

MUSCOVITE

Some prominent absorptions in muscovite (Spectrum 18A-B) are a broad band at $3612-3508\text{ cm}^{-1}$, and strong bands at 1012 and 1006 cm^{-1} .

According to Lyon and Tuddenham [1960], the shape of the 1110 to 1000 cm^{-1} region of the absorption spectra in various micas such as muscovite and biotite can provide information on the amount of Al(III) substitution for Si(IV) (Y number) in the basal, tetrahedrally coordinated level. Using this approach it is estimated that the muscovite spectrum obtained represents a Y value between 1.01 and 1.02.

A comparison of spectrum of two micas shows that the spectrum of muscovite has about five absorptions of medium intensity in the 1200 to 1050 cm^{-1} range while the spectrum of biotite has none.

Table 11. Characteristic Absorptions in Muscovite (DCG, Unk)

3880w	1610w	1438w	1085m	850w	686w	492w
3800w		1139m	1012s	810w	670w	450w
3760-40w		1108m	1009s	734w	600vw	440w
3620-3510b,w			998m		504w	430w
			915w			

BIOTITE

The absorption bands appearing in the $1000-400\text{ cm}^{-1}$ range in muscovite have flattened in biotite due to the

replacement of potassium by iron or possibly other ion exchanges. One can easily recognize one from the other by comparing their spectra. The biotite spectrum has better resolved absorptions in the 1600-1400 cm^{-1} range, with bands at 1600, 1535, 1500 and 1410 cm^{-1} .

Biotite absorbs strongly in the 1100-800 cm^{-1} region as compared to 1200-950 cm^{-1} for muscovite. Its 440 cm^{-1} absorption is less strong as compared to 995 cm^{-1} , while in muscovite both of these peaks are of comparable strength. The biotite spectrum has an absorption at 525 cm^{-1} and the muscovite spectrum does not.

Table 12. Characteristic Absorptions in Biotite
(DCG, Unk)

3795-15w	1600w	1532w	1097w	888w	601w	488w
3648w	2880-2770w	1498vw	997s	880w	522w	466w
3520-3460w		1408w	987s	860w		452w
3128w	2380w	1306vw	950m	845w		440w
	2344w	1296vw	938w	766vw		412w
	2310w			756vw		400w
	2238w					386w
						328vw

FELDSPARS

Feldspar spectra show some spectral similarities to the limestone spectra. Similar absorptions occur in both at 1420-00, 1000, 705, 570, 530, 445 and 410 cm^{-1} . The feldspar spectra have very much the same absorption pattern in the 2000-1200 cm^{-1} as that of phosphate rock. Both have similar absorptions at 1020, 760, 720, 570 and 460 cm^{-1} . Feldspar and kaolinite spectra show more similarities than either feldspar and limestone or feldspar and phosphate rock

spectra, with closely resembling absorption bands at 1610-1410, 1010-00, 650 cm^{-1} and almost all the ones occurring from 570-300 cm^{-1} . This suggests that feldspars are an important road to mineral formation.

Feldspar spectra are characterized by a strong absorption around 1000 cm^{-1} and two absorptions at 638 and 315 cm^{-1} ; the most striking feature of these spectra are three absorption bands between 760 and 705, 572 and 510, and 412 and 360 cm^{-1} , each a paired absorption.

Various absorption bands of ATR-IR spectra of feldspars are sensitive to the relative amounts of different metallic cations; for example, the absorption band which occurs at 630 cm^{-1} in sodium feldspar moves to 637 cm^{-1} in potassium feldspars.

The feldspar spectra will be discussed under five areas of interest. The first covers 1600 to 1400 cm^{-1} , the second, 1200 to 850 cm^{-1} , the third, 850 to 600 cm^{-1} , the fourth, 600 to 450 cm^{-1} , and the fifth from 450 to 300 cm^{-1} .

SODIUM FELDSPAR

The first region of the spectrum of sodium feldspar, SRM # 99a, NBS (Spectrum 20A-B) has a broad band from 1588-1408 cm^{-1} . Second region has five medium intensity bands at 1133, 1080, 950, 896 and 877 cm^{-1} , and three strong absorptions at 1020, 1008 and 995 cm^{-1} . The third region has paired absorptions at 745 and 720-12 cm^{-1} and single absorptions at 700, 690, 680, 664 and 630 cm^{-1} . The fifth region

is comprised of one paired absorption with maxima at 412 and 365 cm^{-1} , and a single band at 318 cm^{-1} . Various absorptions in Sodium feldspar are given in Table 13.

Table 13. Characteristic Absorptions in Sodium Feldspar, SRM # 99a (NBS)

3860w	2900w	1748w	1588-1395b,mp,w	720w	630w	412-345
3790w	2830-18w		1131m	1080m	560w	b,w
	3736-3310b,mp,w			1008s	531m	318w
	3284-3250w			995s		
	2470w			950m		
	2280w					

The paired peaks of the last three regions are not resolved completely. The first two paired peaks have the lower wavenumber absorption band stronger than the higher wavenumber one while the last one has both absorptions of the same strength.

POTASSIUM FELDSPAR

Potassium feldspar, SRM # 70a (Spectrum 21A,B) absorbs at the same wavenumbers as the sodium feldspar with the following differences.

1. The broad absorption band in the 1600 to 1400 cm^{-1} range has moved towards higher wavenumbers by 10 cm^{-1} .
2. The peak around 1000 cm^{-1} is sharper and less complex than the one in the sodium feldspar spectrum.
3. In regions 3,4 and 5 the paired peaks are resolved completely.
4. In regions 3 and 4 the lower wavenumber absorption of

the paired peaks is stronger, while in region 5 the higher wavenumber absorption peak is stronger.

5. The two single absorptions at 674 and 638 cm^{-1} not only are resolved better but moved towards higher wavenumbers by 8 cm^{-1} . The band at 318 cm^{-1} is also better resolved.

These changes are attributed to a decrease of the percentages of CaO, BaO, Na₂O and Al₂O₃ and an increase of the percentages of K₂O and SiO₂.

Table 14. Characteristic Absorptions in Potassium Feldspar, SRM # 70a (NBS)

3860vw	2910w	1728w	1150m	1035s	775w	655w	410m
3815w	2860-2552d,w			1010s	717m	637w	360w
3690-3120b,mp,w		1610-1420b,mp,w		1002s		570m	315w
	2390-2815w			998s		530m	
				982s			

POTASSIUM FELDSPAR

The spectrum of potassium feldspar, SRM # 607 (Spectrum 22A,B) shows no absorption band in the 1600 to 1400 cm^{-1} range. The band around 1000 cm^{-1} is wider compared to the one in SRM # 70a potassium feldspar spectrum. Resolution of the paired peaks in regions three and four is better than sodium feldspar spectrum but not as good as in SRM # 70a spectrum. Both paired peaks in regions three and four and a single peak at 674 cm^{-1} have moved towards lower wavenumbers by about 18 cm^{-1} which probably is due to the trace amounts of rubidium and cesium in this sample of potassium feldspar since other constituents of both feld-

spars are approximately the same as shown by NBS Certificates of Analysis (Appendix I-K). Differences in lattice structure of the two compounds can also be a factor for this change. One single absorption at 638 cm^{-1} in sodium feldspar is absent in this spectrum.

Table 15. Characteristic Absorptions in Potassium Feldspar, SRM # 607 (NBS)

3810w	3084w	1390w	1018s	750w	660w	400m
3780w	3000-2980w	1275w	1010s	708m	628w	358-00
3735w	2900w		998s		560m	mp,w
3664w	2415w		985s		520m	
3585w						
3440-3310w						
3200w						

TALCS

Spectra of three samples of talc (Spectrum 23A-25B) showed a sharp band at 658 cm^{-1} ; no other mineral in this study showed this absorption. All three samples absorbed strongly from 1000 to 970 cm^{-1} and 450 to 400 cm^{-1} .

All talc spectra have the same fundamental absorption bands with slight differences in their appearance and position. Each spectrum has a broad absorption band from 1620 to 1410 cm^{-1} ; a strong band at about 1000 cm^{-1} , which, in the DCG and UOP talc, is broad (approximately 40 cm^{-1} width). Each spectrum also shows a sharp and strong band at 658 cm^{-1} and a broad and strong absorption band at $460-320\text{ cm}^{-1}$. In the low-vis talc spectrum, there is no broad absorption at $460-320\text{ cm}^{-1}$, instead there is one absorption of relatively higher strength at 438 cm^{-1} and a few weak

absorptions. The low-vis talc spectrum also showed one band at $742\text{-}35\text{ cm}^{-1}$ absent in the other two spectra.

Table 16. Characteristic Absorptions in Talc

Talc (Low-Vis) (John K. Bice Company)					
3910-3870w	1618-1426b,mp,w	1003s	742-35w	438s	
3690w	2980w			658m	
3645-15w				600w	
3530w	2900w			516m	
3495w	2750w				
3474w	2640-2570w				
3355w	2500w				
3260w	2400-2374w				
Talc (DCG, Unk)					
3938w	3048-38w	1003-970mp,s	660s	404-00s	
3848-20d,w	1612-1430b,mp,w		885m	335-20w	
3600-3320b,w			780-60w		
3180-50w					
	2715w				
	2515w				
Talc (UOPC, Unk)					
3960w	3020-2965w	1150w	1000-970mp,s	655s	416-09s
3920-3860w	1613-1438b,mp,w	901m	851m	648s	
3845-3795w					
3558w					
3438-3150w					

HIGH SILICA MATERIALS

Glass sand (High iron), SRM # 81a, Glass sand (Low iron), SRM # 165a and Pumice (Rabia-Winters Corporation) spectra (Spectrum 26A-28B) showed a shift of the Si-O absorption band towards lower wavenumber as one would expect due to very low alumina and higher silica content. The same absorption moved towards higher wavenumber in the spectrum of high iron glass sand as compared to low iron glass sand due to the increase of iron content. Both glass sand samples gave a broad band for hydroxyl group stretching at 3480 to 3010 cm^{-1} . The same absorption band in pumice spectrum

comprised small absorption bands, the largest being at 3110 cm^{-1} . Pumice spectrum showed an absorption at 1450-20 cm^{-1} , apparently due to C-O stretch for CO_3^{2-} or HCO_3^- .

GLASS SAND (HIGH IRON)

The spectrum of high iron glass sand (Spectrum 26A,B) has two broad bands at 3410-3010 and 1580-1470 cm^{-1} due to O-H stretching and bending, respectively. Si-O bond stretching occurs at 964-54 cm^{-1} . All absorptions below 800 cm^{-1} in high iron glass sand are stronger than the ones in low iron glass sand.

Table 17. Characteristic Absorptions in High Iron Glass Sand, SRM # 81a (NBS)

3480-3010b,w	1580-1470b,mp,w	678-68w
	991-40m,mp	440-08w
	759w	350w

GLASS SAND (LOW IRON)

Almost all the bands of high iron glass sand are present in the spectrum of low iron glass sand (Spectrum 27A,B) with the difference that its Si-O absorption is flatter and broader, as are the rest of the absorptions below 600 cm^{-1} ; O-H bending did not appear for unexplainable reasons. However, this sample has a band at 605 cm^{-1} which is a little stronger than the one for high iron glass.

Table 18. Characteristic Absorptions in Low Iron Glass Sand, SRM # 165a (NBS)

3480-3010b,w	1010-890b,m,mp	605w	445-386w
	760-20w		

PUMICE

The pumice spectrum (Spectrum 28A,B) is different from both high iron and low iron glass sand in the sense that it has two regions of high absorption. One is from 1200 to 850 cm^{-1} which is the same as high and low iron glass sand but differs in detail; the other, from 470 to 320 cm^{-1} , is very weak in the other two cases. The 800 to 700 cm^{-1} region shows weak absorption as compared to high iron glass sand but shows stronger peaks than low iron glass sand. Its major Si-O absorption occurs at 992 cm^{-1} which is a shift towards higher wavenumber. This means that a number of Si(IV) positions have been substituted by Al(III) or Mg(II) or other lighter atoms and not many Si(IV) are replaced by Fe(III). The absorptions of medium intensity at 1110, 1066, 1046, 982, 978, 962 and 940-35 cm^{-1} indicate more than one type of Si-O environment in pumice lattice structure. Pumice has a band at 1700 cm^{-1} probably due to C-O stretch of HCO_3^- . This band is absent in all the minerals under this study. Its O-H bending absorption occurs as multiplet rather than a single band.

Table 19. Characteristic Absorptions in Pumice
(Rabia-Winters Corporation)

3480-3010b,mp,w	1960-20mp,w	1036m	760w	590w	480w
2315w	1748w	1190w	990s	720-10w	406m
	1700w	1110m	935m		
	1630-1420b,mp,w				

LITHIUM ORES

Three lithium ores, petalite, spodumene and lepidolite (Spectra 29-32B), are a tectosilicate, an inosilicate and a phyllosilicate respectively, according to Gadsden's classification [1975]. Their ATR-IR spectra show differences in location and the shape of absorptions due to O-H stretch. The 1400 to 900 cm^{-1} and 450 to 400 cm^{-1} is the region of strong absorption, the Si-O stretch occurs at 1010 cm^{-1} . Each spectrum of the various ores shows a band at 790 cm^{-1} . The O-H bending in petalite and spodumene occurs at 1600 to 1400 cm^{-1} . The spectra of petalite and spodumene have one band at 1140 cm^{-1} which in lepidolite samples is either absent or very weak. Petalite has some of the characteristic bands of clay minerals and some of lithium ores.

The differences in shape of Si-O stretching absorptions in various lithium ores is attributed to the variation in the Li_2O percentages in the ore samples. The absorption band which occurs at 600 cm^{-1} in petalite and lepidolite is probably due to the Rb_2O because this band is strongest in lepidolite which has the higher percentage of Rb_2O as compared to petalite whereas this peak does not occur in the spodumene spectrum because spodumene does not have any Rb_2O at all (Appendix F). The variation in the percentages of Rb_2O or K_2O or Li_2O or all these together have affected the absorption peak at 515 cm^{-1} which is very weak in the spodumene spectrum as compared to the spectra of other two ores.

PETALITE

The biggest difference between the spectrum of petalite (Spectrum 29A,B) and the spectra of other lithium ores is in the 800 to 600 cm^{-1} range, where its spectrum has three absorption bands of about the same strength. It has two multiplets with prominent paired absorptions at 752 and 735 cm^{-1} and 684 and 663 cm^{-1} , and one multiplet with one obvious band at 600 cm^{-1} . The absorption bands at 400 and 390 cm^{-1} are stronger than the Si-O band at 1012 cm^{-1} . These bands are 30 to 50 cm^{-1} lower when compared to the spectra of spodumene and lepidolite.

Table 20. Characteristic Absorptions in Petalite, SRM # 182 (NBS)

3660-3130b,mp,w	1750w	1138m	1040s	875w	684w	455w
2860w	1650-1418b,mp,w		1012s	790w	662w	400m
2738w			1000s	750w	600w	
2628-2592w				735w	560w	
2310w					525m	
					500w	

SPODUMENE

The spectrum of spodumene (Spectrum 30A,B) has an absorption at 925-00 cm^{-1} which is not present in other lithium ore spectra. Spodumene has a set of absorptions at 870, 860 and 850 cm^{-1} which are better resolved compared to other spectra. Each absorption in the 800 to 500 cm^{-1} range is less resolved and is of lower strength as compared to the other two spectra.

Various absorptions in the spodumene are given in Table 21 on the following page.

Table 21. Characteristic Absorptions in Spodumene, SRM # 181 (NBS)

3790w	2945w	1733-18m,mp	1012s	875w	680w	487vw
3788-3112b,w		1250w	1006s	790w	655w	460w
	2645-20w	1140m	925-00w	725w	618m	438m
	2360-2280w				588m	390w
						375w

LEPIDOLITE

Most absorption bands in the spectra of two samples of lepidolite (one from NBS and the other from DCG) (Spectra 31A-32B), have the same pattern and strength of the bands but slightly shifted towards higher wavenumbers by 10 cm^{-1} in the DCG lepidolite spectrum and the band at 300 cm^{-1} has shifted to 290 cm^{-1} in the same specimen; the absorptions in this region are somewhat flat in the DCG lepidolite spectrum. The 600 and 350 cm^{-1} band is stronger in NBS lepidolite spectrum.

Table 22. Characteristic Absorptions in Lepidolites

Lepidolite, SRM # 183 (NBS)						
3668-3200b,mp,w	1632-1530b,mp,w	1030s	790w	600w	450m	
3000w		1303vw	1015-05s	515m	350w	
2900w		1150w	935w	734-23w	300w	
2510w						
Lepidolite (DCG, Unk)						
3685-3262b,mp,w	1628-1497b,mp,w	1020s	860w	689-79w		
3180-20w		1400w	1010s	796-20w	462-48m	
2840w		1300w	963m	525m	356w	
2478w		1222-12w		515m		
		1150w	905w			
		1100w				

NONSILICATE MINERALS

Carbonate minerals such as argillaceous limestone and

dolomitic limestone can be distinguished from silicate minerals by comparing their ATR-IR spectra. Differences include the higher strength and sharpness of bands in carbonate minerals. The bands which characterize carbonate minerals occur at 1400 cm^{-1} and in the $1020\text{-}850\text{ cm}^{-1}$ region. Neither the strong broad band around 1400 cm^{-1} nor the sharp band at 870 cm^{-1} occurs in silicate minerals or it is very weak. The single sharp band near 1000 cm^{-1} in carbonate minerals appears as a multiplet in silicate minerals.

DOLOMITIC LIMESTONE

Dolomitic limestone (Spectrum 33A,B) shows weak O-H stretching absorptions due to water at 3755 and $3530\text{-}3300\text{ cm}^{-1}$. Strong carbonate absorptions occur at 1420 and 1008 cm^{-1} , in addition to a medium band at 870 cm^{-1} and two weak bands at 714 and 678 cm^{-1} .

Table 23. Characteristic Absorptions in Dolomitic Limestone, SRM # 88a (NBS)

3755w	2920-2810b,mp,w	1420s	1009s	870m	678w	460m
	3530-3300w			714w	658w	450m
	2580w				556w	400s
	2420-00w				530m	340s
						320-10m

ARGILLACEOUS LIMESTONE

All absorptions in argillaceous limestone (Spectrum 34A,B) occur at approximately the same wavenumbers as in dolomitic limestone but are more intense. The absorption at 1420 cm^{-1} in dolomitic limestone occurs as a broad and

strong band at 1420-1390 cm^{-1} in this sample. Absorptions occurring below 710 cm^{-1} are stronger than their counterparts in dolomitic limestone.

Table 24. Characteristic Absorptions in Argillaceous Limestone, SRM # 1b (NBS)

3738w	2925w	1800w	1420-1390b,s	869s,sh	449s
3680-70w				1009s,sh	420m
3288w	2760w			790w	399w
	2570w			770w	375m
	2500w			705m	358m
	2380-00w				515m
					330s
					505m
					305s
					280s

PHOSPHATE ROCK

Phosphate rock (Spectrum 35A,B) shows strong absorption at 1015 cm^{-1} due to P-O stretching of phosphate ions. There is a medium intensity absorption at 1455-20 and weak absorptions at 875 and 860 cm^{-1} due to carbonate ions. These bands are much stronger in the limestone spectra.

Two medium absorptions occur at 600 and 560 cm^{-1} due to P-O bending of phosphate ions. These bands are also much weaker in the limestone spectra. Various absorptions in phosphate rock are given in Table 25.

Table 25. Characteristic Absorptions in Phosphate Rock, SRM # 120b (NBS)

3600w	2920-2800b,mp,w	1455-20b,m	875w	660w	497w
3480w	1775w	1012s,sh		600m	450m
3378w	1750w		860w	560m	420w
3150-20w					322s
					308s
					290-80s

Limestones and phosphate rocks can easily be differentiated by a comparison of their ATR-IR spectra. Major differences exist in the absorption pattern around the 1400, 900 and 600-550 cm^{-1} regions.

Phosphate rocks can be differentiated from silicate minerals conveniently due to their different spectral bands. Limestone spectra, like the phosphate rock spectra, resemble to some extent the spectra of certain silicate minerals.

CHRYSOTILE

Chrysotile spectra (Spectra 36A-56B) of all grades show absorption bands for O-H stretching and bending, the former in the 3800 to 3000 cm^{-1} and the latter in the 1600 to 1400 cm^{-1} ranges. These absorptions do not follow any systematic pattern, sometimes even in the same grade of chrysotile by different manufacturers which means that it probably is not possible to classify the various grades based on their ATR-IR spectra. The absorption band for Si-O stretch occurs at approximately 50 cm^{-1} lower wavenumber as compared to clay minerals. Either it is present in the 950 to 900 cm^{-1} or as a broad band in the 1000 to 900 cm^{-1} range. Peak area, strength and pattern of bands is different in all grades of chrysotile but it is rarely indicative of the fiber size, especially if the grades are made from asbestos obtained from different sources. This is stated based on the study of spectra of chrysotile grades discussed in the following pages.

In the 800 to 600 cm^{-1} region almost every grade of chrysotile shows no significant absorption. The only exceptions are the serpentine, which has bands at 768, 720, 710 and 620-05 cm^{-1} , and a few other chrysotile grades.

Chrysotile spectra have at least two absorption bands in the region from 600 to 300 cm^{-1} ; the shapes and wavelengths varied from one chrysotile grade to another.

Chrysotile discussion will be limited to 2000-300 cm^{-1} region because the 4000-2000 cm^{-1} region is not very informative due to high noise level. For reference however, absorptions in this region will be listed along with others in the form of Tables.

Serpentine (Spectrum 36A,B) shows strong absorption due to Si-O stretching at 1006 cm^{-1} and Si-O bending at 440-14 cm^{-1} ; a weaker broad band occurs at 1640-1430 cm^{-1} in addition to the absorption bands listed in Table 26. The Si-O stretching in SWC asbestos (Spectrum 37A,B) has shifted to 915 cm^{-1} due to high alumina content. Other absorptions have also been shifted towards lower wavenumbers. Major change in the absorption of remping fiber asbestos (Spectrum 38A,B) is the narrowing of the band due to O-H bend at 1450 cm^{-1} . Absorptions of all three chrysotile grades are given in Table 26 on the following page.

The chrysotile grade 4K (Spectrum 39A,B) exhibits Si-O stretching absorption as a doublet with maxima at 1010-90 and 951-40 cm^{-1} and a medium absorption at 600 cm^{-1} . The Si-O bending absorption occurs at 440 cm^{-1} . Grade 4T

Table 26. Various Absorptions in Chrysotiles

Serpentine (DCG, Unk)					
	1640-1430b,mp,w	1075w	875w	620-08w	
	1283w	1006s	769w	550w	440-14
	1265w	955m		534w	m,mp
					370w
					345-30w
Asbestos (SWC)					
3535-3482w	1667-1380b,mp,w	1046w	888m	600w	422-00w
3380-20w	1150w	1028w		520-00w	
		943m			342w
		933m			
		915m			
Asbestos, Remping Fiber (UOPC, Unk)					
3418w	1450w	990m		542-13w	
3220w	1395w	929s			400-388m
3160w	1165-40w				

(Spectrum 40A,B) has a broad multiplet at $555-518\text{ cm}^{-1}$ and a strong band at 398 cm^{-1} . Chrysotile grade 4T-2 (Spectrum 41A,B) has one broad band at $600-520\text{ cm}^{-1}$ and one band at $390-365\text{ cm}^{-1}$; both bands have multiple absorptions. In 4K grade the paired Si-O stretching absorptions are of the same strength. The peak of the low wavelength band decreases in strength with finer fiber in changing from grade 4K to 4T-2. Another noticeable difference is that the bands in the 600 to 500 cm^{-1} get broader as the fiber becomes fine which probably is due to the fine size of fiber and resulting better contact. Various absorptions of the samples of this group are given in Table 27 on the following page.

Chrysotile grade 5RNS (Spectrum 42A,B) shows strong paired absorption for Si-O stretch in addition to strong bands at $600-530$ and $418-395\text{ cm}^{-1}$. The spectrum of 6DN chrysotile (Spectrum 43A,B) shows a broad multiple absorption band at $950-20\text{ cm}^{-1}$ due to Si-O stretch. The Si-O

bending occurs at 430 cm^{-1} . The absorptions of Chrysotile grade 5RNS and 6DN are given in Table 27.

Table 27. Absorptions in Various Chrysotile Grades

Chrysotile, 4K (UOPC, Unk)					
3650w	1600-1405b,mp,w	740w	600m	440s	
3600w		1031m	540m	395m	
3530w		1010-90mp,s			
3400w		951-40s			
3300w					
3160w					
Chrysotile, 4T (UOPC, Unk)					
3680-3500b,w	1738-1450b,mp,w	1008s	555-18m		
2870w		970s		460m	
2586w		950-25s		398s	
Chrysotile, 4T-2 (UOPC, Unk)					
3680w	1600-1396b,mp,w	990-80s	600-52m		
3600w		1260-20mp,w	730w	420w	
3460w		1140w	972s	390-65s	
3360w		958s			
3220w		946-30mp,s			
Chrysotile, 5RNS (PAC)					
3820w	2640w	1550-1490mp,w	600-530mp,w		
3740w		1010s		418-395s	
3700w		995s		348m	
3660w		975s		320w	
3620w		956s			
3490w		948s			
3320w		940s			
3110w		930s			
Chrysotile, 6DN (PAC)					
3650w	2960w	950-20mp,s	600m	430m	
3625w	2880w		530m	410-370m	
3240w	2620w			345m	
3220w	2480w				
3175w	2400w				
3130w					

Absorption due to Si-O in 7EK-3 chrysotile (Spectrum 44A,B) occurs at $930-890\text{ cm}^{-1}$ and is the only prominent band. A second sample of 7EK-3 (Spectrum 45A,B) has a medium broad band at $1560-1400\text{ cm}^{-1}$ due to O-H bending and a strong Si-O stretching band at $928-10\text{ cm}^{-1}$. SWC 7EX-3

chrysotile (Spectrum 46A,B) shows a weak absorption at 1580-1450 cm^{-1} and strong absorptions at 993, 979 and 950-37 cm^{-1} . Absorptions at 600-545 and 430-384 cm^{-1} are broad, multiple and strong. A second sample of 7EX-3 (Spectrum 47A,B) exhibits weak absorption at 1630-1390 cm^{-1} ; strong absorptions due to Si-O occur at 1010, 1000 and 950 cm^{-1} in this sample. Spectrum 48A,B is for 7EX-3A and shows absorptions at 560-20 and 430-370 cm^{-1} in addition to the ones listed in Table 28. The 7MS-1 chrysotile (Spectrum 49A,B) shows an absorption band at 1550-1395 cm^{-1} due to O-H bending. It has strong absorptions at 585-40, 430-15 and 370-30 cm^{-1} . Absorptions in grade 7 chrysotile members are given in Table 28 on the following page.

No clearly defined shifting pattern is shown by the grade seven chrysotile between coarse and fine fibers. However, the doublet or multiplet (due to Si-O stretch) of the coarse grades became somewhat sharper singlets in the spectra of finer grades.

The spectrum of KB-753 (Spectrum 50A,B) gives absorptions at 1810-1700, 1604-05 cm^{-1} and a strong band at 937-06 cm^{-1} . The rest of the absorptions did not resolve. The spectrum of JM-7M02 (Spectrum 51A,B) has a broad but weak multiplet at 1610-1378 cm^{-1} and strong Si-O stretching bands at 980, 944 and 940-30 cm^{-1} . The JM-7M05 chrysotile (Spectrum 52A,B) shows weak O-H bending at 1580-42 cm^{-1} and strong Si-O stretching bands at 998, 992, 970, 960-40, 928 and 916 cm^{-1} . A second sample of JM-7M05 (Spectrum 53A,B)

Table 28. Various Absorptions in Grade 7 Chrysotile

Chrysotile, 7EK-3, Sample 1, (PAC)						
3790w	2900w	1950-1800b,mp,w	930-890m		600-345b,mp,w	
3760w		1490w				
3460-3060b,mp,w		1410w				
Chrysotile, 7EK-3, Sample 2, (PAC)						
3580w	2990w	1690-65mp,w	950m		578m	465w
3555w	2850w		1560-1400b,m,mp			416-360
3400w	2780w		1330m	928-10mp,s		mp,w
3370-20w			1138w			
3270w	2760w					
	2650					
	2635w					
	2320w					
	2150w					
Chrysotile, 7EX-3, Sample 1, (SWC)						
3680-3260b,mp,w			1580-1450b,mp,w		600-545m,mp	
3150w	3050w		993s	770w	525m	430-384s
3130w	2880w		979s			350m
3100w	2760w		950-37s			
	2660w					
	2580w					
	2320w					
Chrysotile, 7EX-3, Sample 2, (UOPC, Unk)						
3684w	2620w	1630-1390b,mp,w	1010s	796w	650m	416-375s
3530w	2570w	1250w	1000s	756-09mp,w		352m
3380w		1230w	950s		630m	
3340w		1204w			595-36m,mp	
		1150w				
Chrysotile, 7EX-3A (UOPC, Unk)						
3880w	2520w	1675-1500b,mp,w	1059w	855m	560-20mp,w	
3855w	2360-00w	1336w	980-74w			430-370
3810w		1111w	950-28mp,s			m,mp
3790w				823m		
3640-20w				740w		
3505w						
3490w						
3482w						
Chrysotile, 7MS-1 (CC)						
3836-25w			1550-1395b,m,mp		590-39m,mp	
3635w	2490-2390w		990s	725-20w		430-330
3580w			968s			m,mp
3460-3120b,mp,w			948-34s			

shows different absorptions. There is no significant absorption in the 2000 to 1100 cm^{-1} range. The Si-O stretching bands also differ to some extent. Analysis of JM-7 chrysotile grade spectra show a broadening of the Si-O

stretching band and sharpening of the band around 400 cm^{-1} as one moves towards the finer grades.

Table 29. Various Absorptions in Chrysotile Grades

Chrysotile, KB-753 (UOPC, Unk)							
3520w	2120w	1810-1700b,mp,w	937-06s	605w	470w		
3192w		1640-05mp,w		590-88w			
3100w				560w	460w		
				538w	400w		
					370w		
Chrysotile, JM-7M02 (UOPC, Unk)							
3648w	2965w	1610-1378b,mp,w	980s	644w	427-380		
3595w			944s	600m	mp,s		
3536w			940-30s	580-40m,mp			
3240w							
3180w							
3100w							
Chrysotile, JM-7M05, Sample 1, (UOPC, Unk)							
3665-20w		1750w	1580-42mp,w	750-38w	412-38m,		
3586w	2980w	1648w	1450w	998s	593-50m,mp	mp	
3306w	2900w	1615w		992s		370m	
3280w	2292w			970s		350m	
				960-40s			
				928s			
				915s			
Chrysotile, JM-7M05, Sample 2, (UOPC, Unk)							
3800w	2910w	1900w	1529w	992s	710w	590m	468m
3720w	2840-18w		1460-48w			540m	416s
3688w	2710w	1830w	1420w	942-30s		505m	390-80s
3520-3400b,w		1800w	1195w	910s			370m
3180w	2620-2540w		1160-36mp,w				355m
	2515-2470w						348m
		1750w					322w
		1730w					
		1652w					
		1628-13w					

The ATR-IR of 10A chrysotile (Spectrum 54A,B) shows absorption due to O-H bending at $1620-1430\text{ cm}^{-1}$ and strong absorption at $956-30\text{ cm}^{-1}$ due to Si-O stretch. The 10B chrysotile (Spectrum 55A,B) shows significant bands at 1030, 1002-973 and $958-40\text{ cm}^{-1}$. These bands are less distinct in the 10C chrysotile spectrum. The band at 600 cm^{-1} is

stronger than the one at 570 cm^{-1} in the 10B spectrum while the opposite is true for the 10A spectrum. The absorptions in the vicinity of 400 cm^{-1} in the 10C spectrum (Spectrum 56A,B) more resemble 10B and less 10A. The absorptions in the 600 to 400 cm^{-1} are shifted by 10 to 30 cm^{-1} towards lower wavenumbers. The Si-O stretching band is sharper than 10A and 10B.

Table 30. Absorptions of chrysotile grade 10

Chrysotile, 10A (UOPC, Unk)							
3800w	3040w	1800-1730b,mp,w	956-30mp,s	600m	400s		
3690w	2895w	1620-1430mp,w		580-35m,mp			
3580w	2850w	1365w			370s		
3345w	2840w	1340w			350s		
3280w	2680-70w				319m		
3176w	2580w						
3142w	2400w						
	2240w						
Chrysotile, 10B (UOPC, Unk)							
3780w	2855-2785w	1580-60mp,w		612s	460m		
3690w	2735-2684w	1450w	1030s	600s	430-12s		
3680w	2584-76w	1240-12mp,w		577-40m,mp			
3600-3120b,mp,w	1800w	1002-973mp,s			401-394s		
		958-40s			382s		
					318m		
Chrysotile, 10C (UOPC, Unk)							
3800w	3050w	1800w	1580w	1034m	890m	600m	415s
3750-3240b,mp,w	1750w	1525w	992m	805m	545m	530m	396-70s
	3000w	1625w	1505w	930s			340m
	2980w		1458w				
	2900w		1448w				
	2400w		1420w				
			1200w				
			1170w				

CHAPTER SIX

CONCLUSION

ATR-IR is a viable technique in mineral analysis, and spectra of powdered mineral samples are excellent. They show more sensitivity in the 2000-300 cm^{-1} as compared to the 4000-2000 cm^{-1} range. The contact problem faced by Anderson [1975], a major source of the errors and distortions mentioned in his thesis, was solved by employing various methods such as using scotch tape on the sample, changing incident angle and increasing pressure on the sample. Superior and reproducible spectra were obtained by this improved ATR-IR technique.

Clay minerals with different structures can be conveniently identified without a knowledge of various band assignments. For example, kaolinite can be identified because: (1) It has some characteristic bands of its own which other clay minerals and the rest of the minerals do not, and (2) It gives more absorption bands in the 1100 to 900 cm^{-1} range than other clay minerals. Many more samples of different minerals should be taken in order to be positive about the band assignments, but the spectra run were sufficiently different to enable identification of clay mineral from other clay minerals, from nonclay minerals such as mica, feldspar, talc, high silica minerals, lithium ore, or

from rocks such as limestone and phosphate rock.

Between groups of silicate minerals, there is a change in intensity and position of many absorption bands of the ATR-IR spectra, the latter often by several wavenumbers. This is attributed to two factors analogous to the case with transmission spectra. One factor is the isomorphous substitutions of some cations such as Al(III) by other cations in the crystal lattice. The nature and extent of ionic substitutions in the tetrahedral and octahedral layer-lattice silicates have been shown by Stubican and Roy [1961] to have an effect on transmission spectral bands; this is equally true for ATR-IR spectra of various minerals. A second factor which can cause gradual shifting is the orientation of the hydroxyl groups in the crystal; that is, the orientation of the bond axis. This can be observed in the case of muscovite and biotite.

It is difficult to make exact assignments of the various bands in silicates not only because of the isomorphous substitutions but also because some minerals occur as mixtures of various compounds as shown by the percentages of the oxides in various minerals in Chapter Two and from Certificates of Analysis of the NBS Standard Reference Materials in Appendices C to O.

In some cases tentative assignment of bands has been made based on the theoretical and experimental evidence collected as a result of this study. Spectra of many more minerals of variable composition should be taken in order to

enable accurate understanding and enhanced interpretation of the absorption bands of minerals using ATR-IR techniques.

Assignments of some of the bands found in the two limestone and one phosphate rock spectra should be accurate as they correlate well with those obtained using transmission techniques and they are relatively monomineralic; their spectra are easily distinguishable from those of the silicate minerals.

ATR-IR in spite of its excellence as a qualitative tool in distinguishing one mineral or mineral group from another, unfortunately failed to provide spectra with useful and meaningful correlations between the fiber size and spectral bands of various chrysotile grades.

ATR-IR can be successfully used both as a qualitative and quantitative tool especially for the purpose of classification of minerals. More useful qualitative work can be done in geoanalytical chemistry by putting emphasis on band assignments by preparing artificial minerals of variable but known composition from known compounds and studying the effects of changing composition of various components on spectral bands. The information obtained from ATR-IR spectra can be used in conjunction with other traditional methods of analysis such as X-ray diffraction, TG, EGA, electron microscopy, neutron activation analysis, etc. for a more reliable analytical study. It is recommended that response time = 4 and scan time = 24 minutes for Perkin-Elmer IR Model 283 be used in future work as it provides more resolved spectra

throughout the length of spectrum.

BIBLIOGRAPHY

1. American Society for Testing Materials. Book of Standards. Philadelphia: ASTM, 1971.
2. Anderson, Donald F. Analysis of Rocks and Minerals by Attenuated Total Reflection With Atlas. M. S. Thesis. UOP Science Library, July 1975.
3. Brugel, Werner. An Introduction to Infrared Spectroscopy. New York: Wiley, 1962.
4. Correns, C. W., D. M. Shaw, K. K. Turekian, and J. Zemann. Handbook of Geochemistry. Vol 1. New York: Springer-Verlag, 1978.
5. _____. Handbook of Geochemistry. Vol II-1. New York: Springer-Verlag, 1978.
6. _____. Handbook of Geochemistry. Vol II-2. New York: Springer-Verlag, 1978.
7. _____. Handbook of Geochemistry. Vol II-3. New York: Springer-Verlag, 1978.
8. CRC Press. CRC Handbook of Chemistry and Physics. 1973-74.
9. Fripiat, J. J. and F. Toussaint. Predehydroxylation State of kaolinite. Nature 166: 627-8 (1960)
10. Gadsden, John. Infrared spectra of Minerals and Related Inorganic Compounds. London: Butterworths, 1975.
11. Gordy, W. J. A Relation Between Bond Force Constants, Bond Orders, Bond Lengths, and the Electronegativities of the Bonded Atoms. J Chem Phys 14: 305-20 (1946)
12. Harrick, N. J. and B. H. Riederman. Infrared Spectra of Powders by Means of Internal Reflection Spectroscopy. Spectrochim Acta 21: 2135 (1965)
13. Harrick, N. J. Internal Reflection Spectroscopy. New York: Interscience, 1967.
14. Hirschfeld, Tomas. Solution for the Sample Contact Problem in ATR. Appl Spectry 21: 235-6 (1967)
15. Houghton, J. T. and S. D. Smith. Infrared Physics. Oxford: Clarendon Press, 1966.

16. Hunt, John M., Mary P. Wisherd, and Lawrence C. Bonham. Infrared Absorption Spectra of Minerals and Other Inorganic Compounds. Anal Chem 22: 1478-97 (1950)
17. Hussain, Fazal-i- and M. Ghazi-u-Din. Physical Chemistry. Lahore: Ilmi Kitab Khana, 1971.
18. Keller, W. D. and E. E. Pickett. The Absorption of Infrared Radiation by Clay Minerals. Am J Sci 248: 264-73 (1950)
19. Kirk, R. and D. Othmer. Encyclopedia of Chemical Technology. Vol 6. New York: Wiley-Interscience, 1979.
20. _____. Encyclopedia of Chemical Technology. Vol 5. New York: Wiley-Interscience, 1979.
21. _____. Encyclopedia of Chemical Technology. Vol 4. New York: Interscience, 1949.
22. _____. Encyclopedia of Chemical Technology. Vol 3. New York: Interscience, 1948.
23. Larson, Sylvia J., G. W. F. Pardoe, and H. A. Gebbie. The Use of Far Infrared Interferometric Spectroscopy for Mineral Identification. Am Mineral 57: 998-1002 (1972)
24. Lyon, R. J. P. and W. H. Toddenham. Infrared Determination of the Kaolin Group Minerals. Nature 165: 835-6 (1960)
25. _____. Determination of Tetrahedral Aluminum in Mica by Infrared Absorption Analysis. Nature 185: 374-5 (1960)
26. Manghnani, Murli H. and John Hower. Glauconites: Cation Exchange Capacities and Infrared Spectra; Part II. Infrared Absorption Characteristics of Glauconites. Am Mineral 49: 1930-42 (1964)
27. Mellor, J. W. A Comprehensive Treatise on Inorganic and Theoretical Chemistry. Vol VI. London: Longman, Green and Co., 1925.
28. Miller, Foil A. and Charles H. Wilkins. Infrared Spectra and Characteristic Frequencies of Inorganic Ions. J Anal Chem 24, No 8: 1253-94 (1952)
29. Nakamoto, Kazuo. Infrared and Ramam Spectra of Inorganic and Coordination Compounds. New York: Wiley-Interscience, 1978.
30. Nicol, Alstair W. Physicochemical Methods of Mineral Analysis. New York: Wiley-Interscience, 1978.
31. Nyquist, Richard A. and Ronald O. Kagel. Infrared Spectra of Inorganic Compounds 3800-45 cm⁻¹. New York: Plenum

Press, 1975.

32. Perkin-Elmer Corp. Model 283 Double Beam Recording Infrared Spectrophotometer Catalog. Norwalk, Connecticut. 1979.
33. Rogers, Austin F. Introduction to the Study of Minerals. New York-London: McGraw-Hill Book Co., 1937.
34. Simon, Ivan. Infrared Radiation. Princeton, New Jersey: D. Van Nostrand Company, 1966.
35. Thompson, Sheldon and Milton E. Wadsnorth. Determination of the Composition of Plagioclase Feldspars by Means of Infrared Spectroscopy. Am Mineral 42: 334-41 (1957)
36. Wainerdi, R. E. and E. A. Uken. Modern Methods of Geochemical Analysis. New York-London: Plenum Press, 1971.
37. Wilks Scientific Corp. Internal Reflection Spectroscopy. Vol 1. Instructions for Operation of Wilks Scientific Internal Reflection Infrared Spectrophotometers and Accessories. South Norwalk, Connecticut. 1965.
38. Winchell, N. H. and A. N. Winchell. Elements of Optical Mineralogy-An Introduction to Microscopic Petrography. New York: Wiley, 1949.

APPENDICES

APPENDIX A

LIST OF SPECTRA OF MINERALS BY ATR-IR

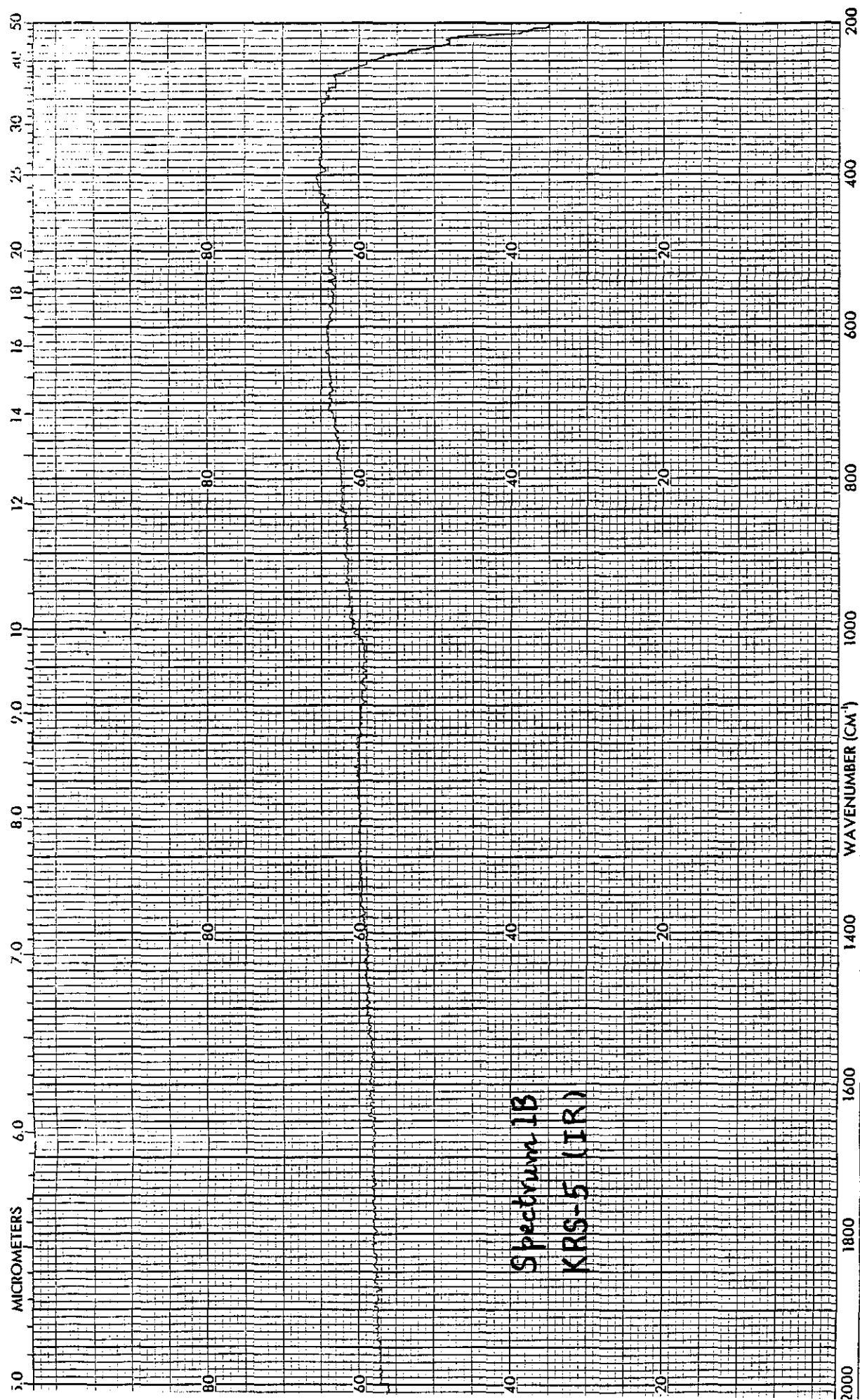
Name of Mineral	Spectrum #	Page #
KRS-5 [IR]	1A, B	93, 94
KRS-5 [ATR-IR]	2A, B	95, 96
Talc, comparative slit program spectrum	3A, B	97, 98
Kaolinite, Langley	4A, B	99, 100
Kaolinite, Bath	5A, B	101, 102
Kaolinite, DCG	6A, B	103, 104
Kaolinite, UOP	7A, B	105, 106
Bentonite, Rock River ..	8A, B	107, 108
Bentonite, Osage	9A, B	109, 110
Halloysite, Eureka	10A, B	111, 112
Halloysite, Bedford	11A, B	113, 114
Bauxite (Dominican)	12A, B	115, 116
Bauxite (Jamaican)	13A, B	117, 118
Bauxite (Arkansas)	14A, B	119, 120
Bauxite (Surinam)	15A, B	121, 122
Flint Clay	16A, B	123, 124
Plastic Clay	17A, B	125, 126
Muscovite	18A, B	127, 128
Biotite	19A, B	129, 130
Sodium Feldspar	20A, B	131, 132
Potassium Feldspar, SRM # 70a	21A, B	133, 134
Potassium Feldspar, SRM # 607	22A, B	135, 136

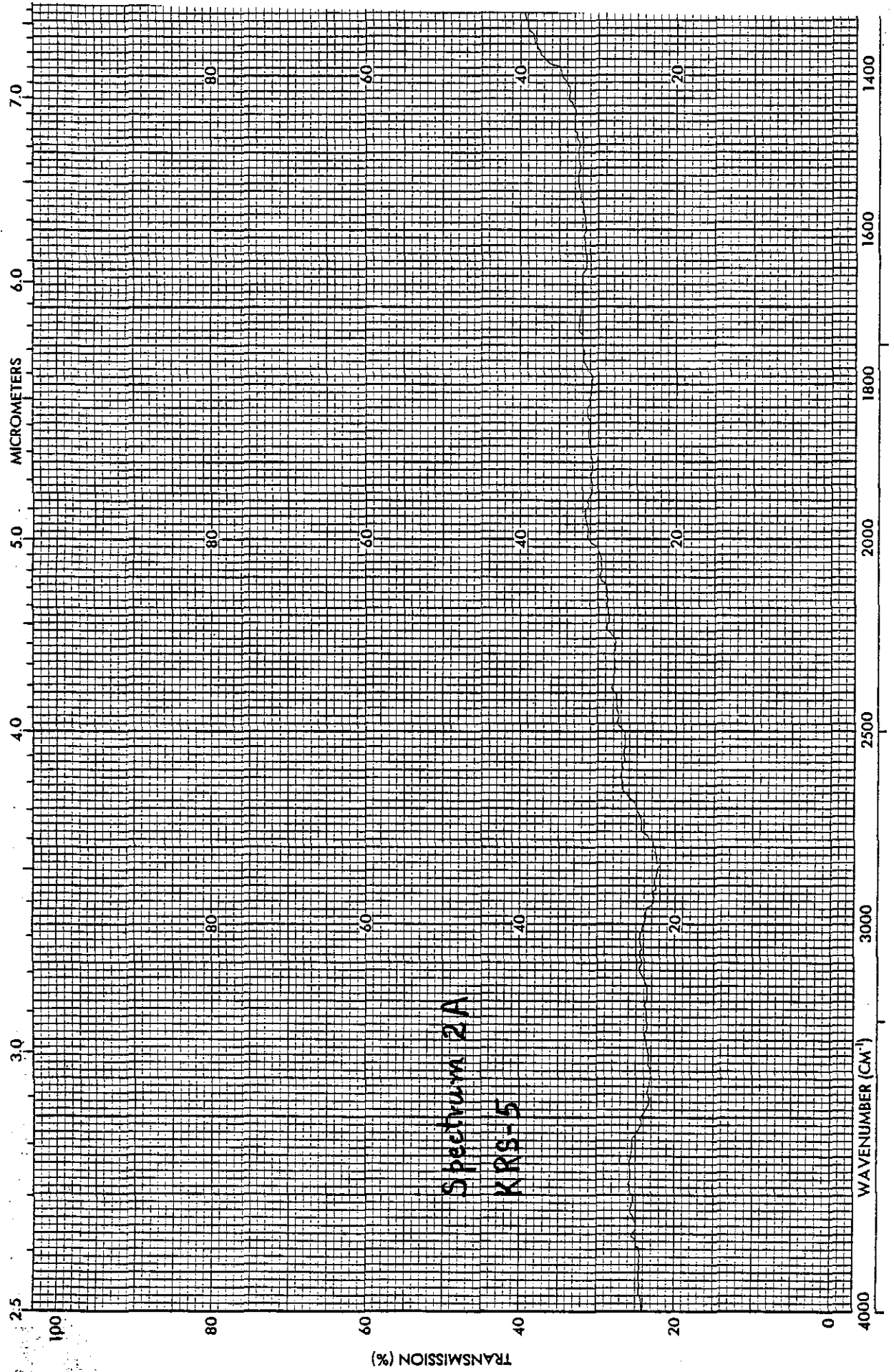
Name of mineral	Spectrum #	Page #
Talc (Low-Vis)	23A, B	137, 138
Talc (DCG)	24A, B	139, 140
Talc (UOPC)	25A, B	141, 142
Glass Sand (High Iron)	26A, B	143, 144
Glass Sand (Low Iron)	27A, B	145, 146
Pumice	28A, B	147, 148
Petalite	29A, B	149, 150
Spodumene	30A, B	151, 152
Lepidolite, SRM # 183 .	31A, B	153, 154
Lepidolite (DCG)	32A, B	155, 156
dolomitic Limestone ..	33A, B	157, 158
Argillaceous Limestone	34A, B	159, 160
Phosphate Rock	35A, B	161, 162
Serpentine	36A, B	163, 164
Asbestos (SWC) i.....i.e.	37A, B	165, 166
Asbestos, Remping Fiber	38A, B	167, 168
Chrysotile, 4K	39A, B	169, 170
Chrysotile, 4T	40A, B	171, 172
Chrysotile, 4T-2	41A, B	173, 174
Chrysotile, 5RNS	42A, B	175, 176
Chrysotile, 6DN	43A, B	177, 178
Chrysotile, 7EK-3, Sample 1	44A, B	179, 180
Chrysotile, 7EK-3, Sample 2	45A, B	181, 182
Chrysotile, 7EX-3 (SWC)	46A, B	183, 184

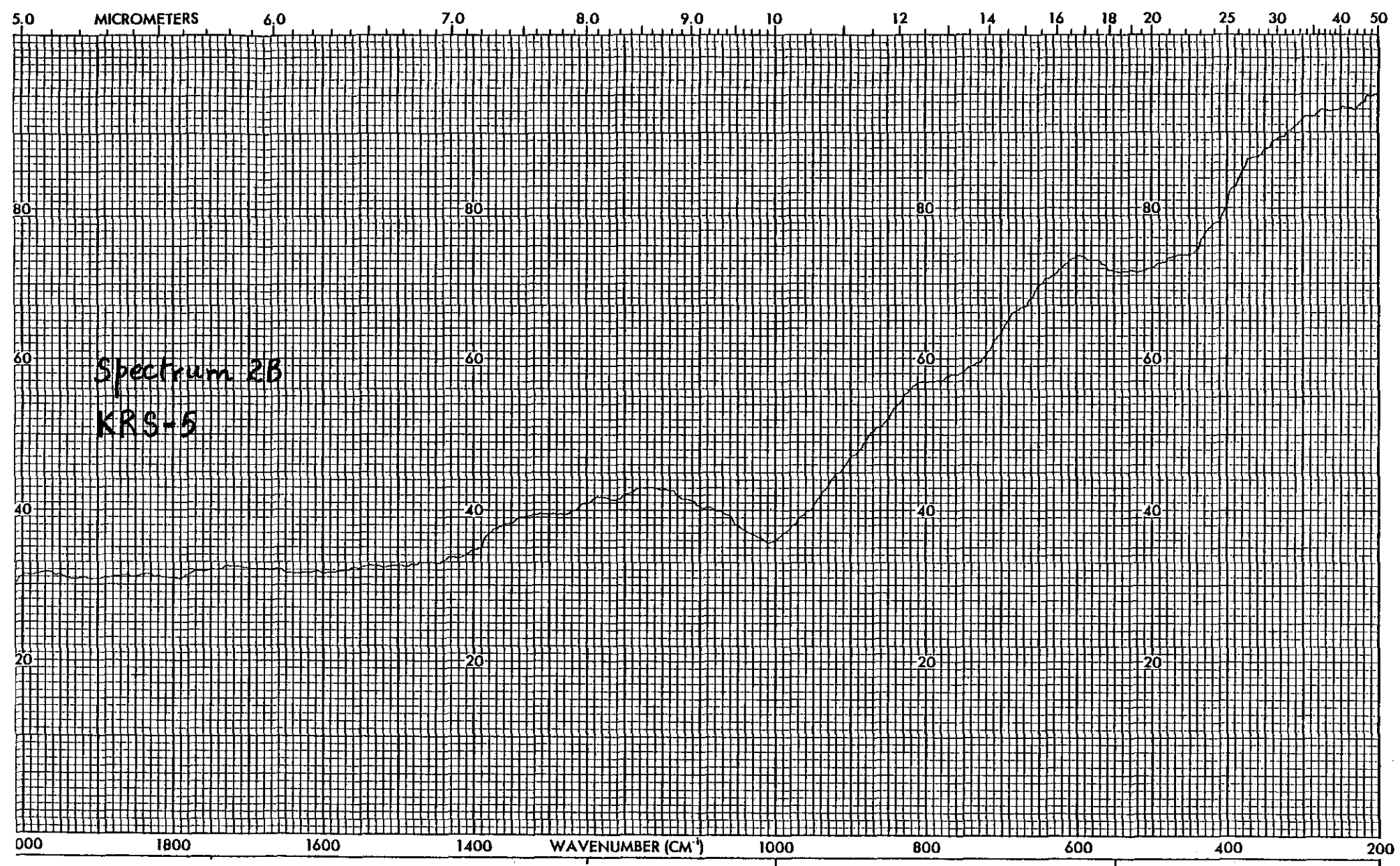
<u>Name of Mineral</u>	<u>Spectrum #</u>	<u>Page #</u>
Chrysotile, 7EX-3 (UOPC)	47A, B	185, 186
Chrysotile, 7EX-3A	48A, B	187, 188
Chrysotile, 7MS-1	49A, B	189, 190
Chrysotile, KB-753	50A, B	191, 192
Chrysotile, JM-7M02 ...	51A, B	193, 194
Chrysotile, JM-7M05 Sample 1	52A, B	195, 196
Chrysotile, JM-7M05 Sample 2	53A, B	197, 198
Chrysotile, 10A	54A, B	199, 200
Chrysotile, 10B	55A, B	201, 202
Chrysotile, 10C	56A, B	203, 204

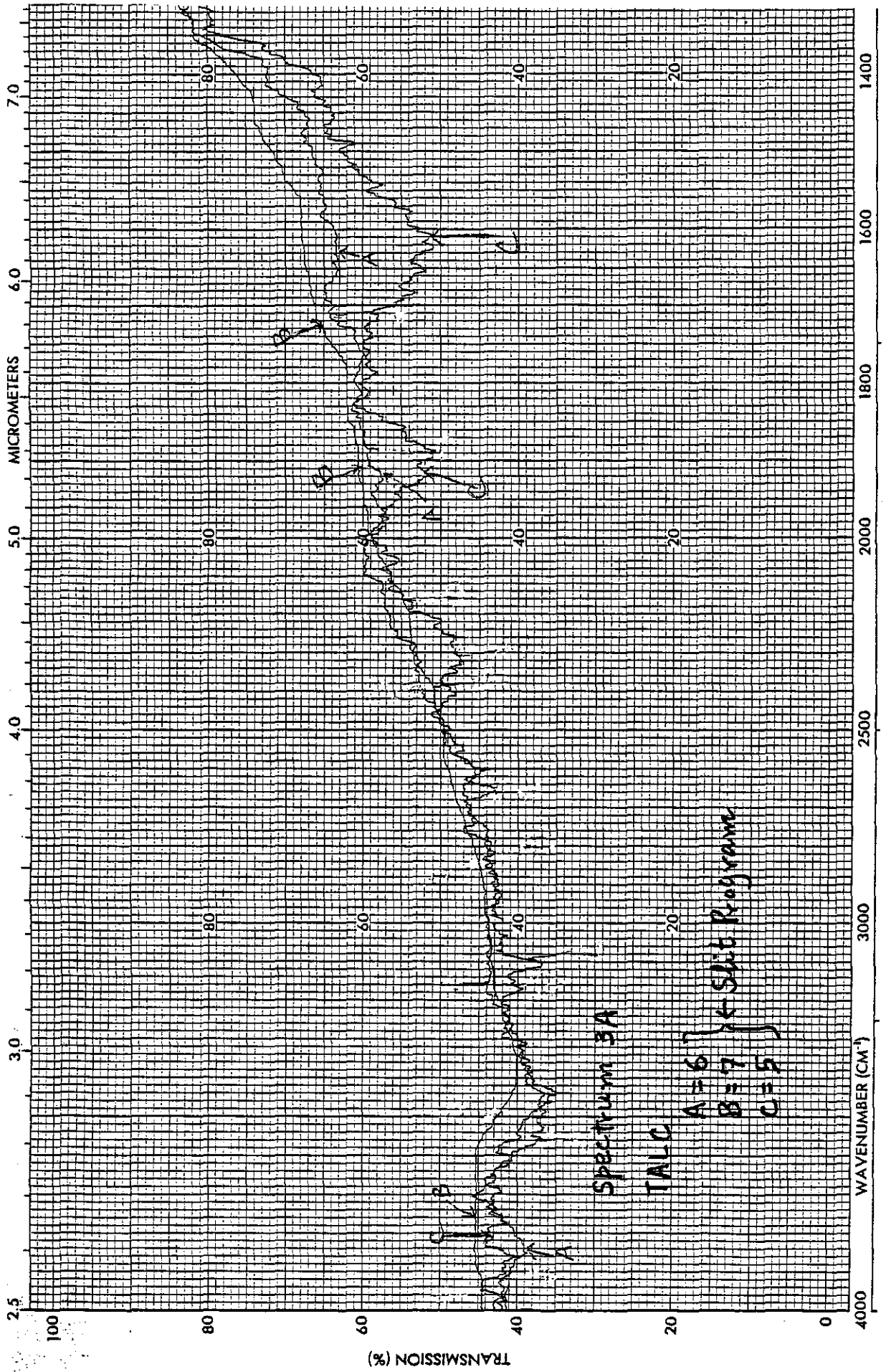


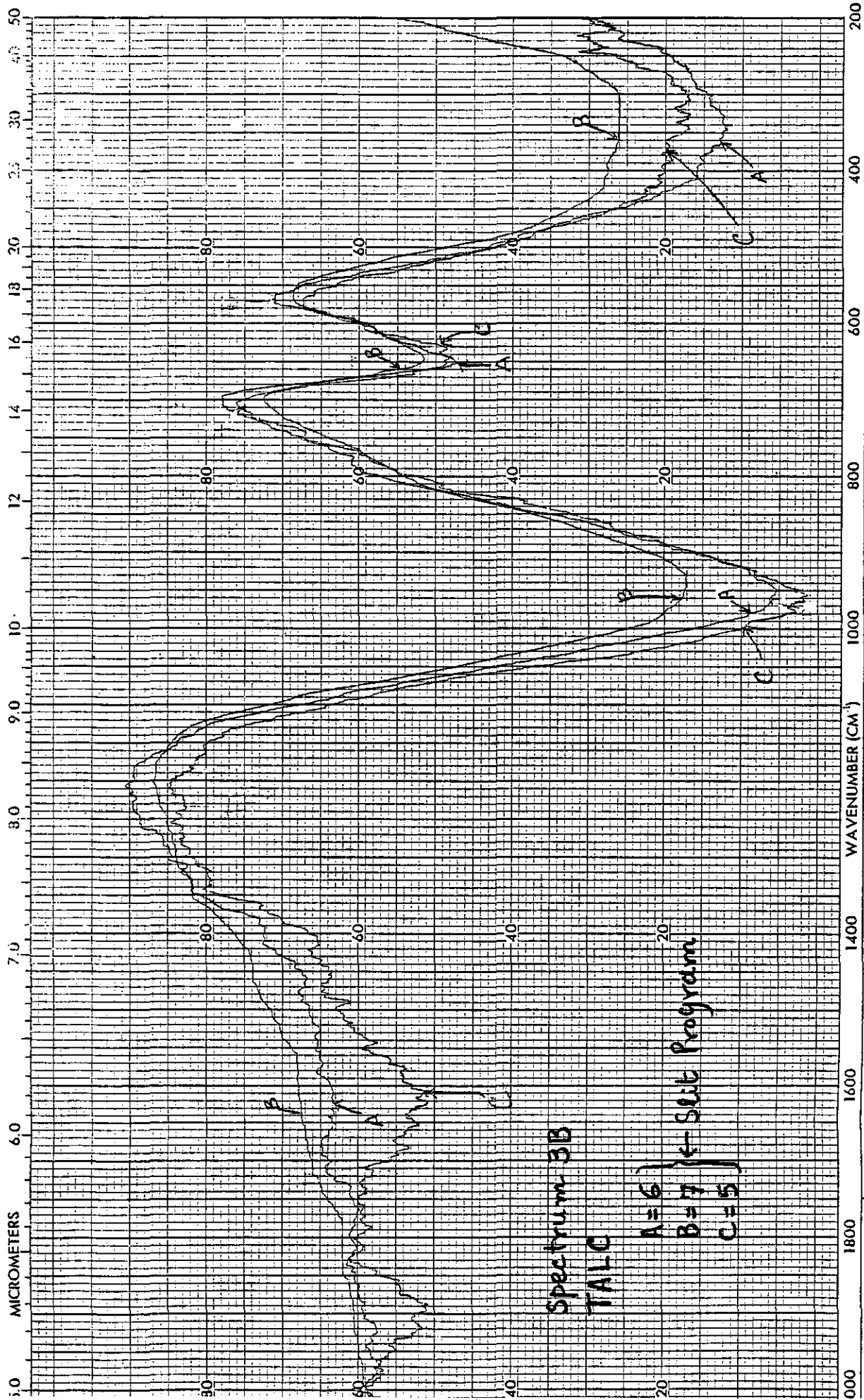
Spectrum 1A
KRB-5 (IR)







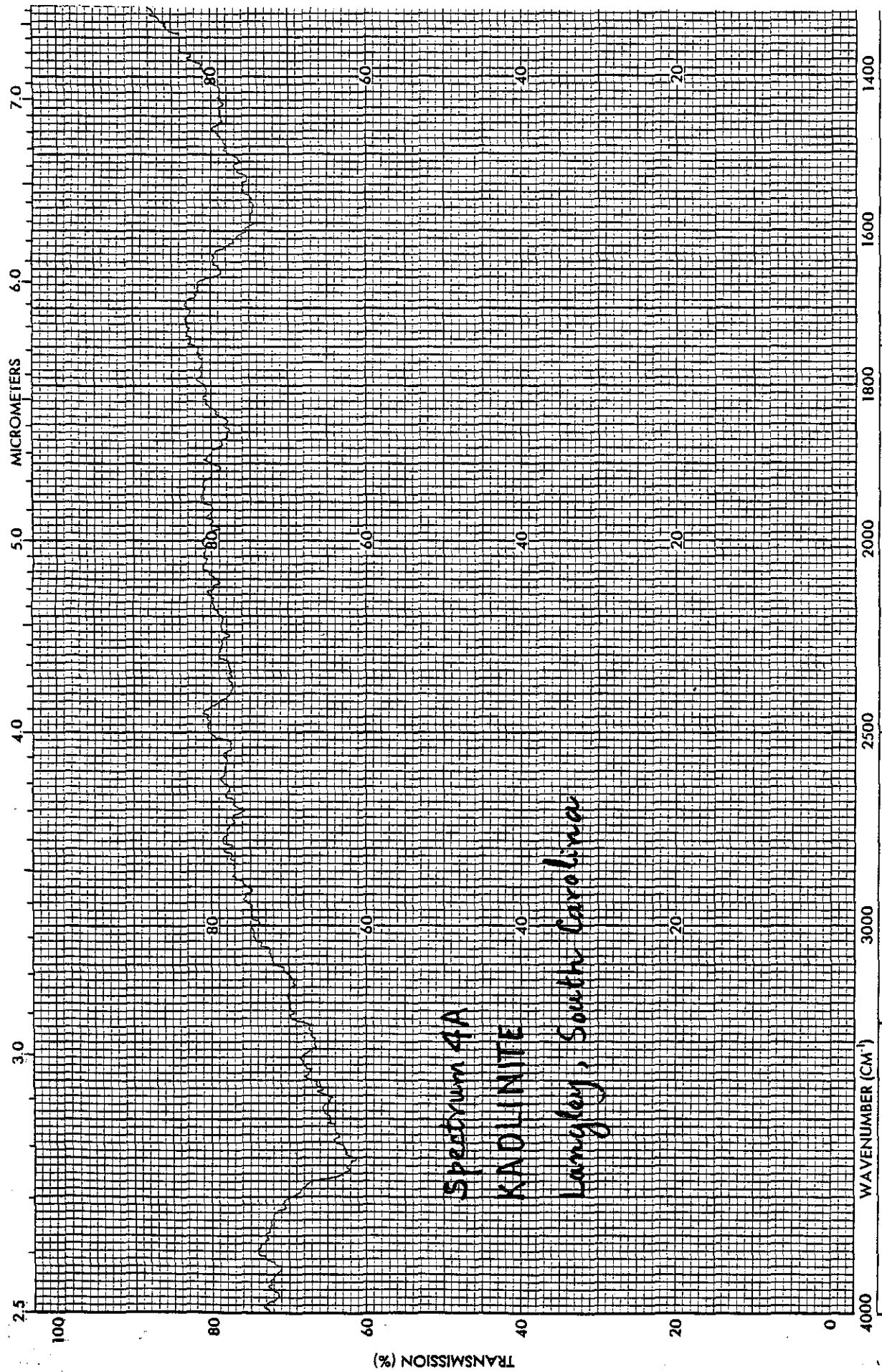




Spectrum 3B

TALC

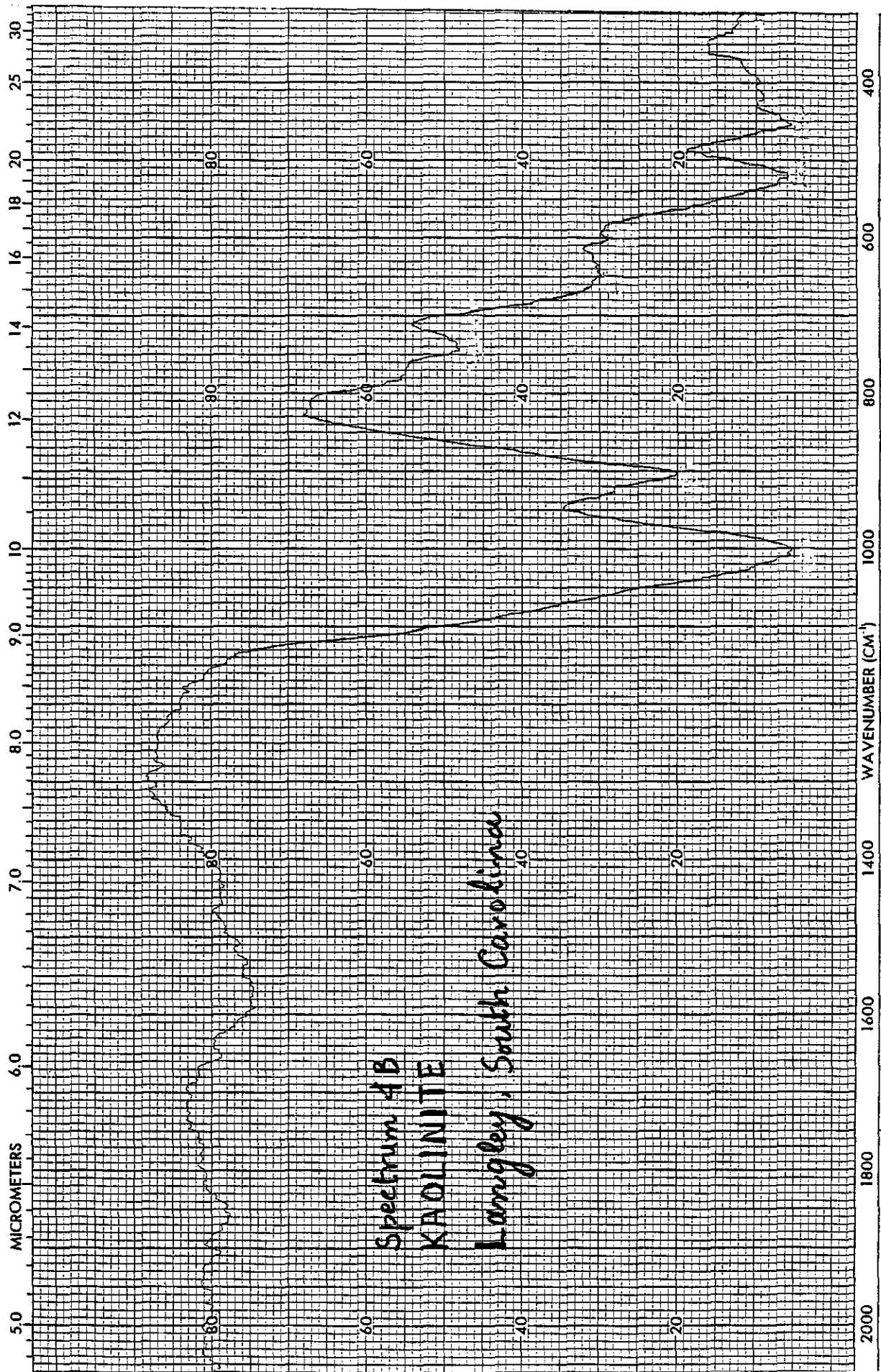
A=6
B=7
C=5
← Slit Program



Spectrum 4A

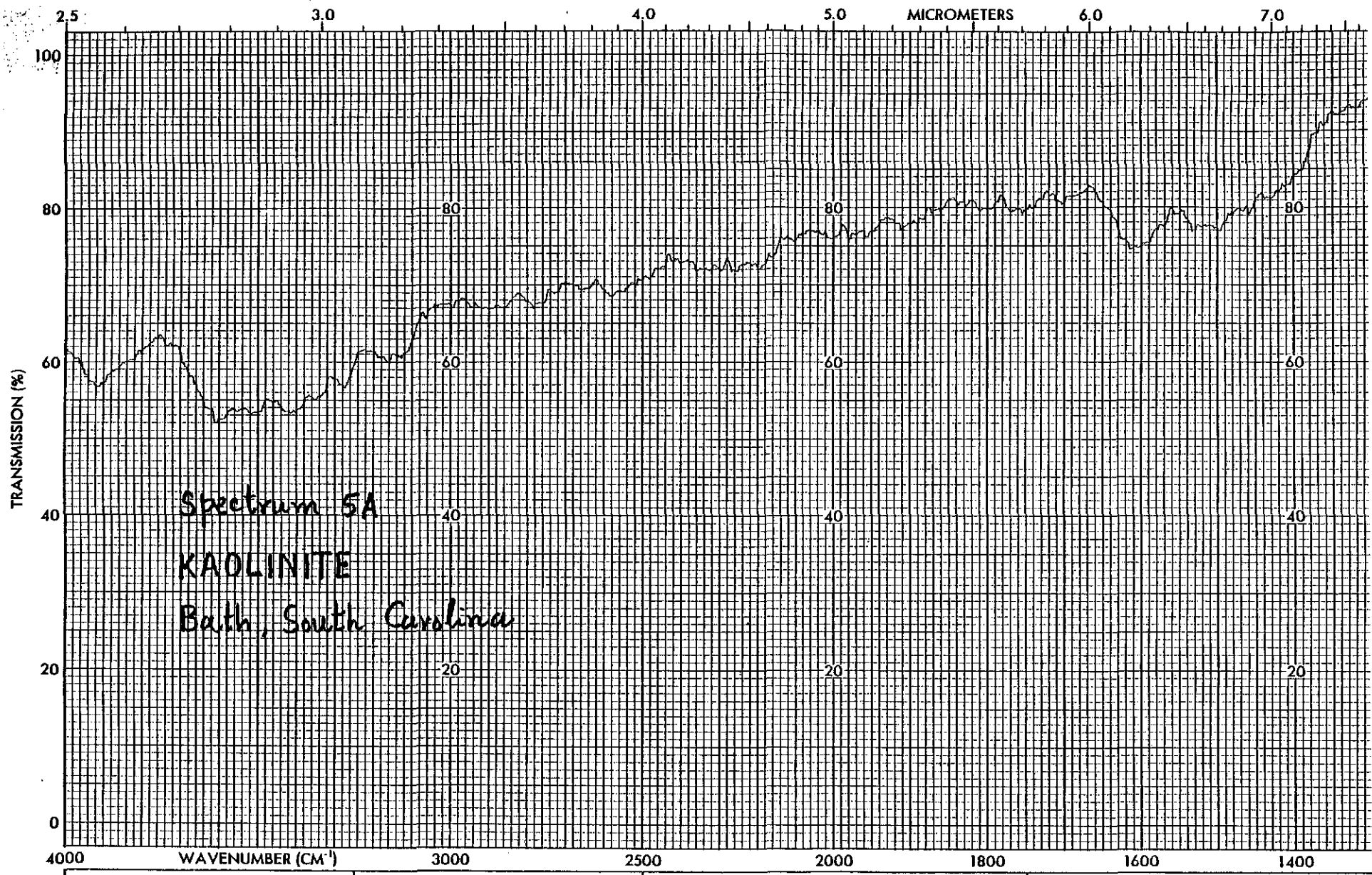
KADLITE

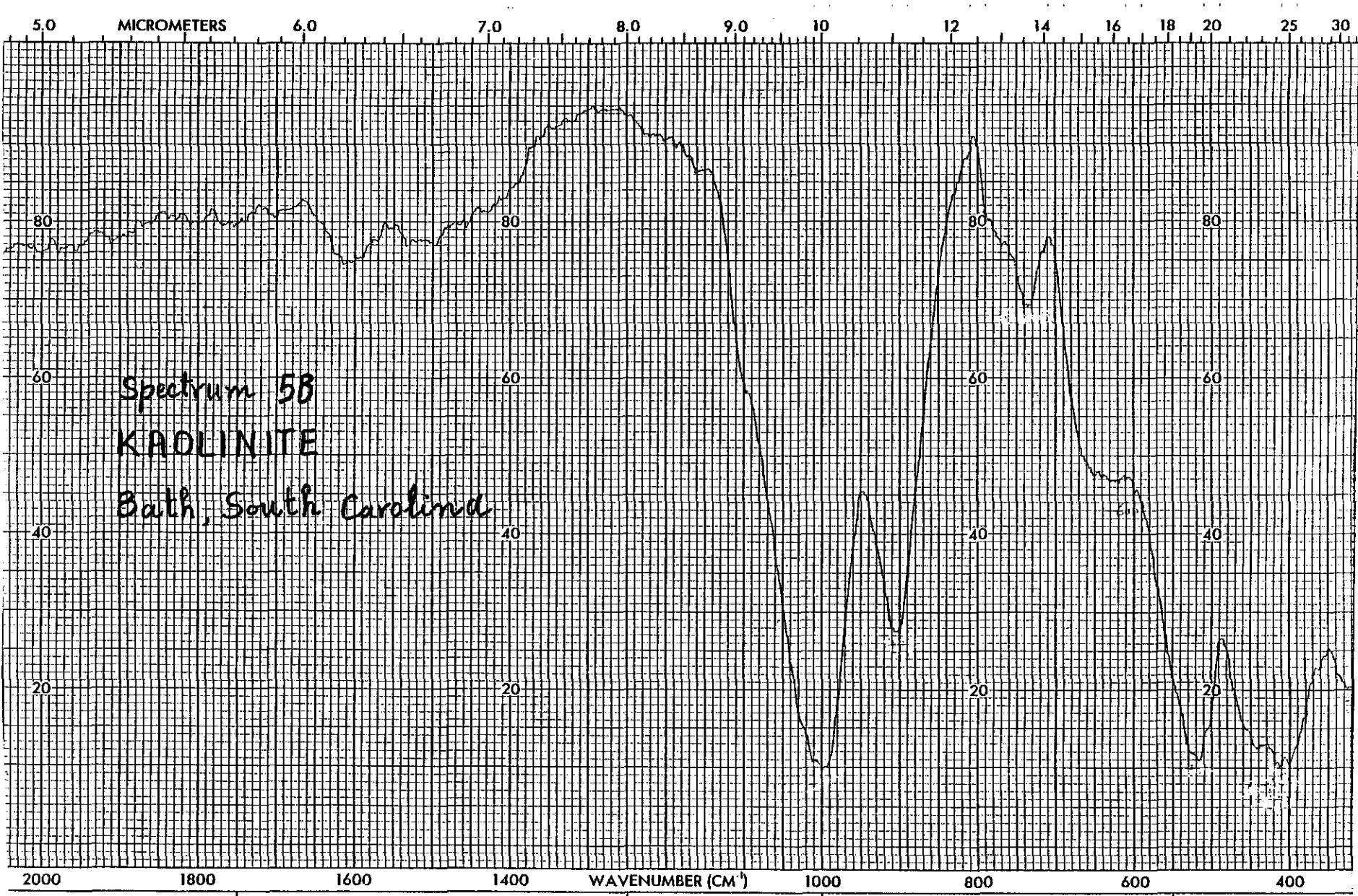
Langley, South Carolina



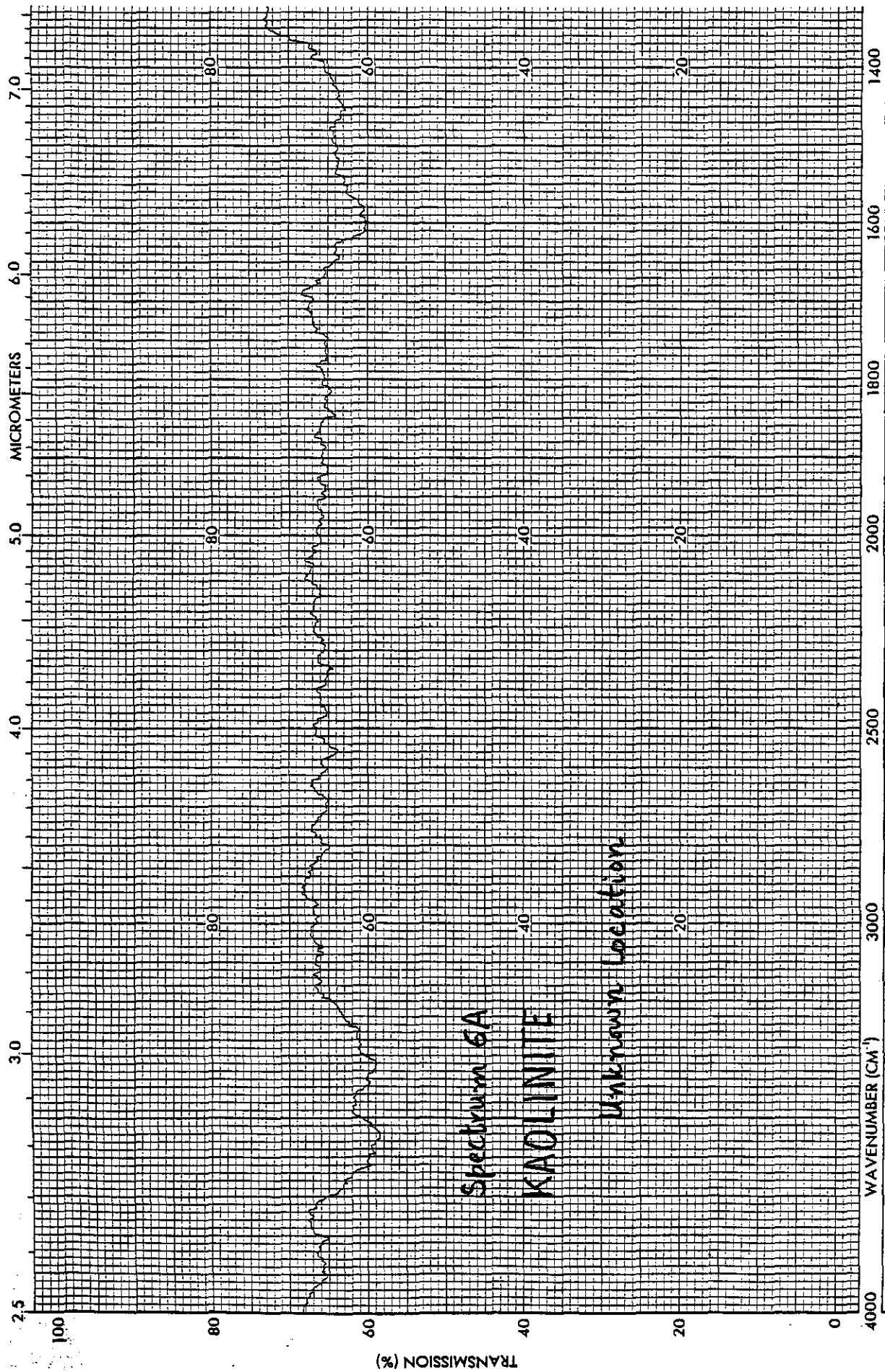
Spectrum 4B
KAOLINITE

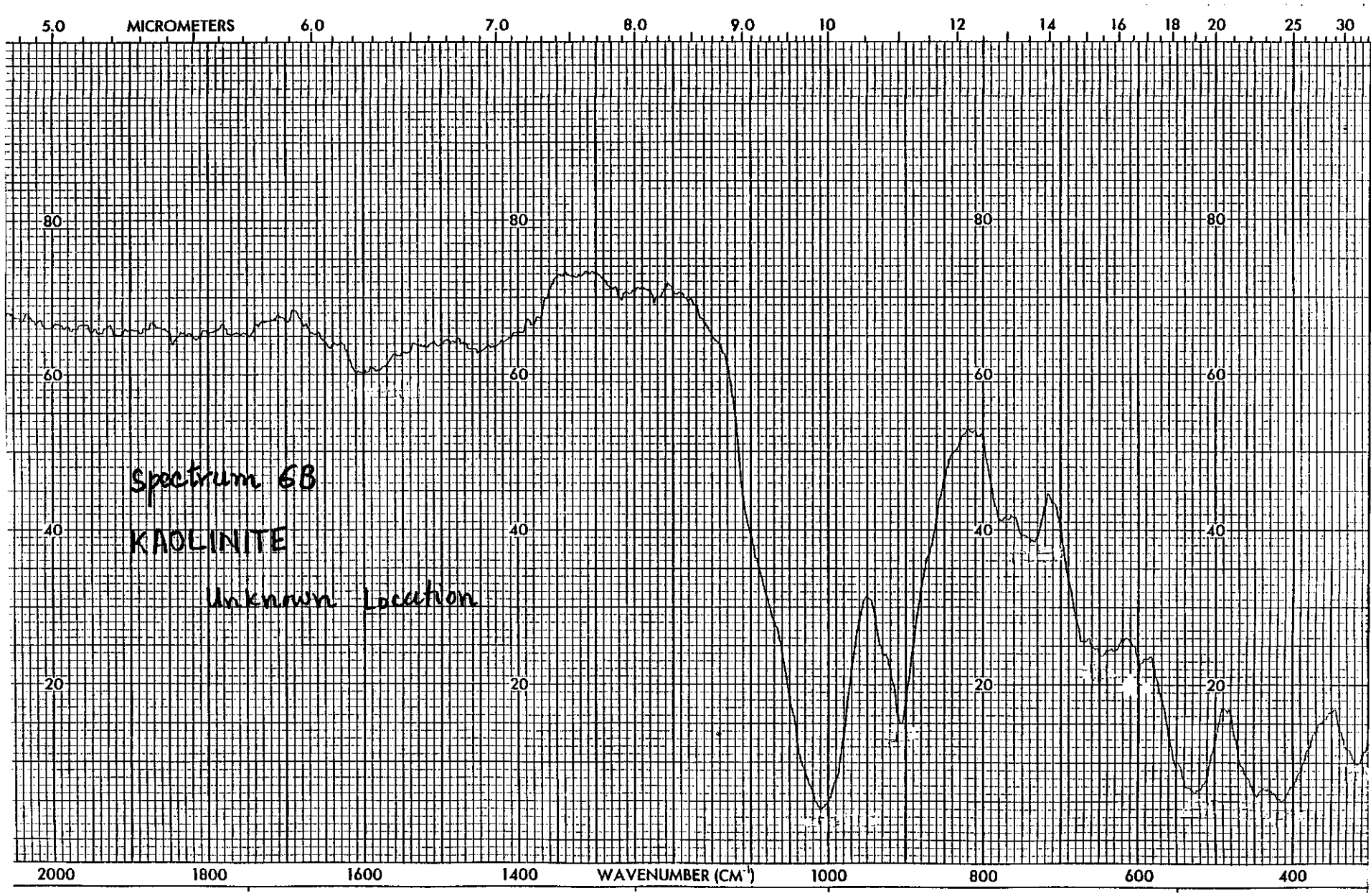
Langley, South Carolina

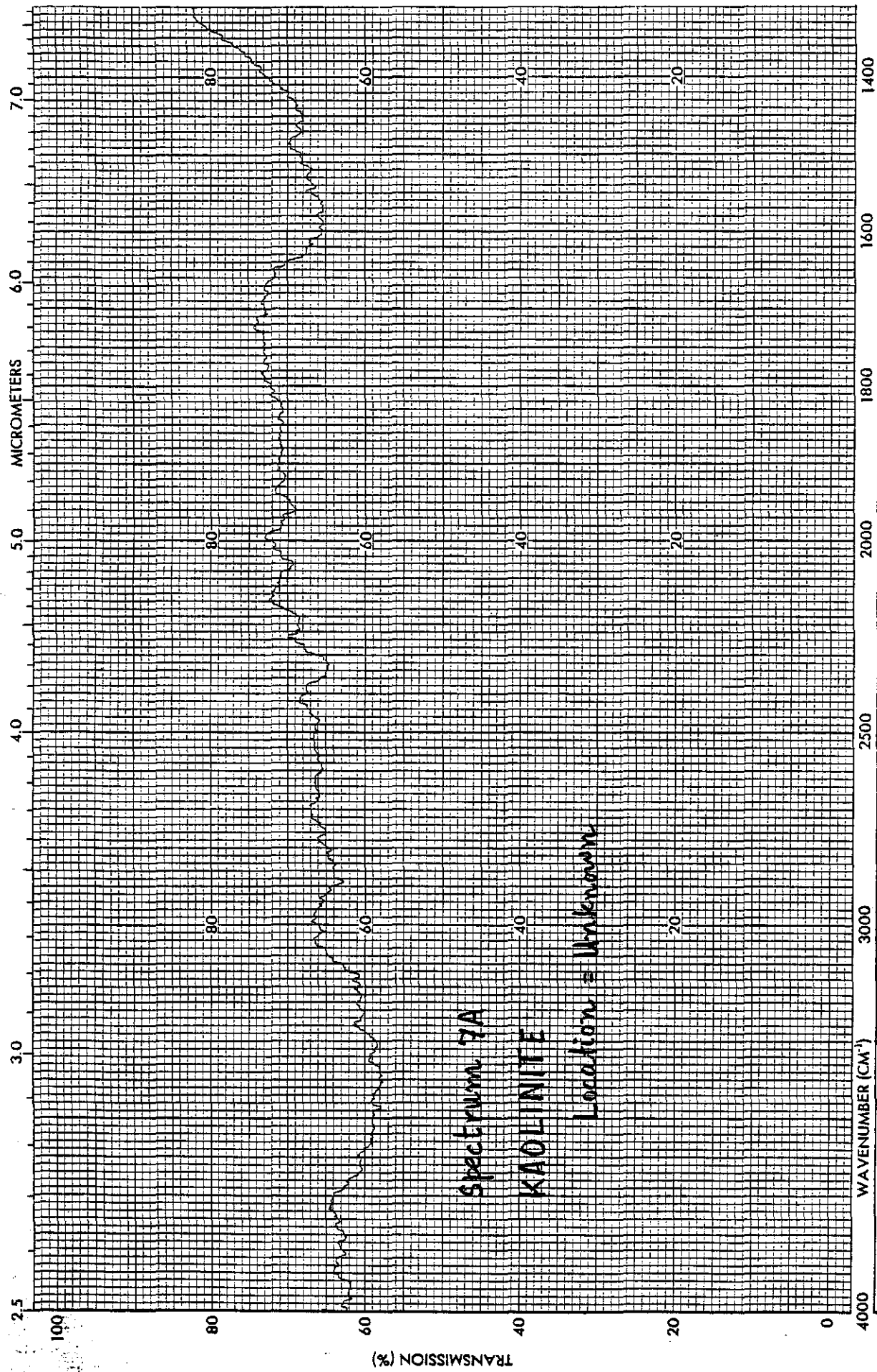


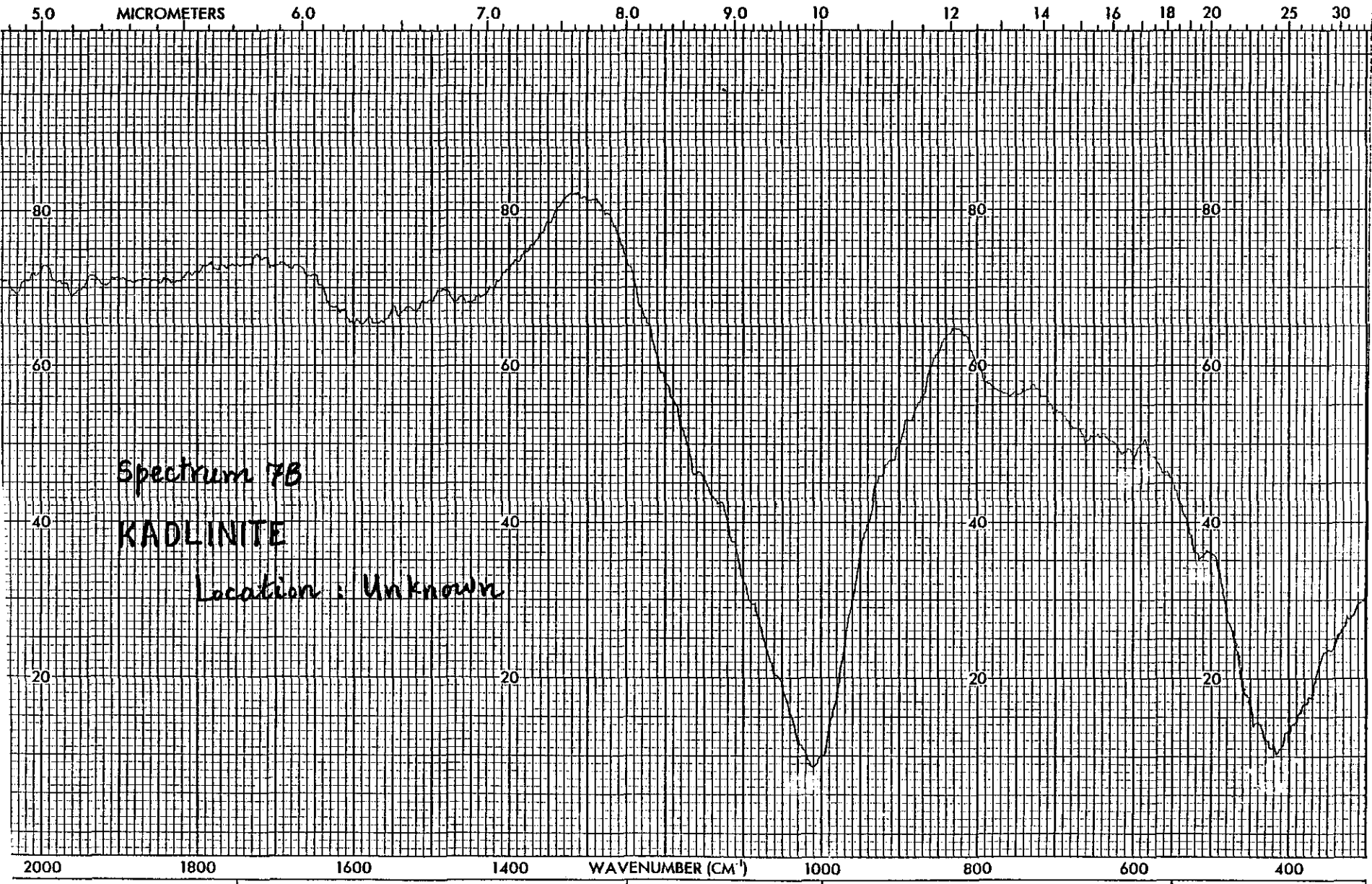


Spectrum 58
KAOLINITE
Bath, South Carolina





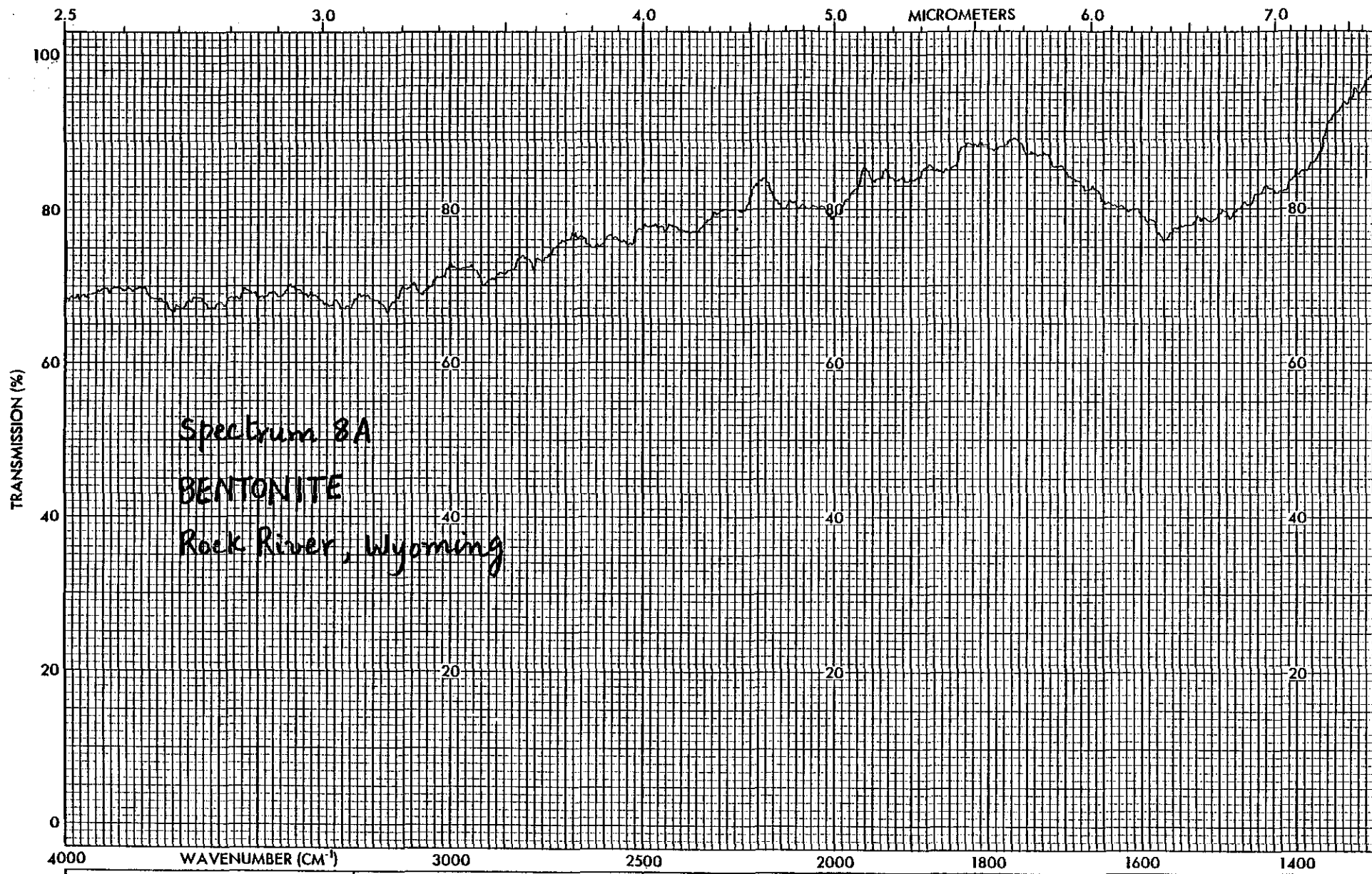


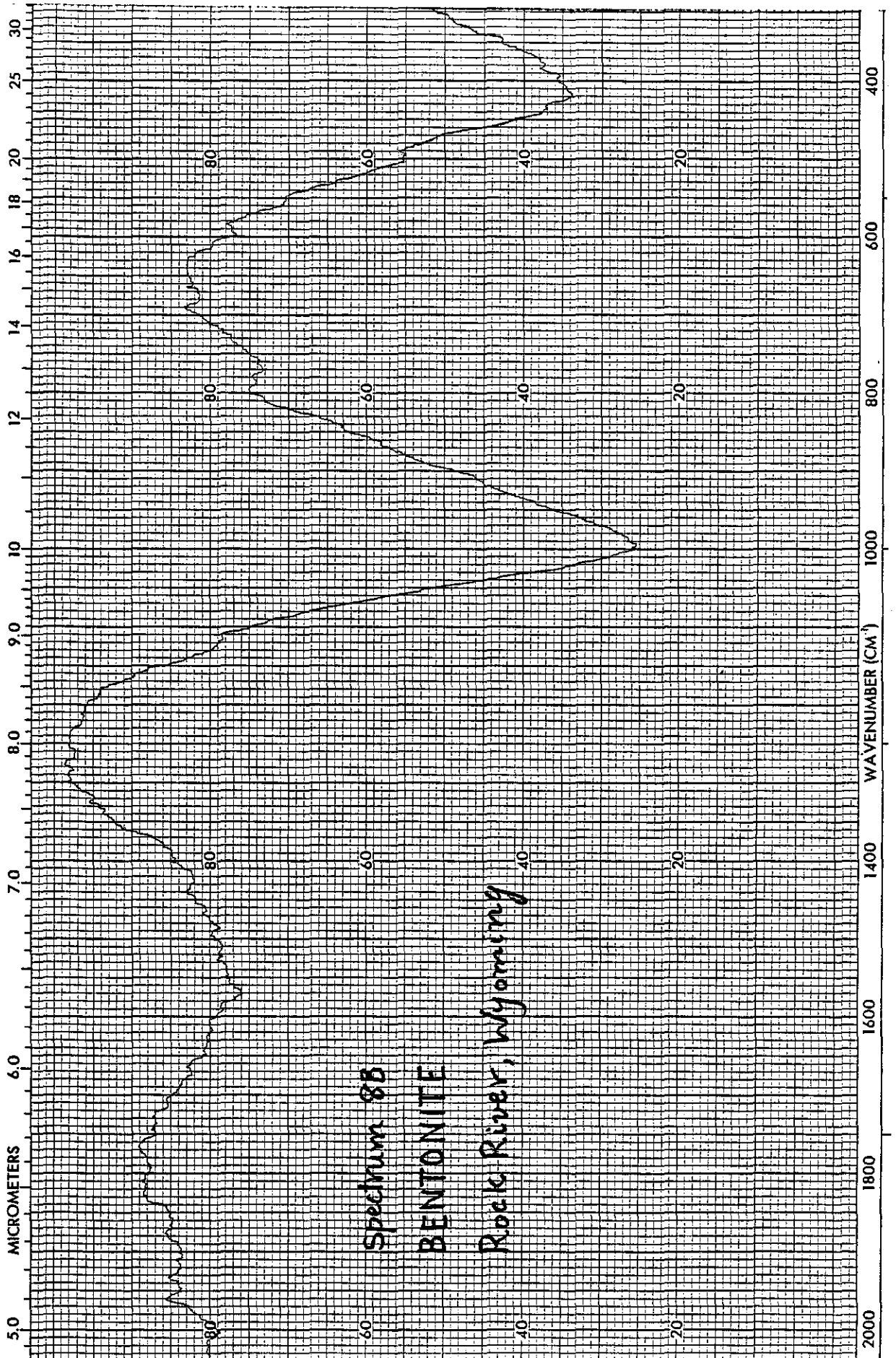


Spectrum 7B

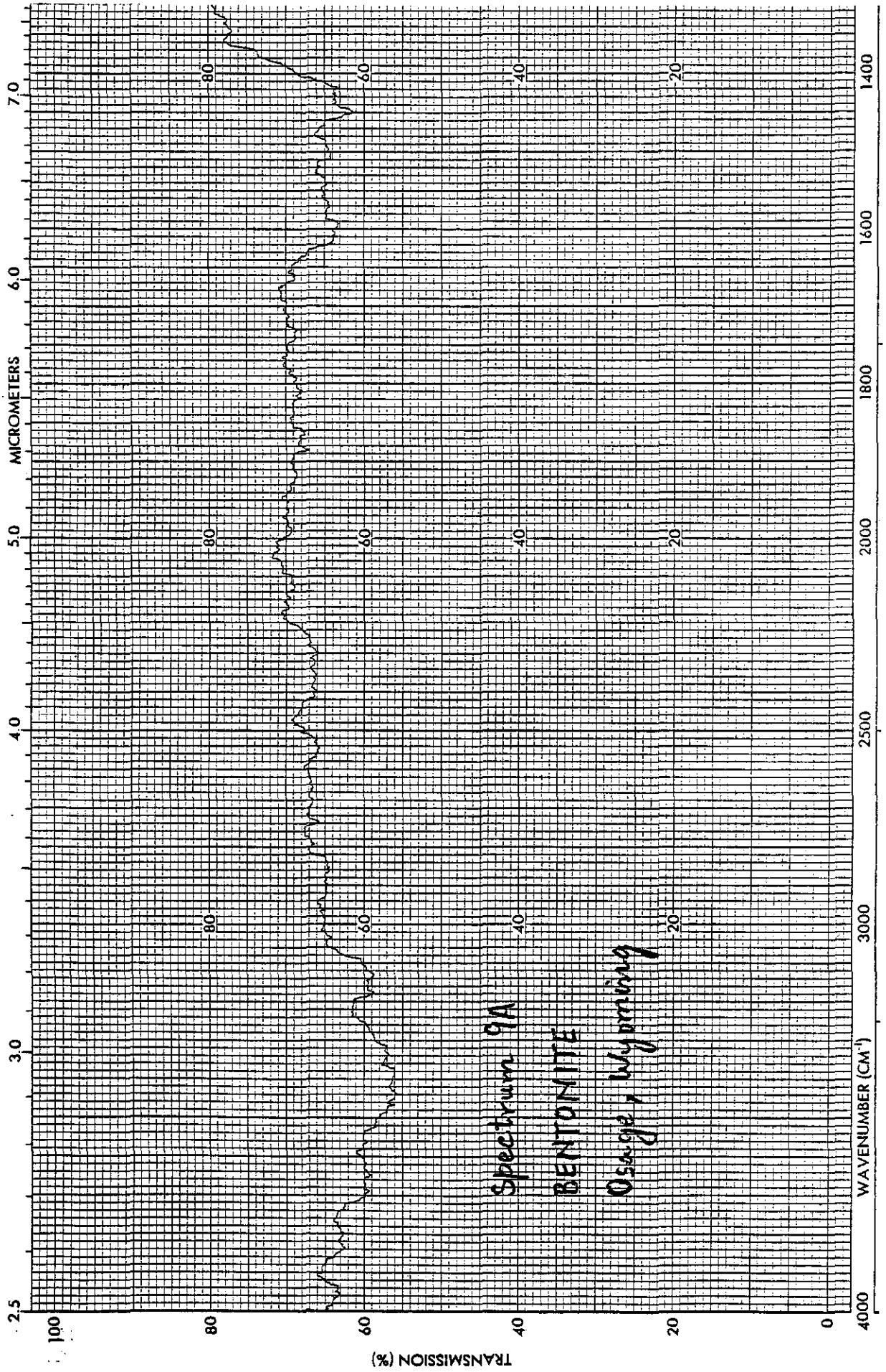
KADLINITE

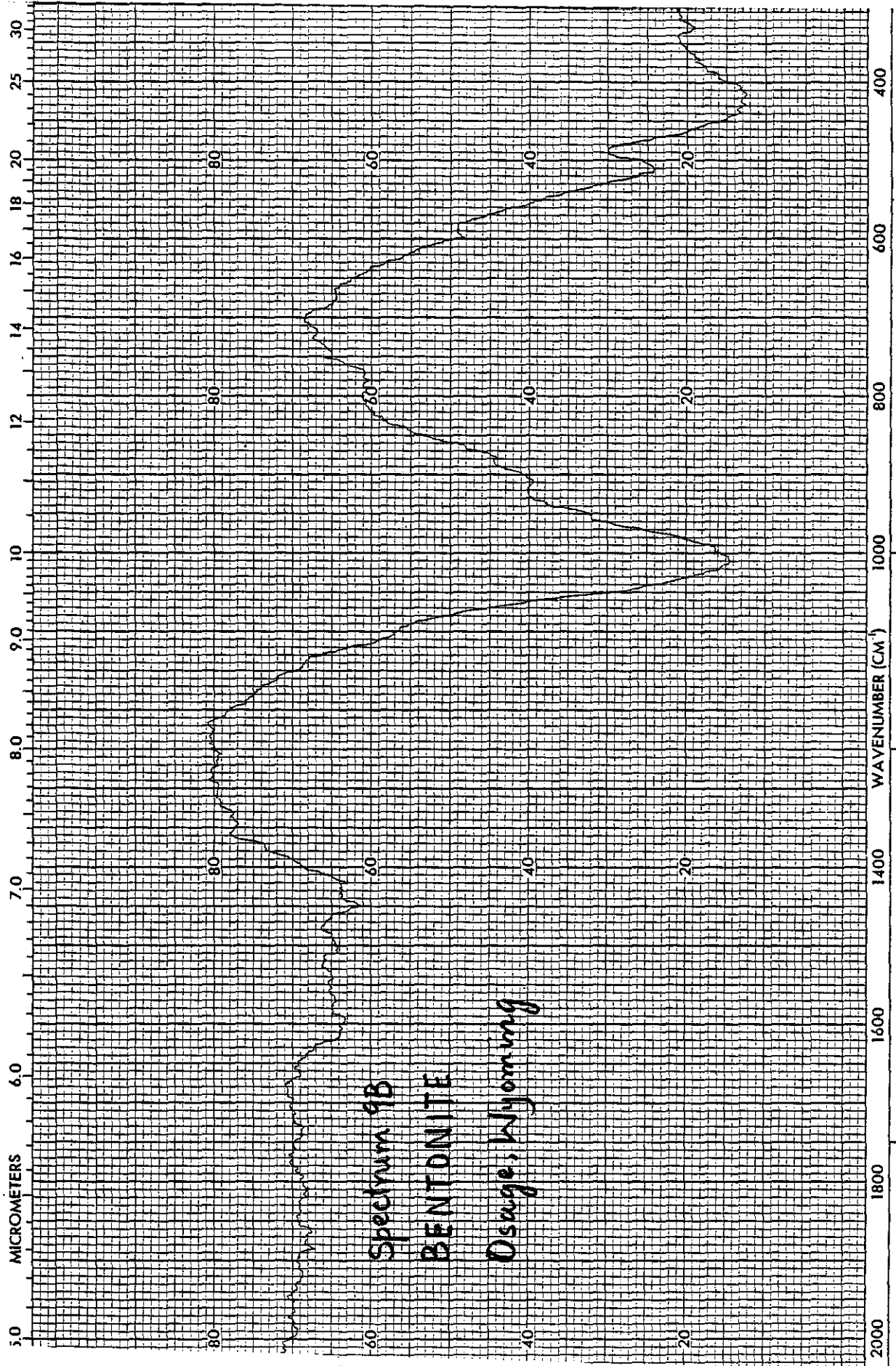
Location: Unknown

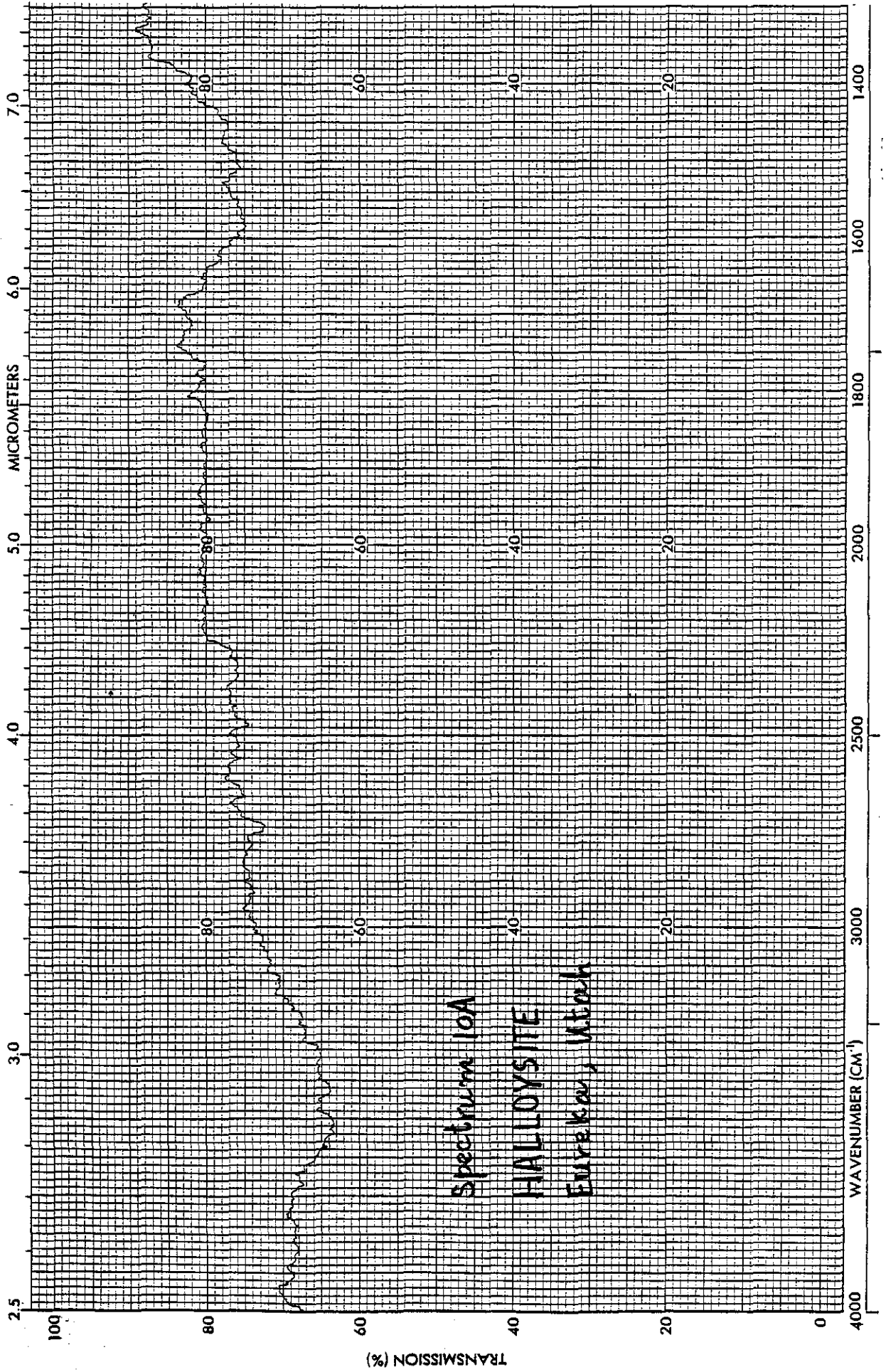




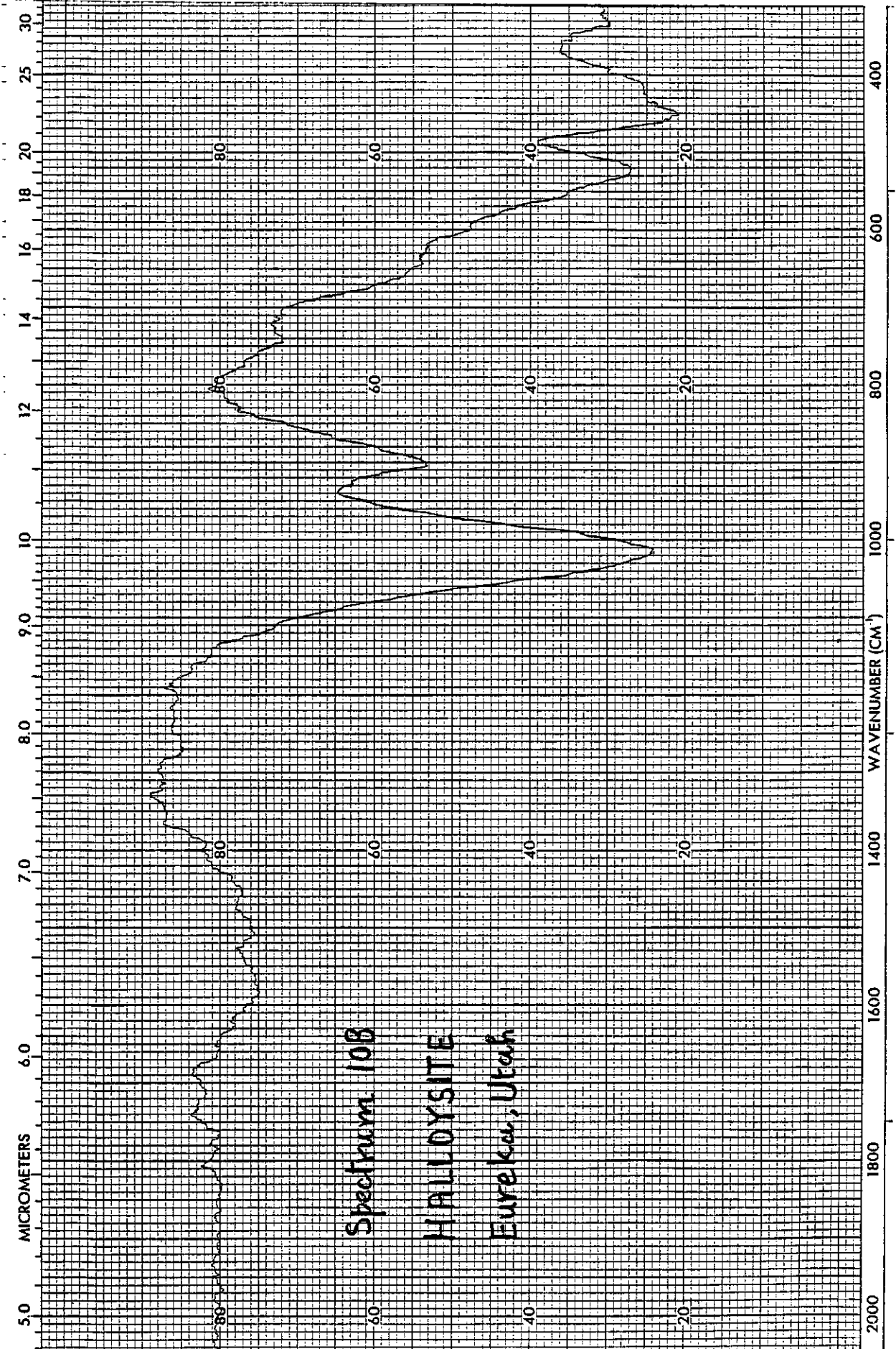
Spectrum 8B
BENTONITE
Rock River, Wyoming

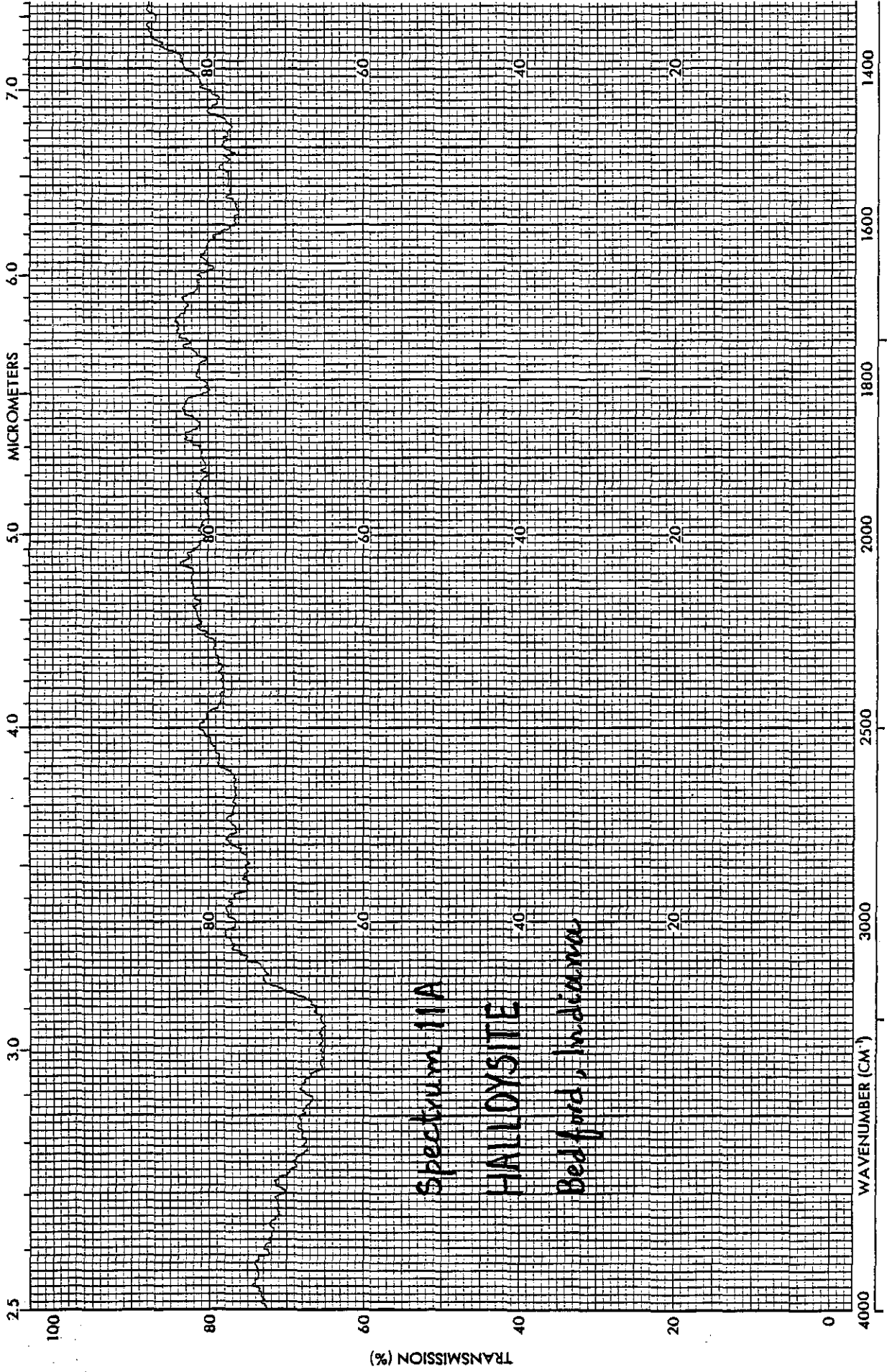


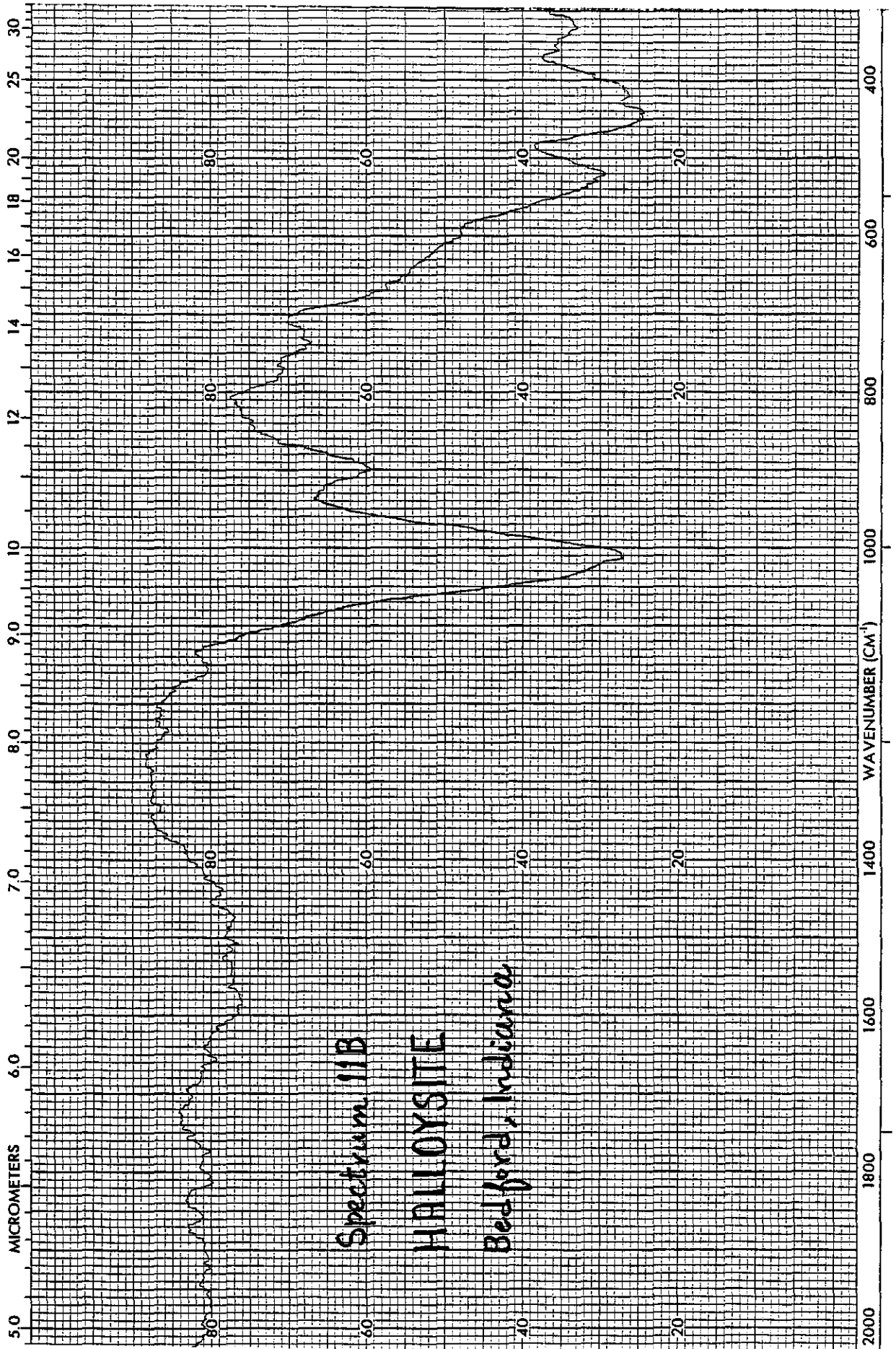




Spectrum 10A
HALLOYSITE
Eureka, Utah



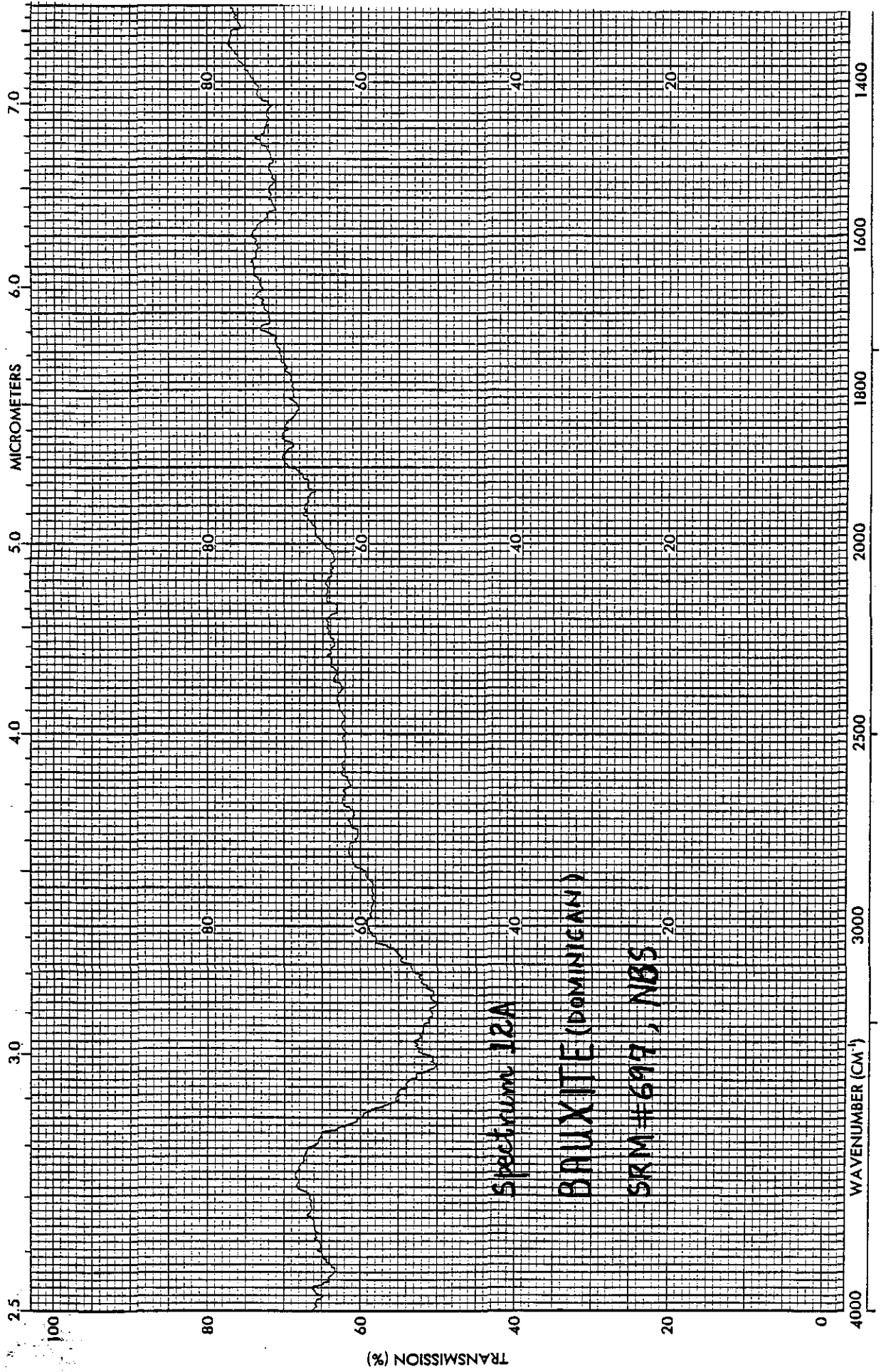


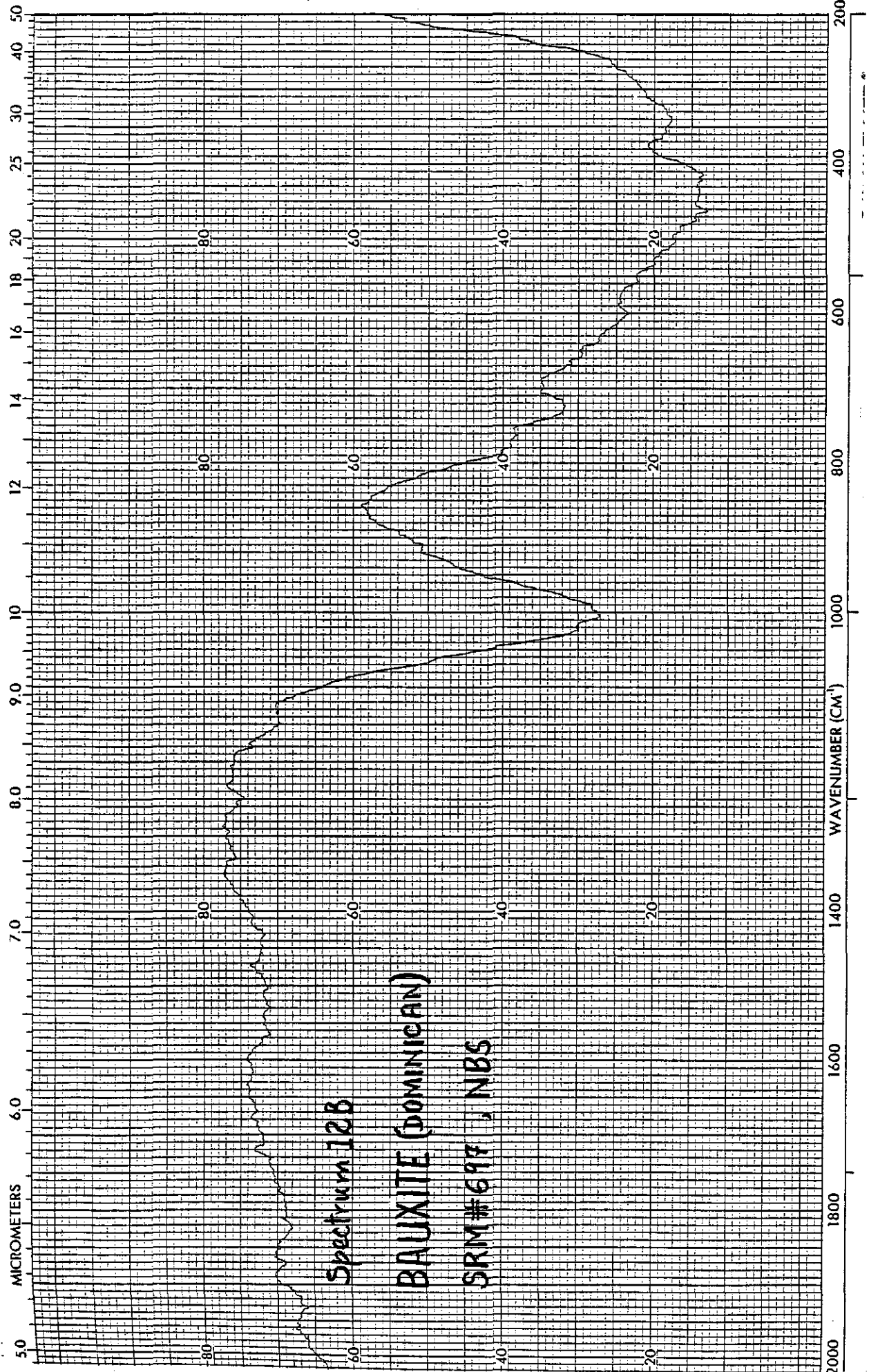


Spectrum 11B

HALLOYSITE

Bedford, Indiana

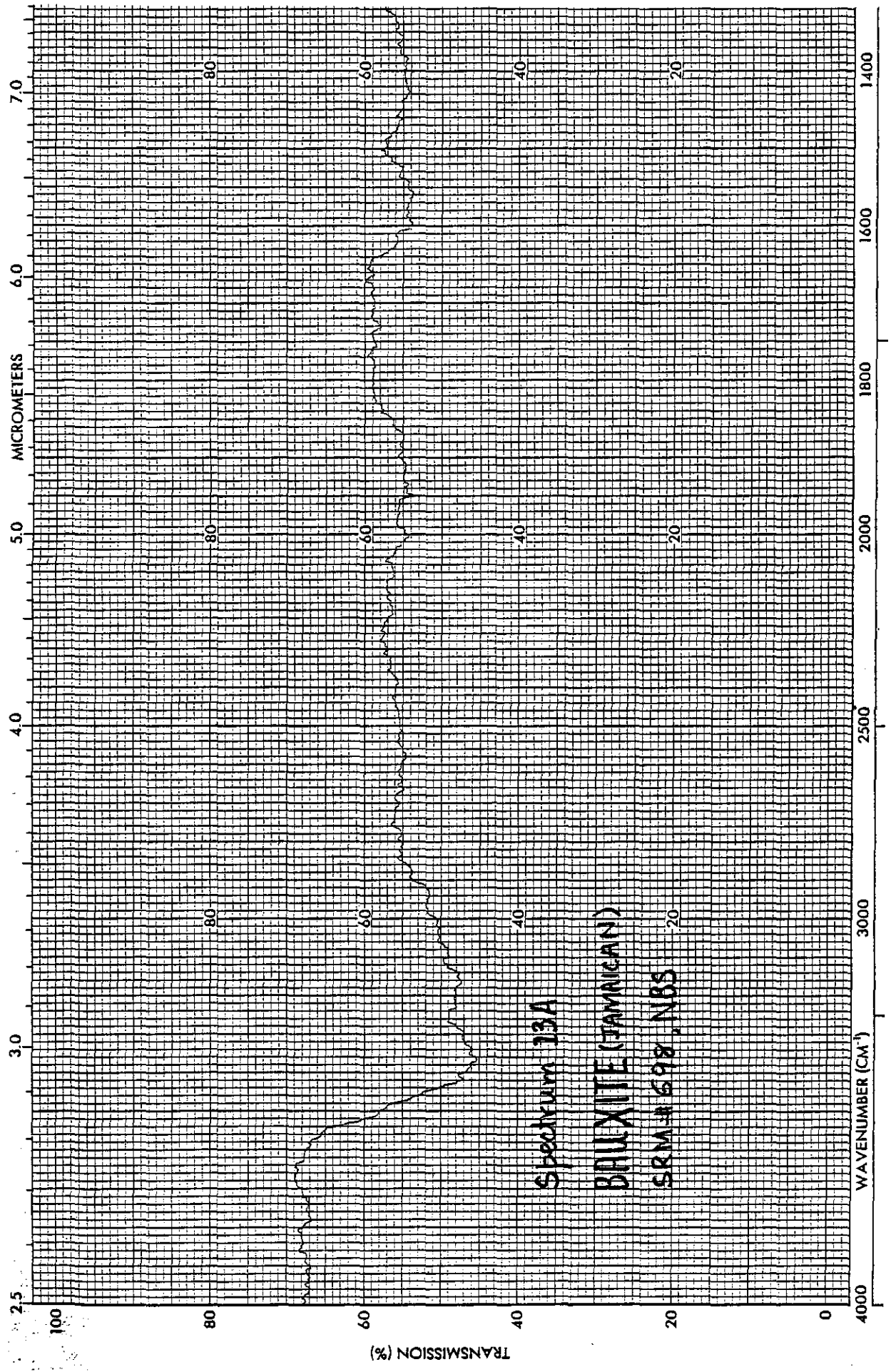


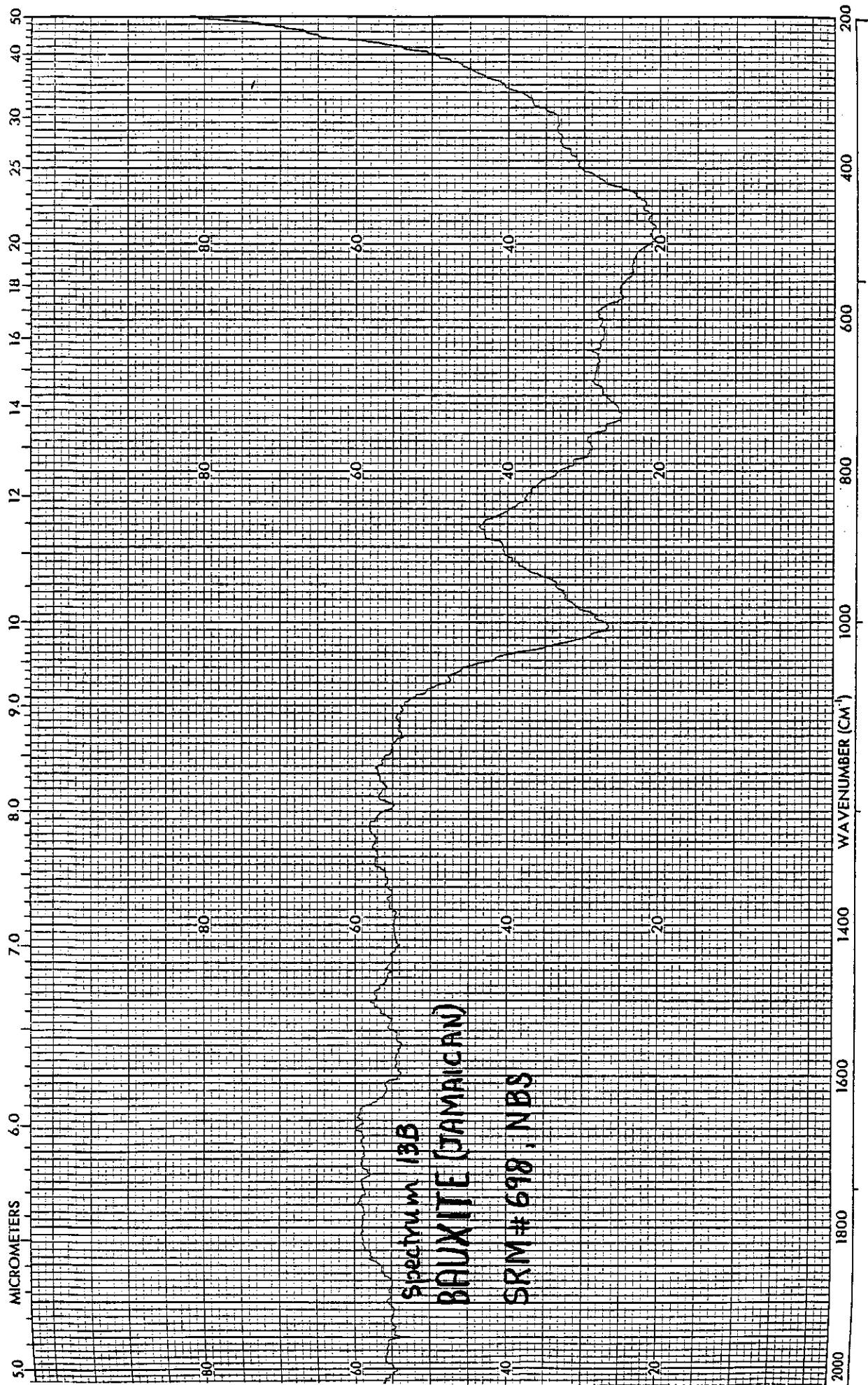


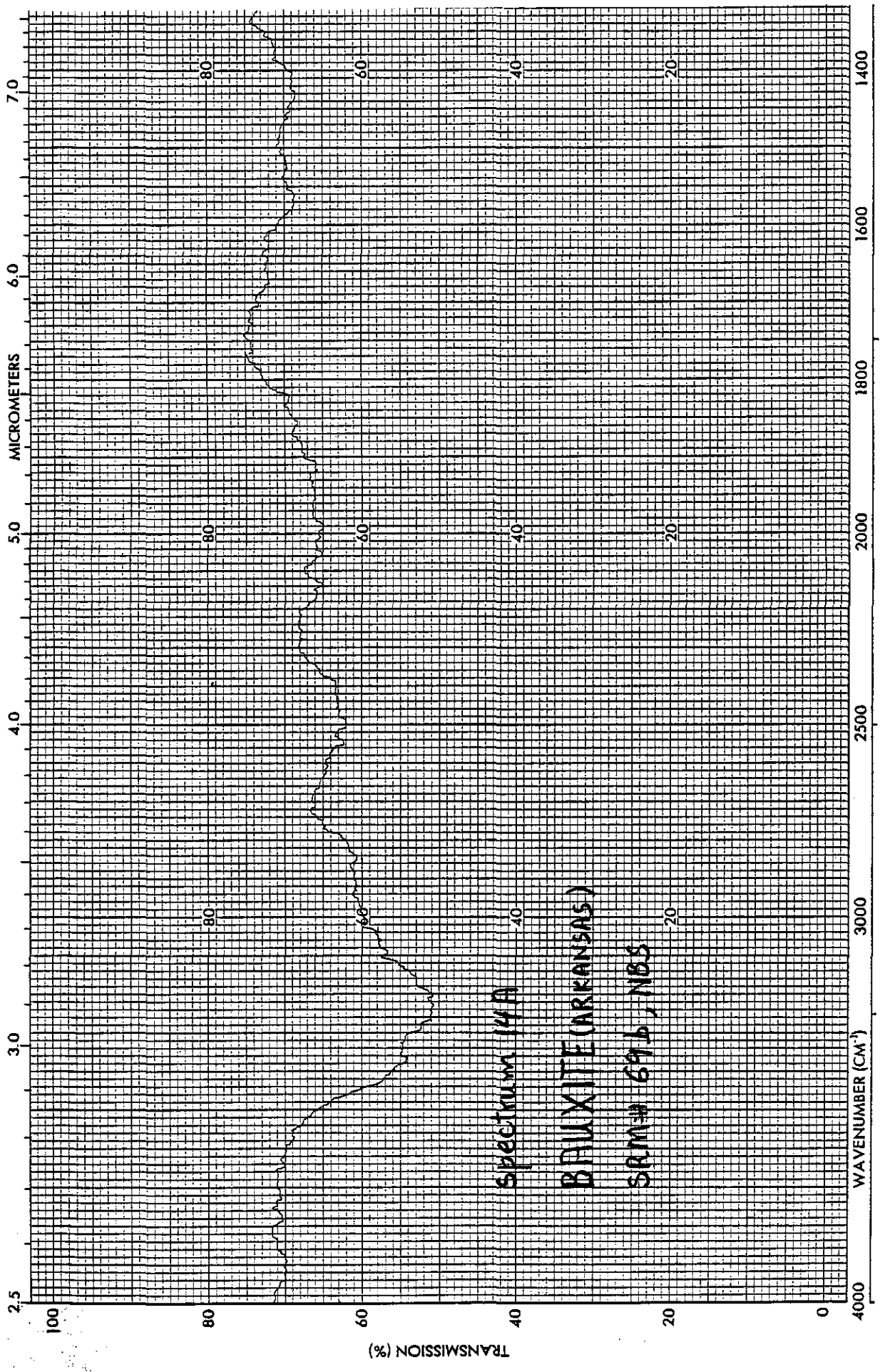
Spectrum 128

BAUXITE (DOMINICAN)

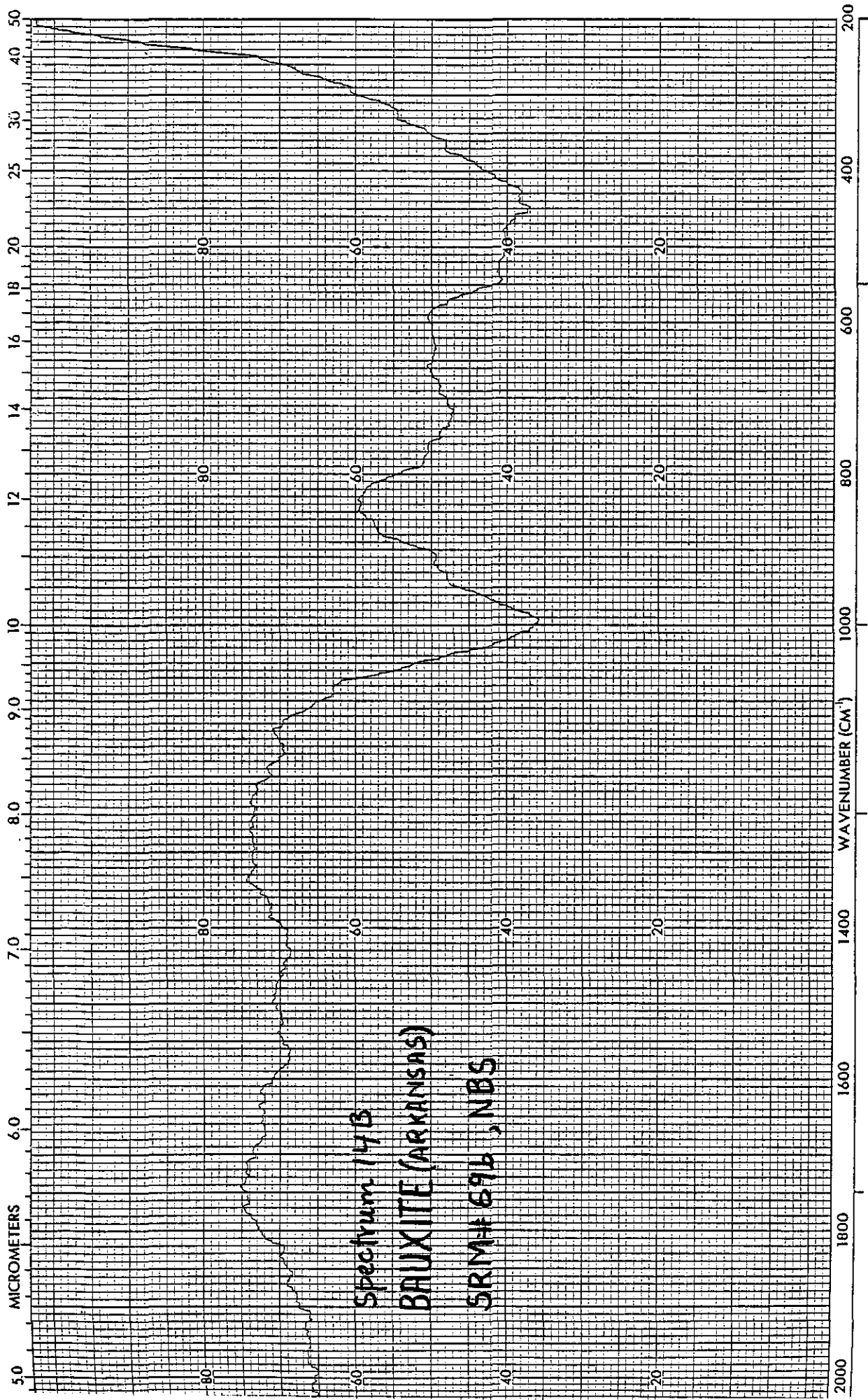
SRM #697, NBS



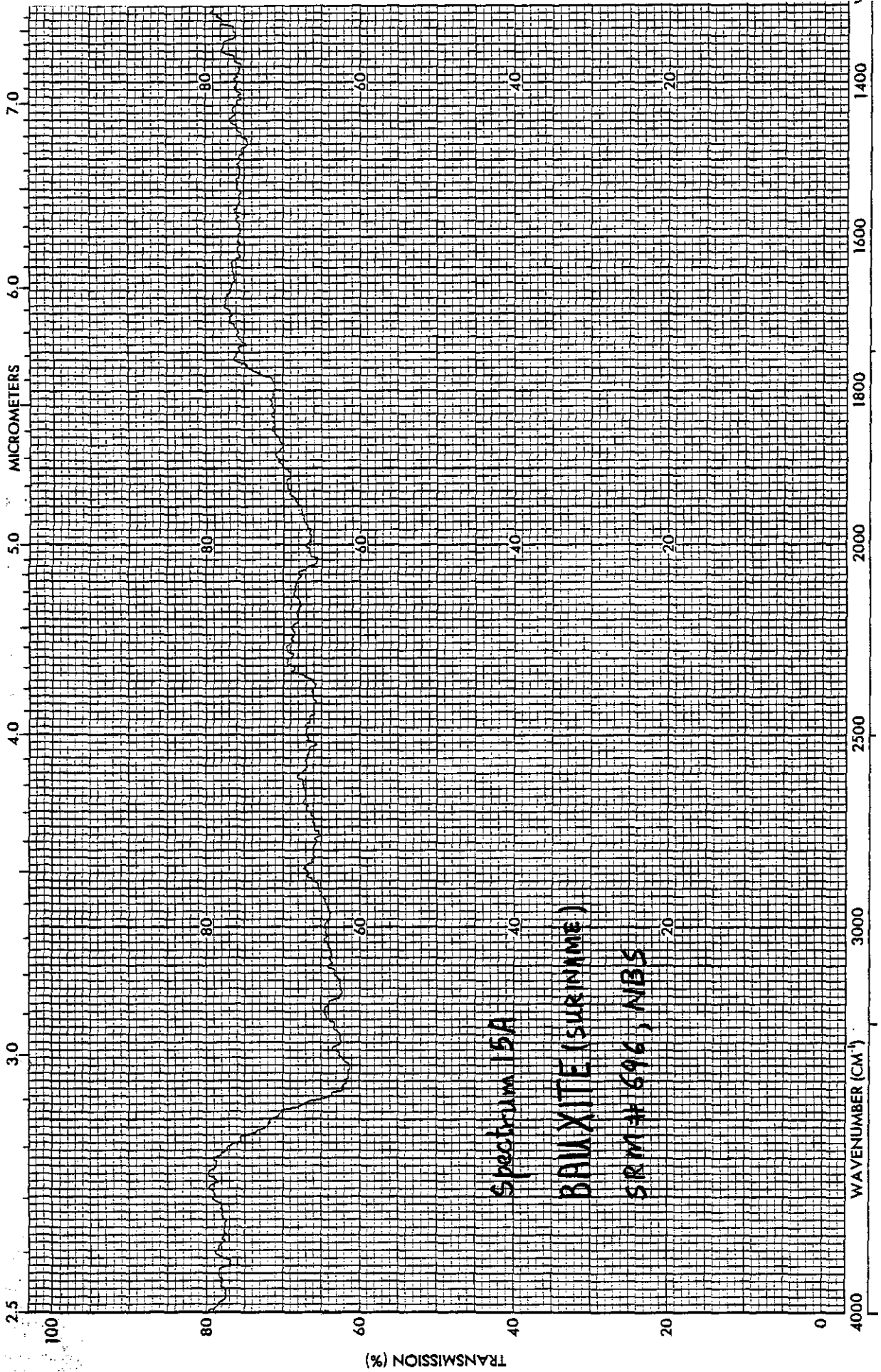


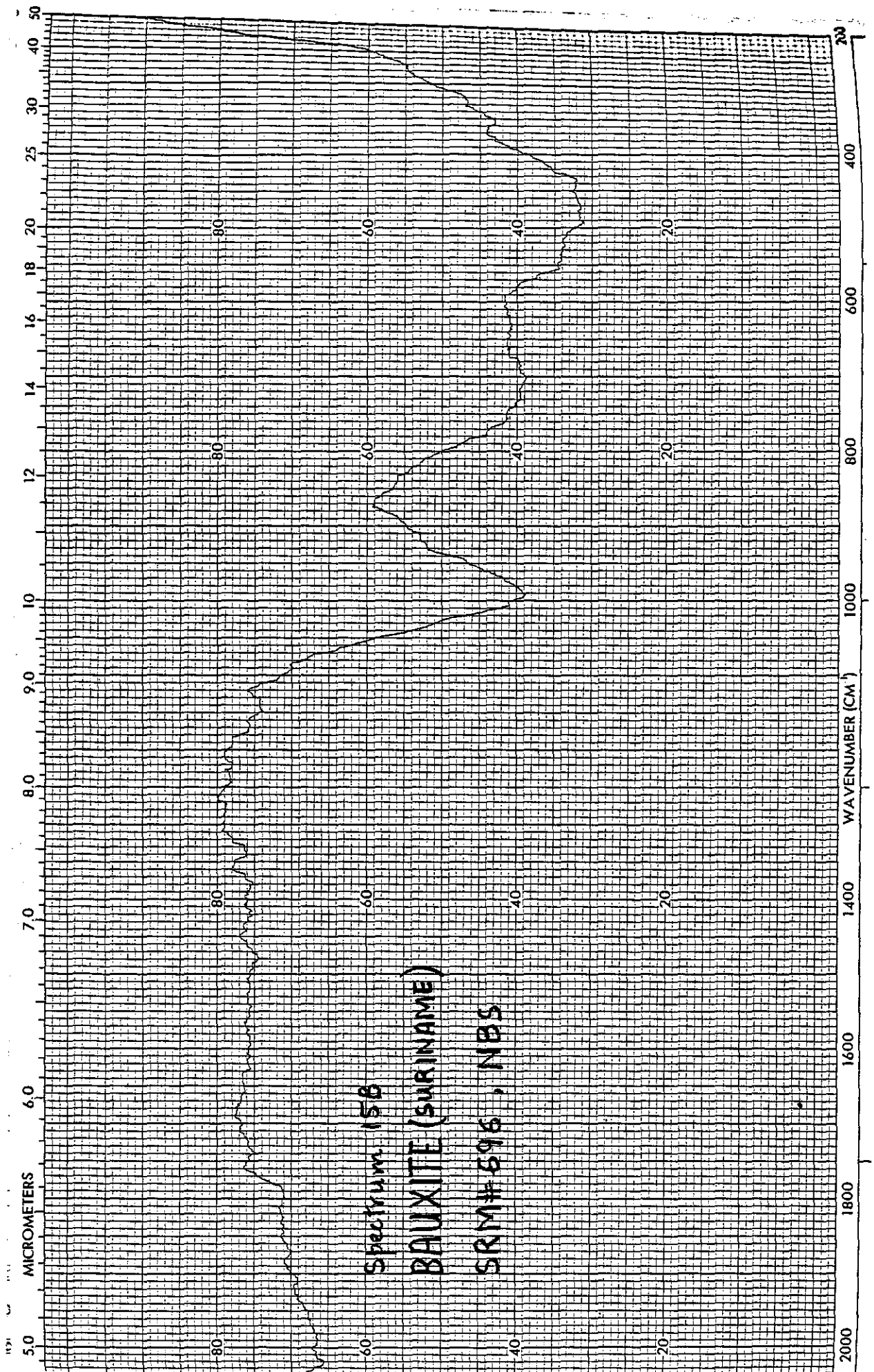


SPECTRUM (4A)
BAUXITE (ARKANSAS)
SAM# 6916, NBS

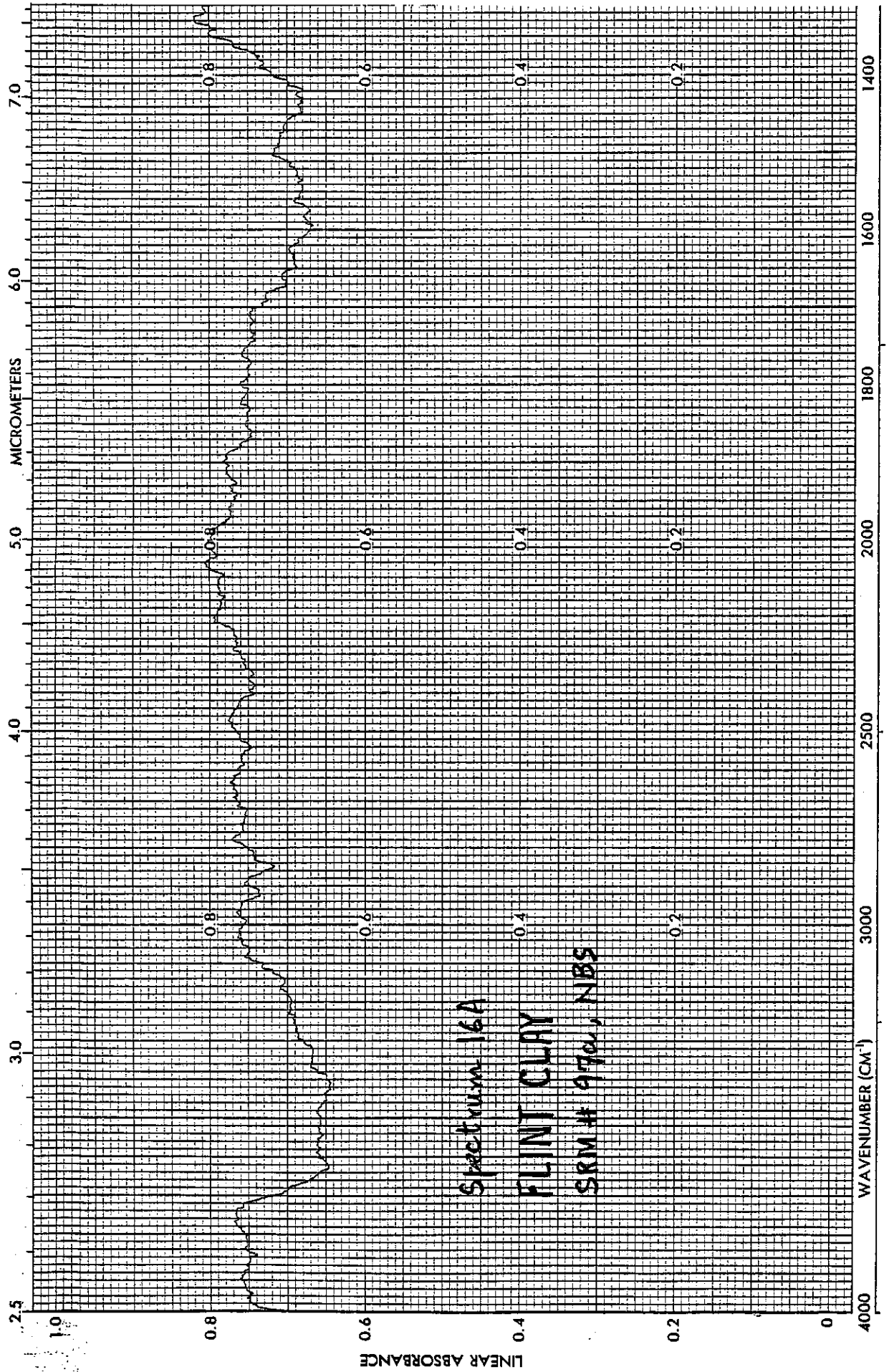


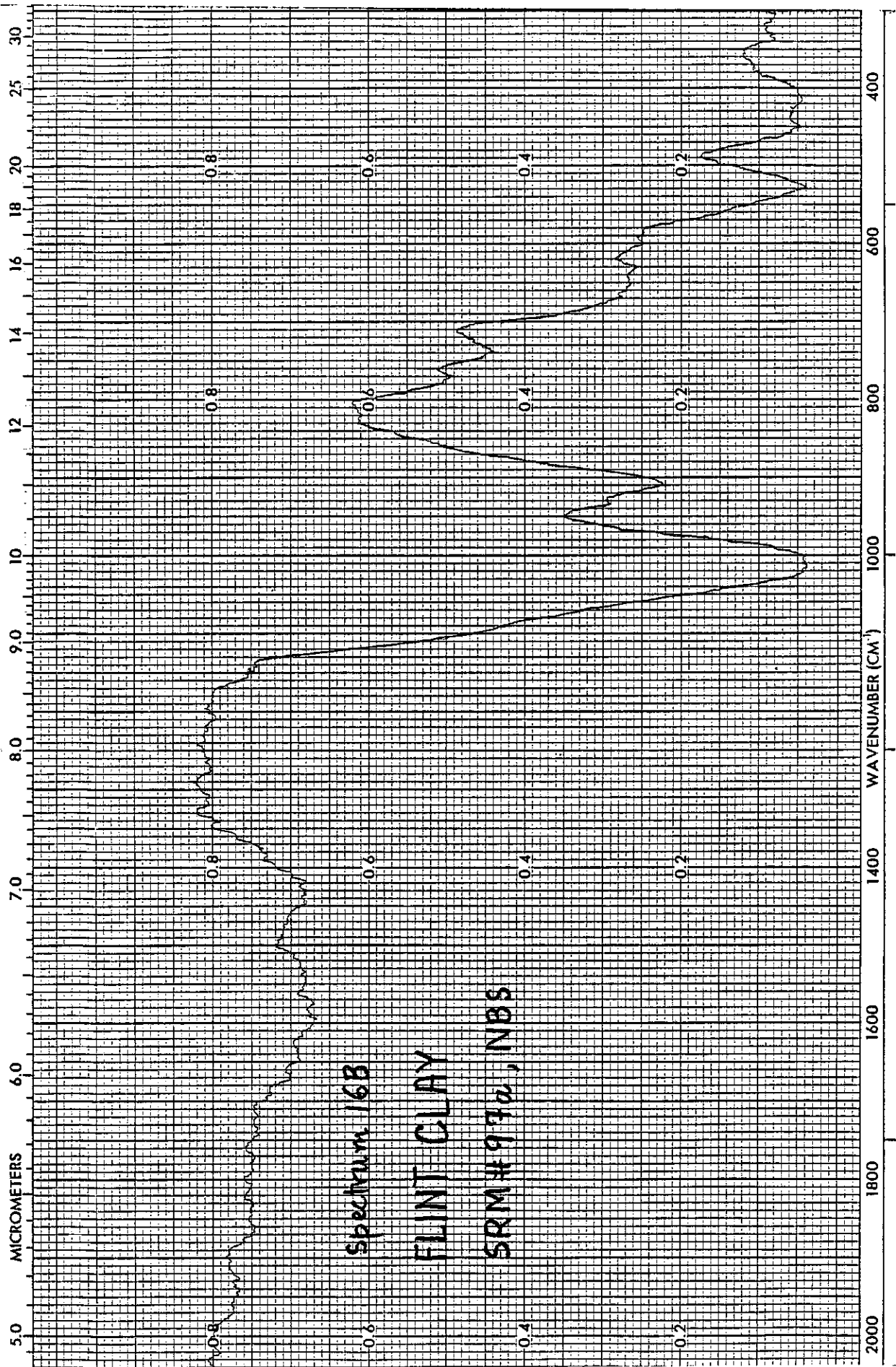
Spectrum 143
BRAUXITE (ARKANSAS)
SRM# 696, NBS

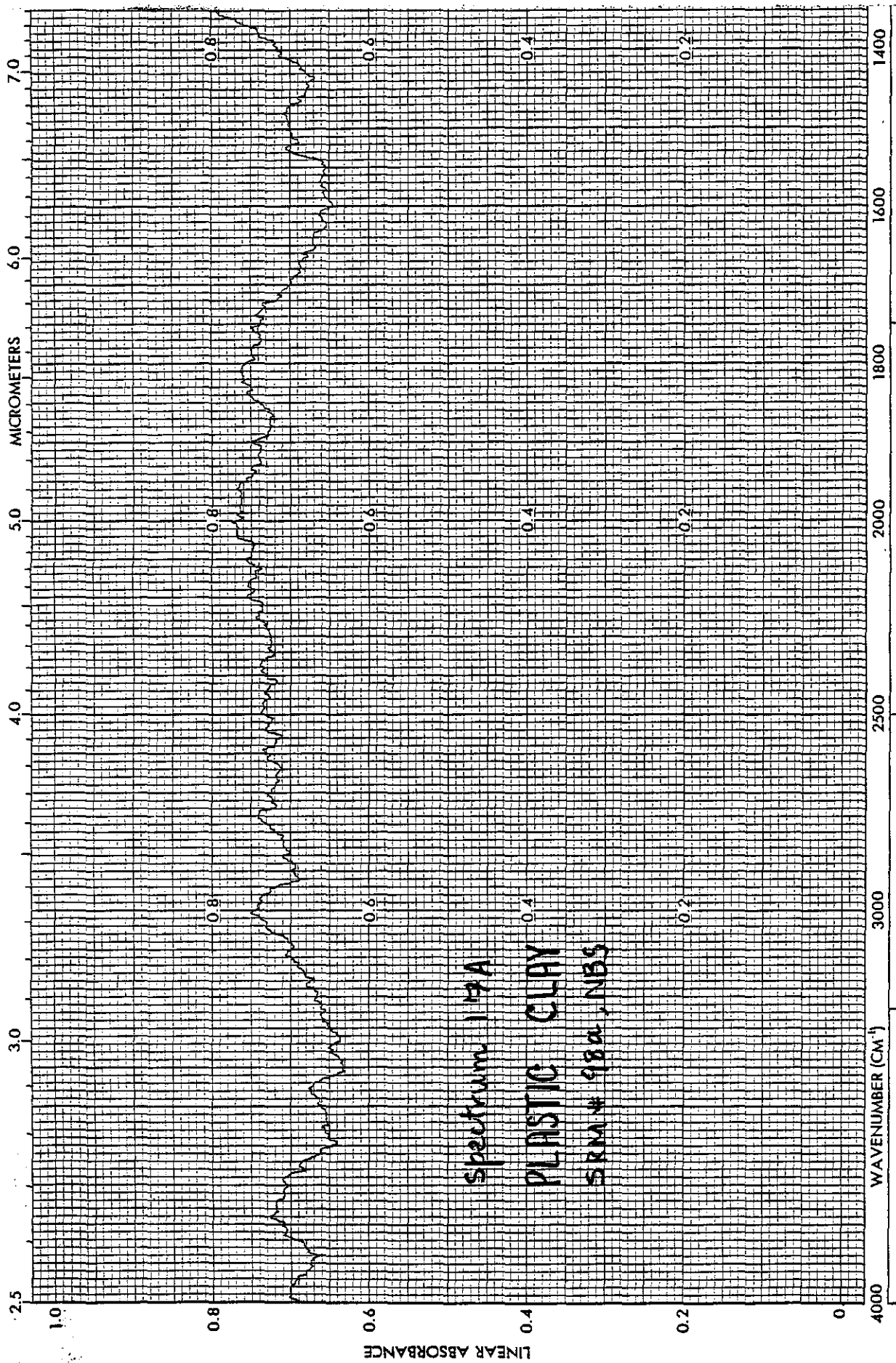


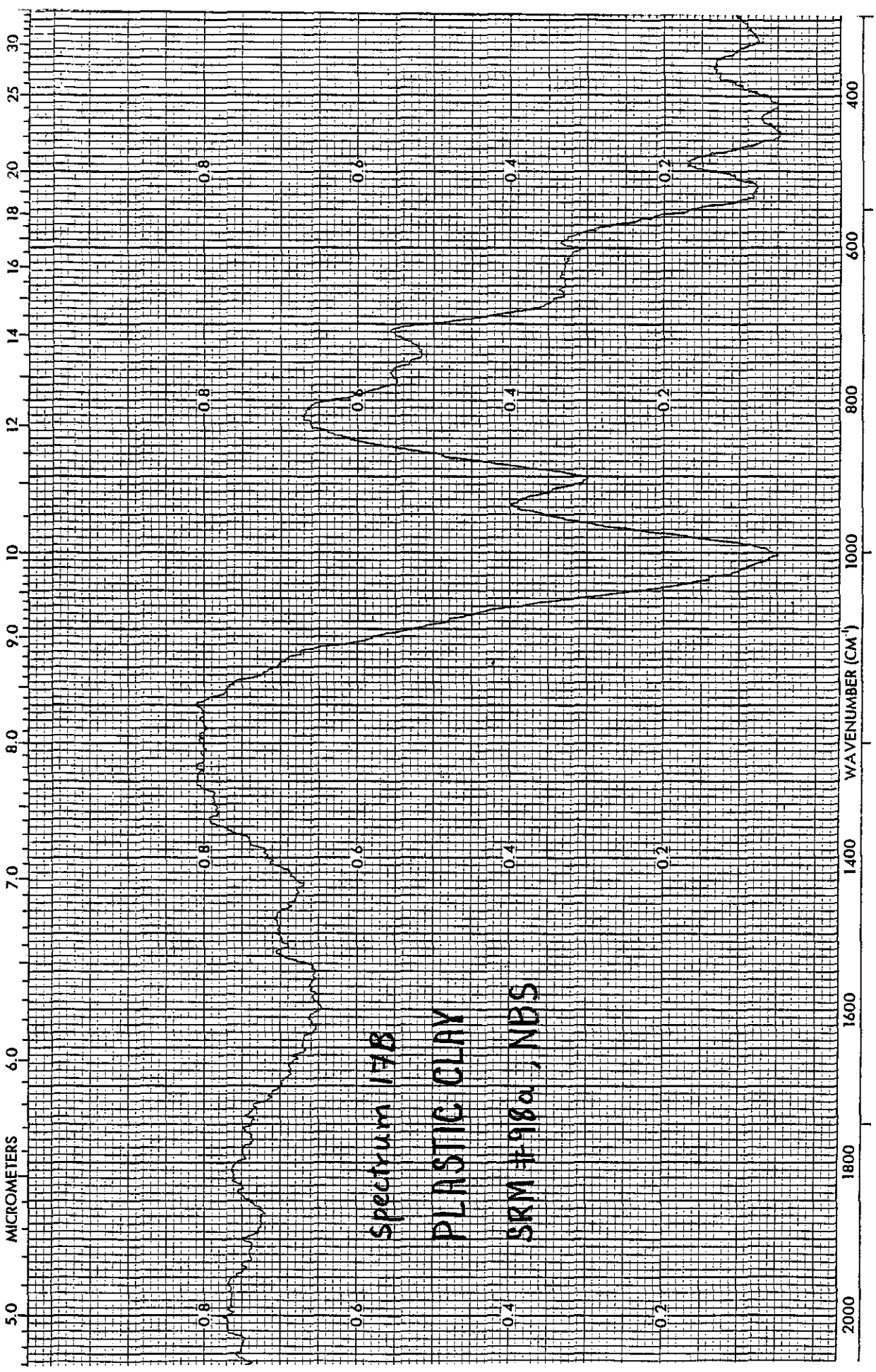


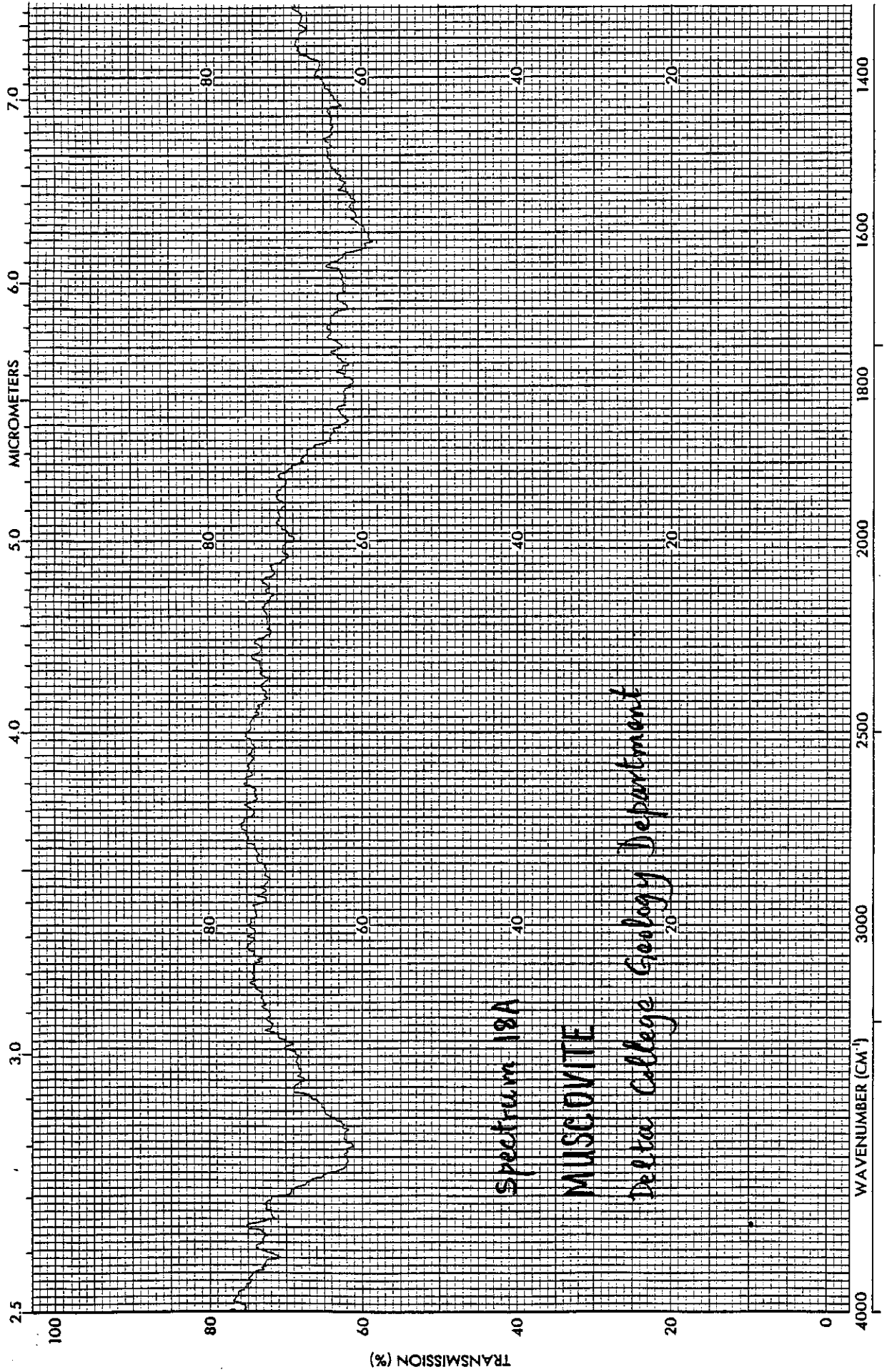
Spectrum 158
BAUXITE (SURINAME)
SRM# 5916, NBS







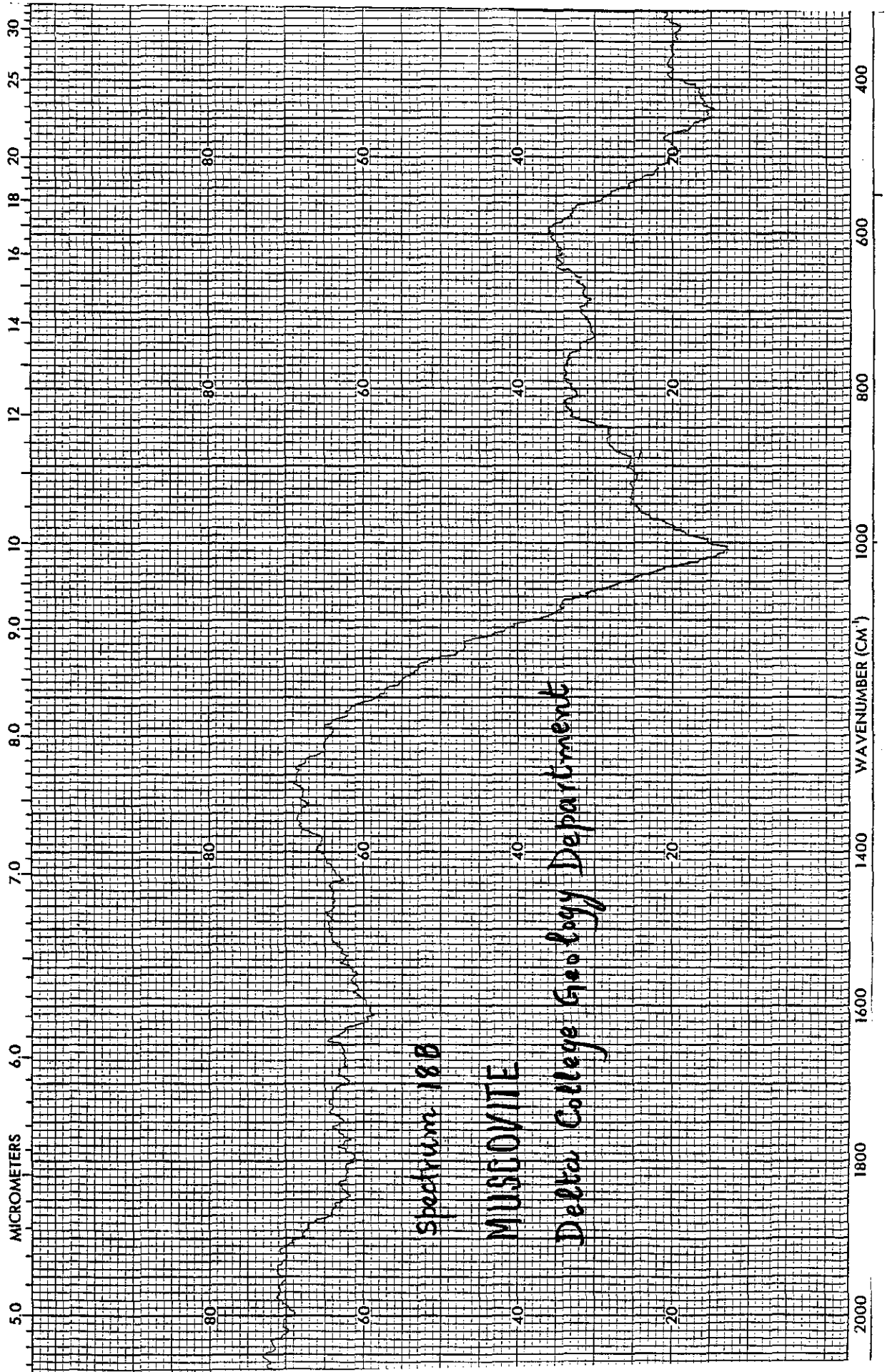




Spectrum 18A

MUSCOVITE

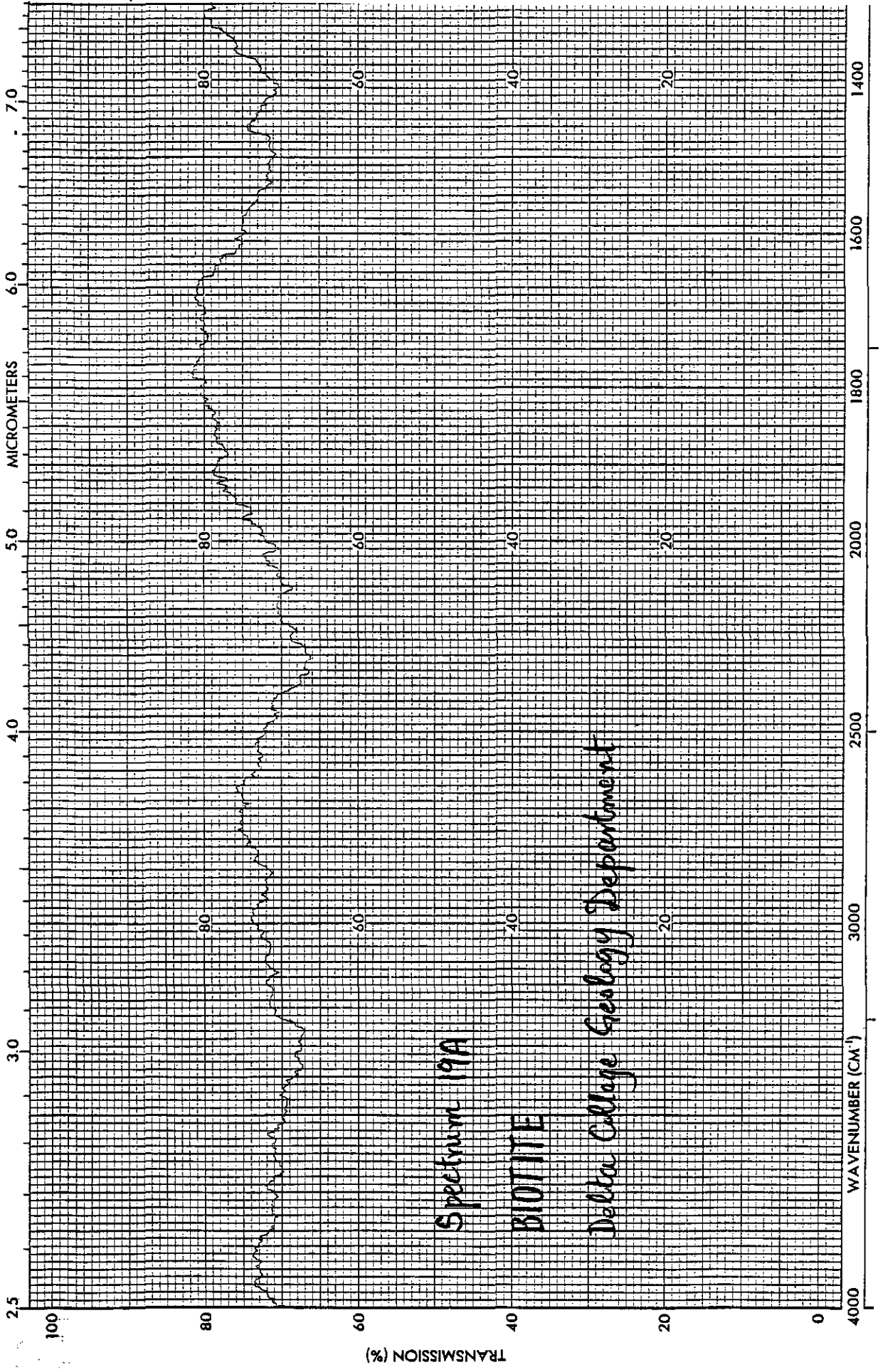
Delta College Geology Department



Spectrum 18B

MUSCOVITE

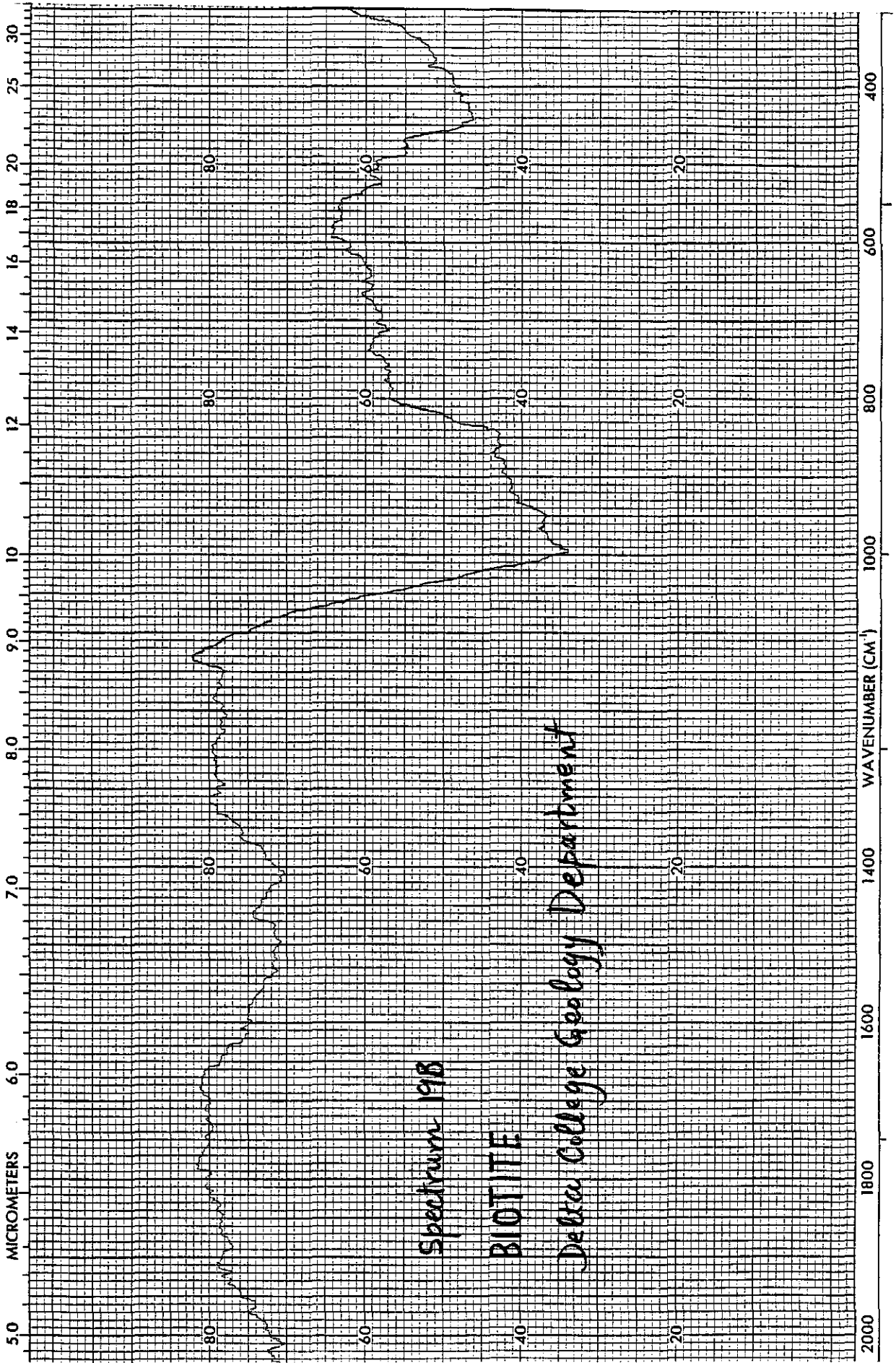
Delta College Geology Department



Spectrum 19A

BIOTITE

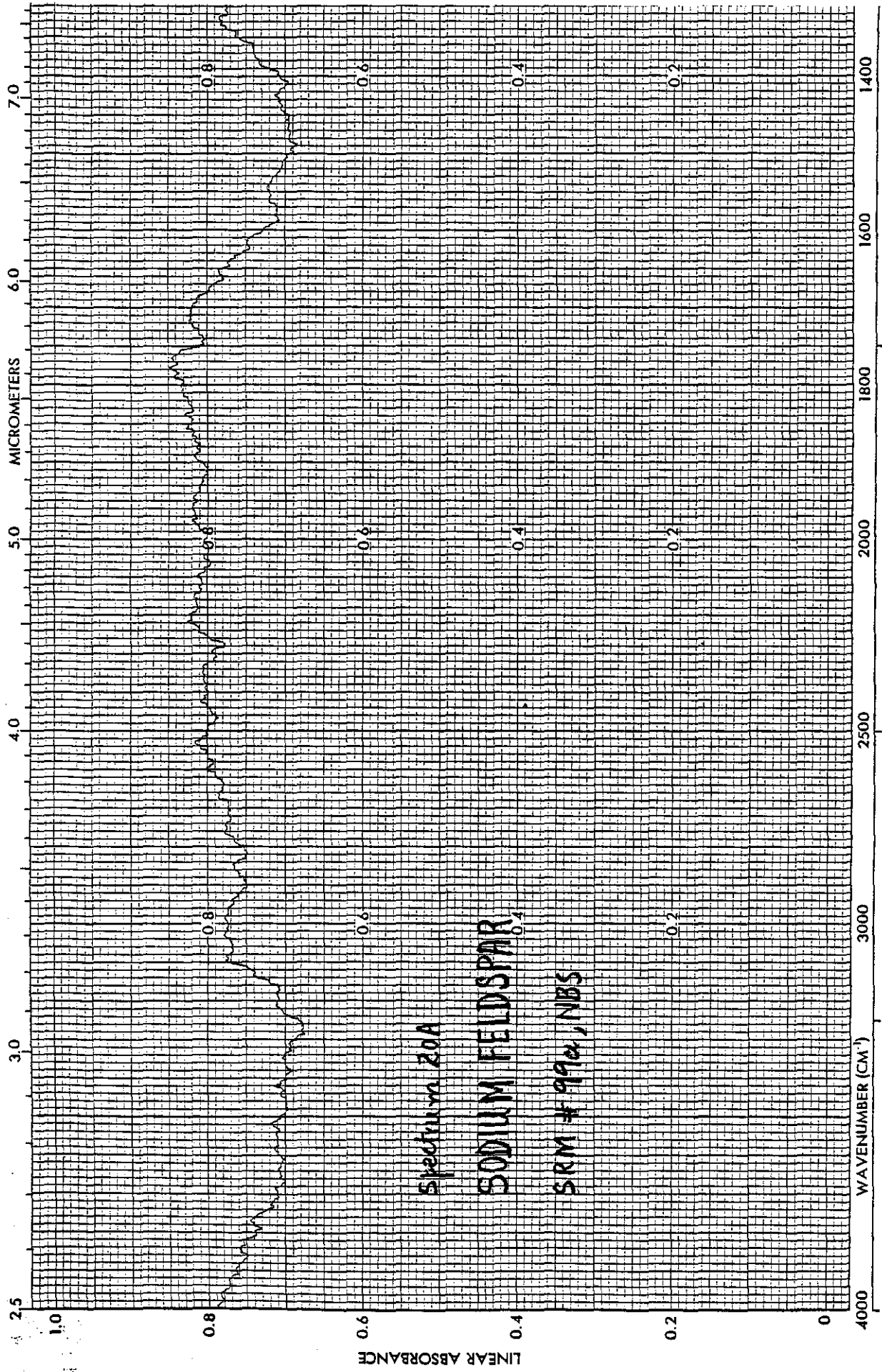
Delta College Geology Department



Spectrum 19B

BIOTITE

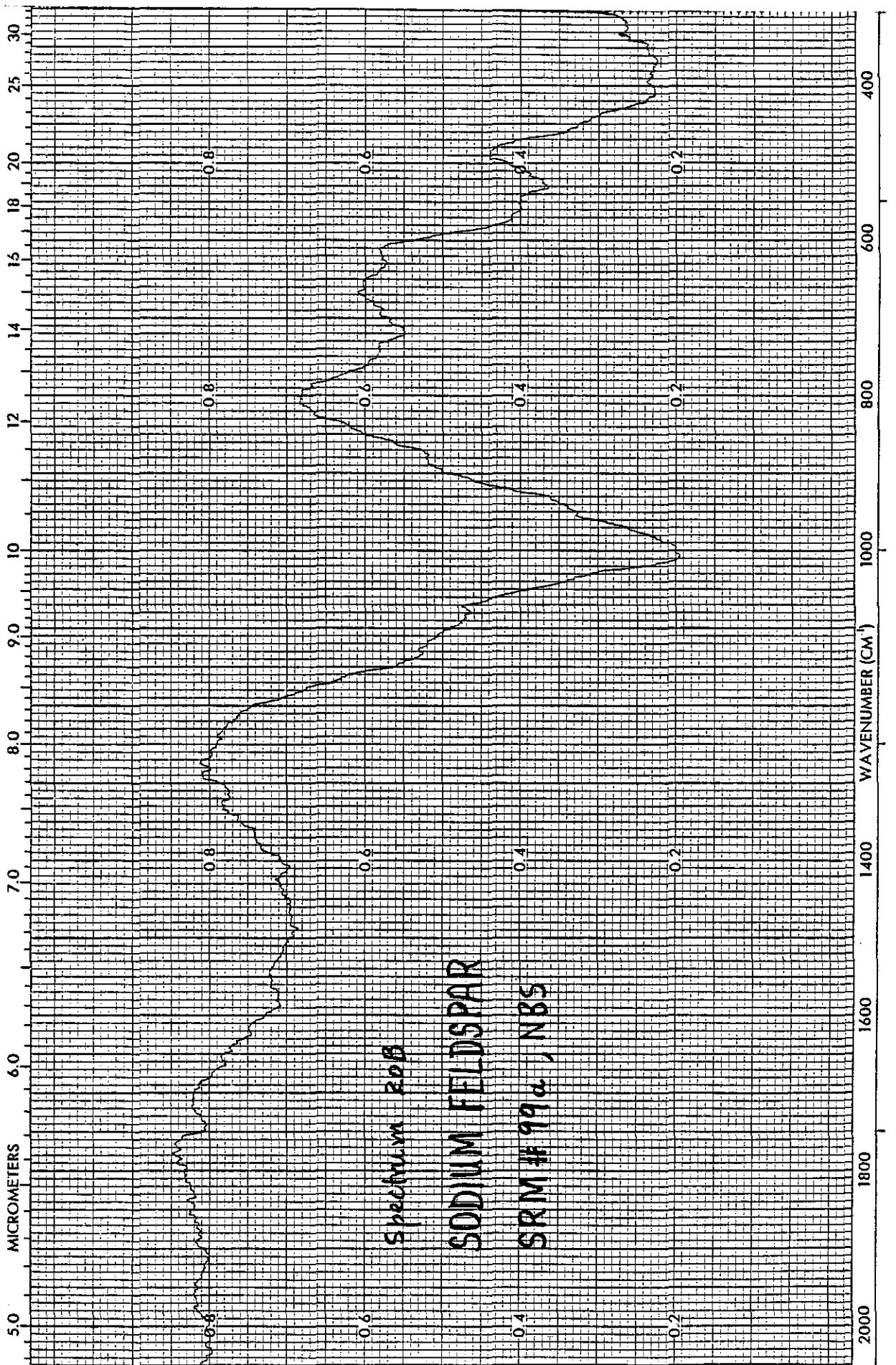
Delaware College Geology Department

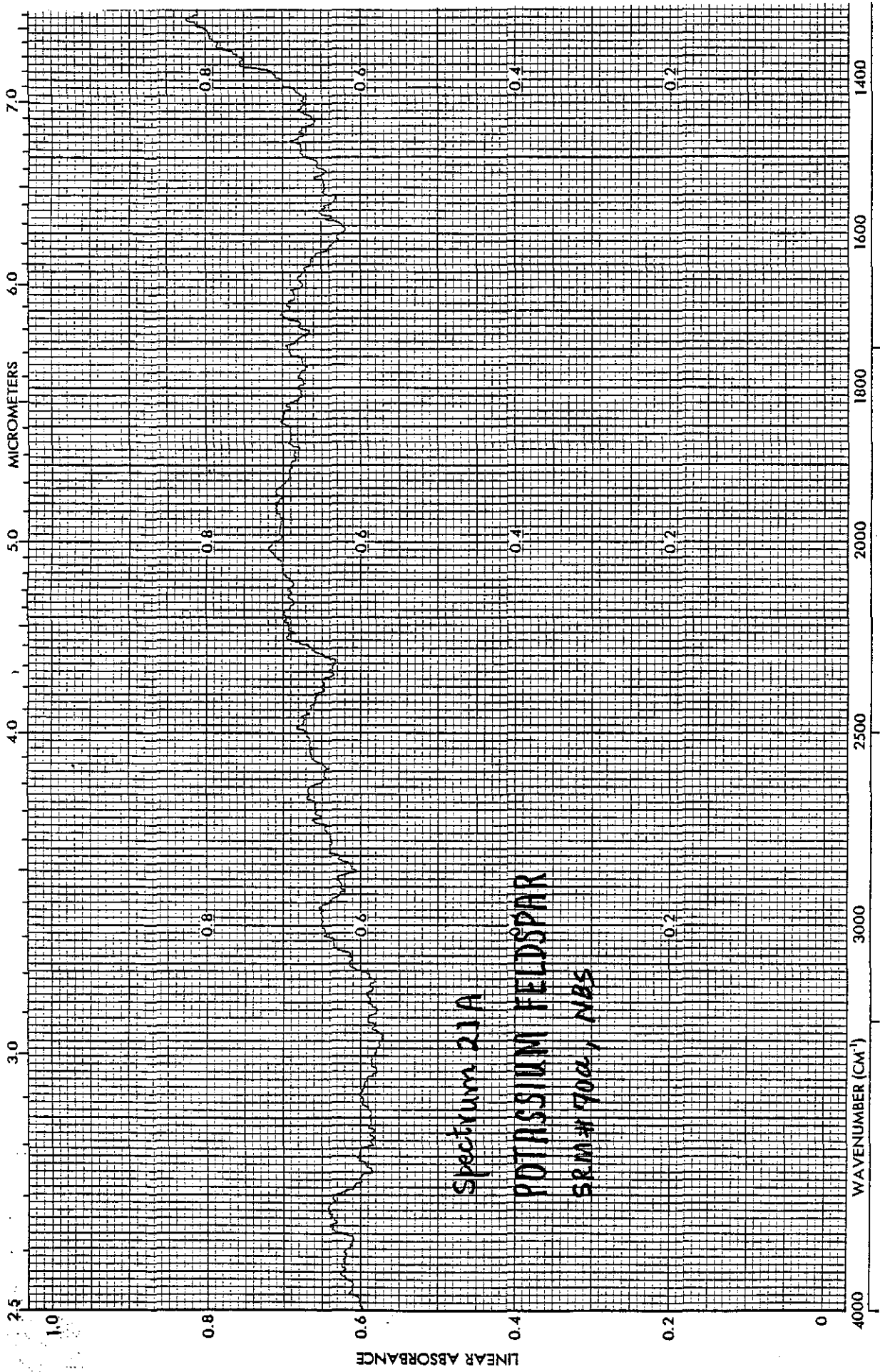


Spectrum 20A

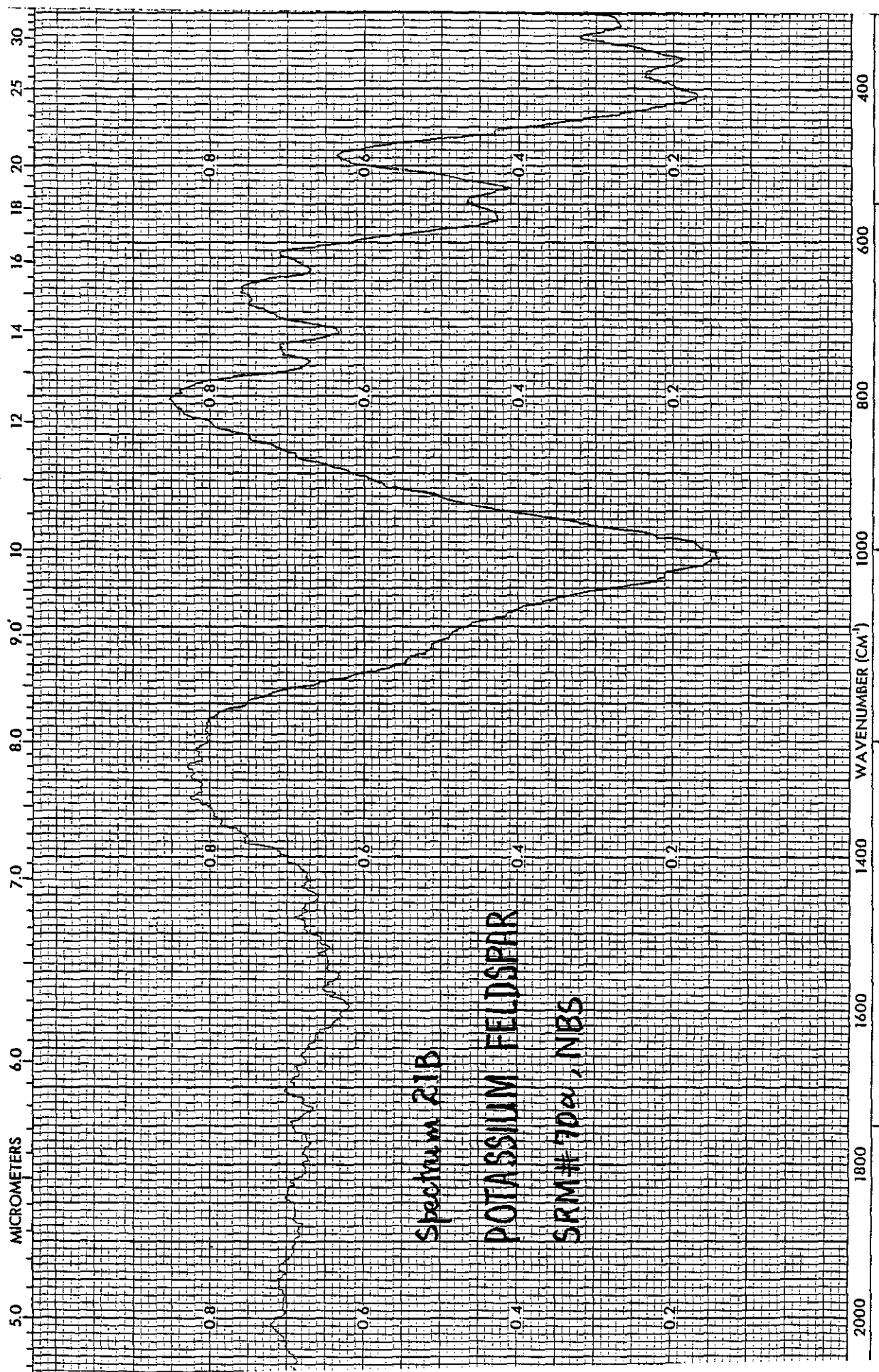
SODIUM FELDSPAR

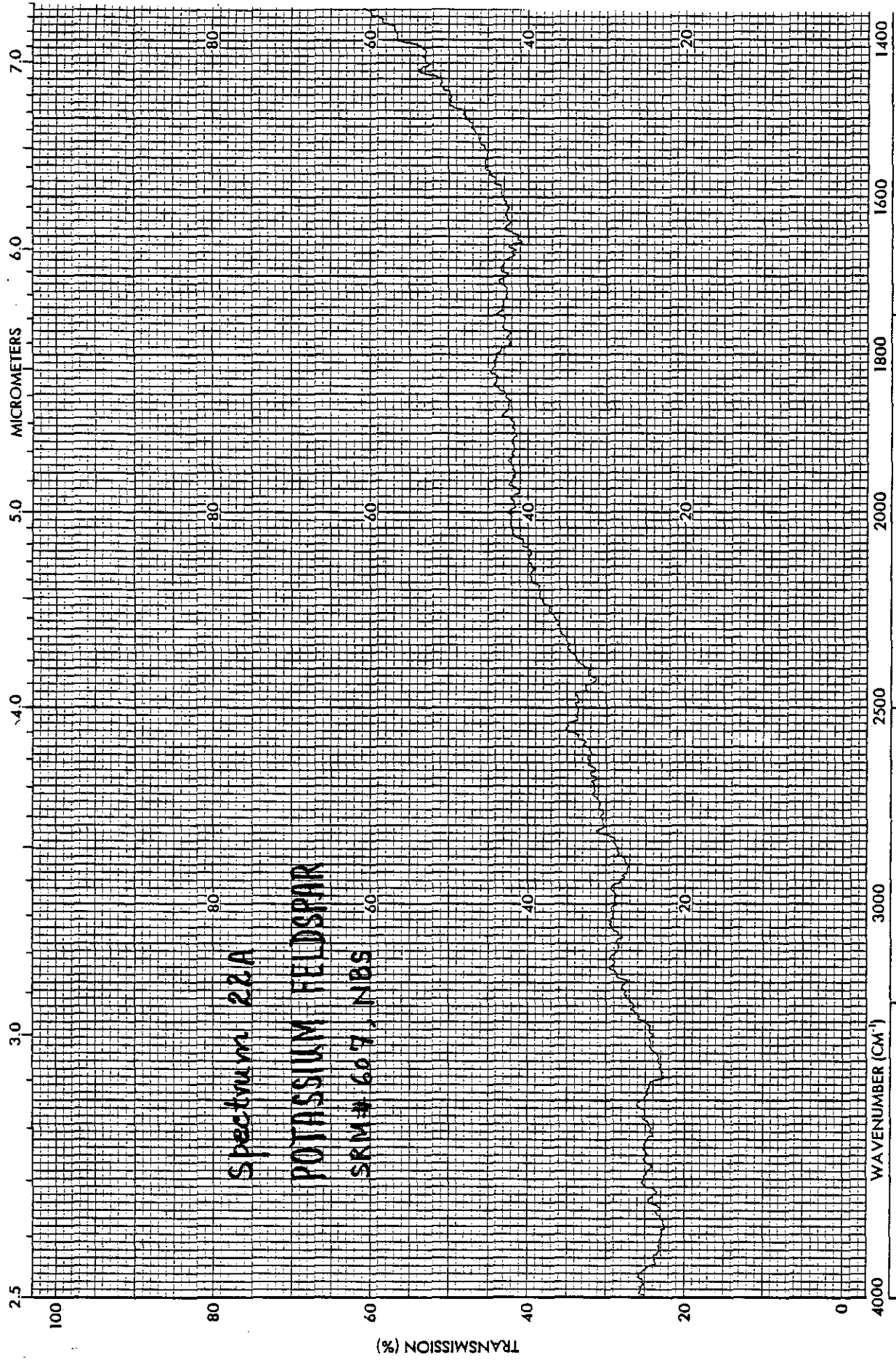
SRM # 99a, NBS

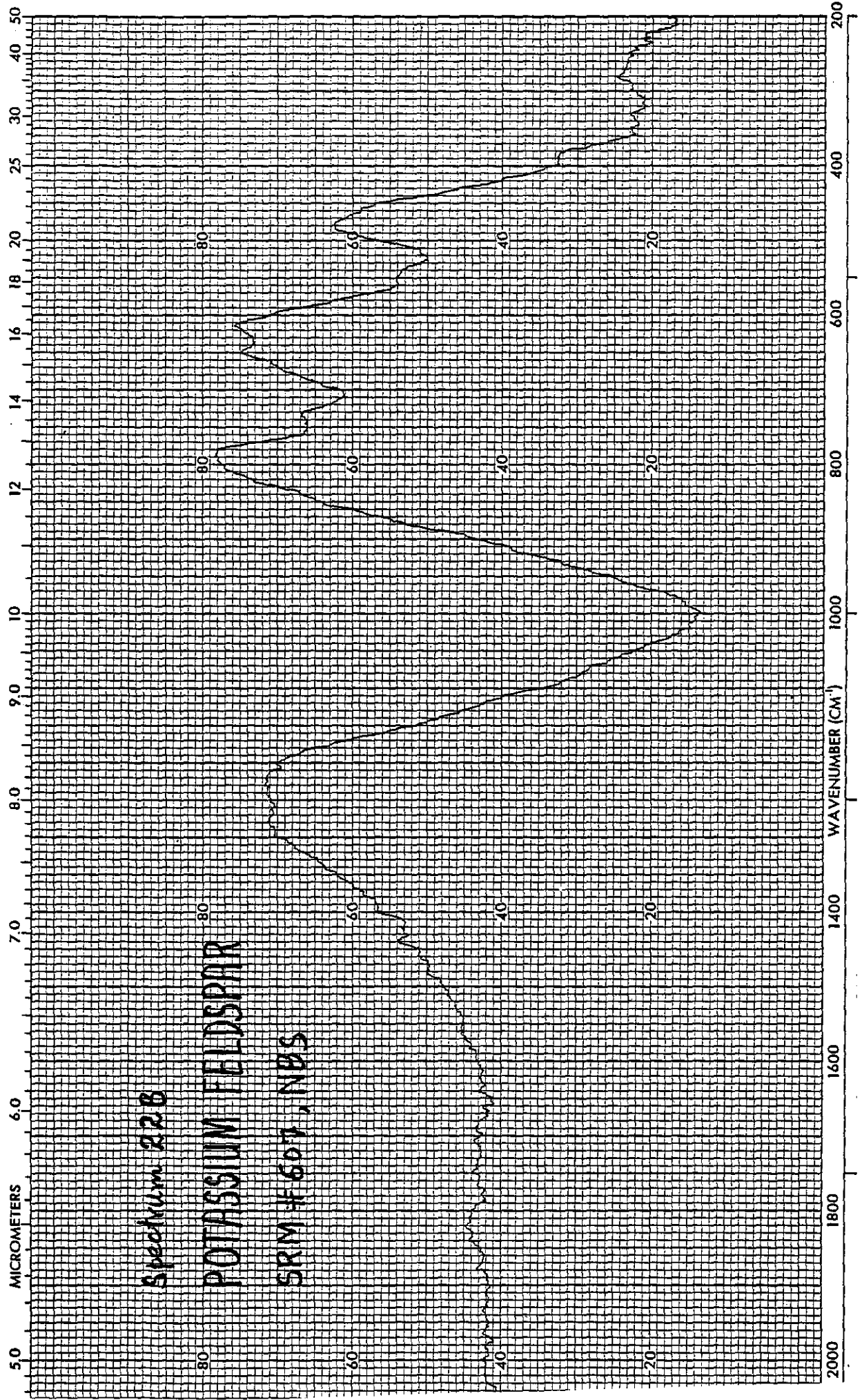


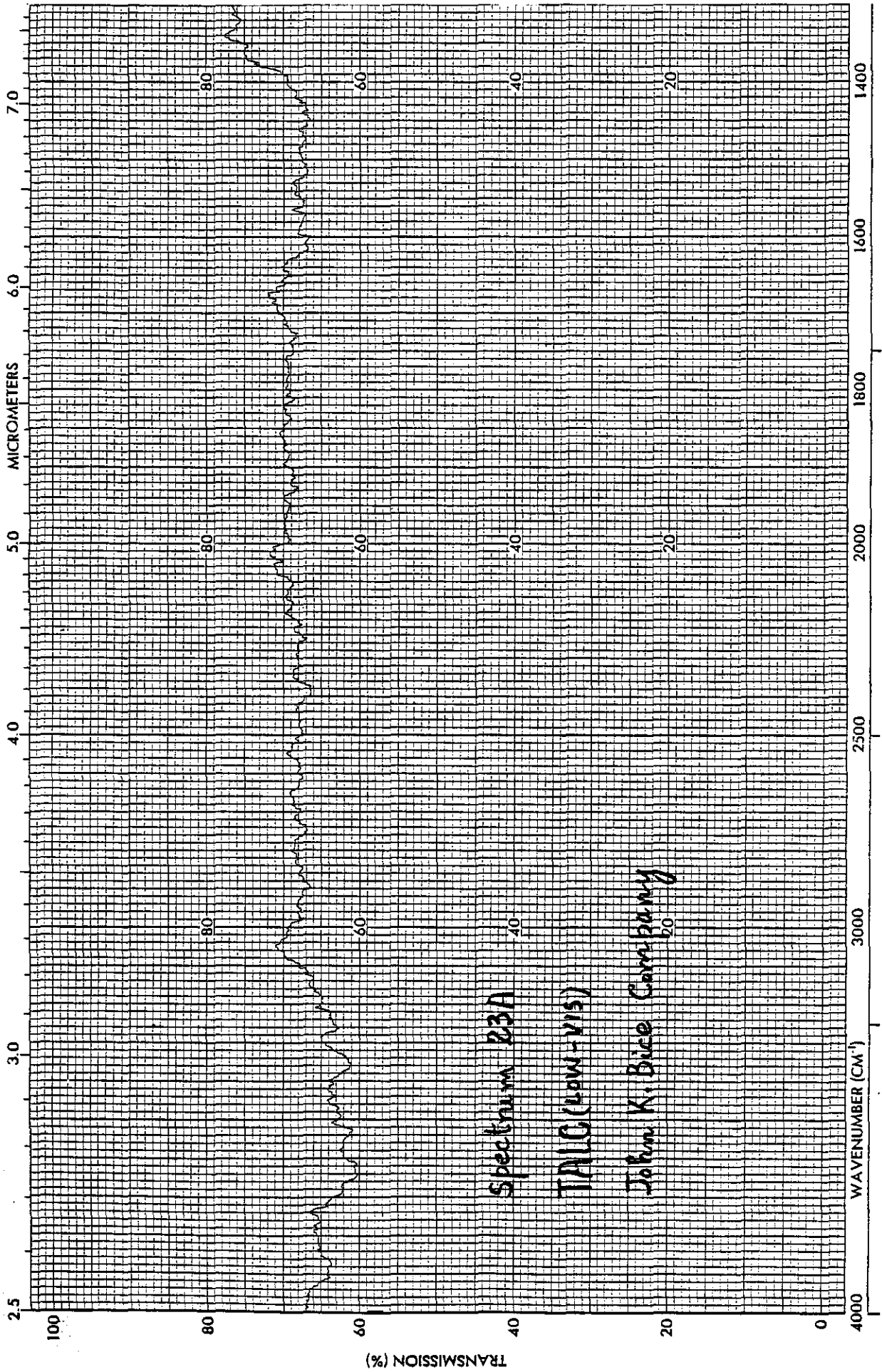


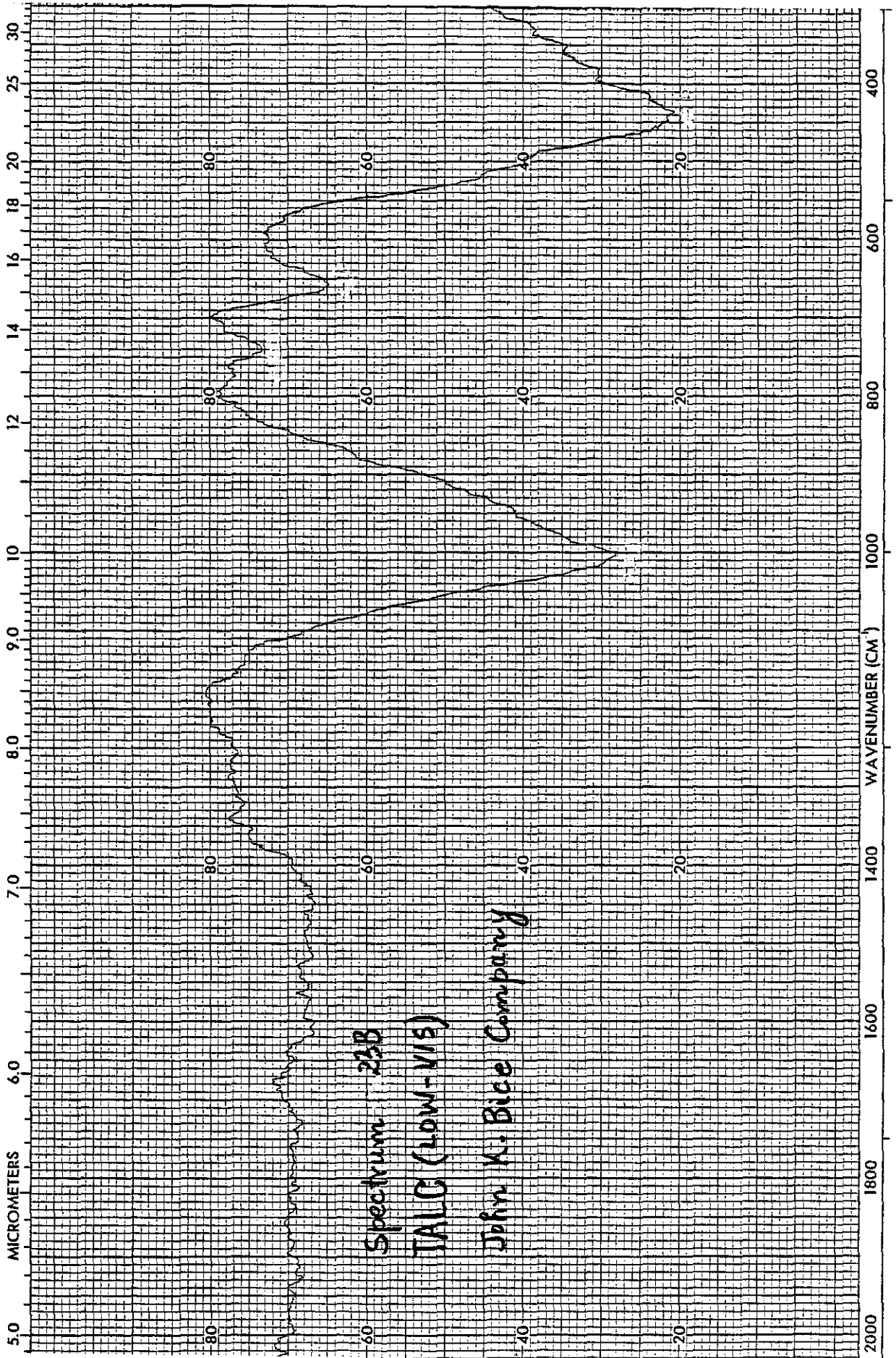
Spectrum 21A
POTASSIUM FELDSPAR
SRM # 70c, NBS

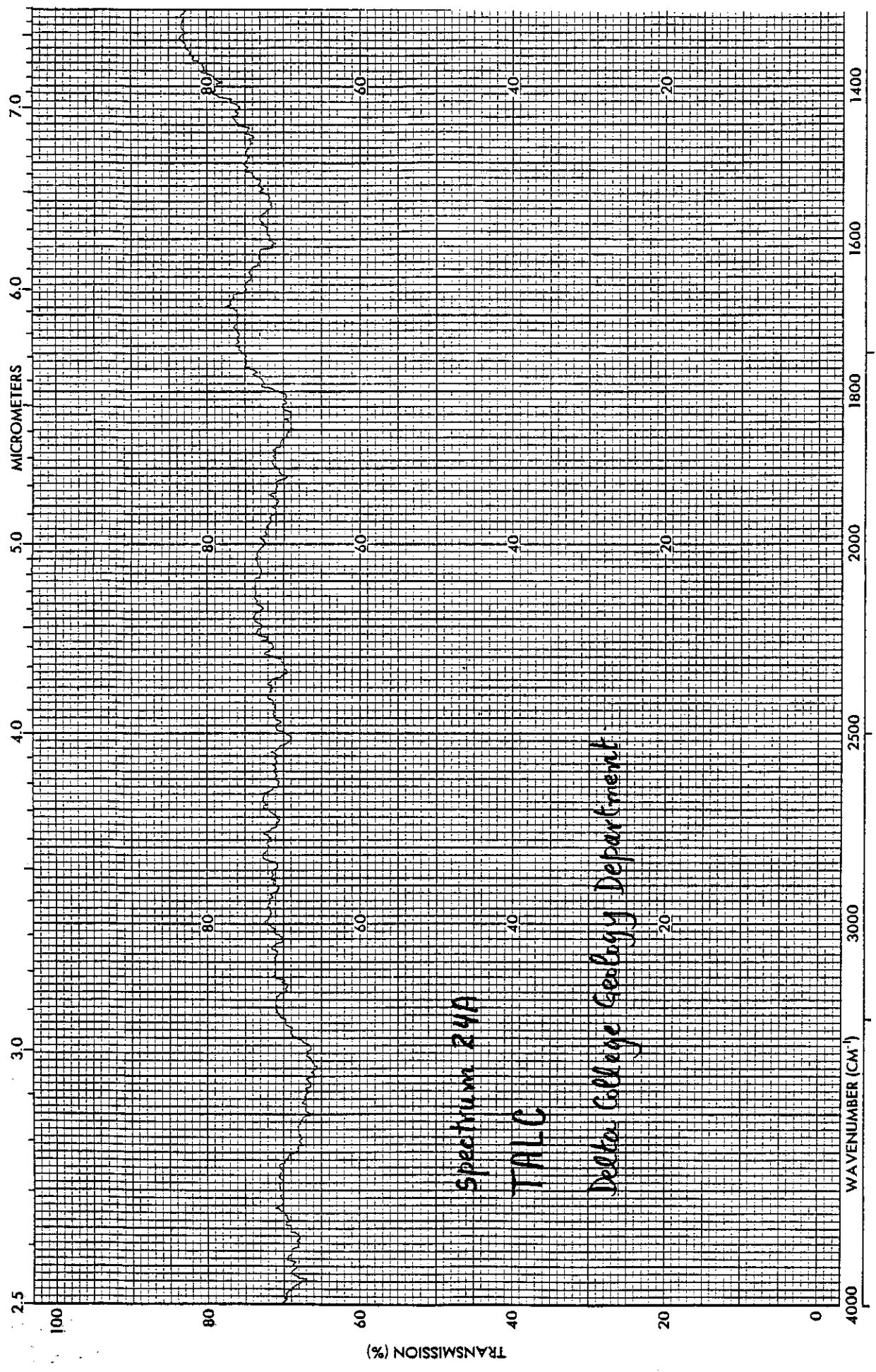








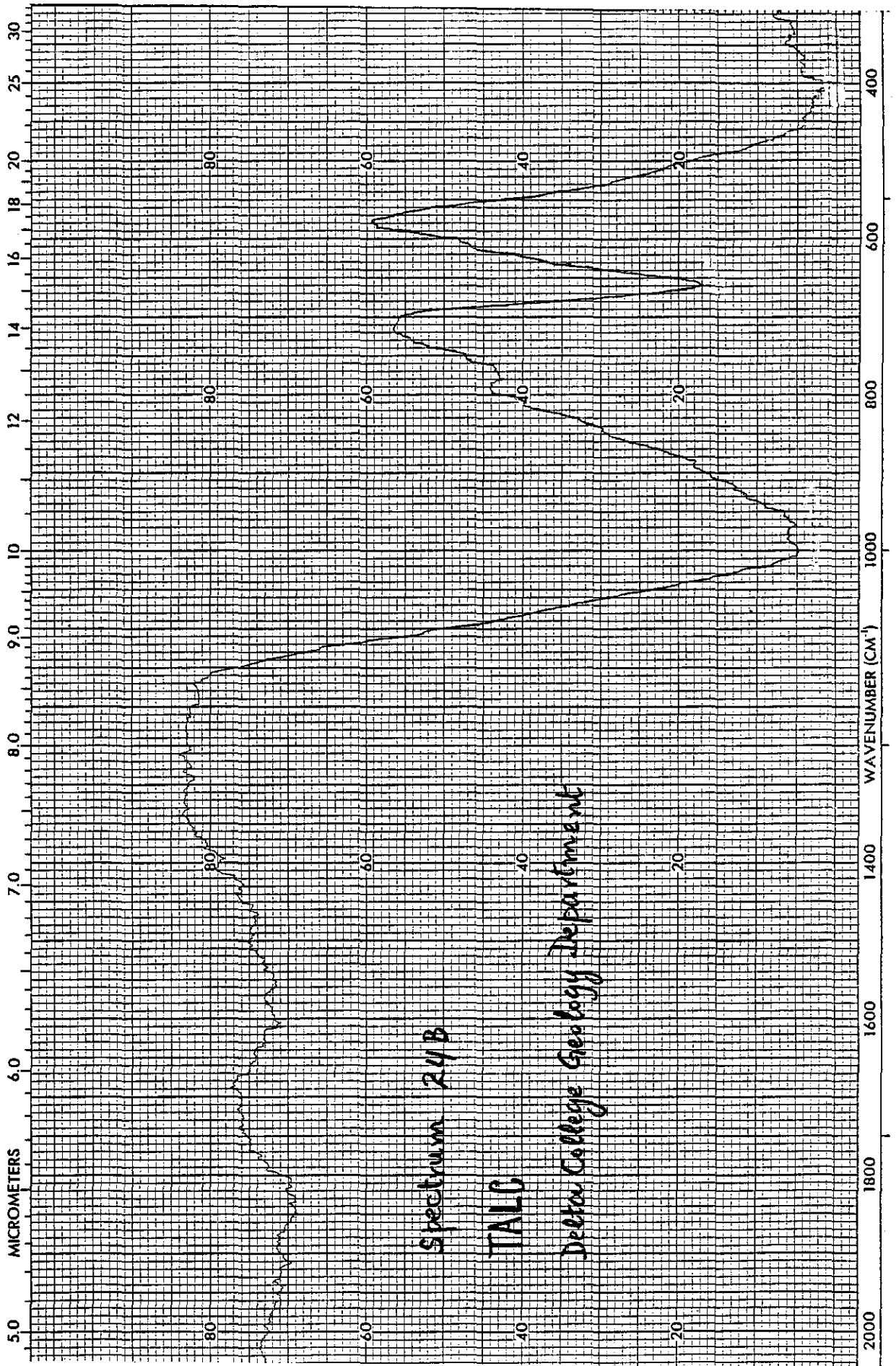




Spectrum 24A

TALC

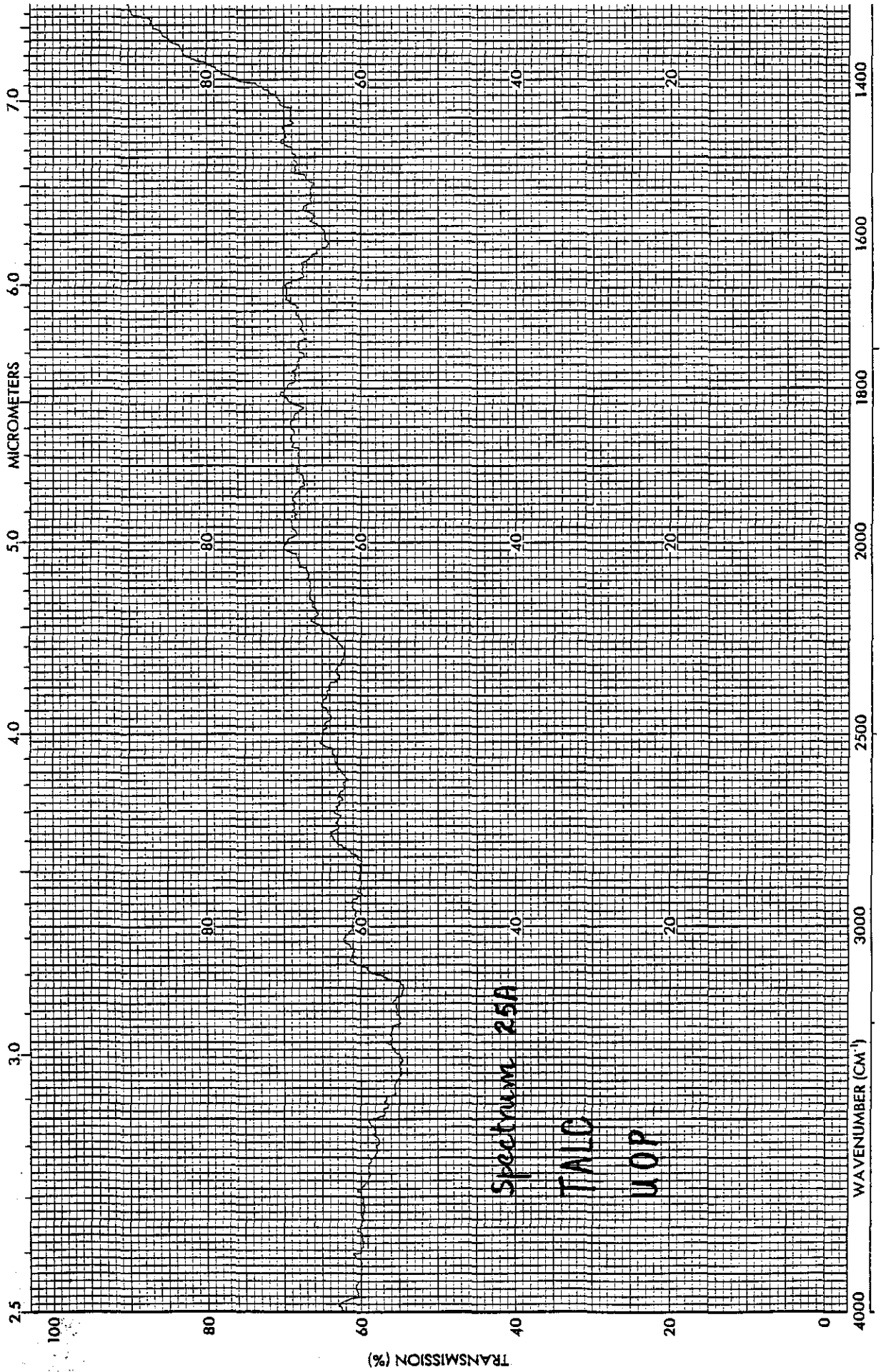
Delta College Geology Department

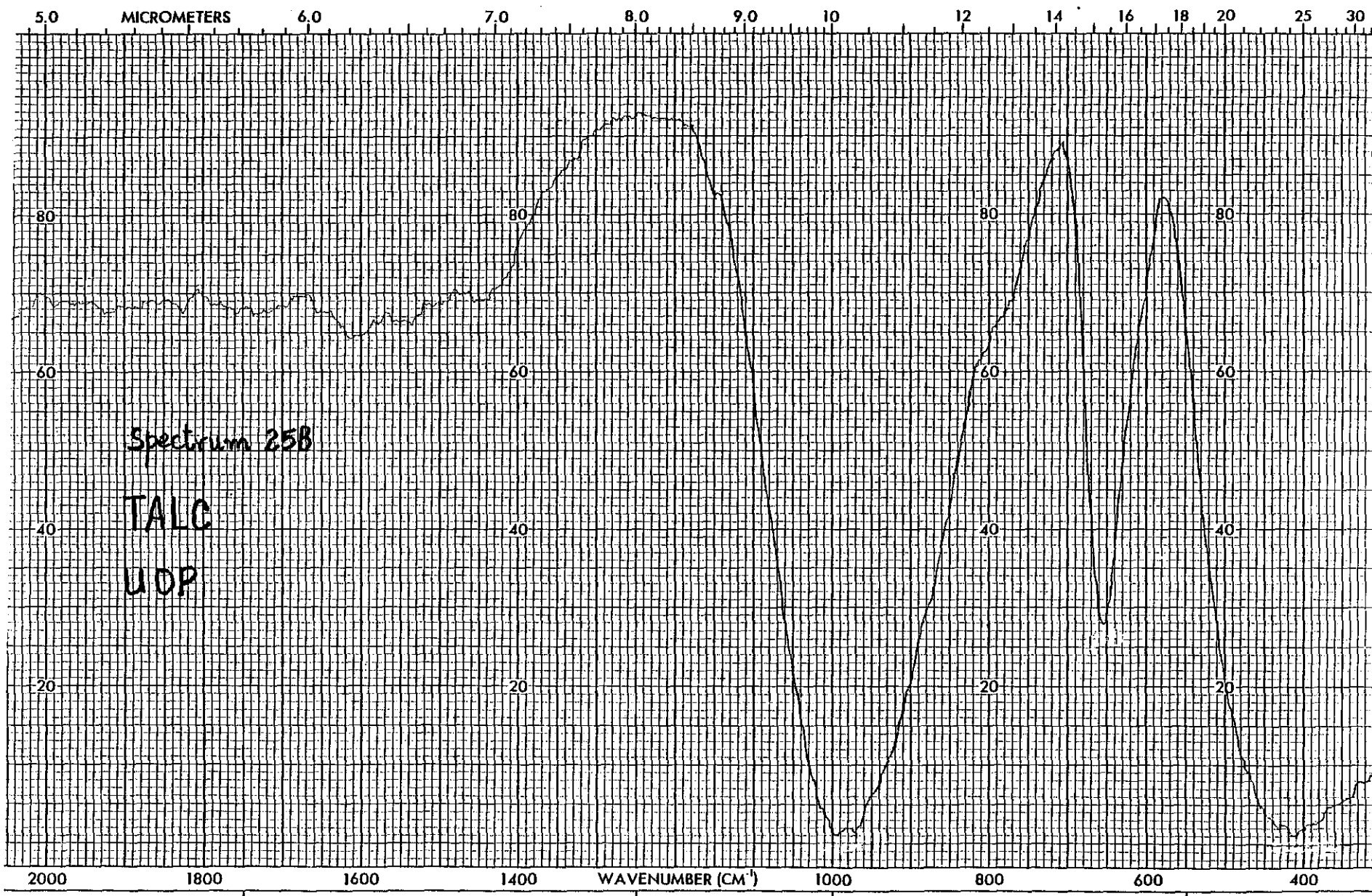


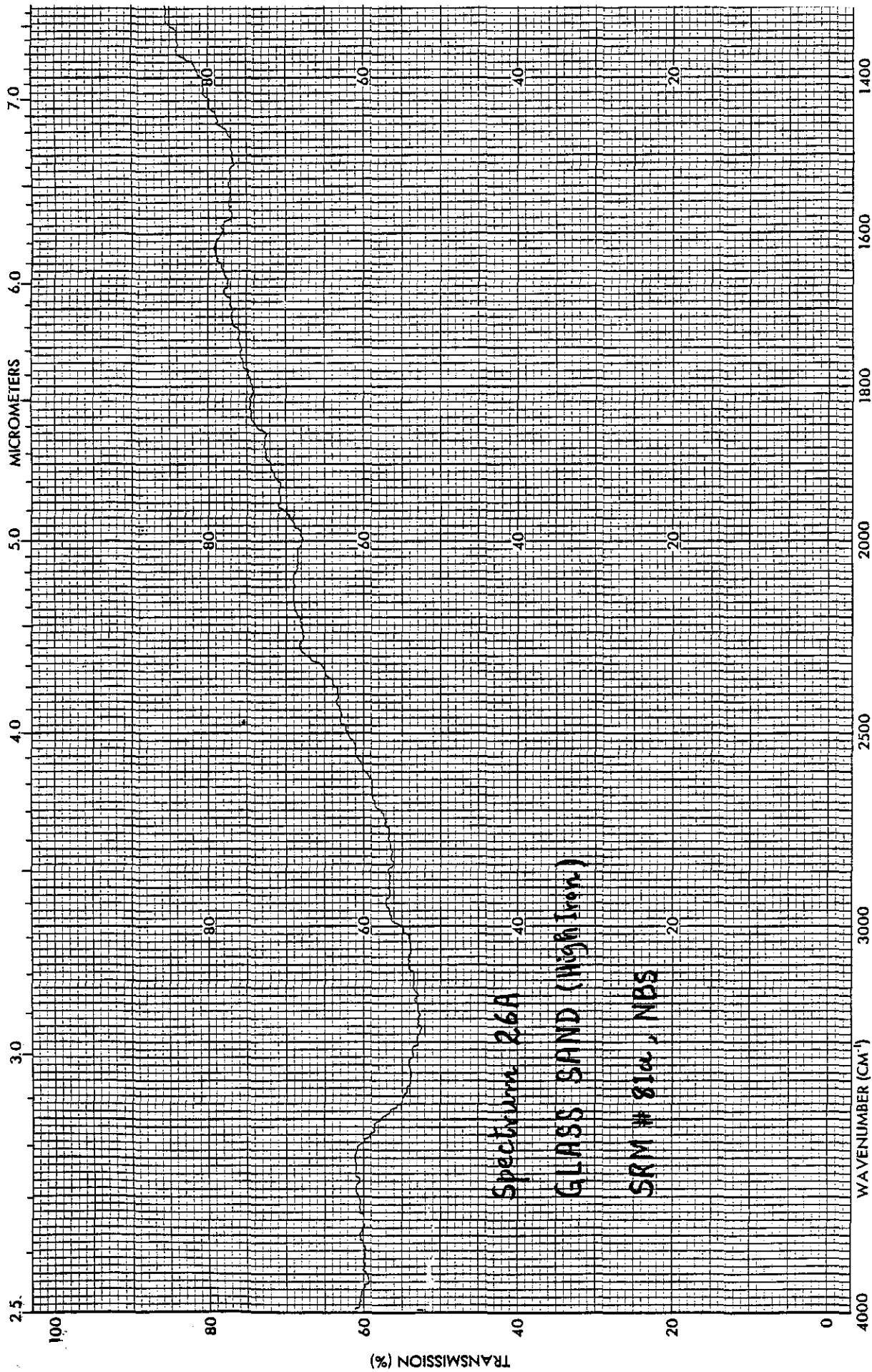
Spectrum 24B

TALS

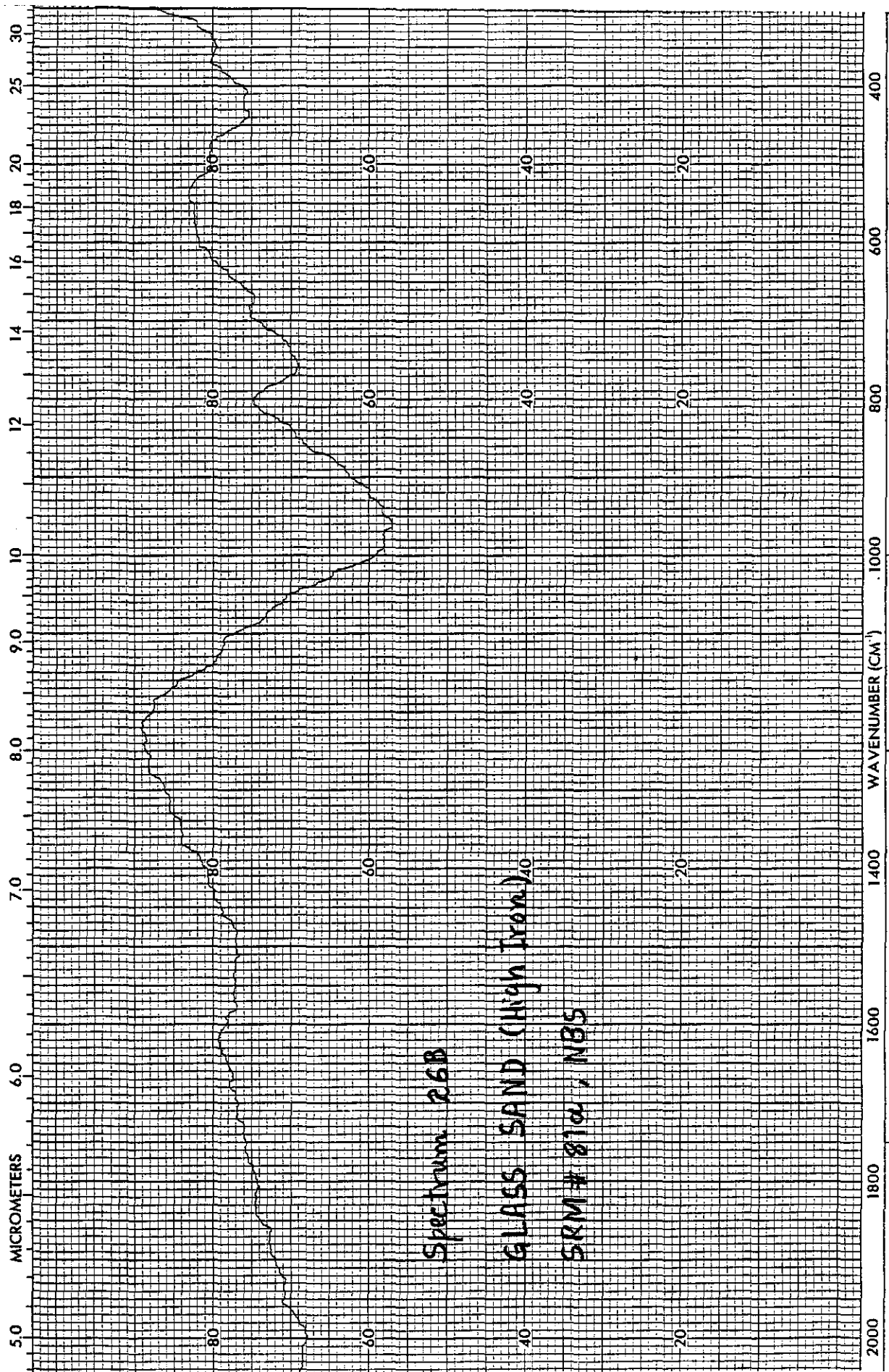
Delta College Geology Department

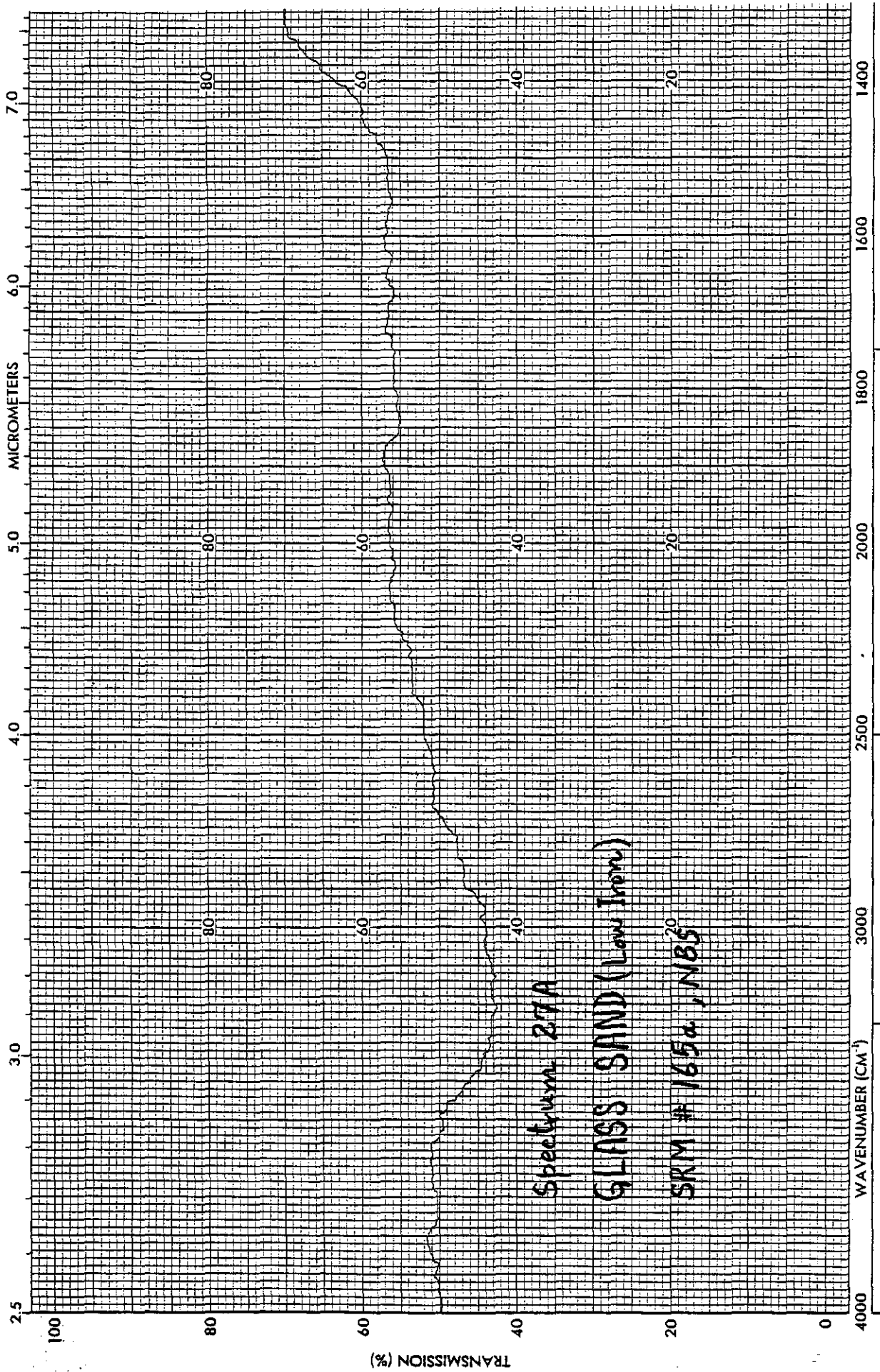






Spectrum 26A
GLASS SAND (High Iron)
SRM # 81a, NBS

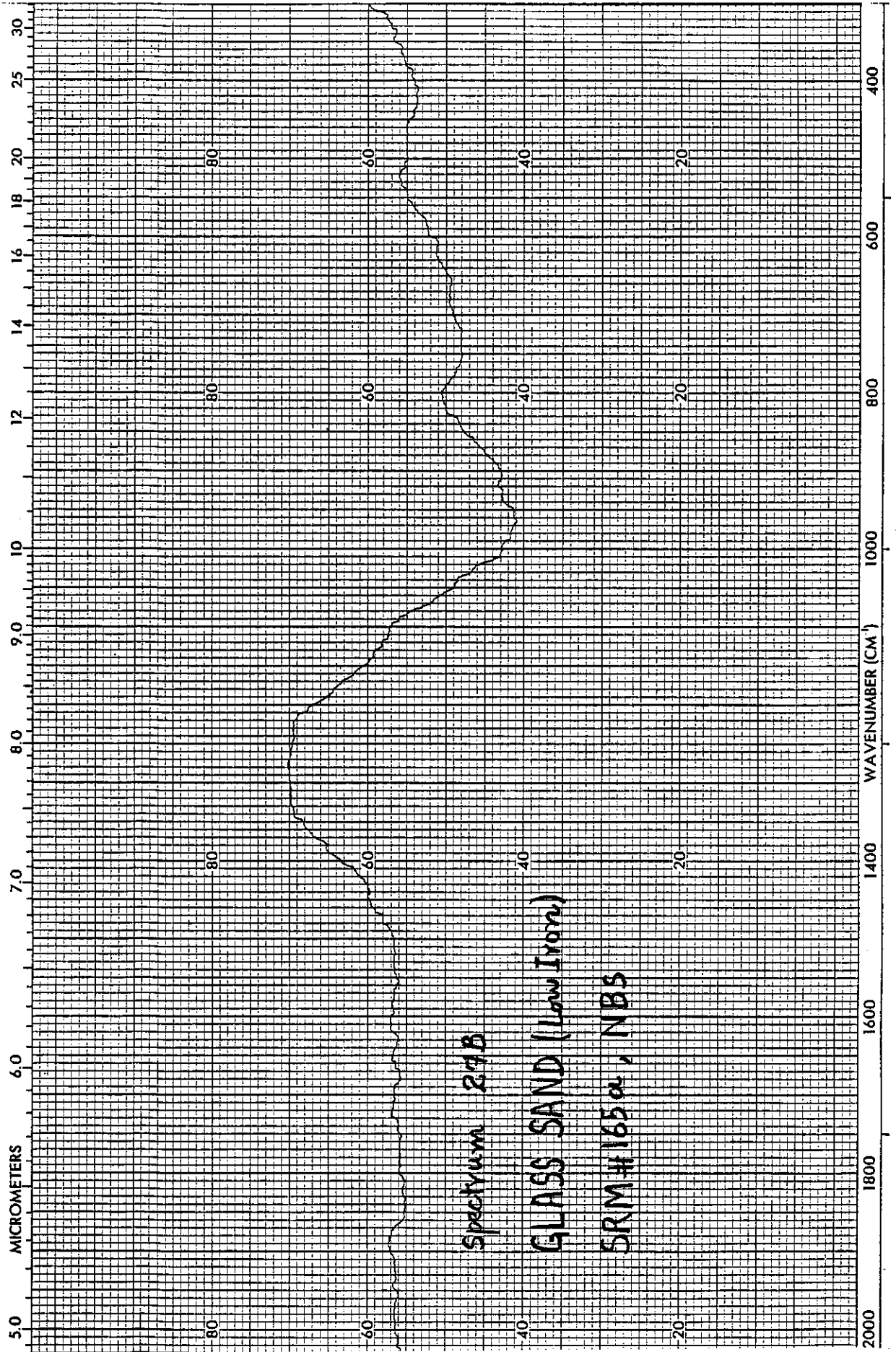


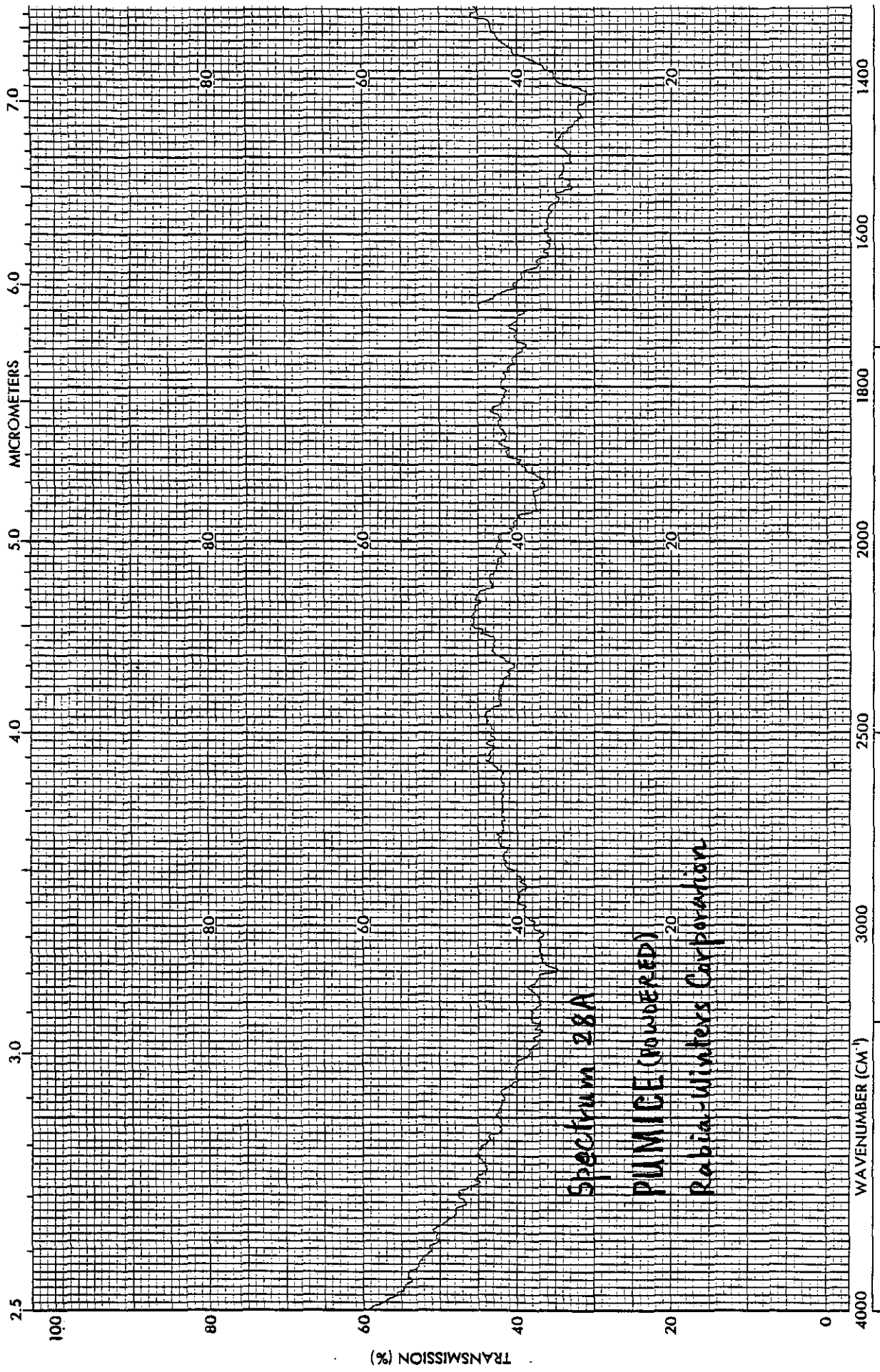


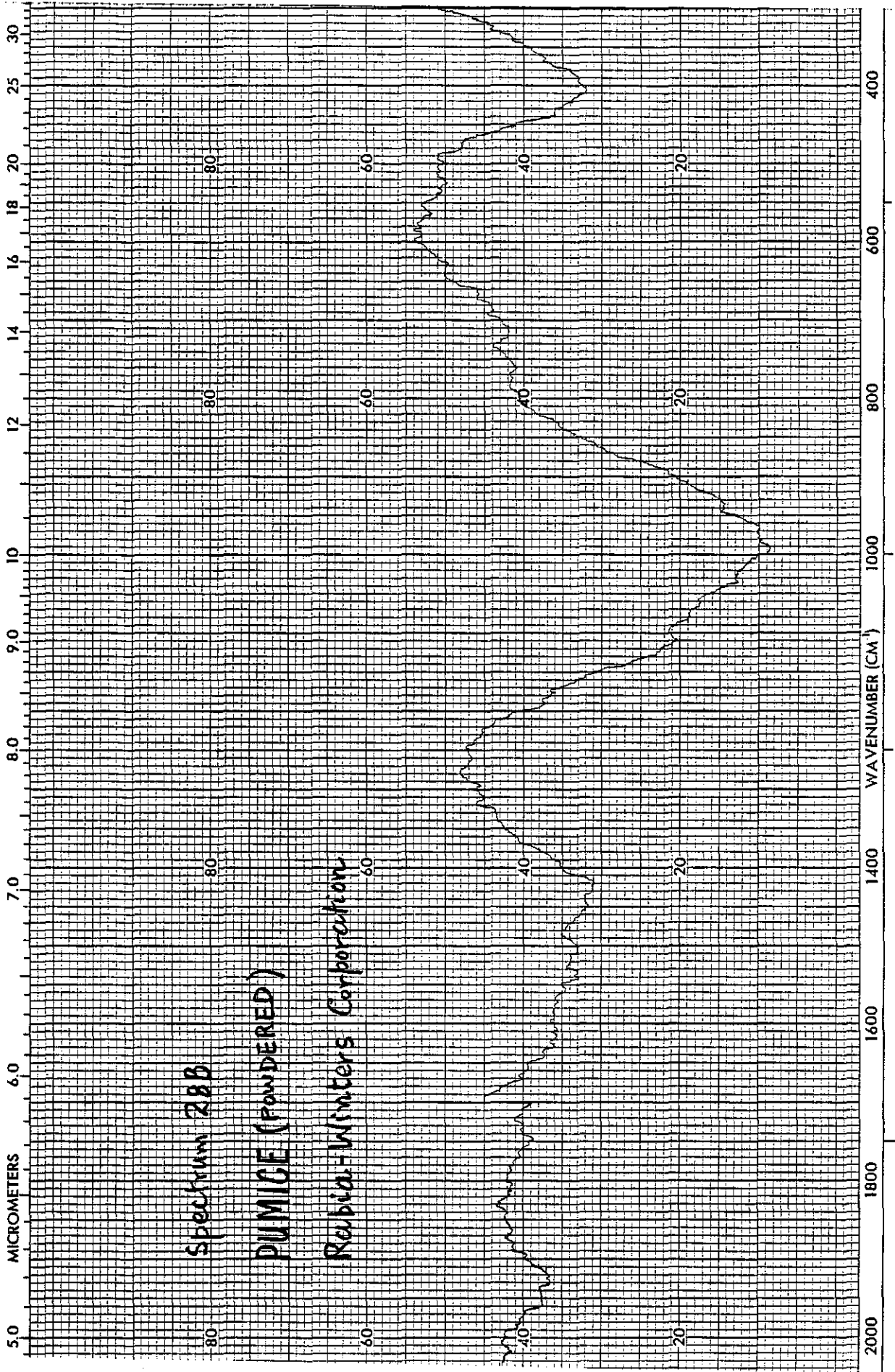
Spectrum 27A

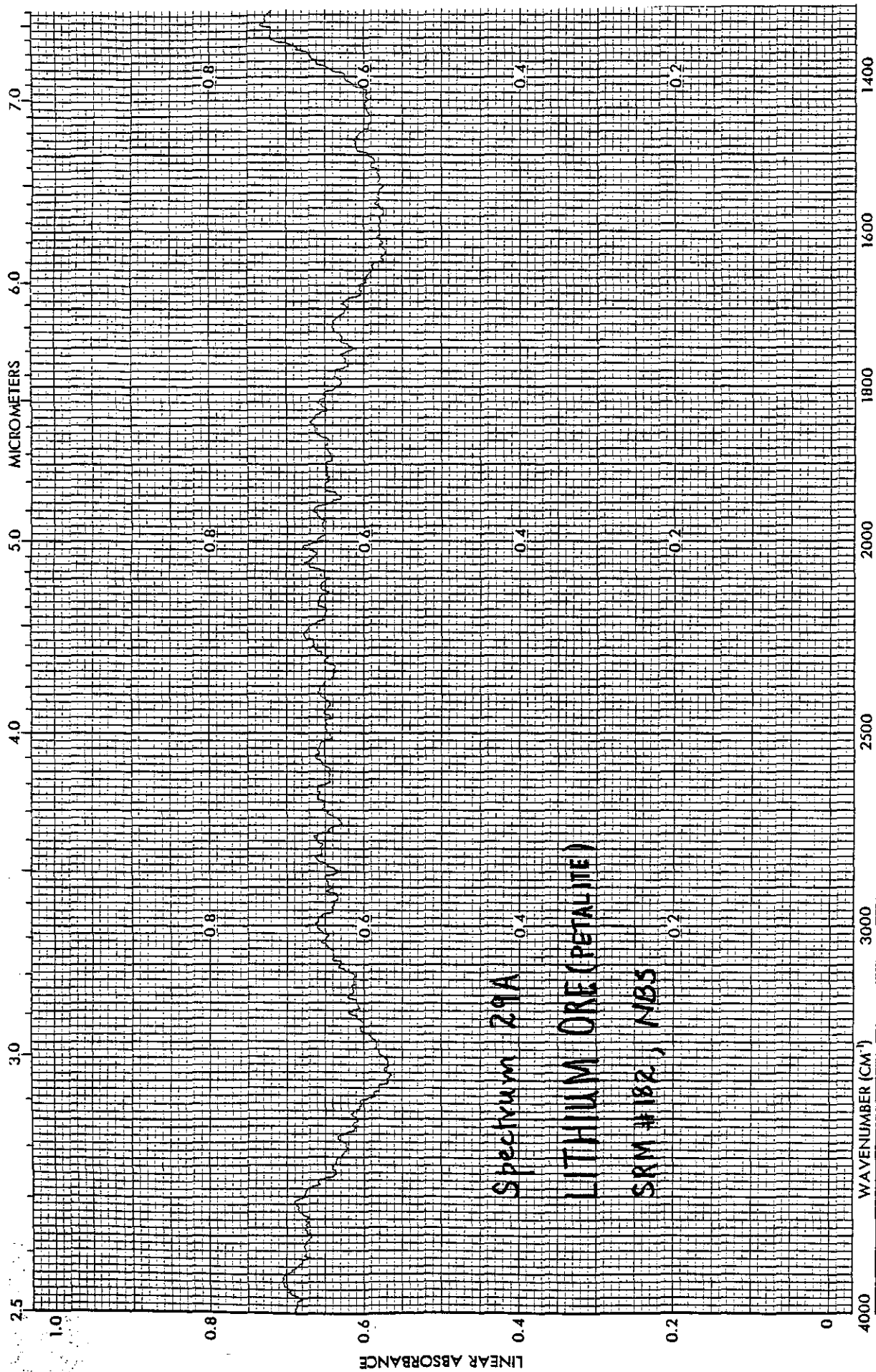
GLASS SAND (Low Iron)

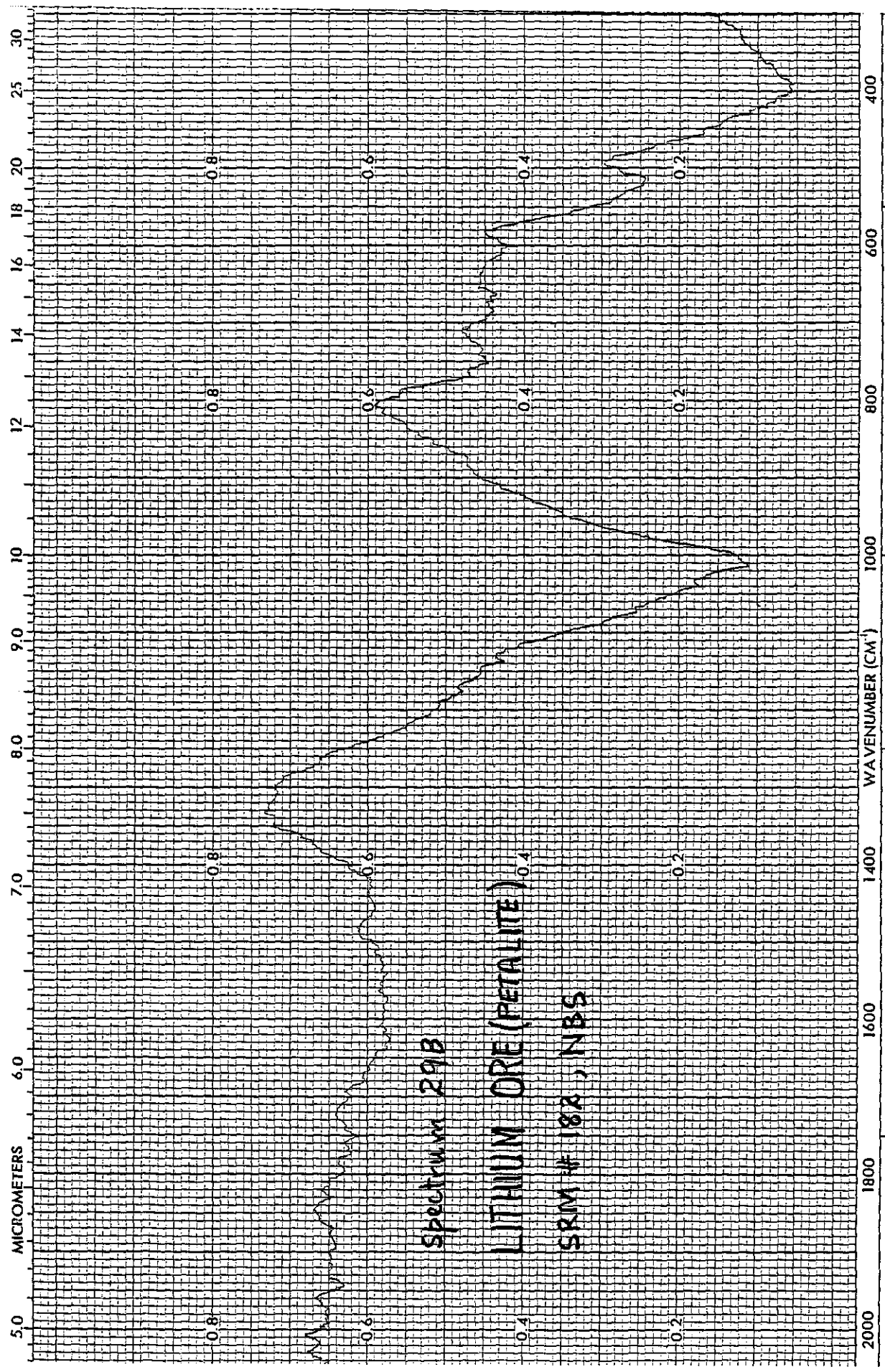
SRM # 165a, NBS

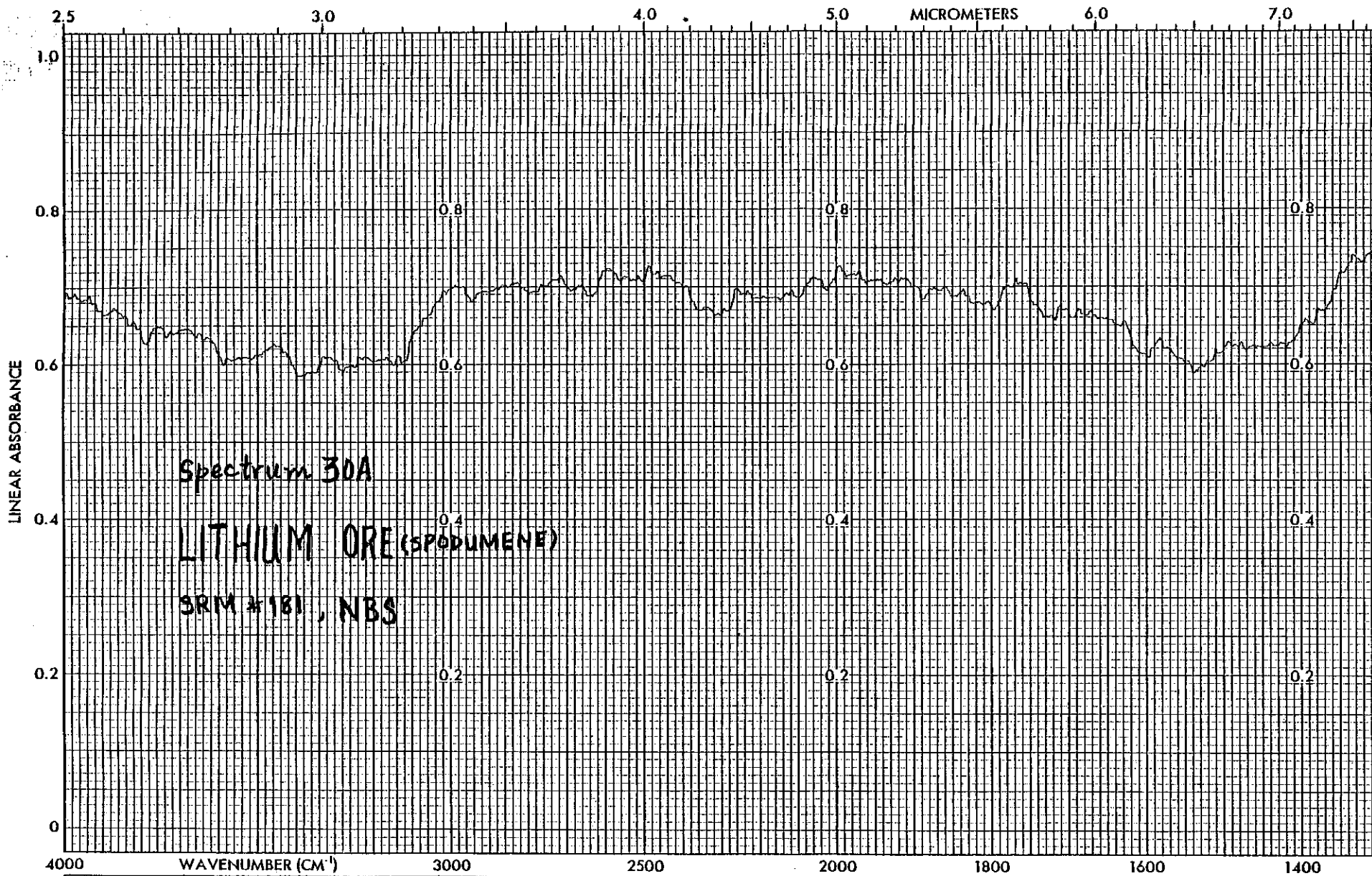


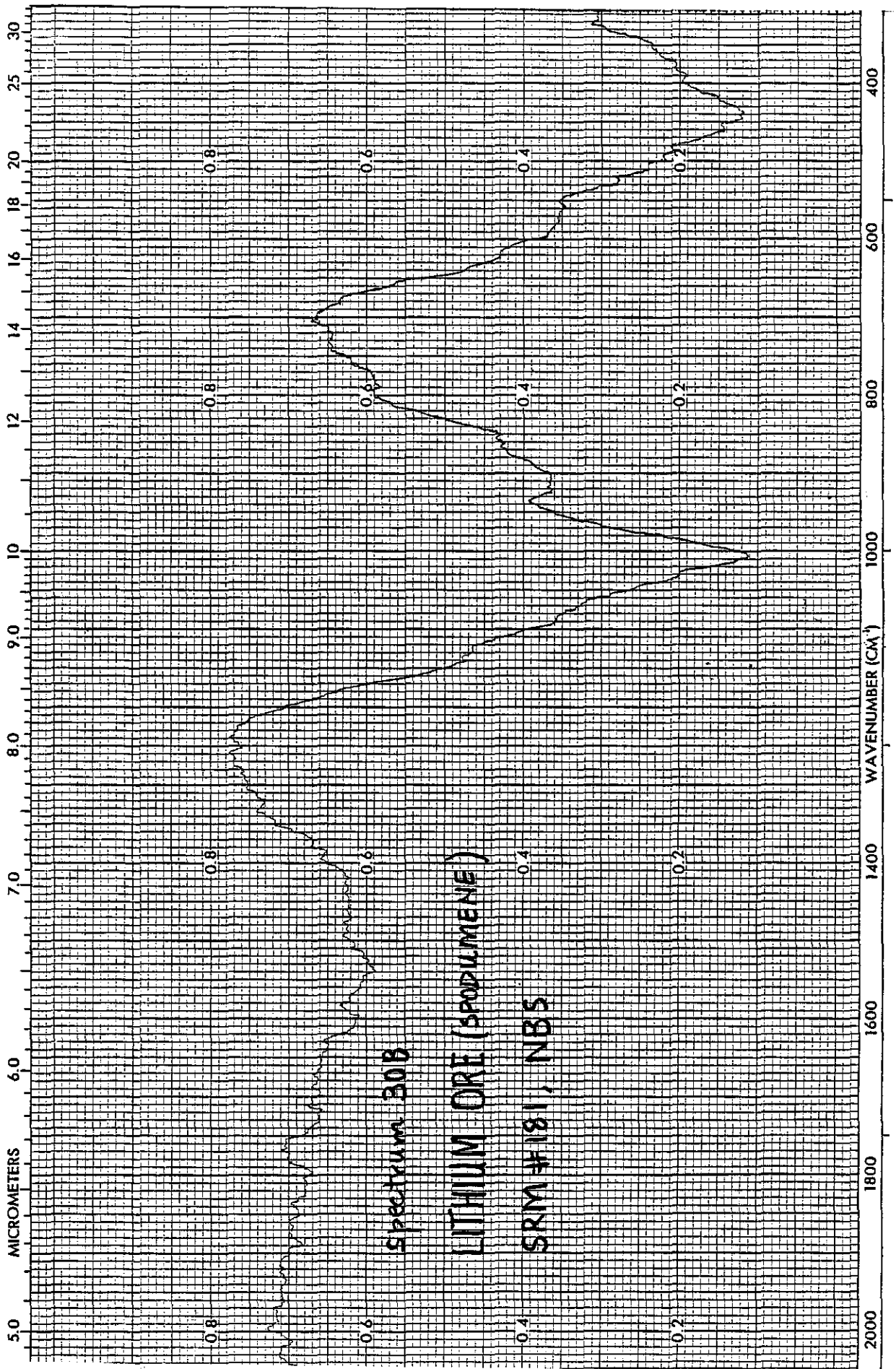


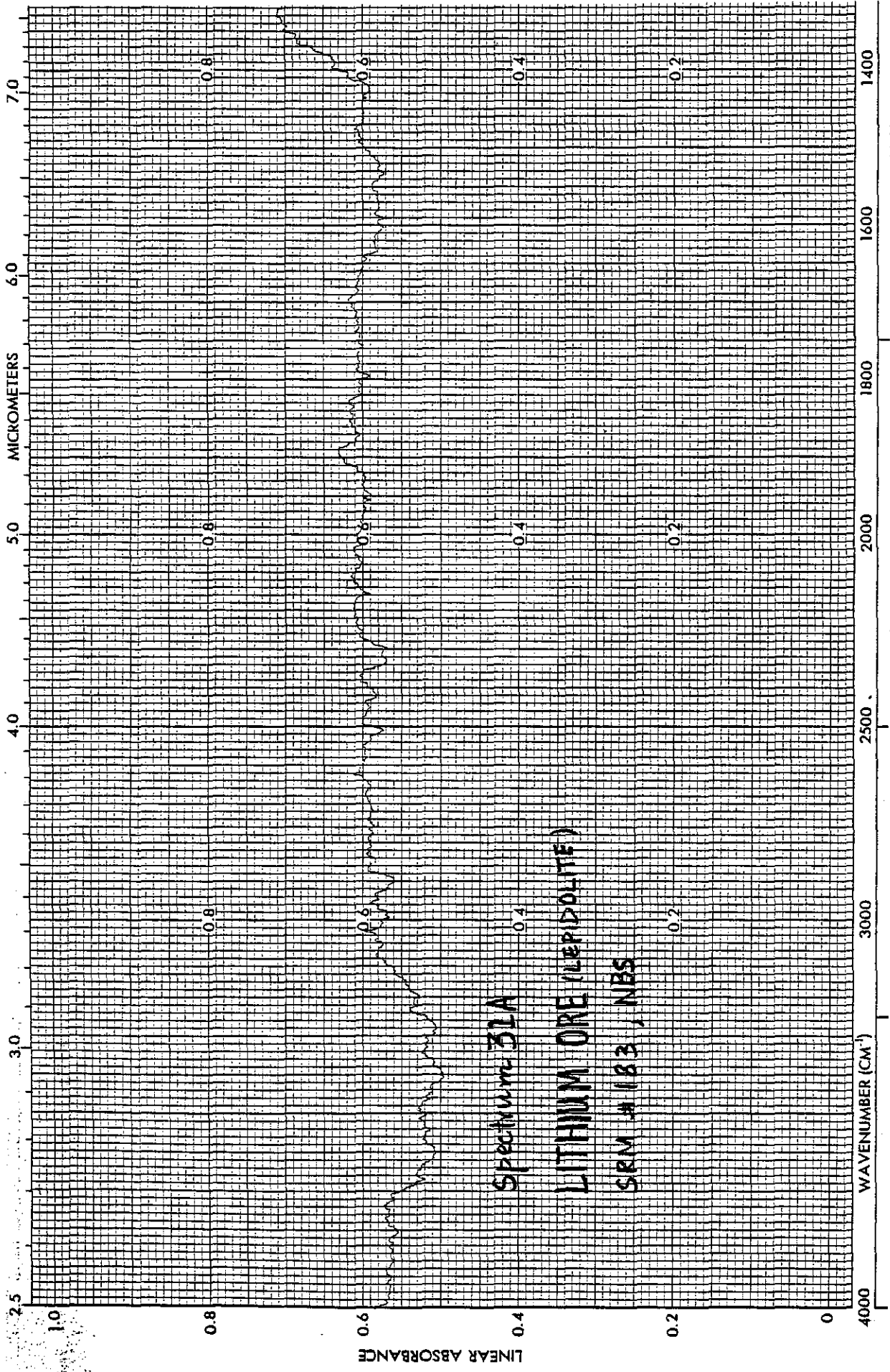


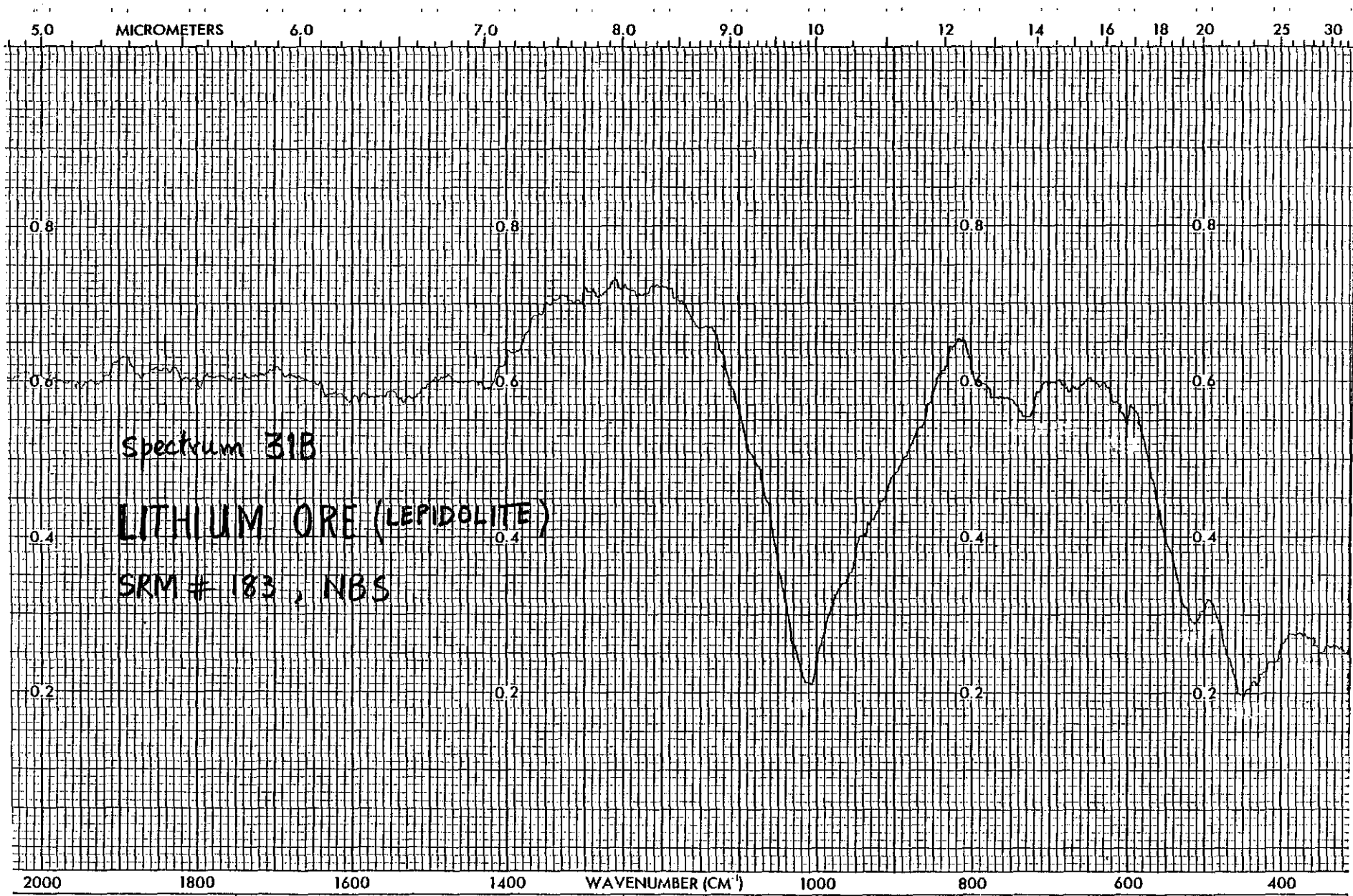


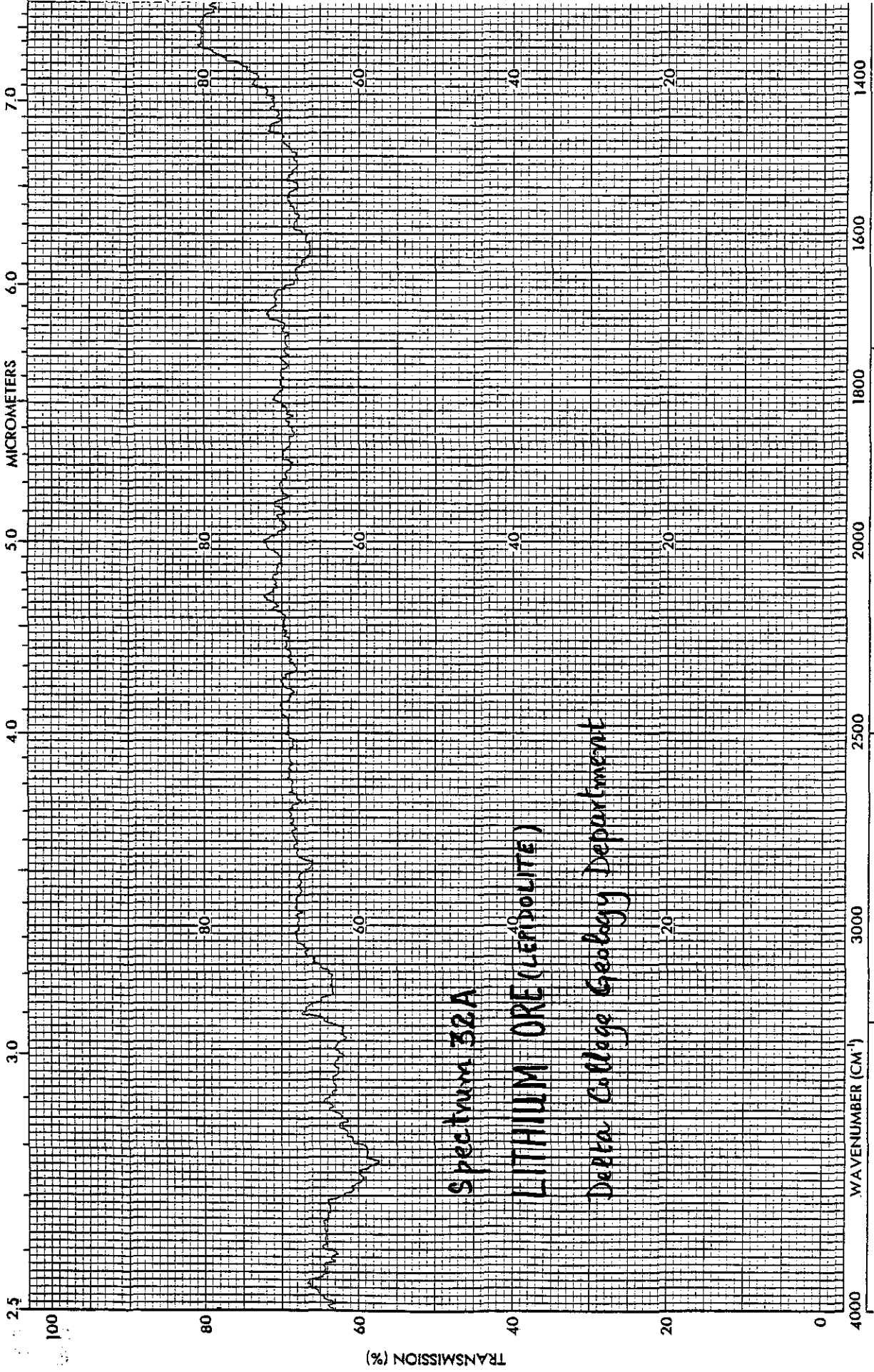


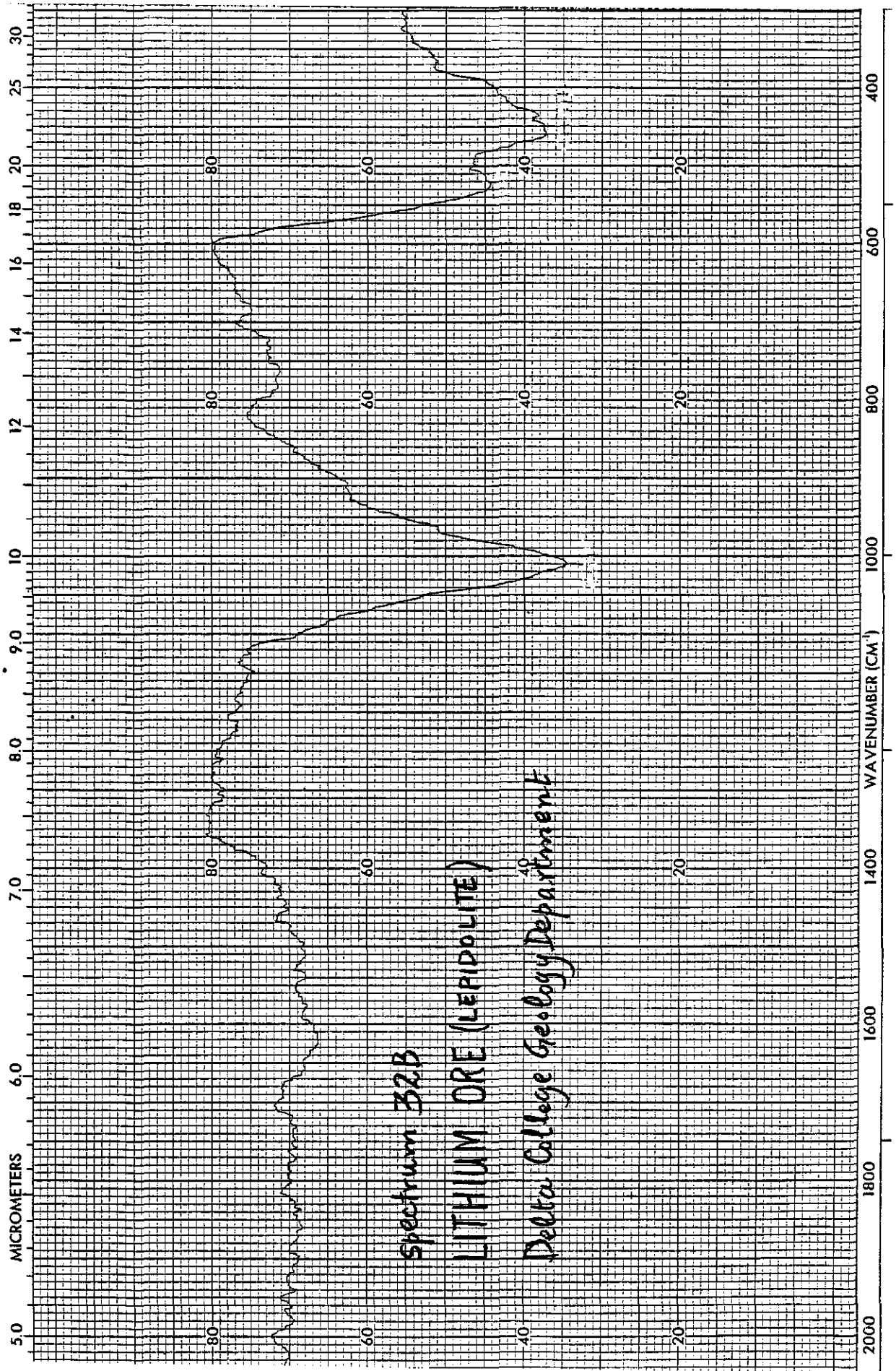








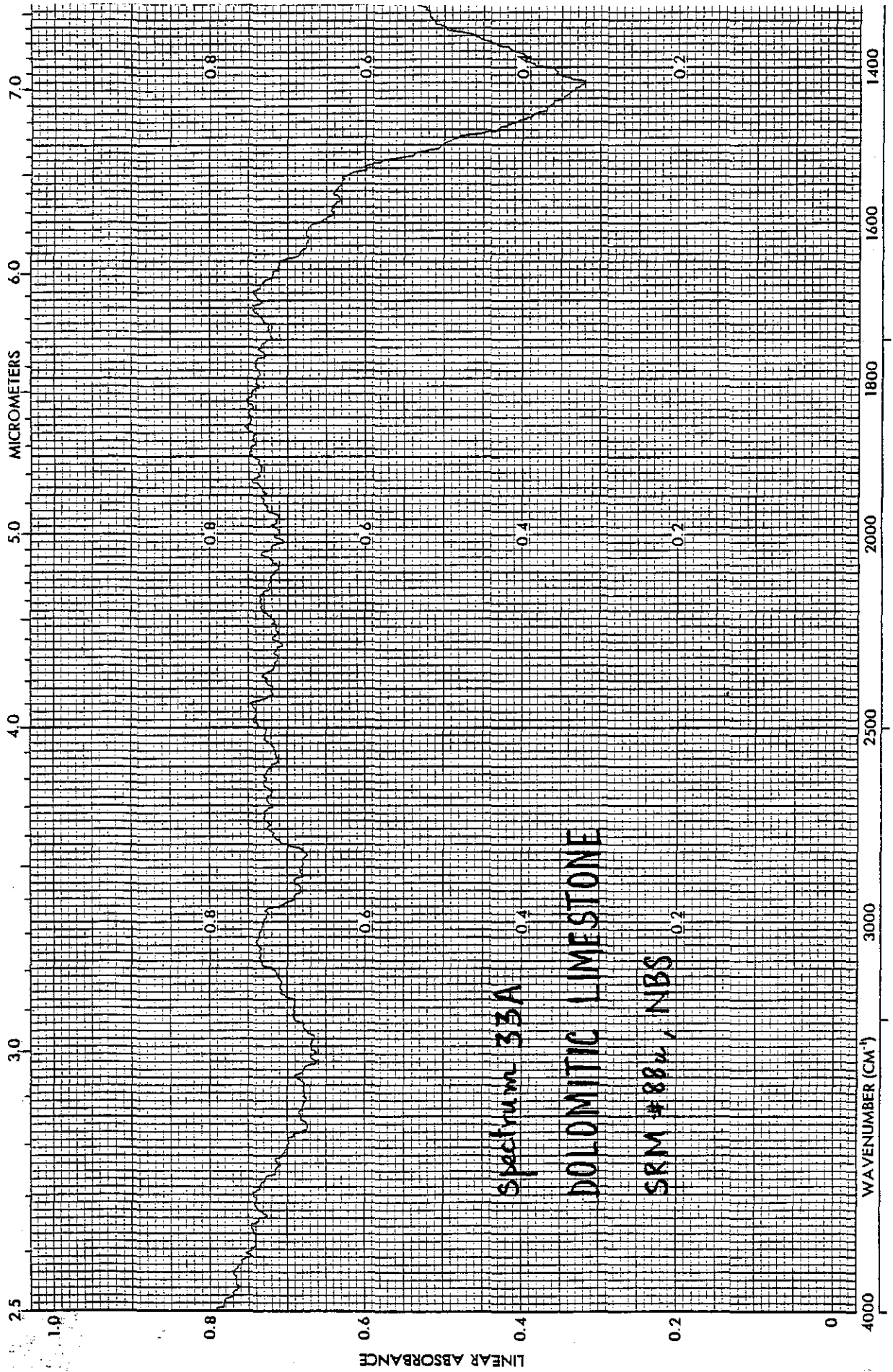


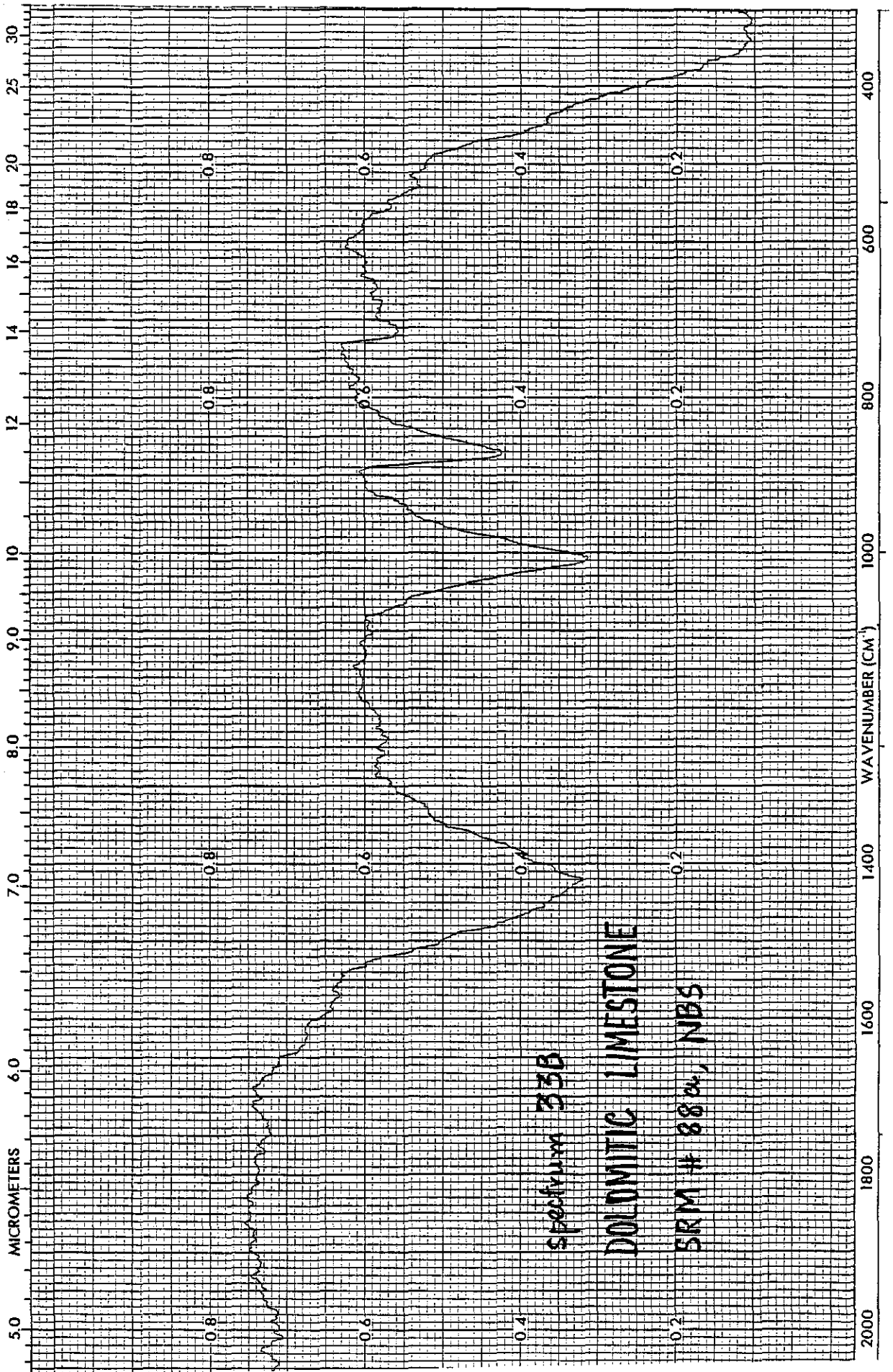


Spectrum 32B

LITHIUM ORE (LEPIDOLITE)

Delta College Geology Department

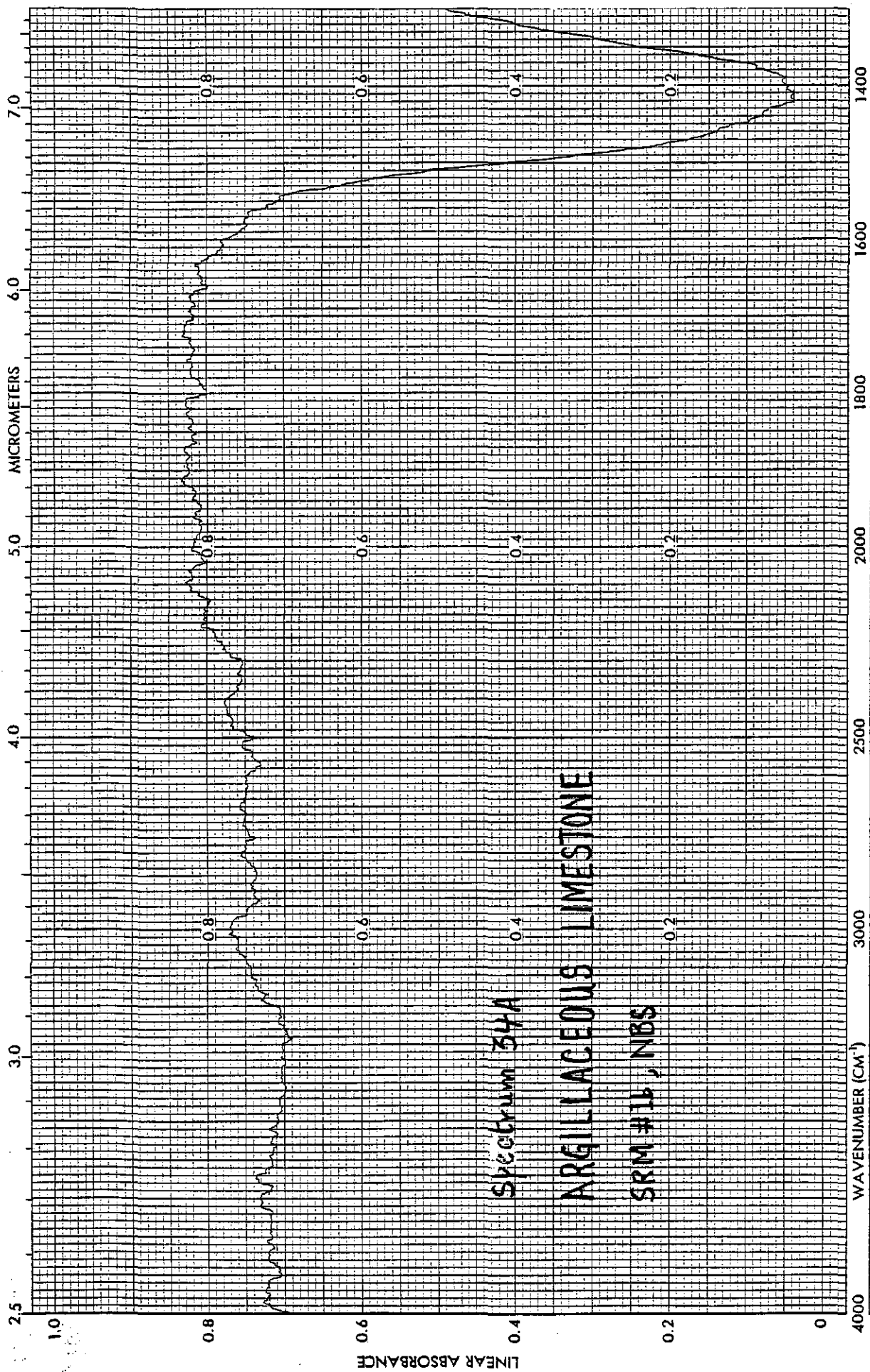




Spectrum 33B

DOLOMITIC LIMESTONE

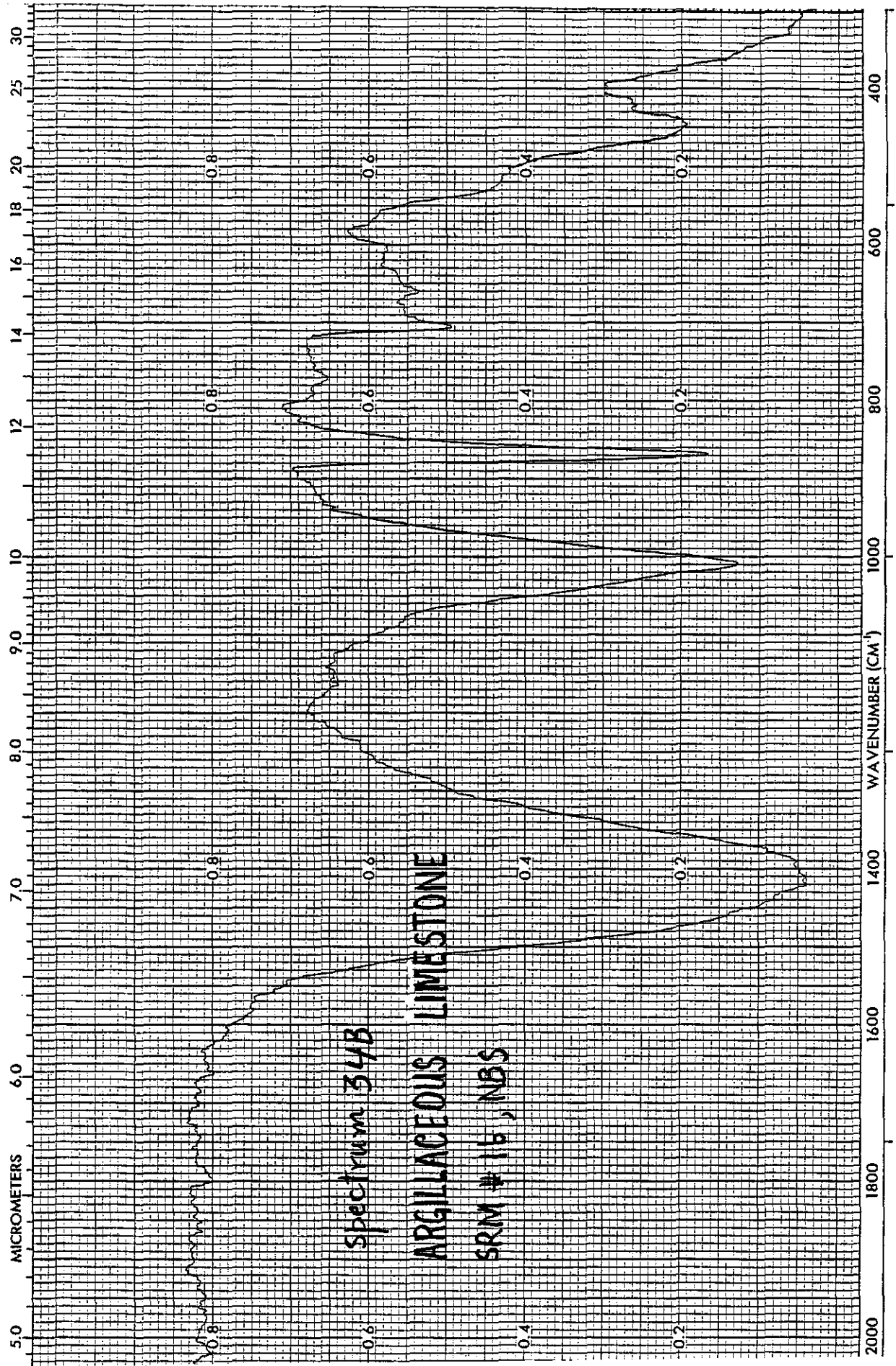
SRM # 88a, NBS

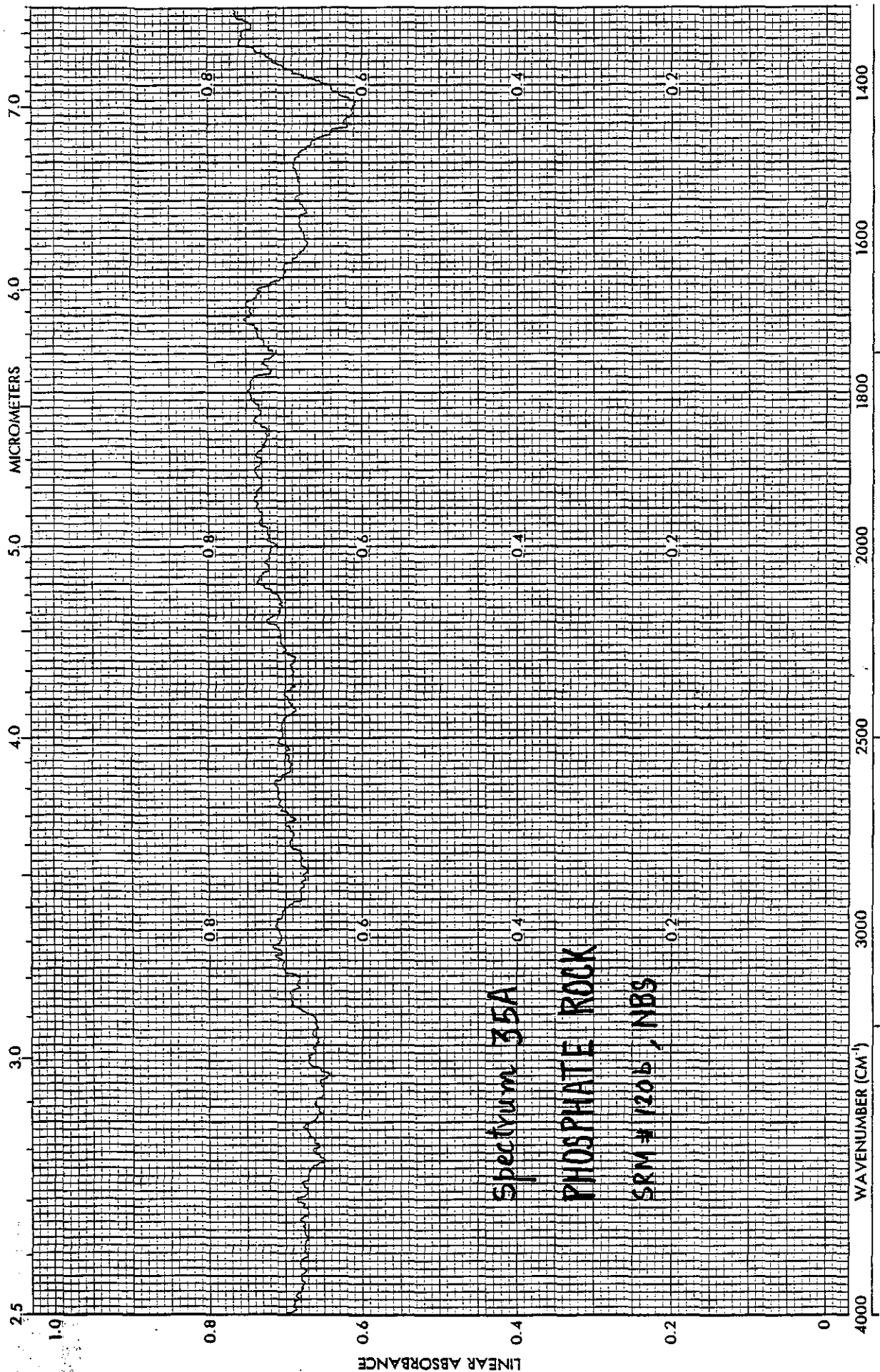


Spectrum 37A

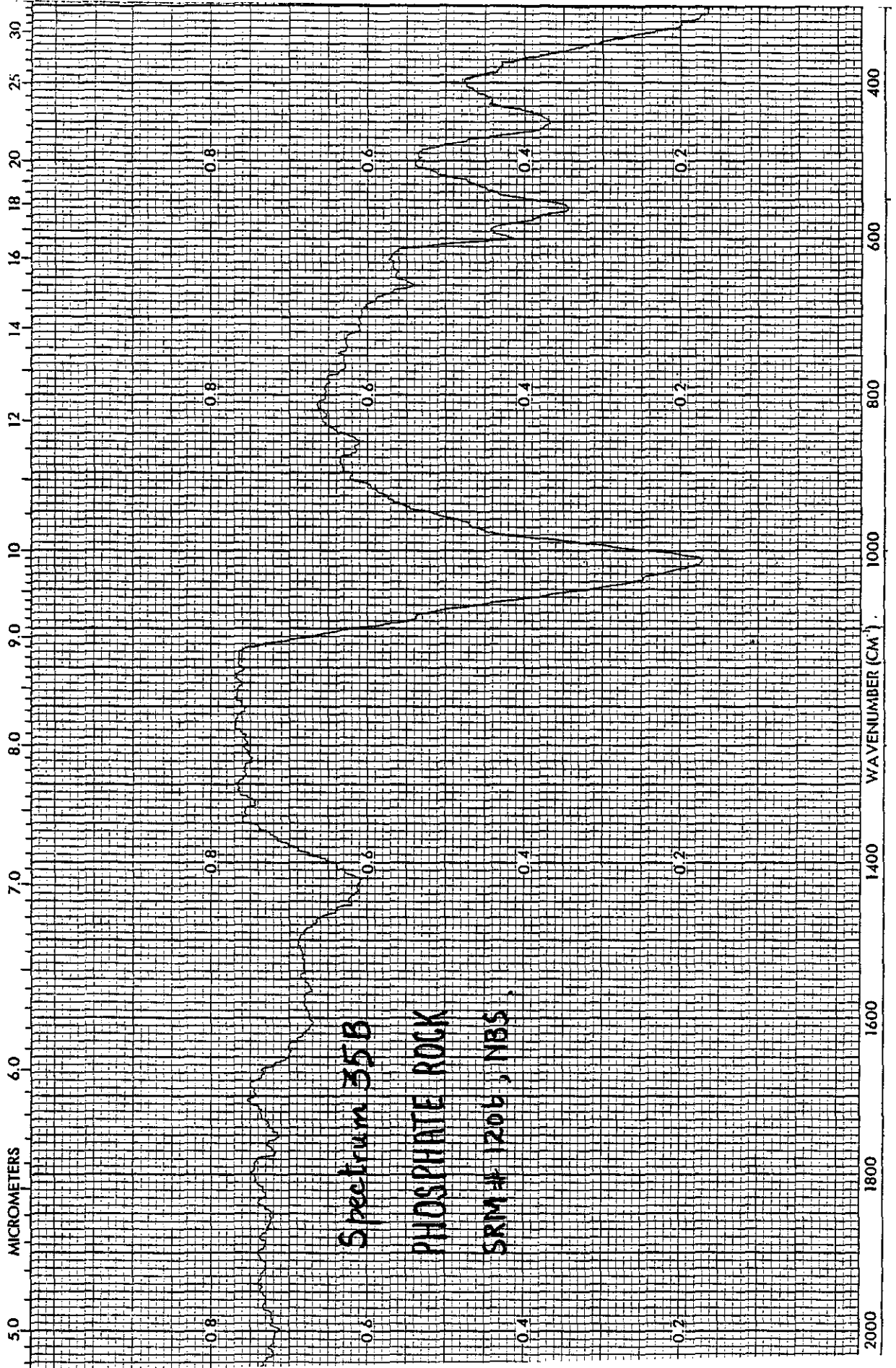
ARGILLACEOUS LIMESTONE

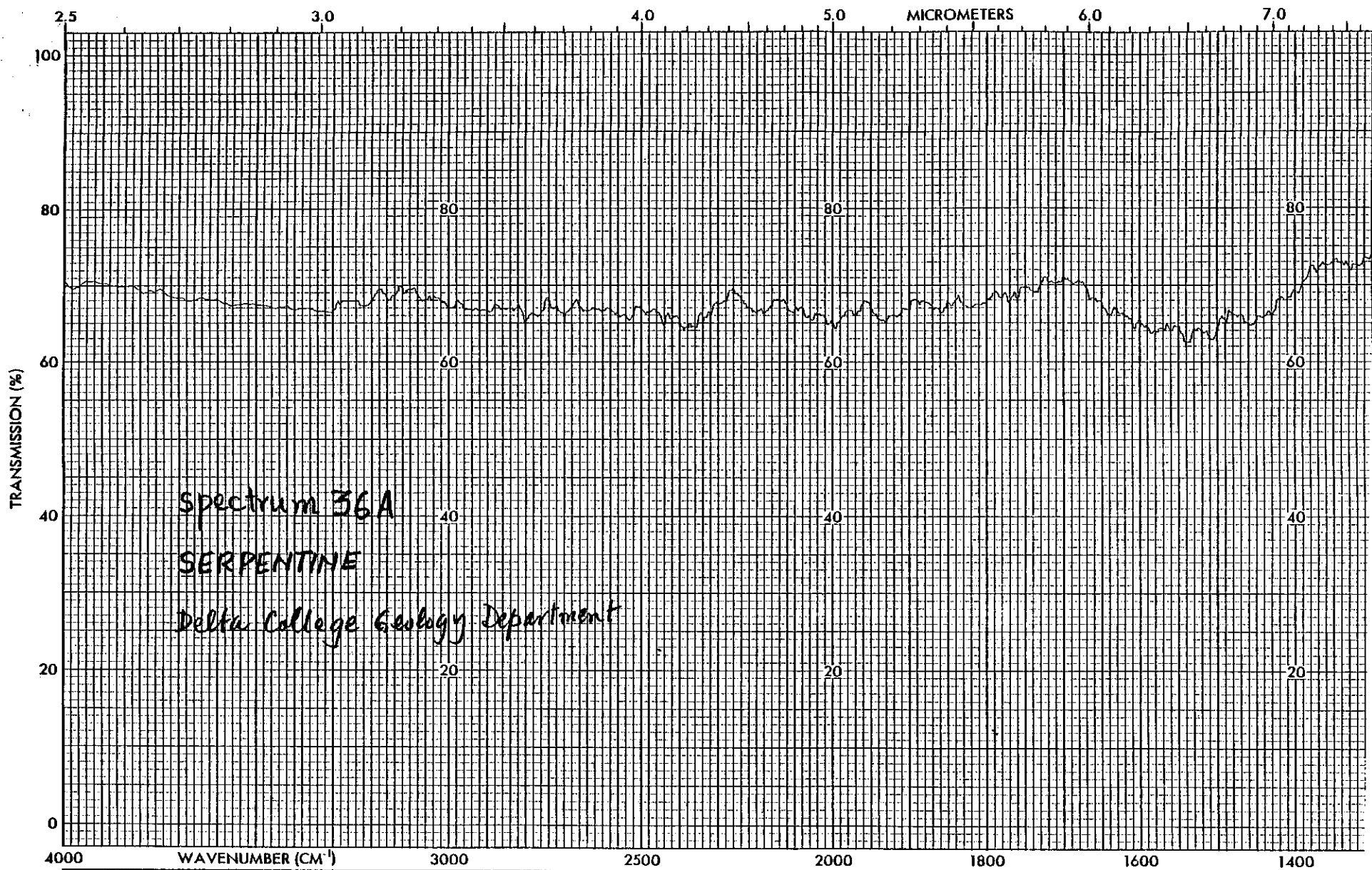
SRM #1B, NBS

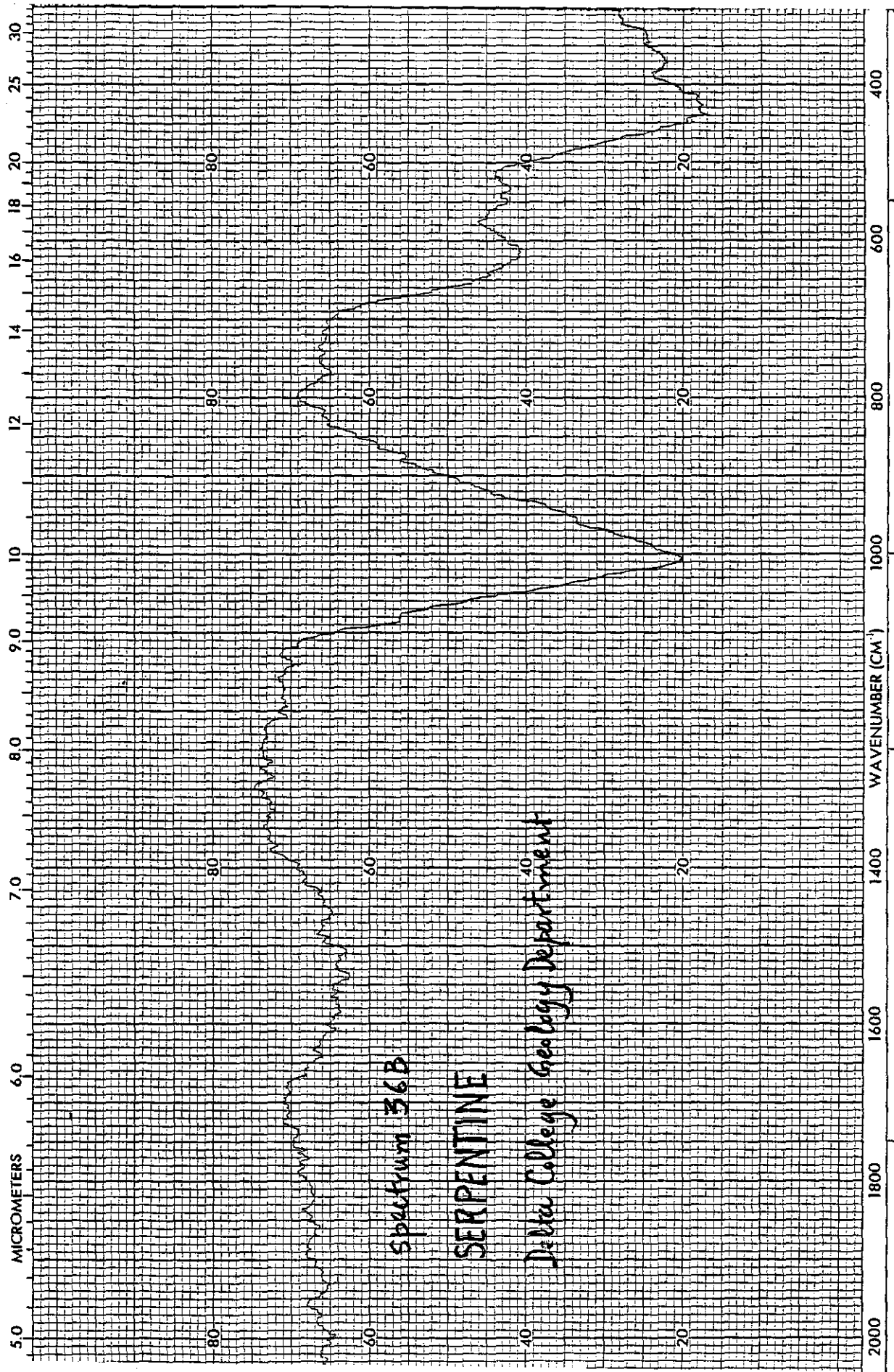




Spectrum 35A
PHOSPHATE ROCK
SRM #120b, NBS



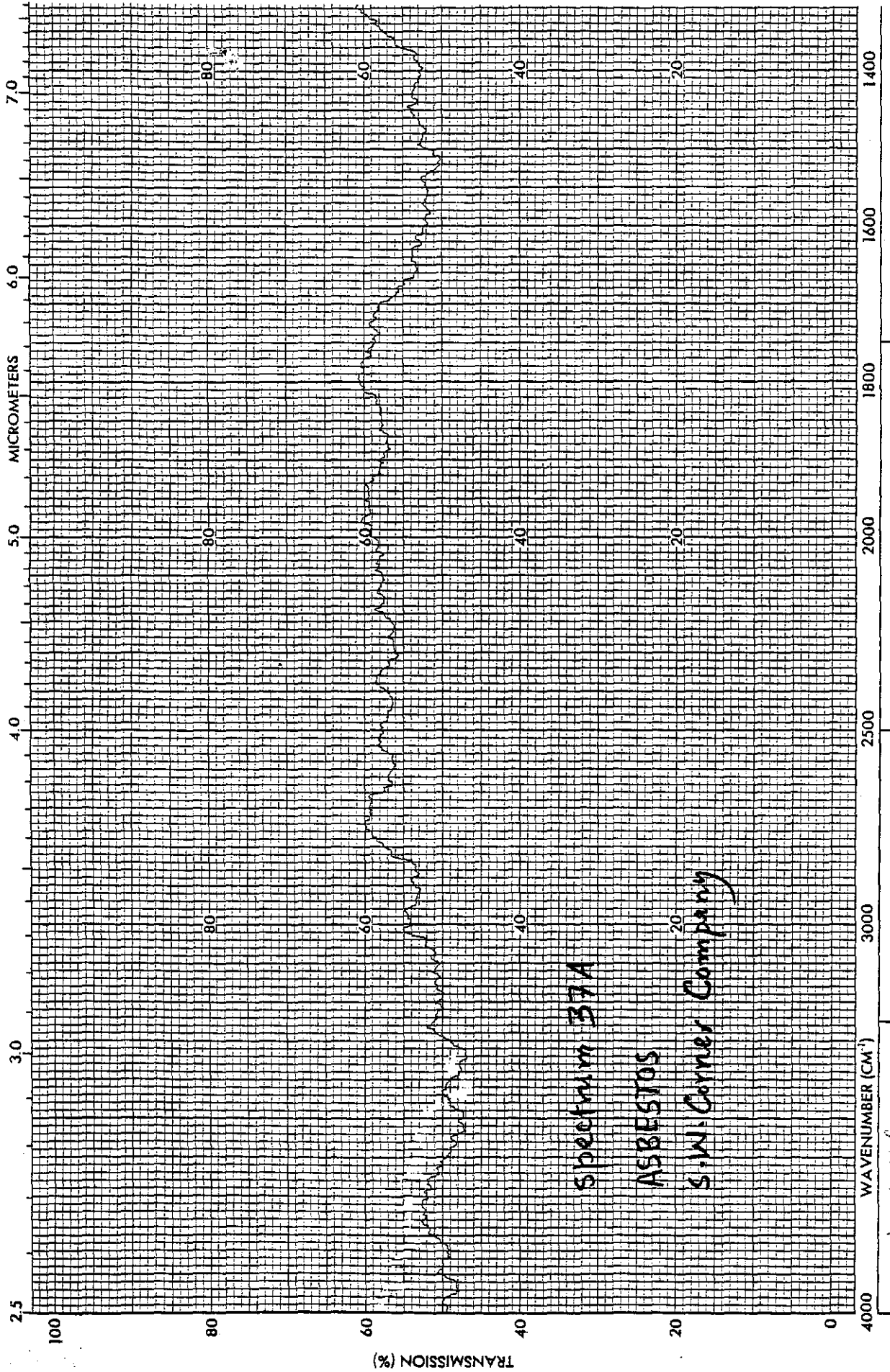




Spectrum 36B

SERPENTINE

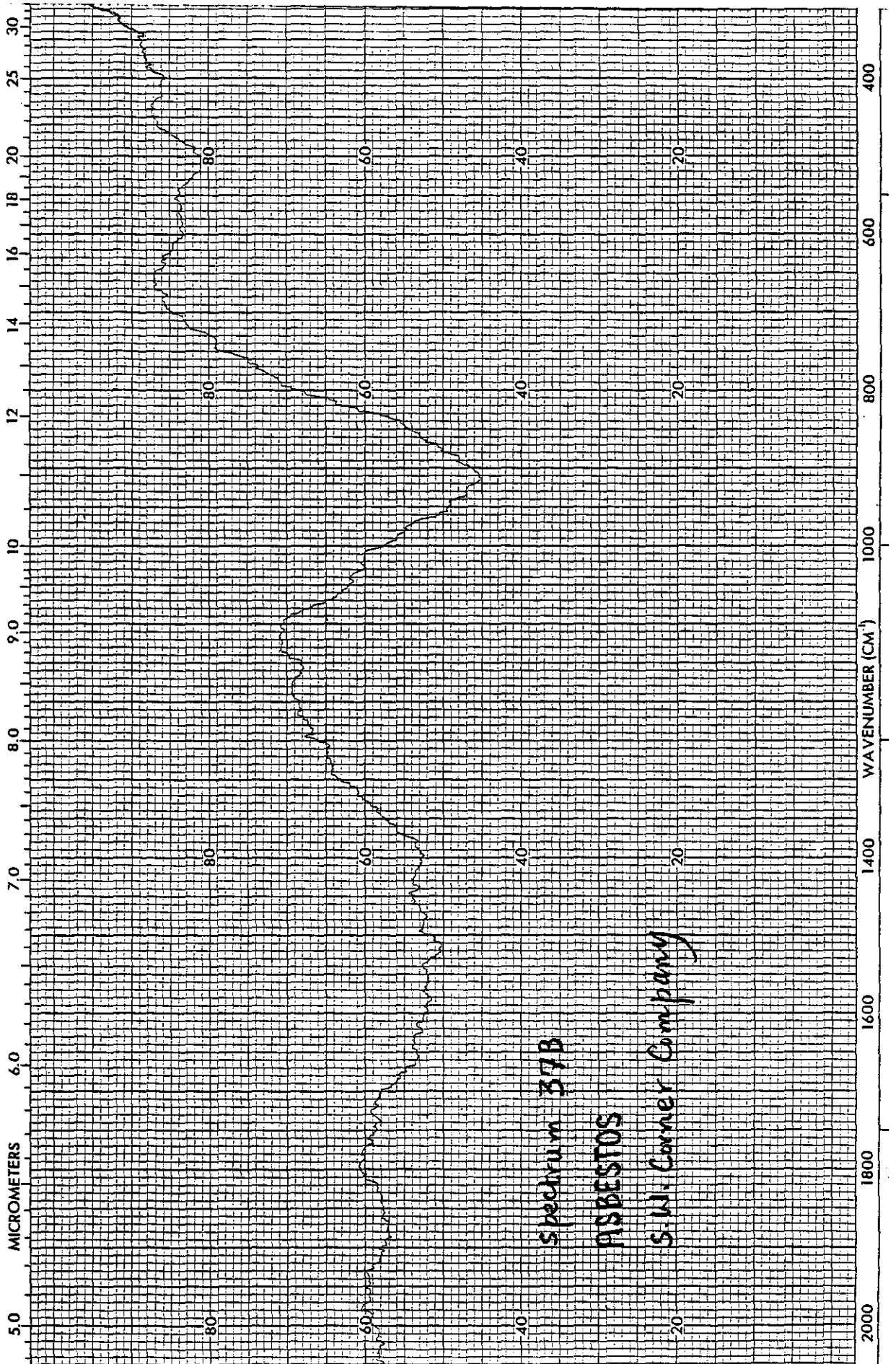
DeWitt College Geology Department

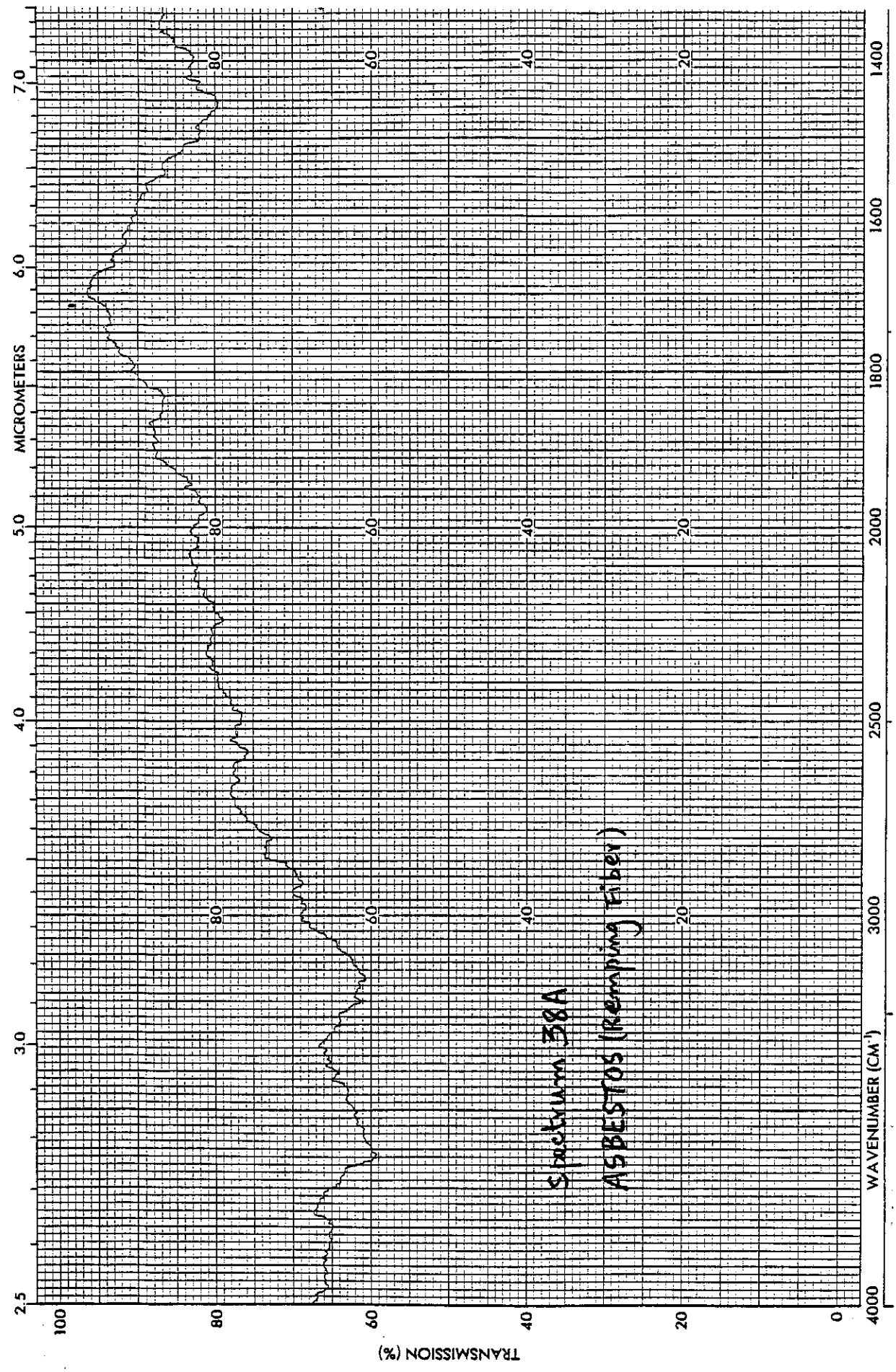


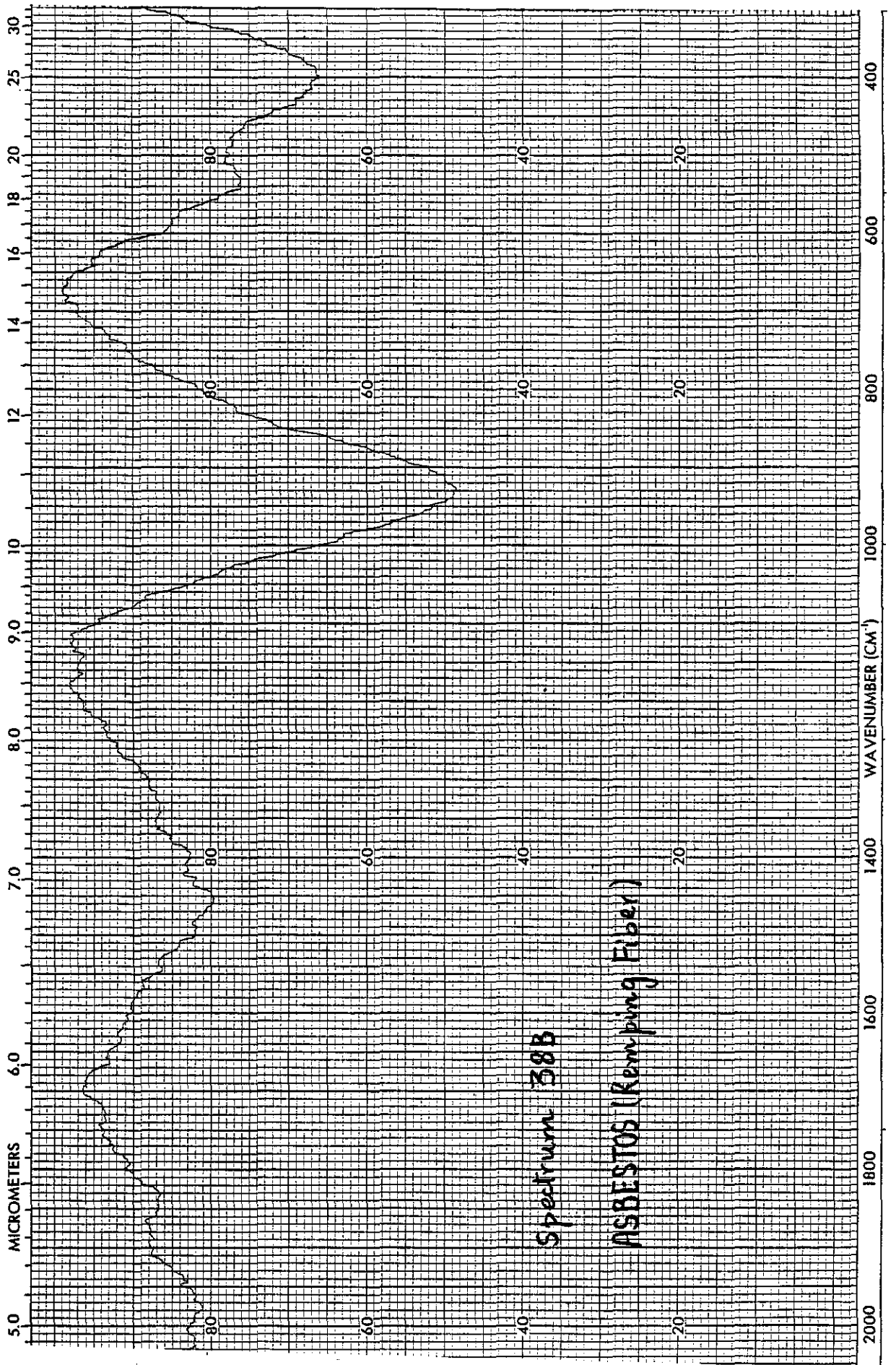
Spectrum 37A

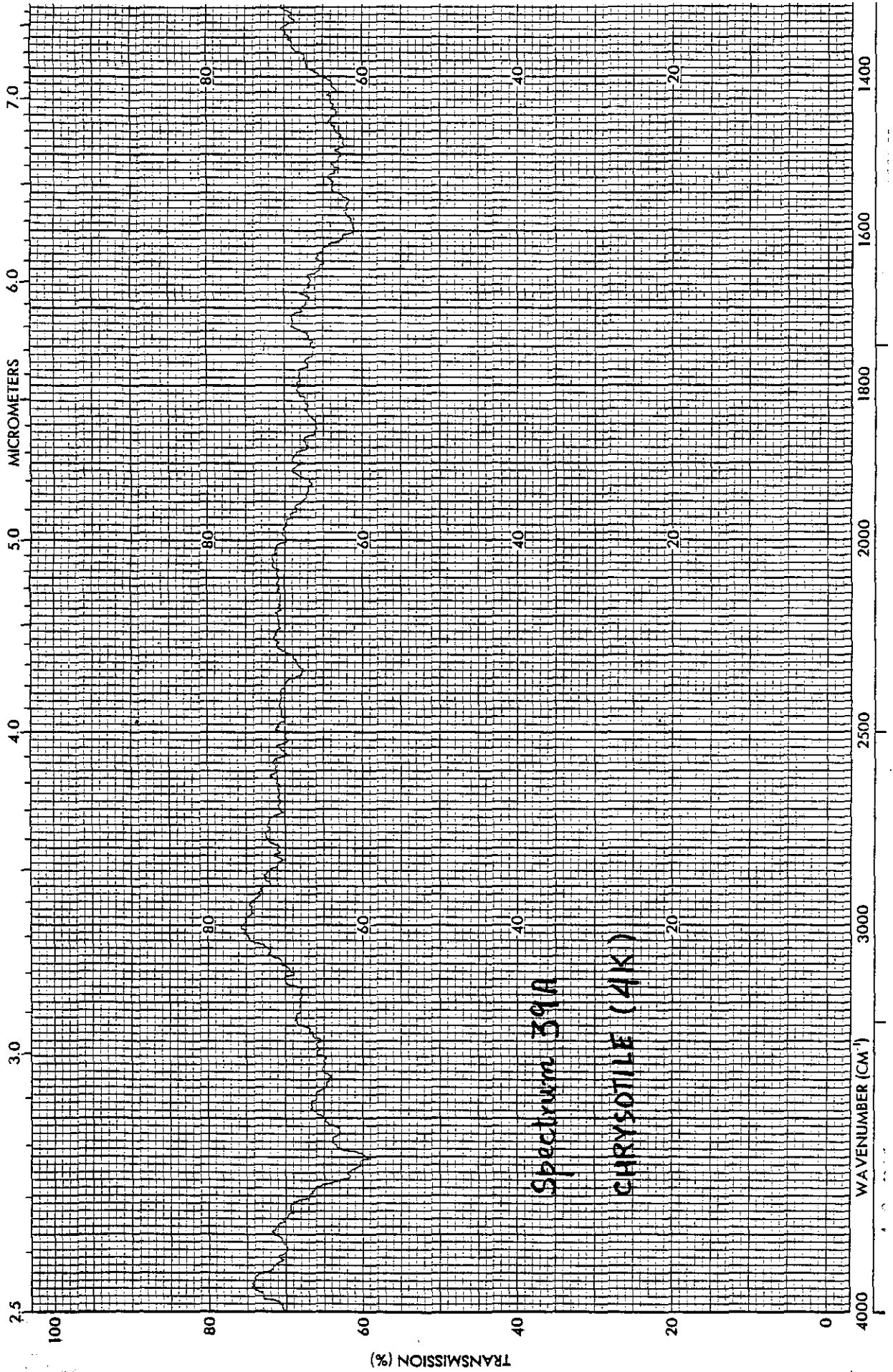
ASBESTOS

S.W. Corrier Company

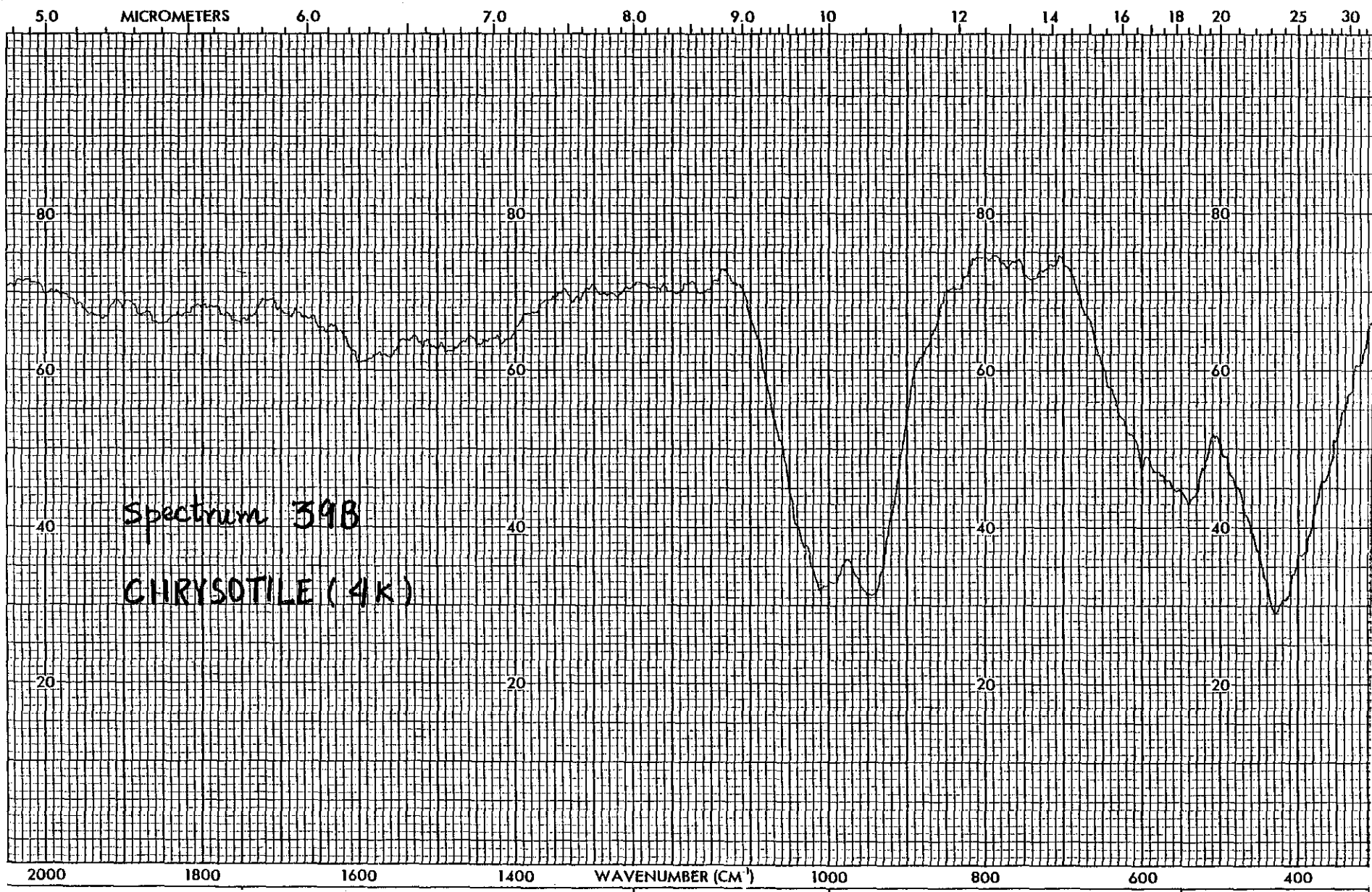


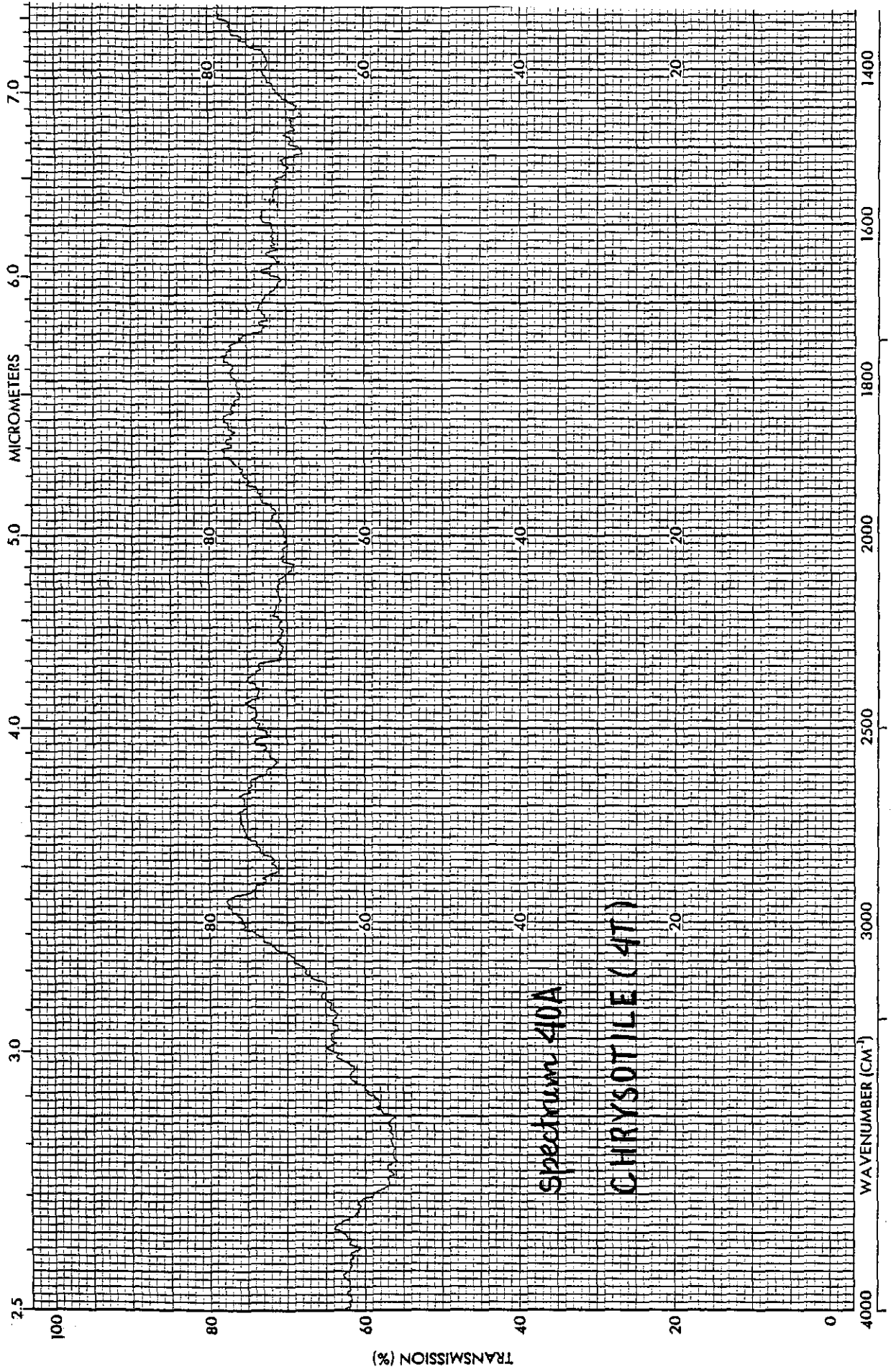




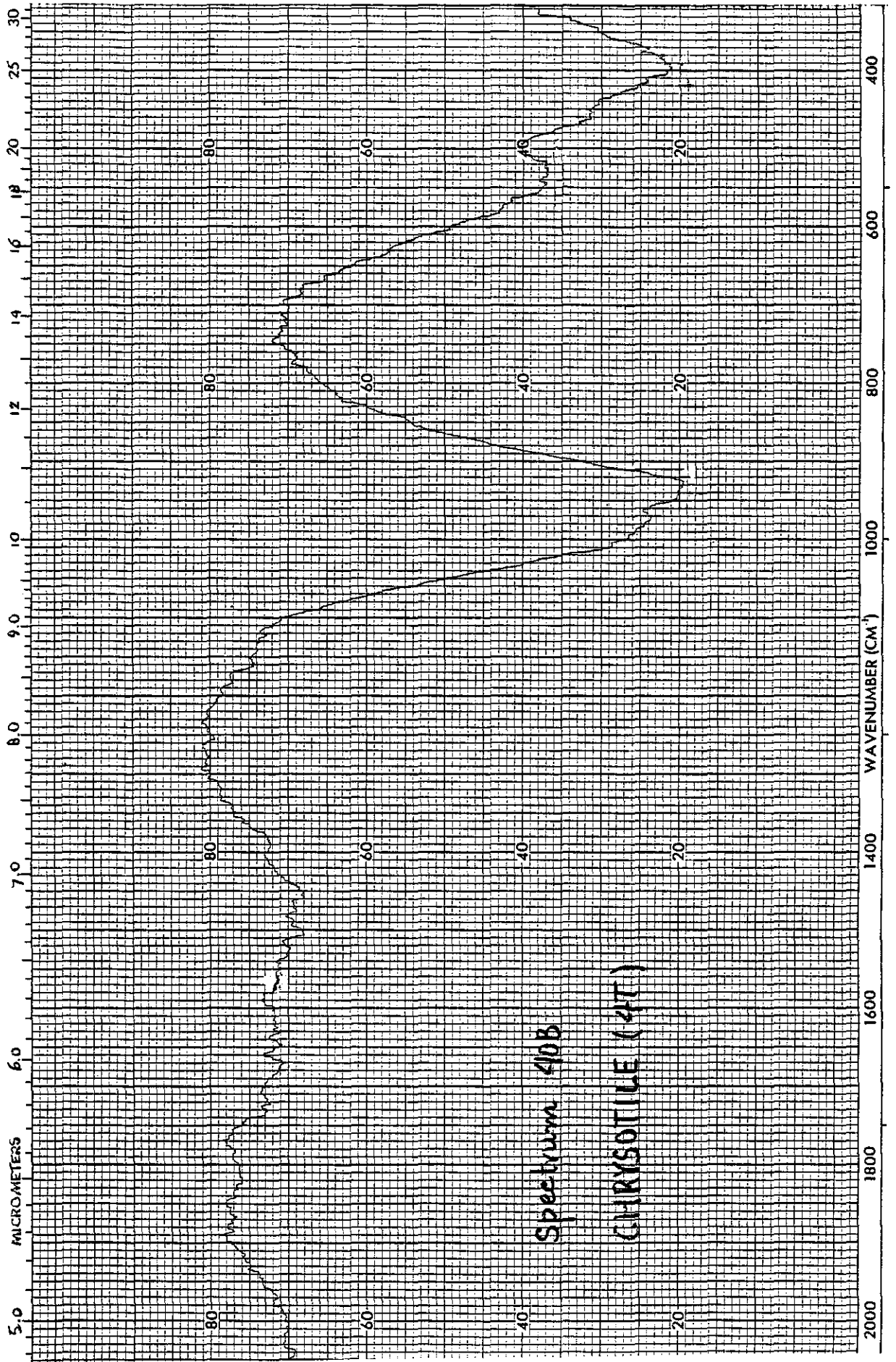


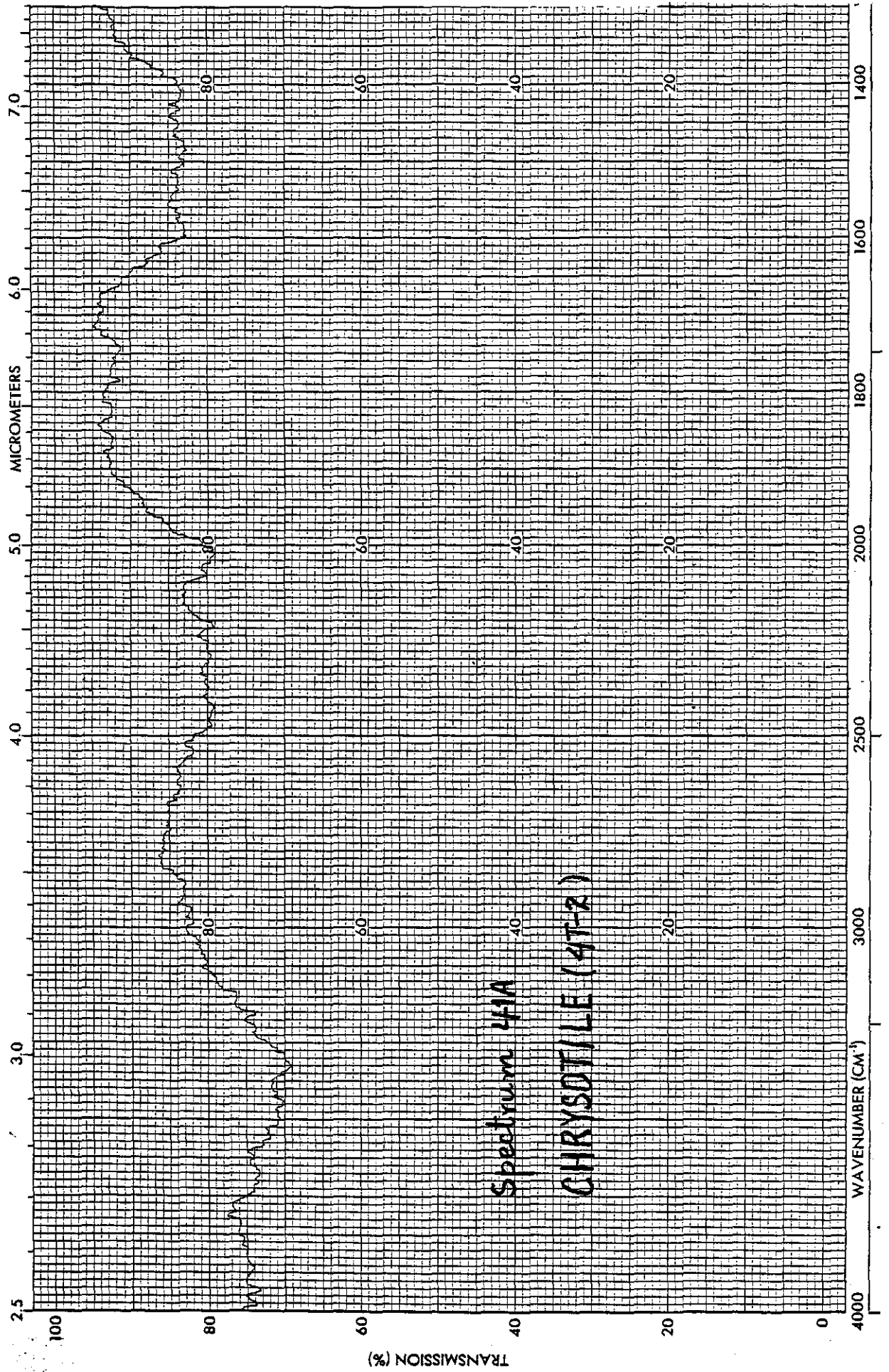
Spectrum 391A
CHRYSOTILE (4K)



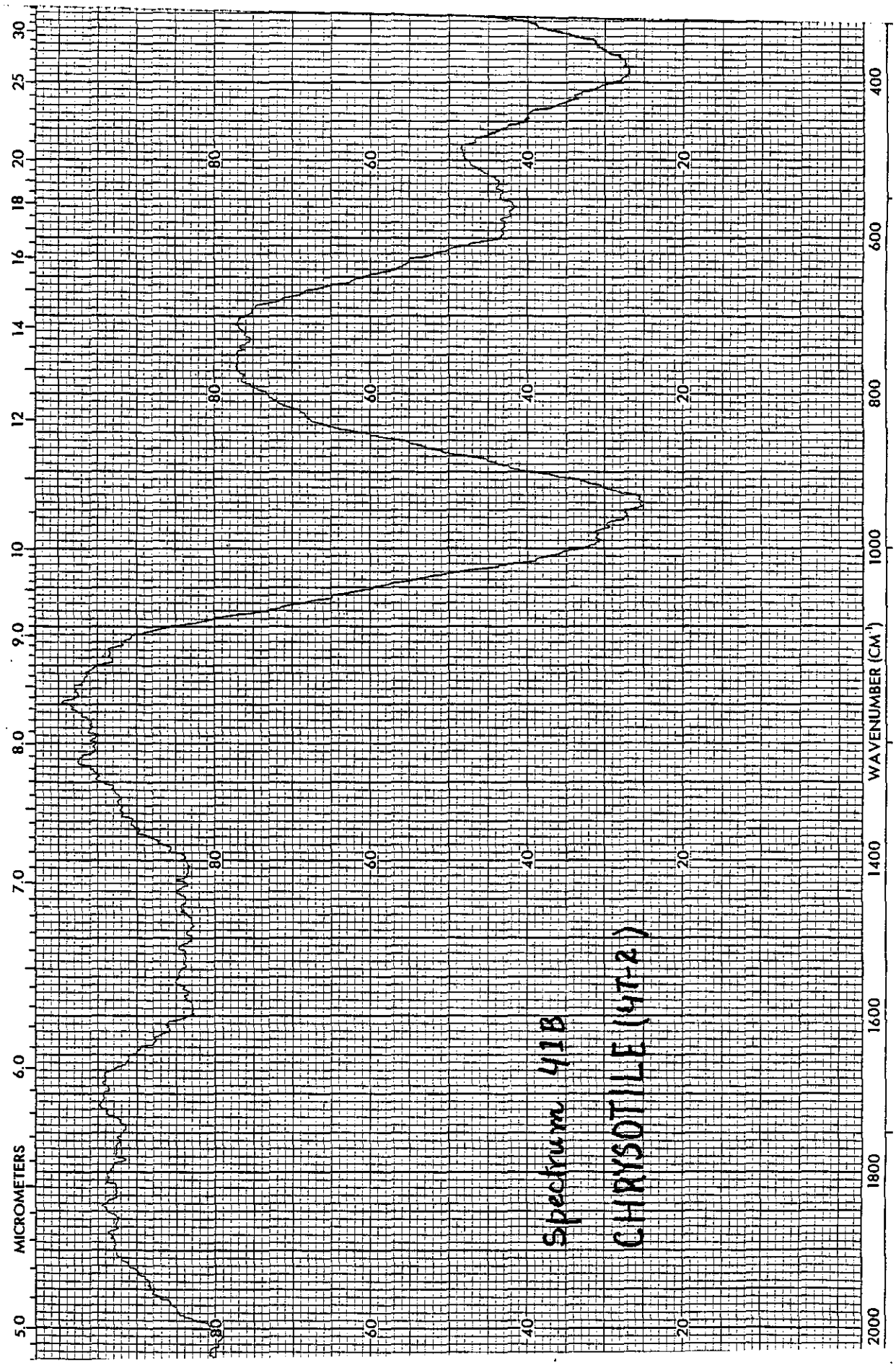


Spectrum 40A
CHRYSOTILE (4T)



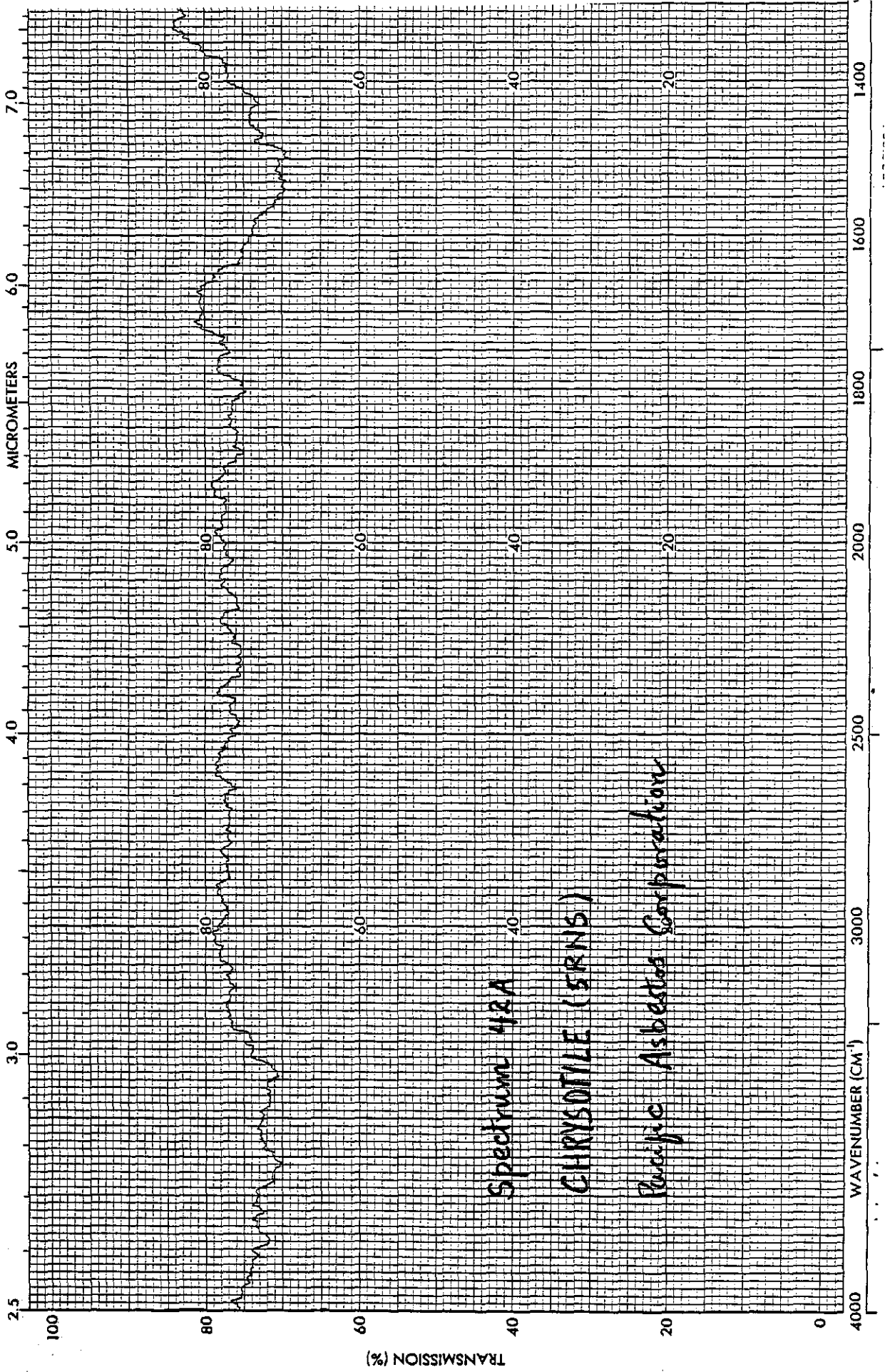


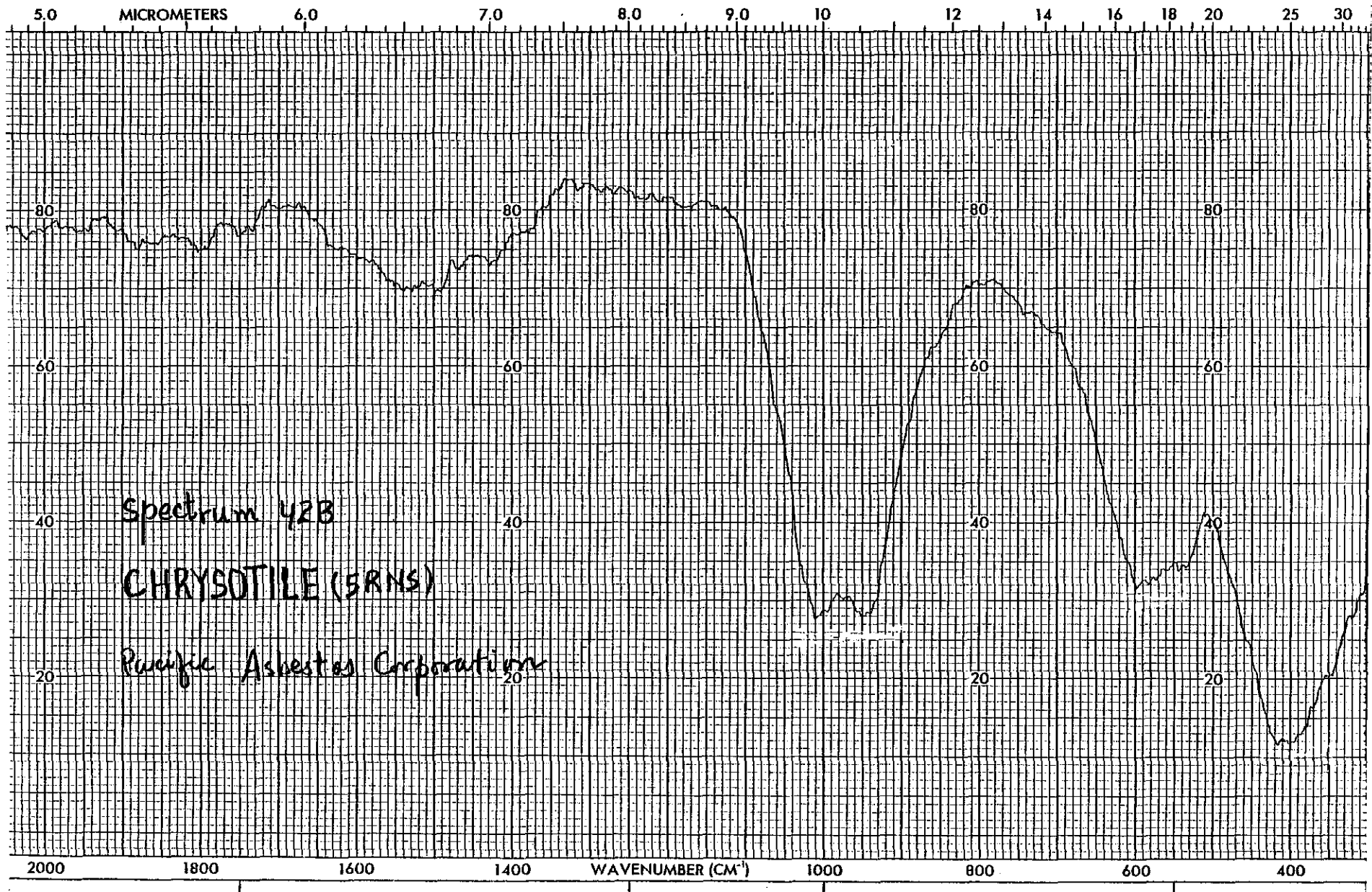
Spectrum 41A
CHRYSOTILE (4T-2)

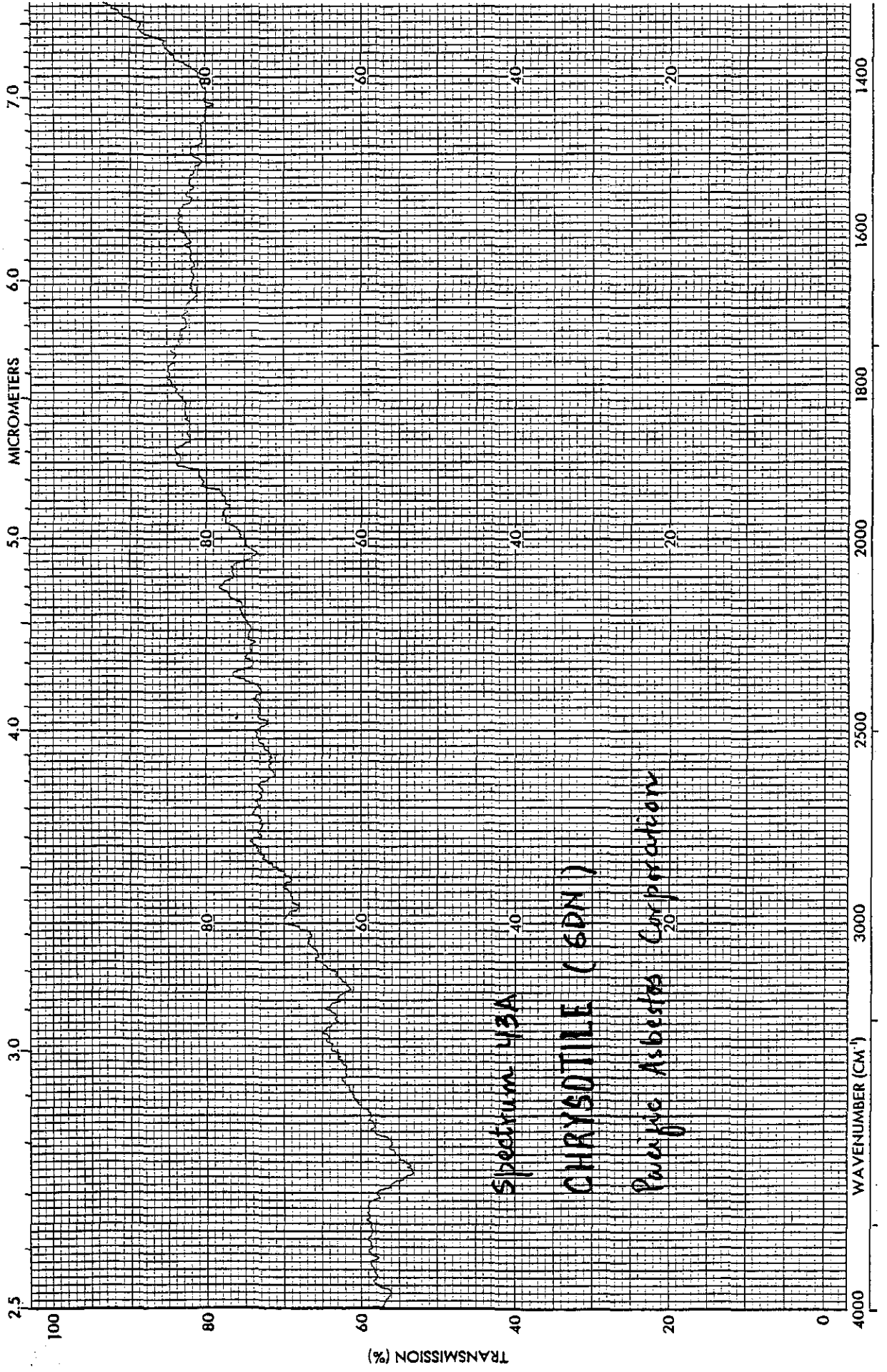


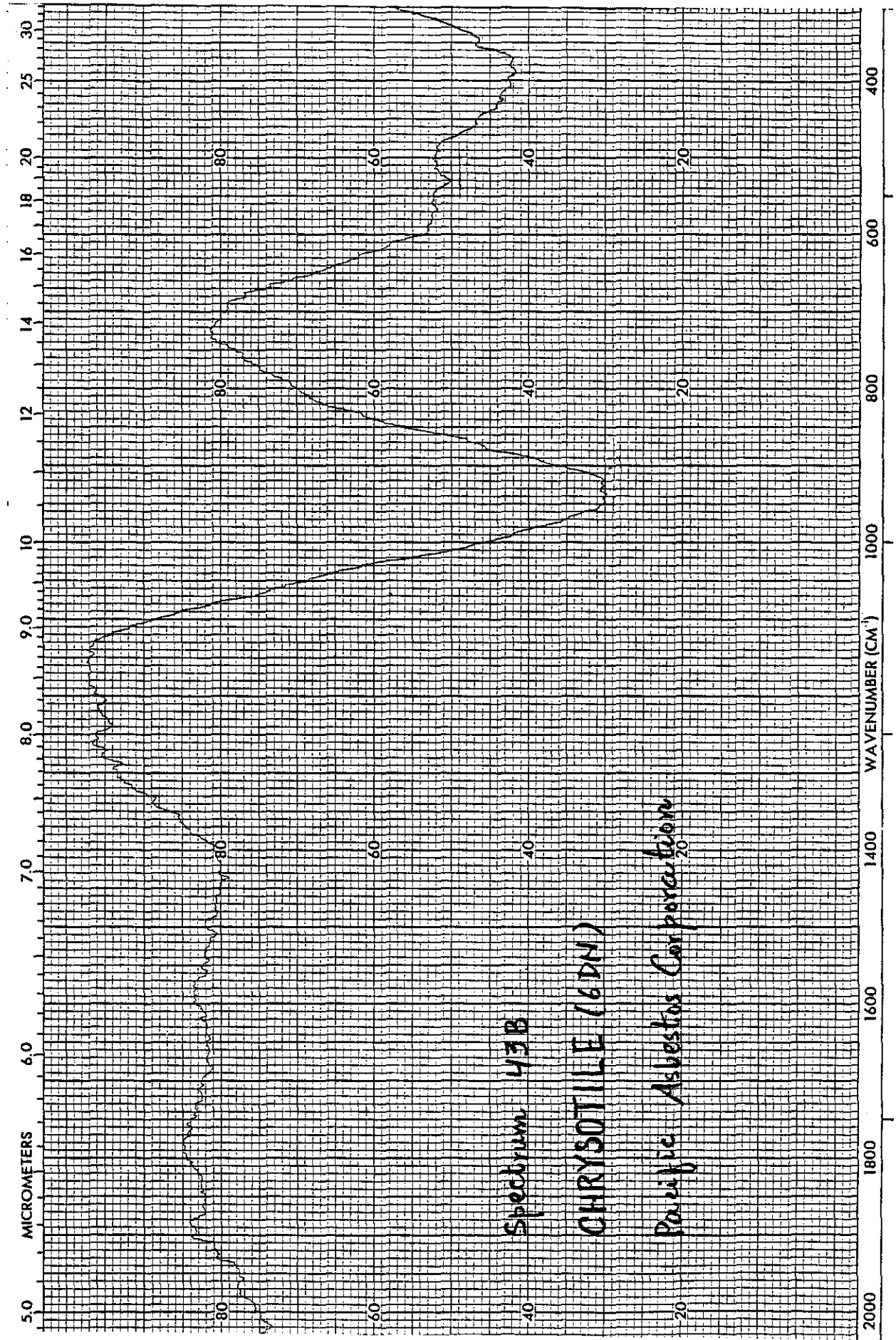
Spectrum 41B

CHRYSOTILE (4T-2)





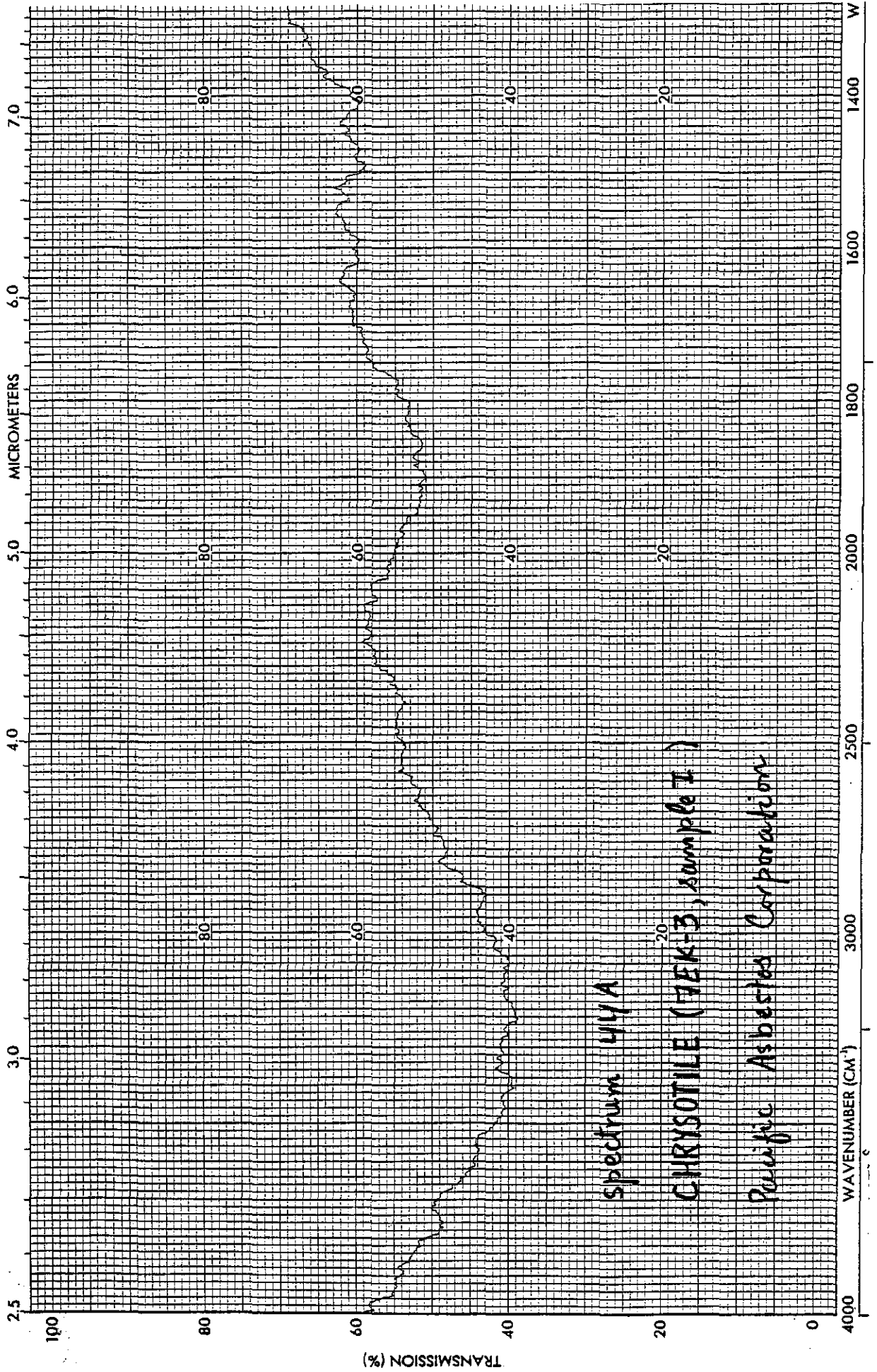




Spectrum 43B

CHRYSOITILE (6DN)

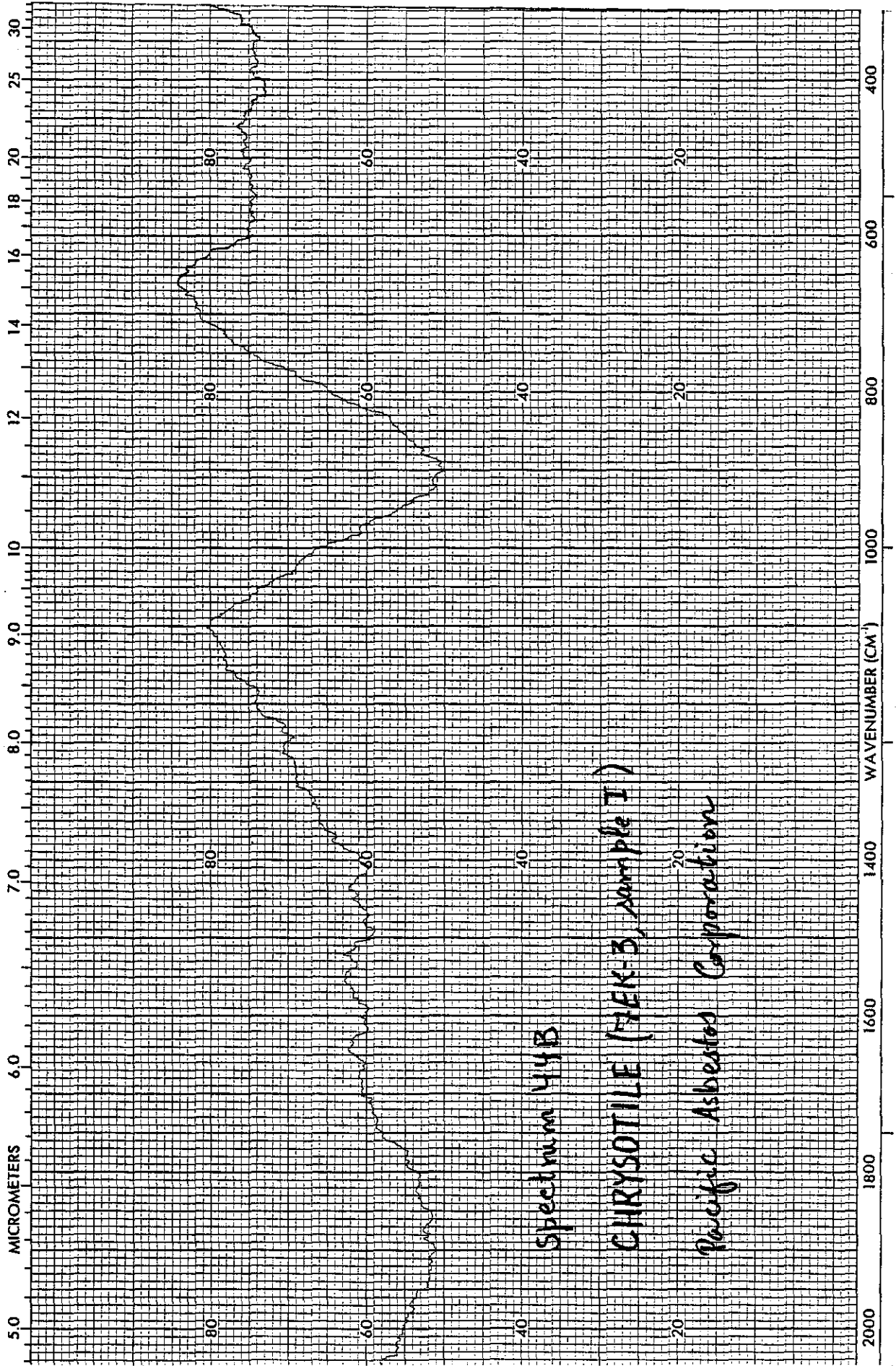
Pacific Asbestos Corporation

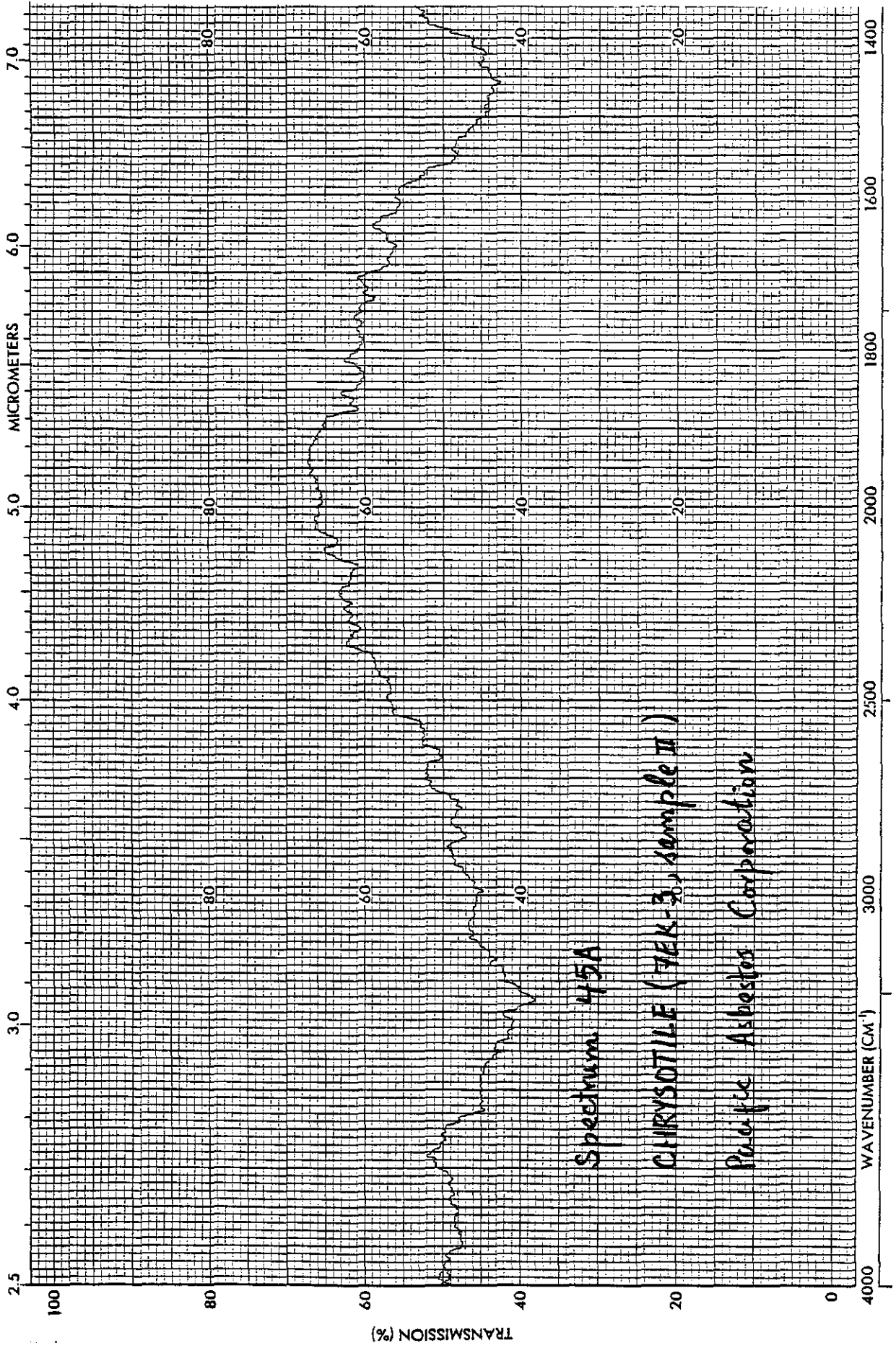


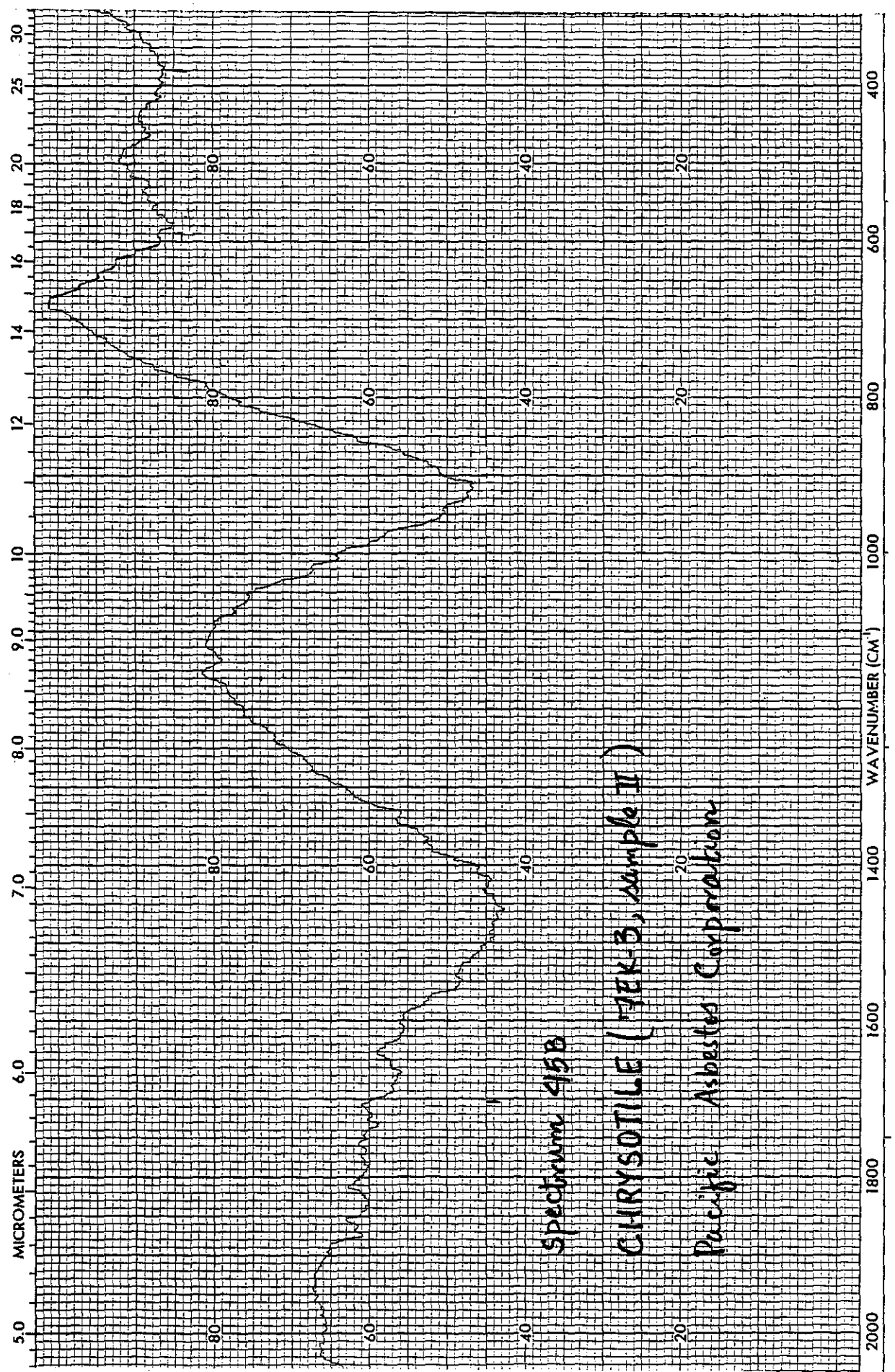
Spectrum 44A

CHRYSOTILE (TEK-3, sample I)

Pacific Asbestos Corporation



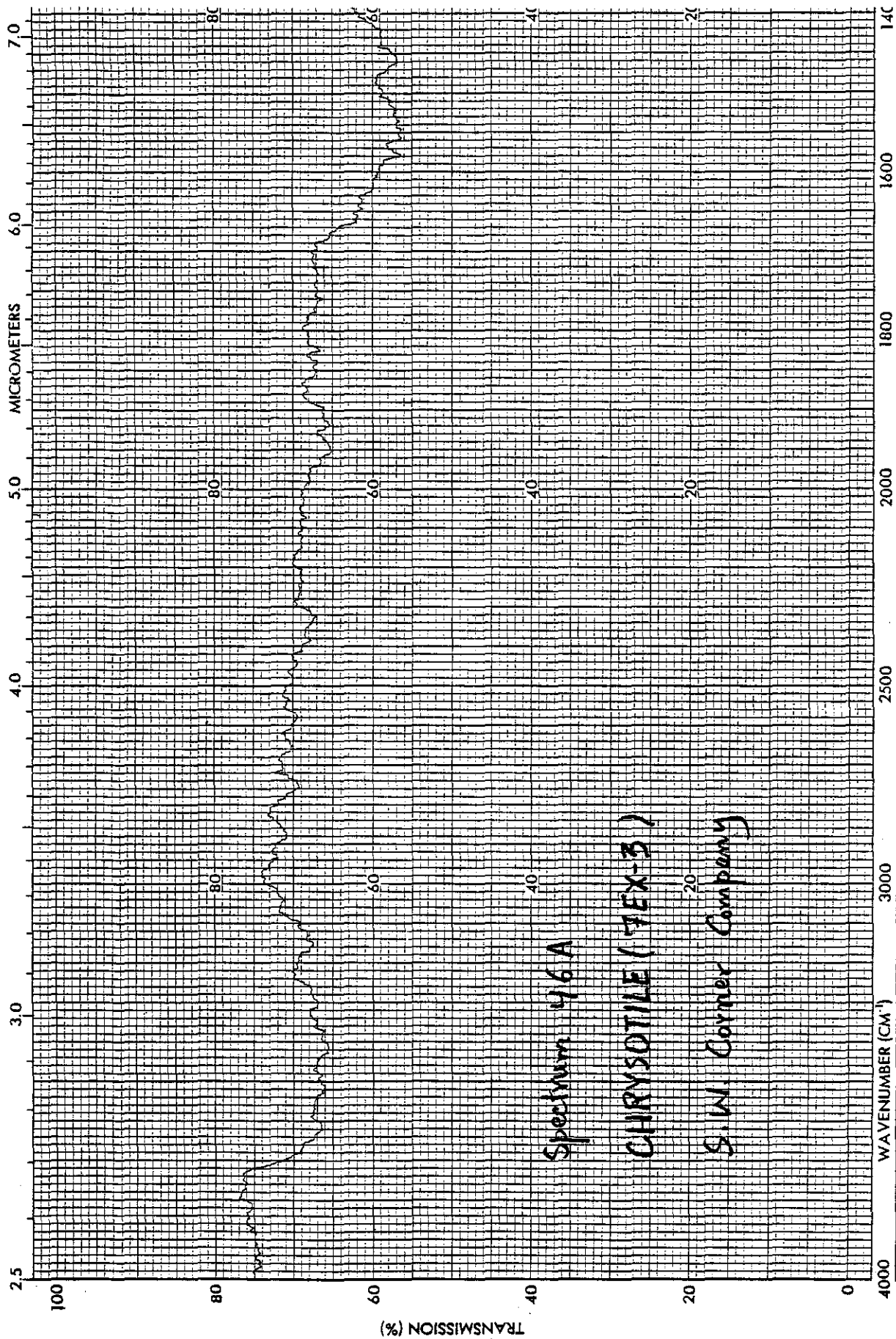


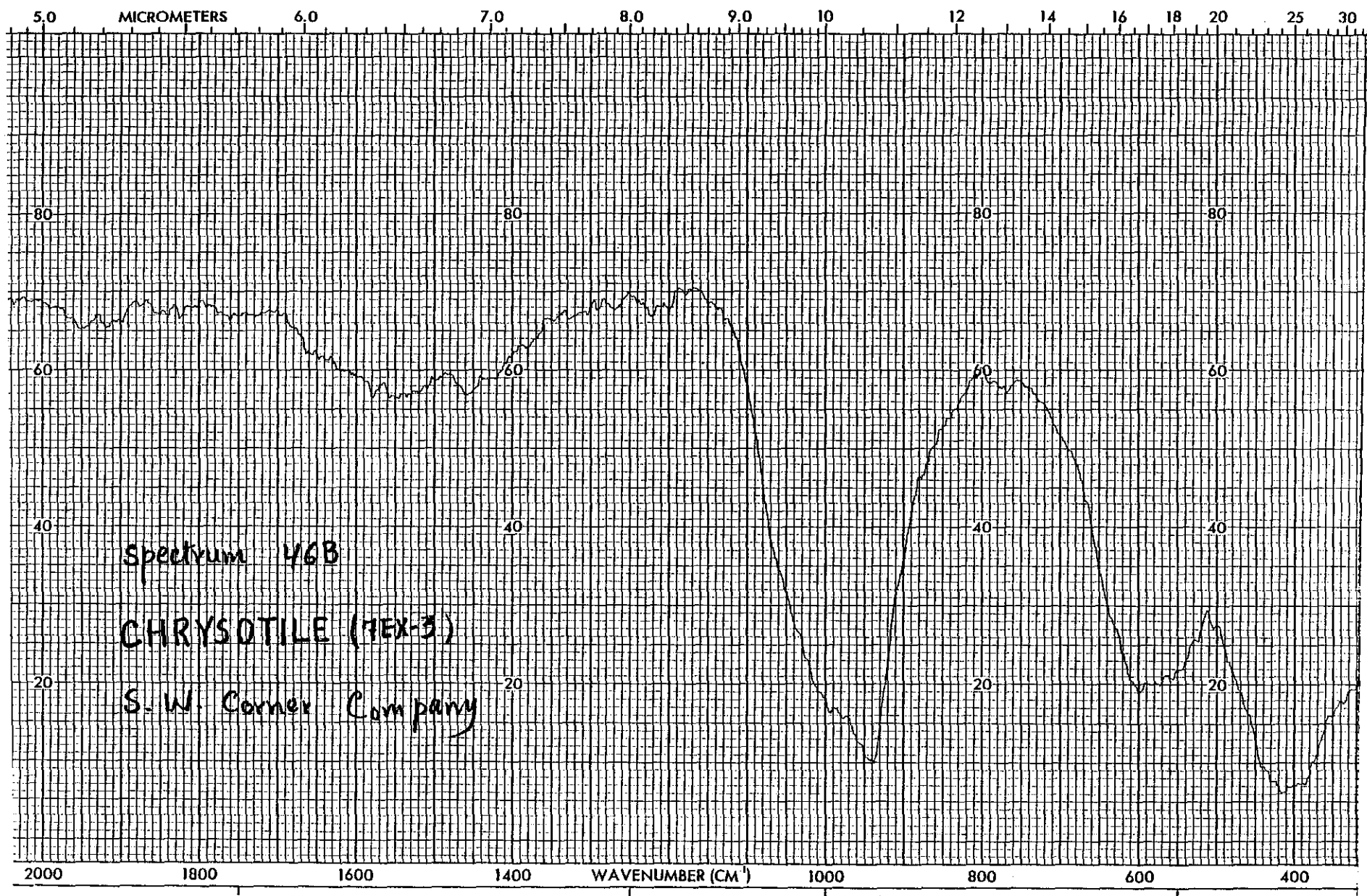


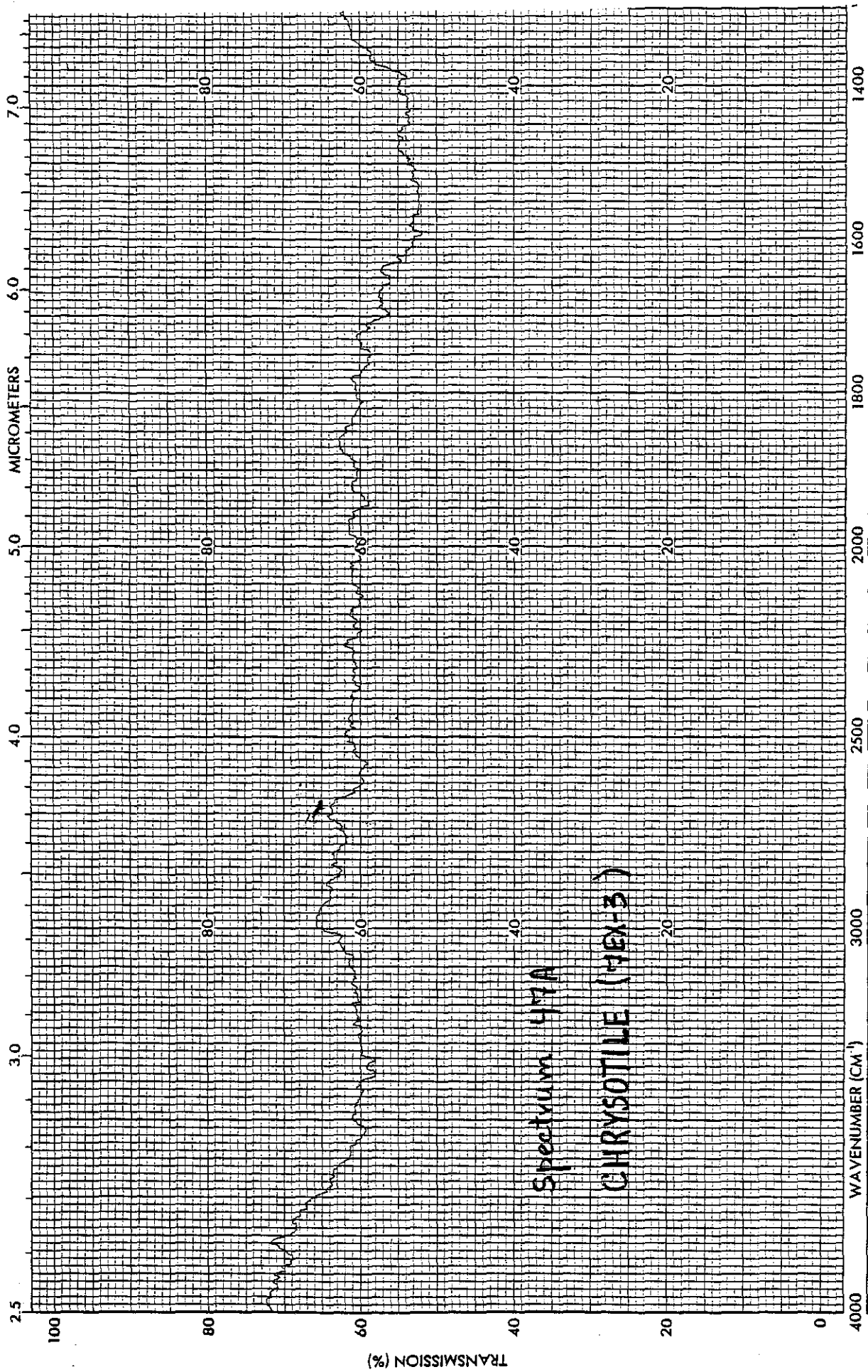
Spectrum 415B

CHRYSOTILE (FEK-B, sample II)

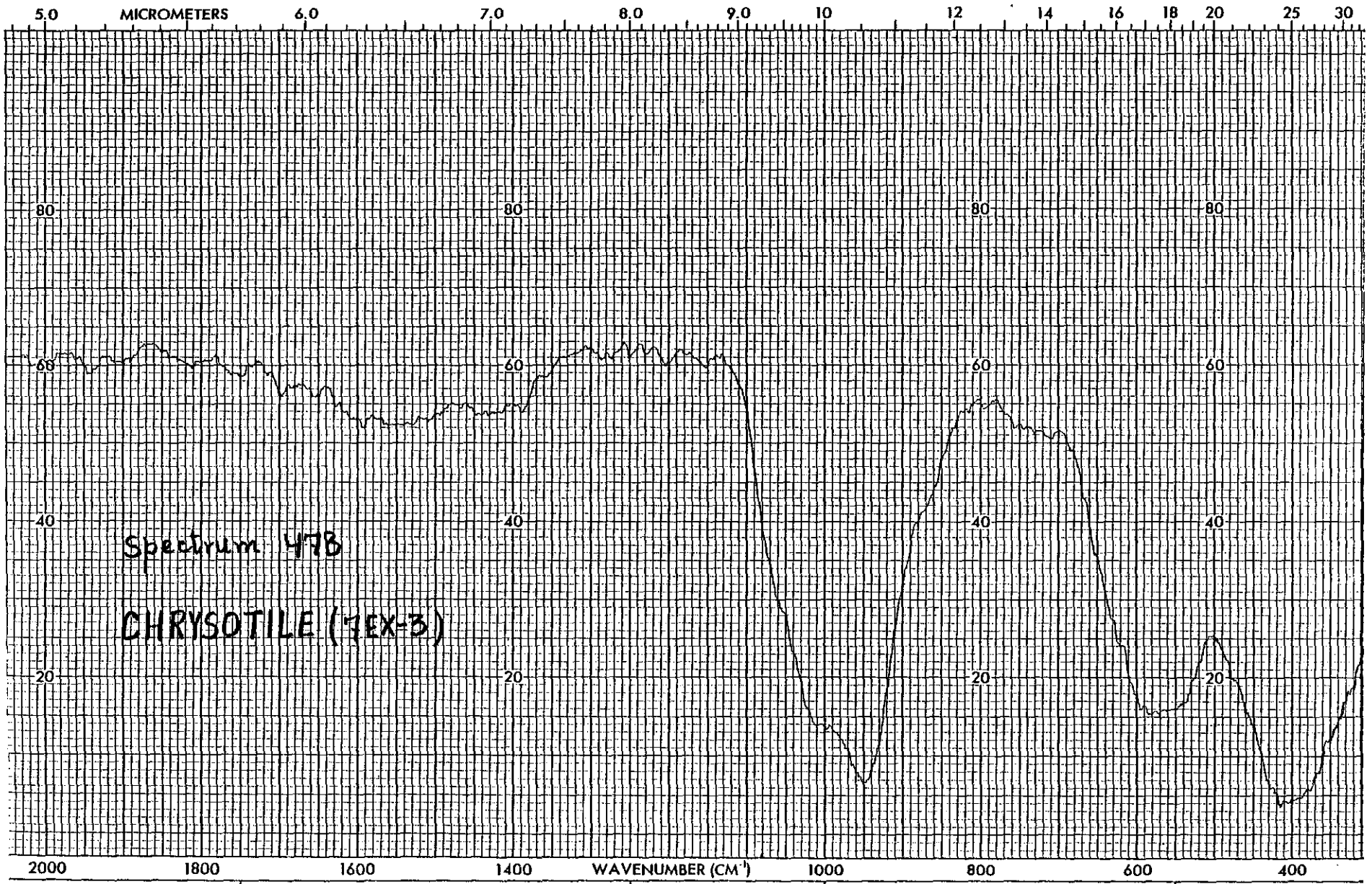
Pacific Asbestos Corporation

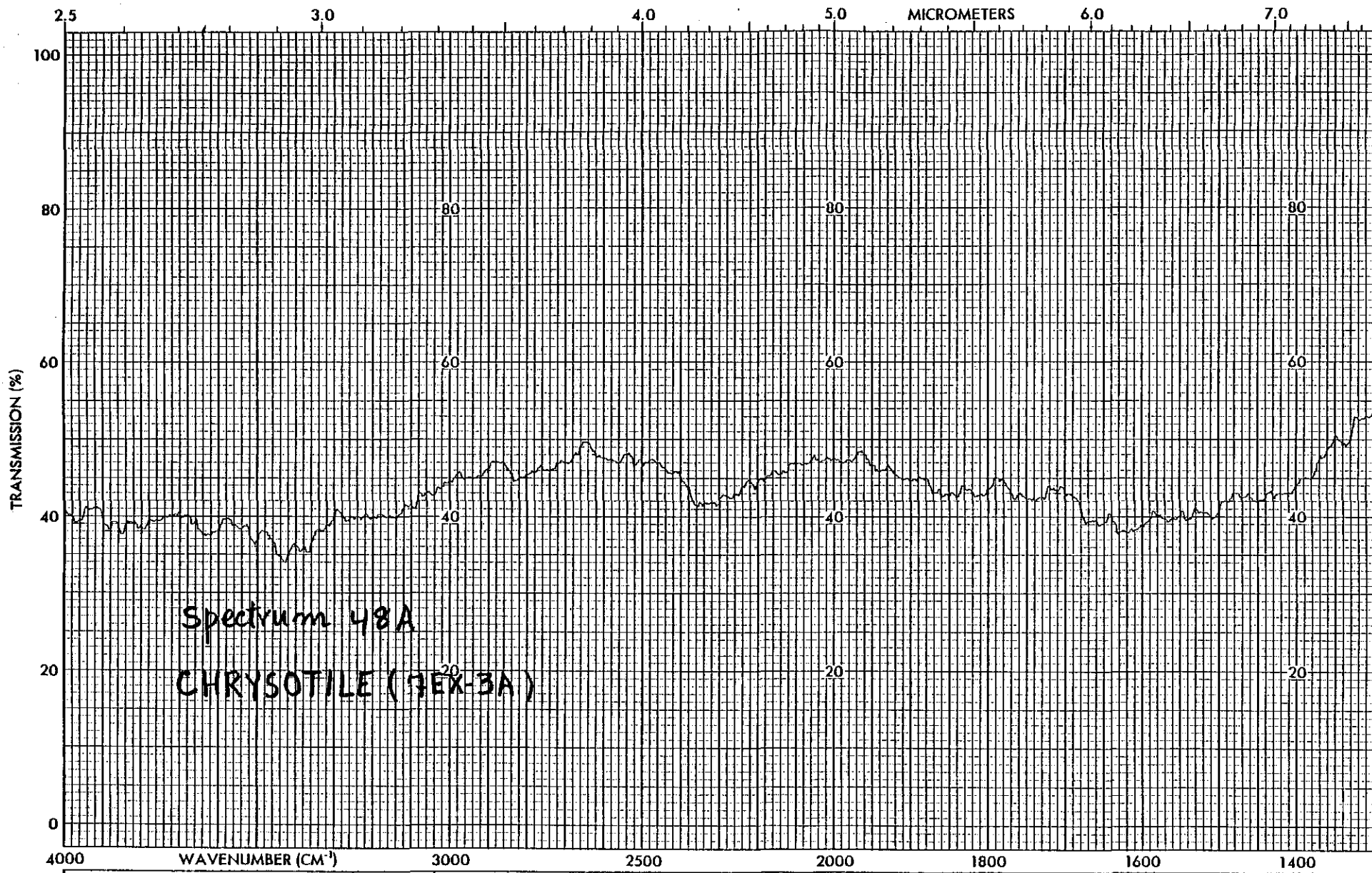


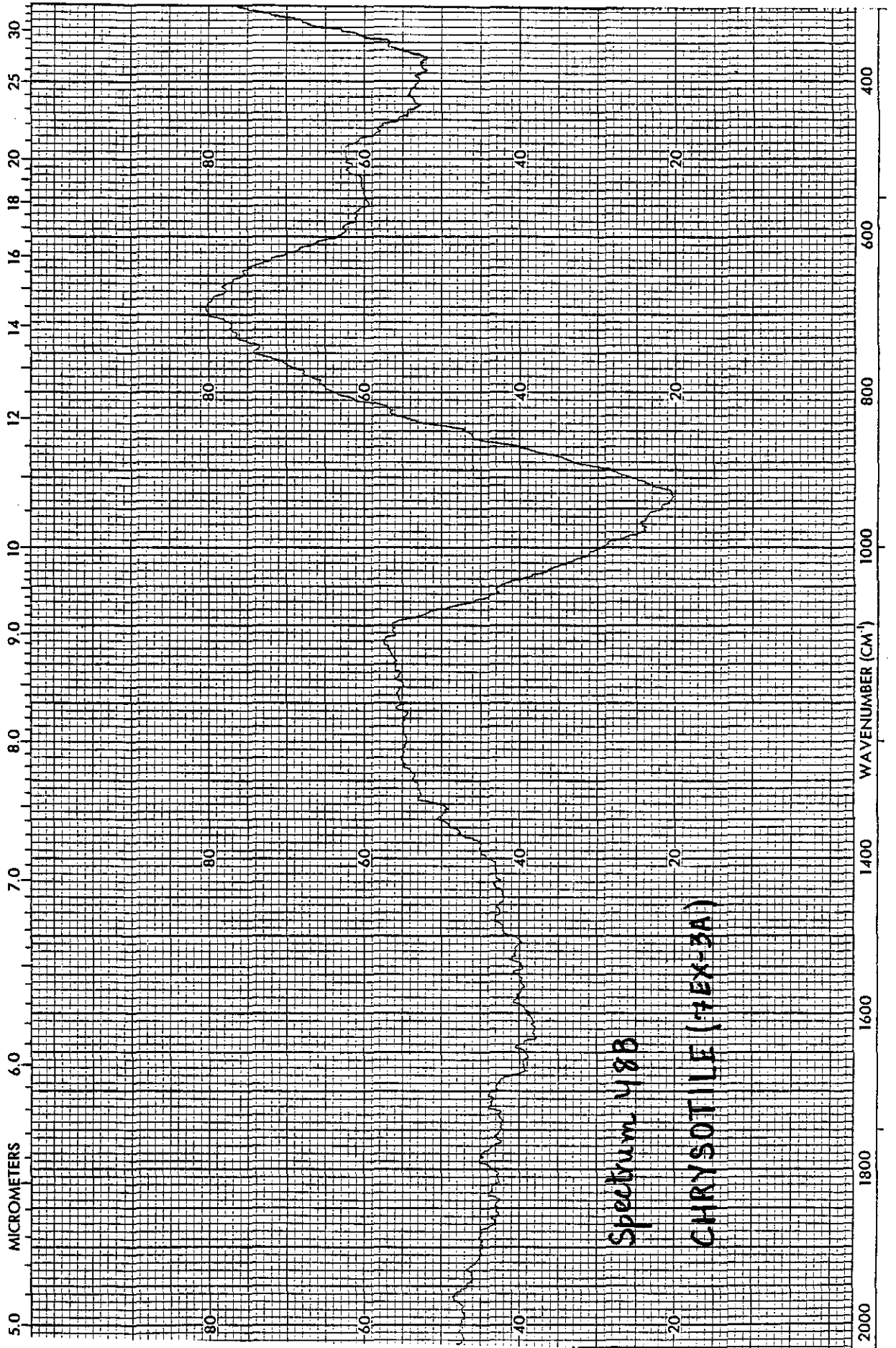




Spectrum 477A
CHRYSOTILE (HEX-3)

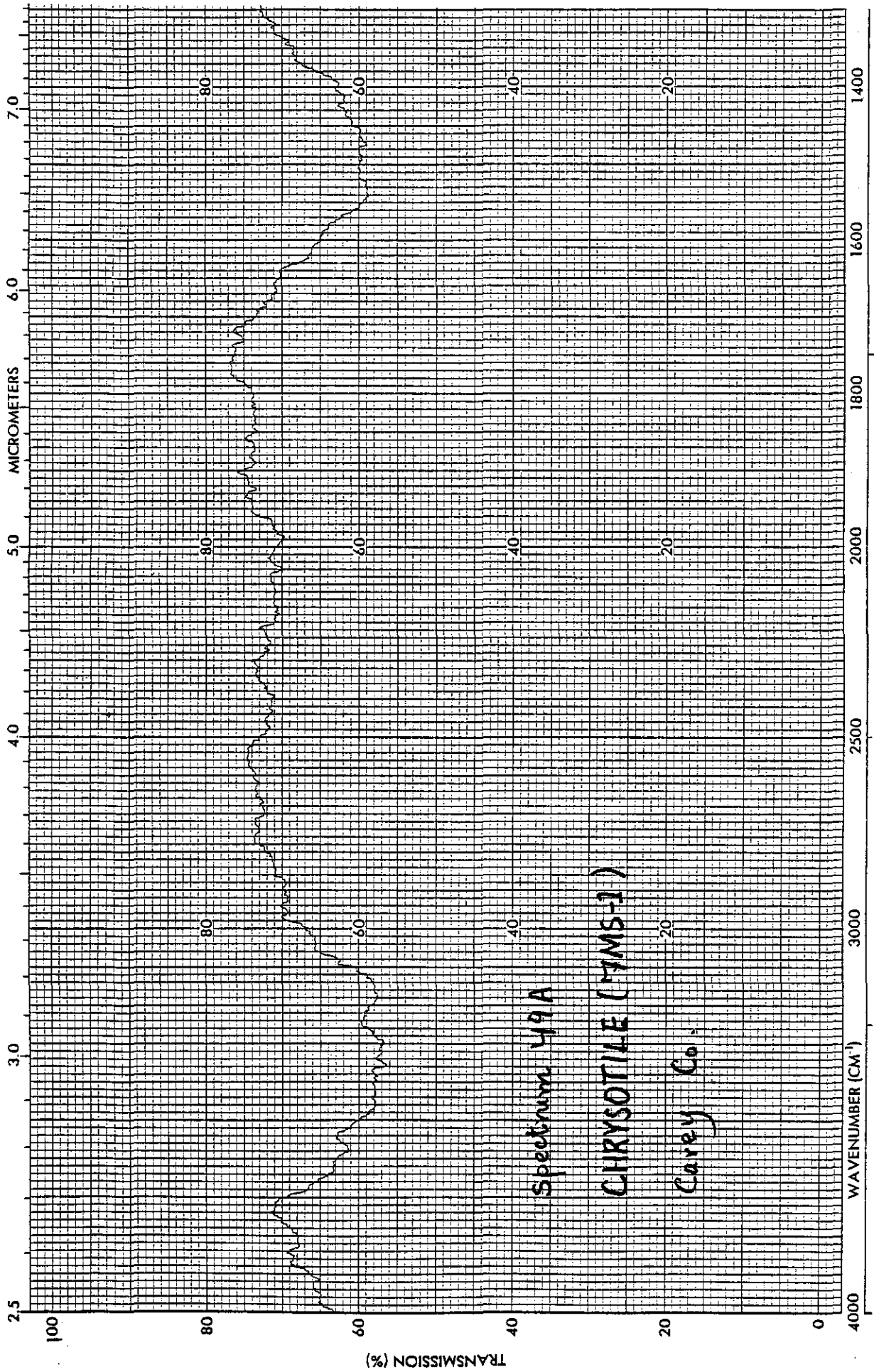


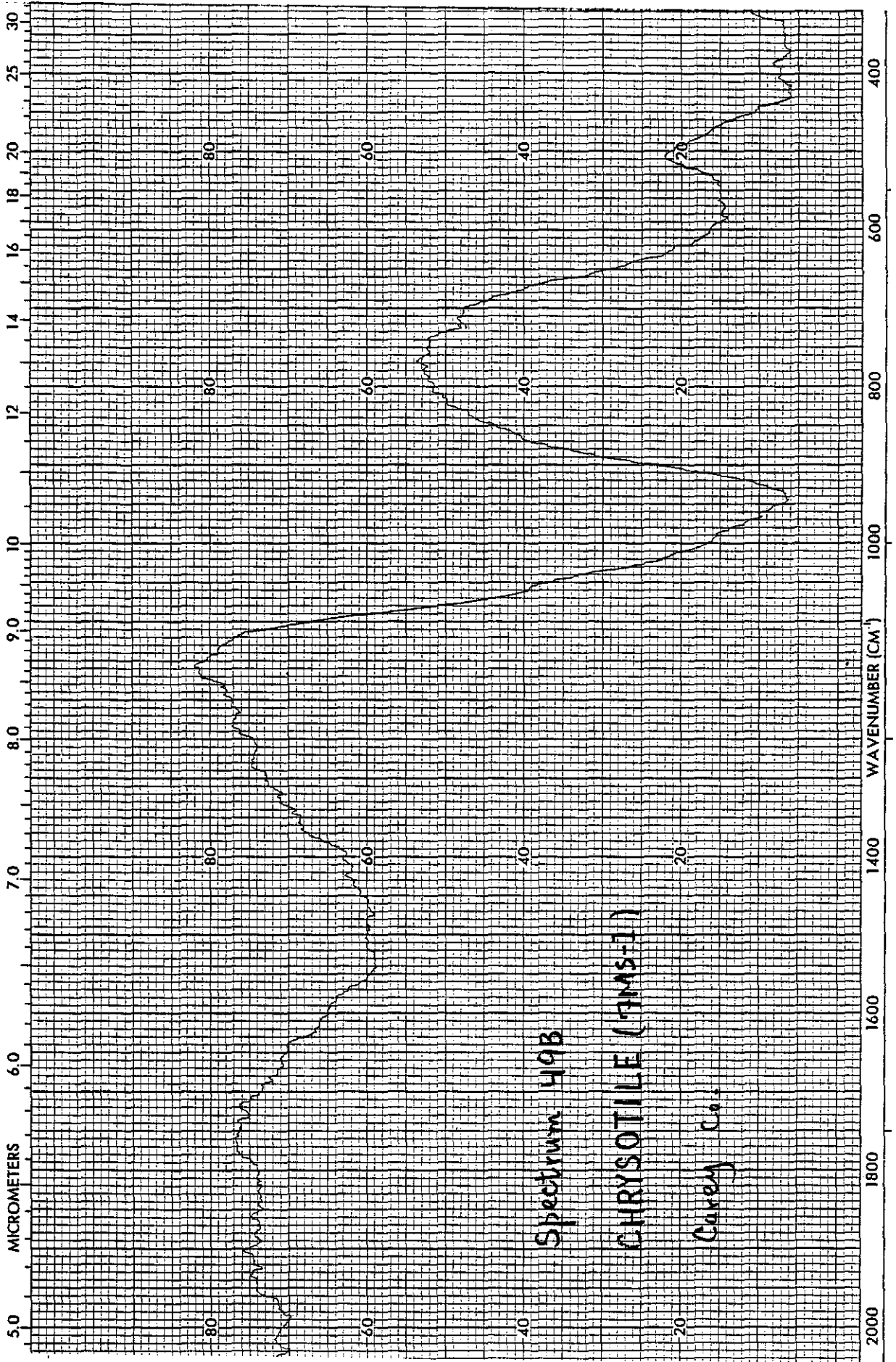


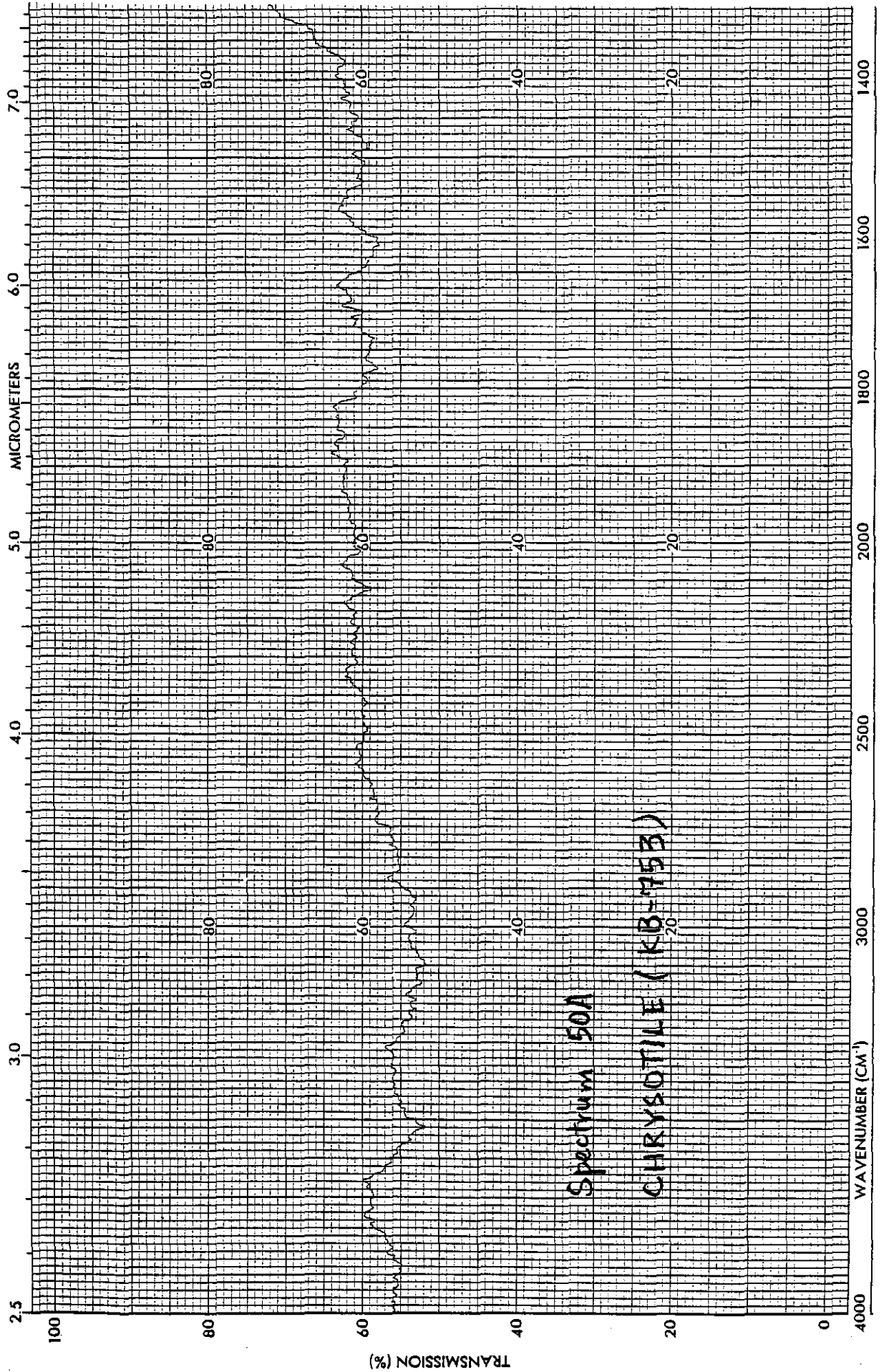


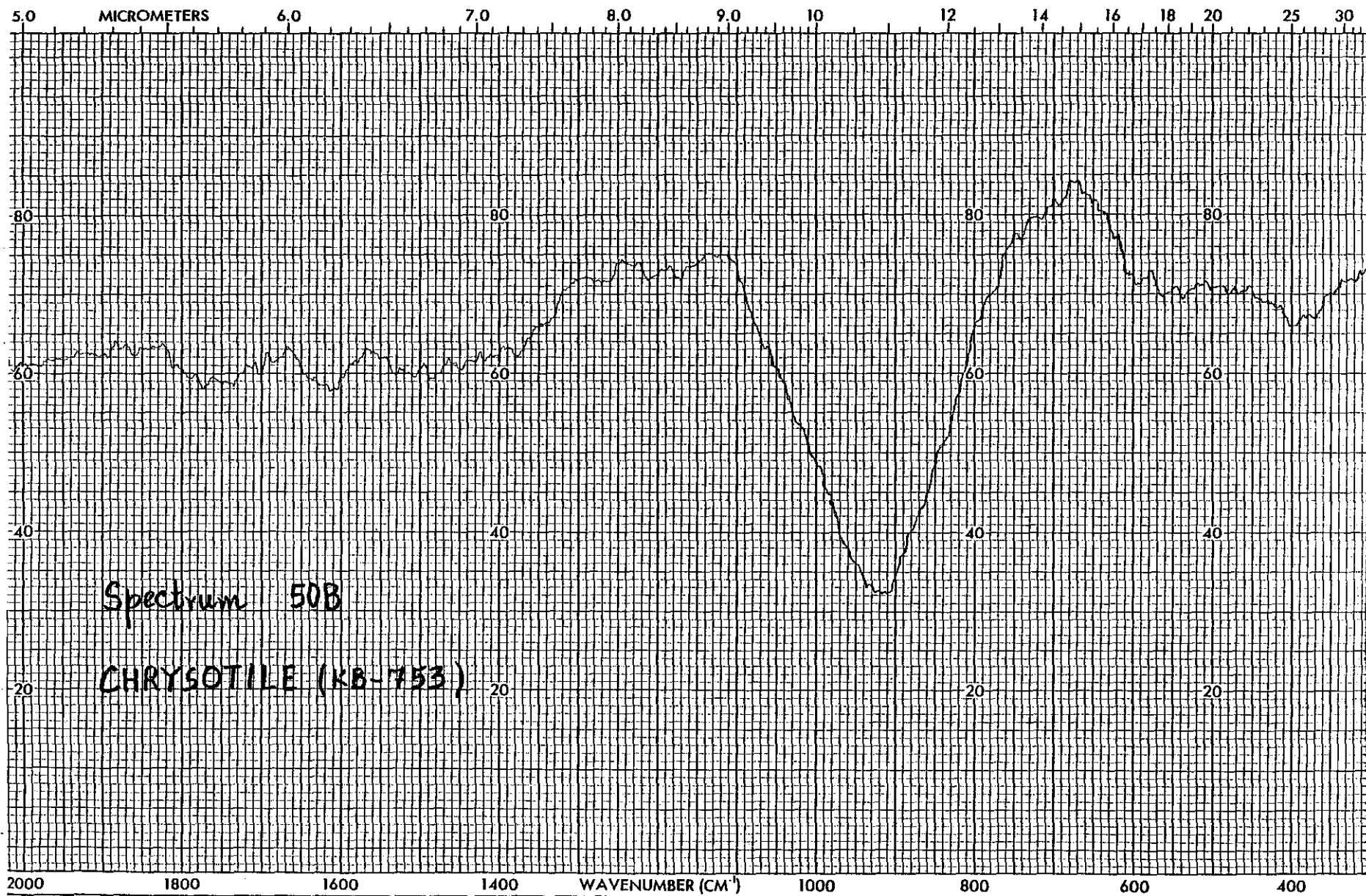
Spectrum 488

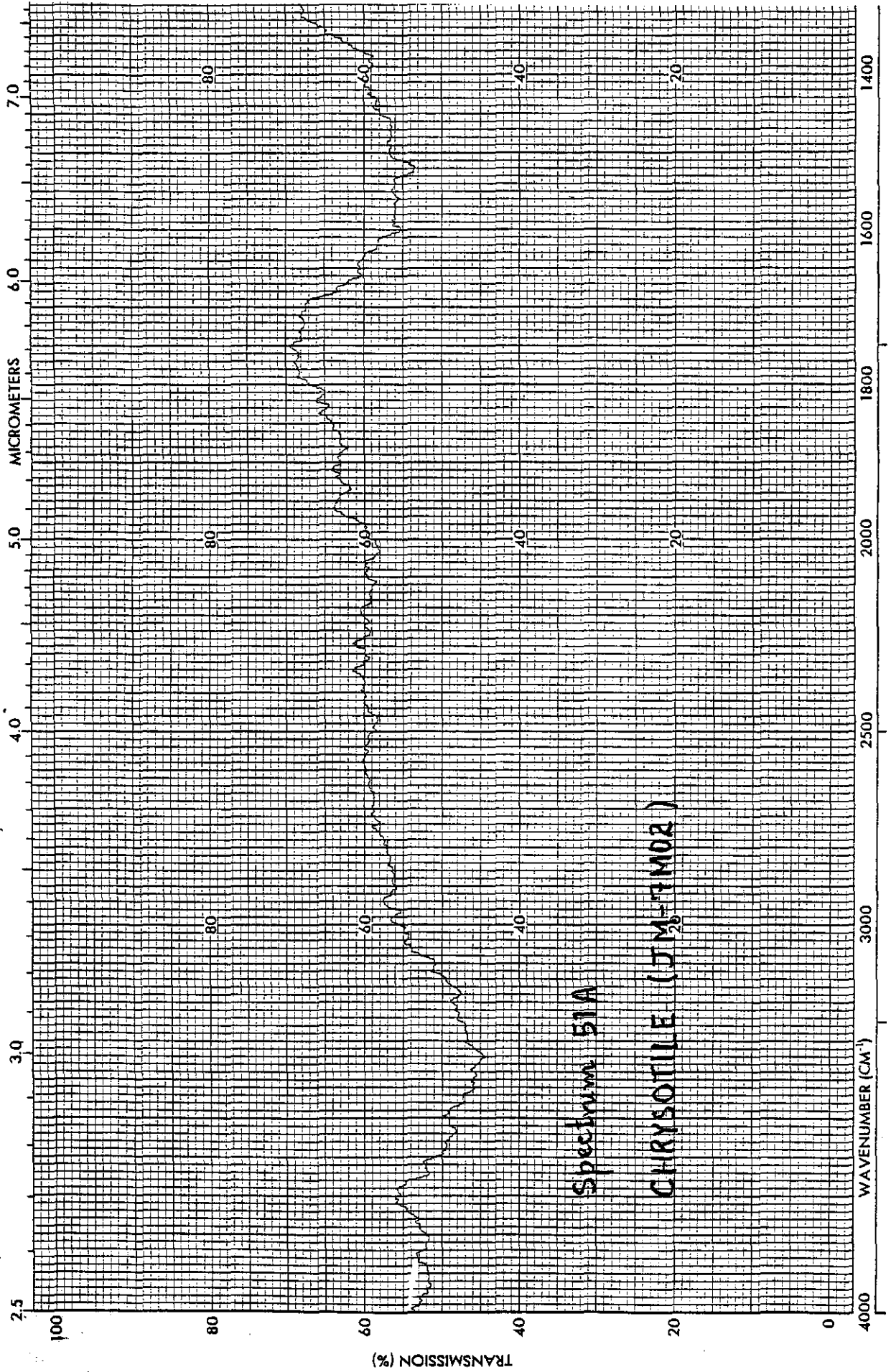
CHRYSOTILE (7EX-3A)







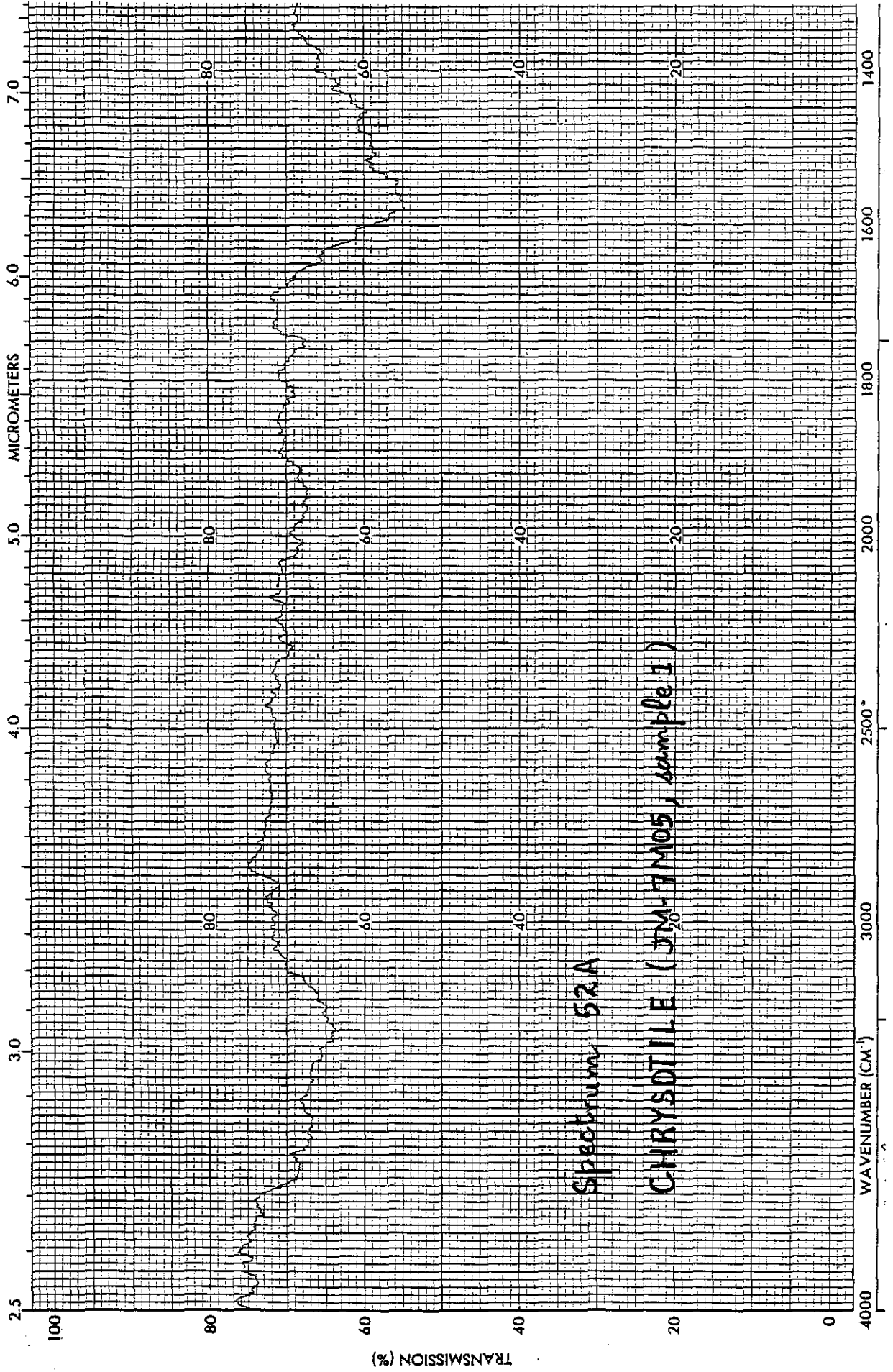




Spectrum 51A

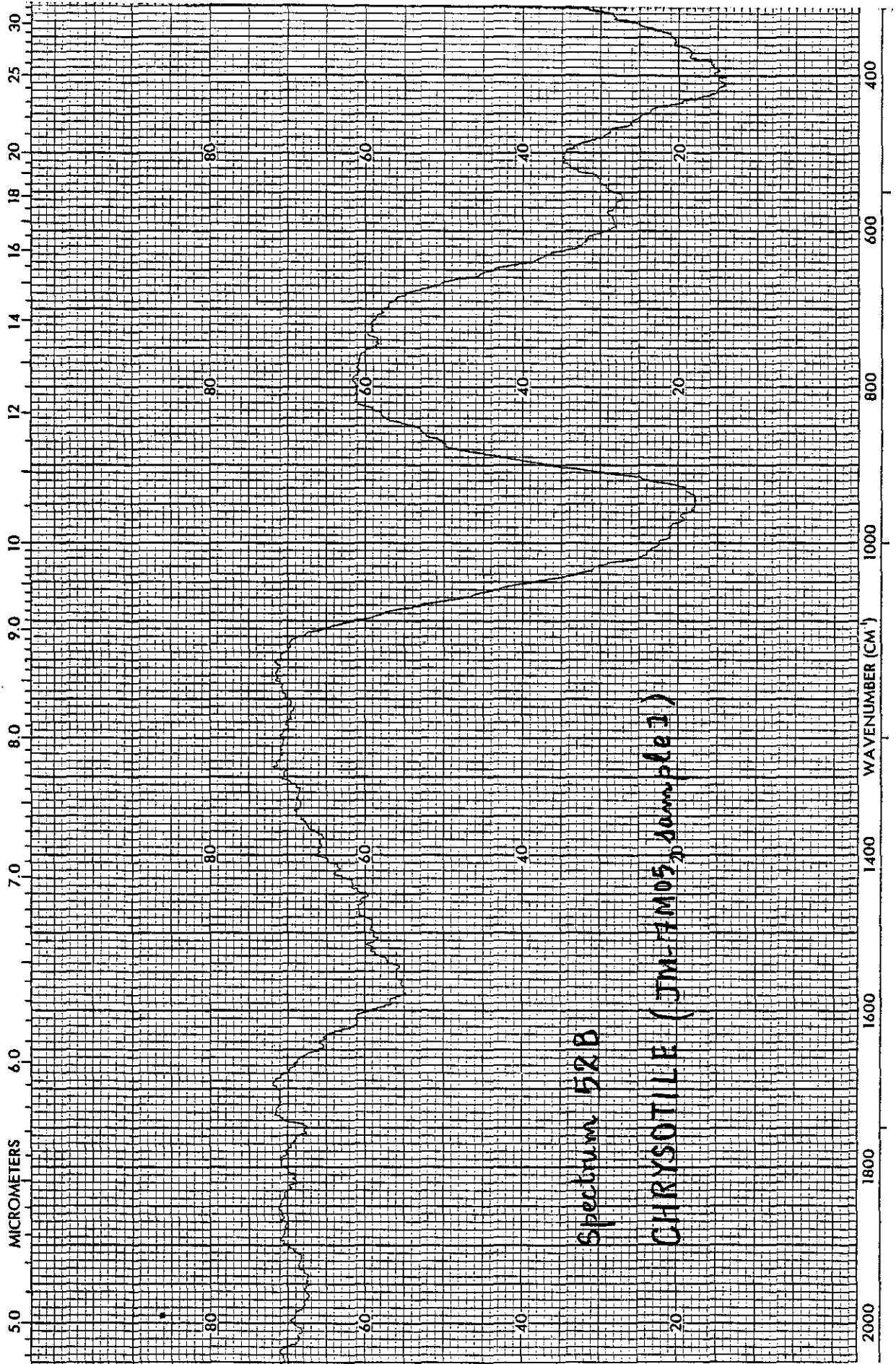
CHRYSOTILE (JM-7M02)





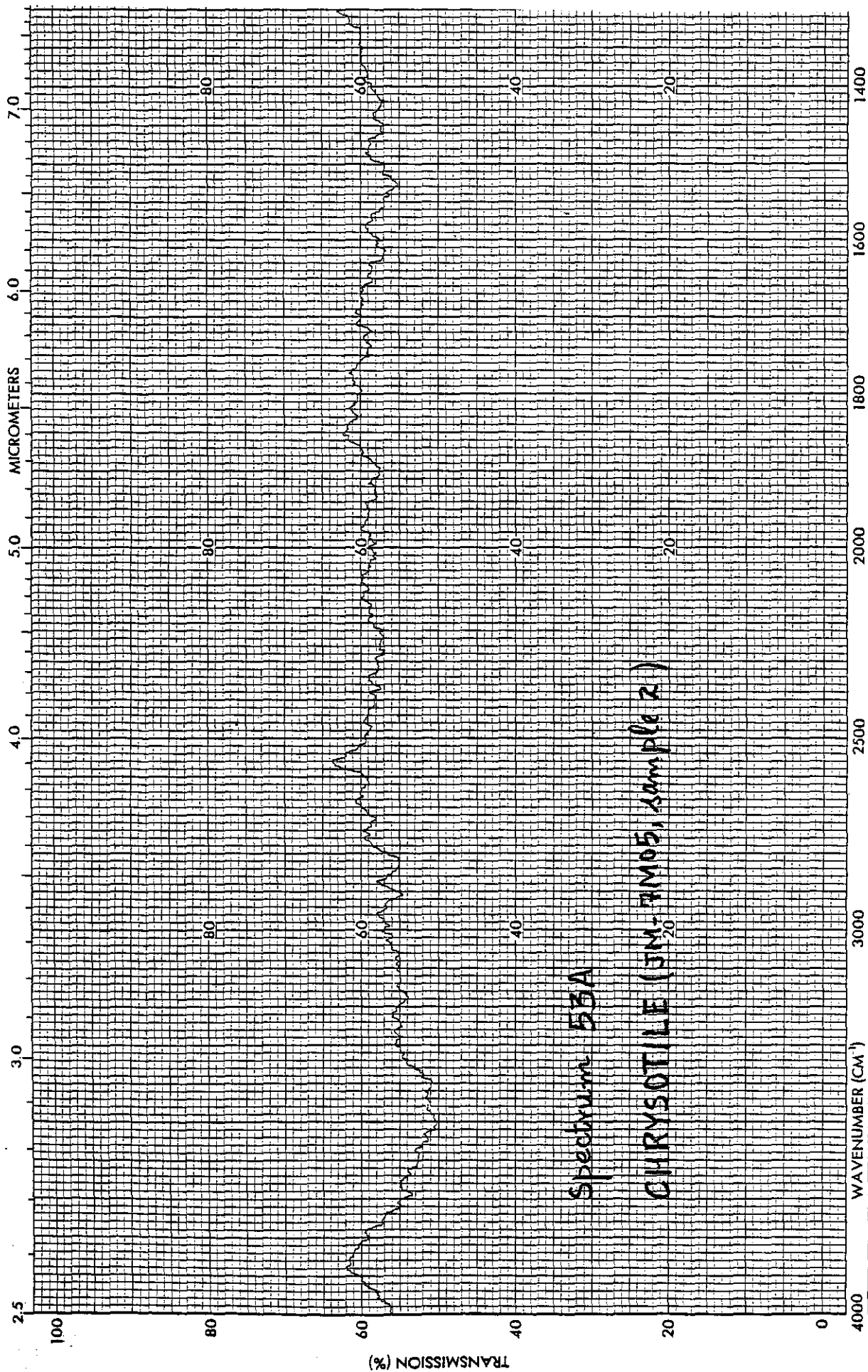
Spectrum 52A

CHRYSOTILE (JM-7M05, sample 1)



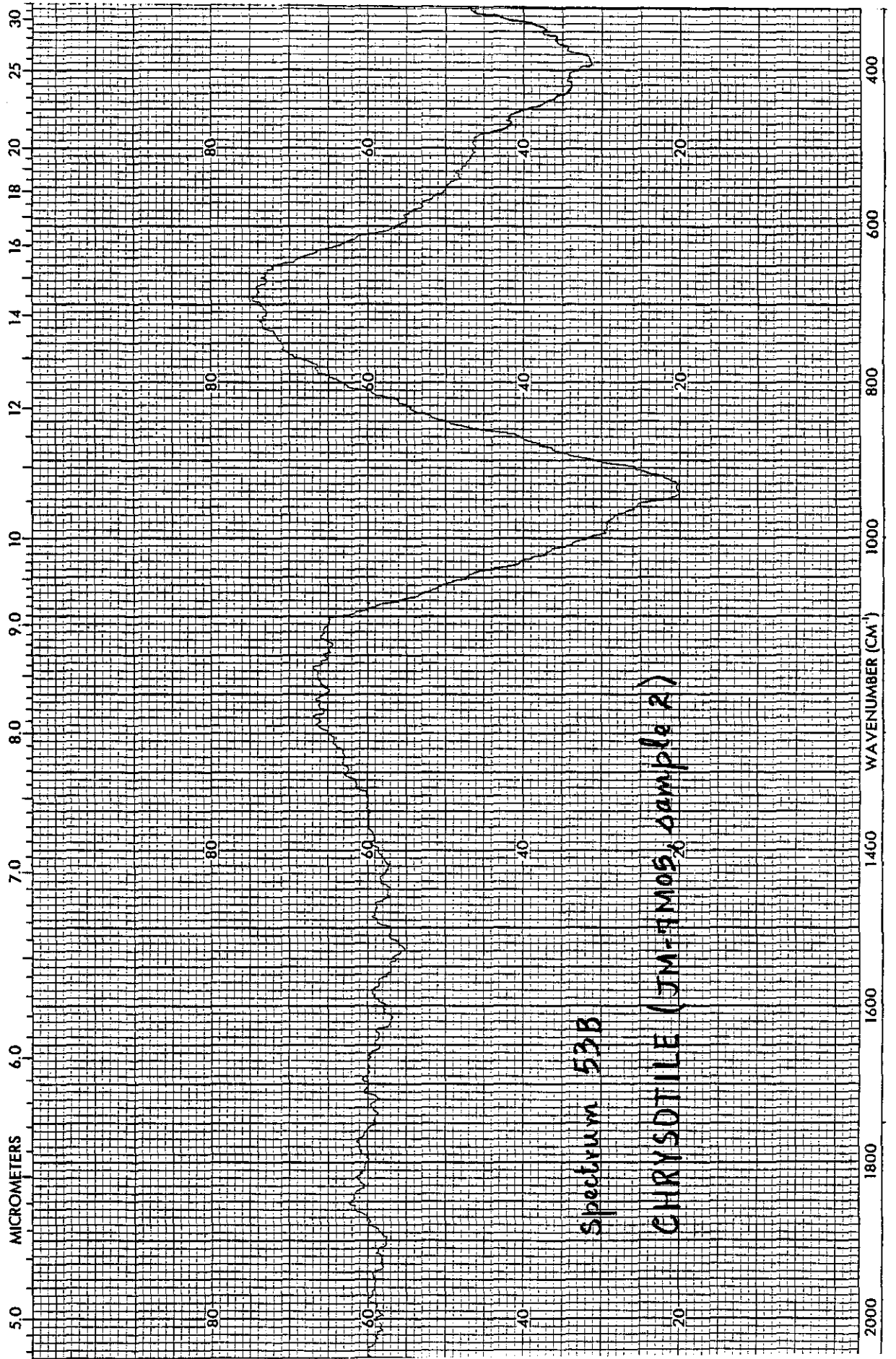
Spectrum 52B

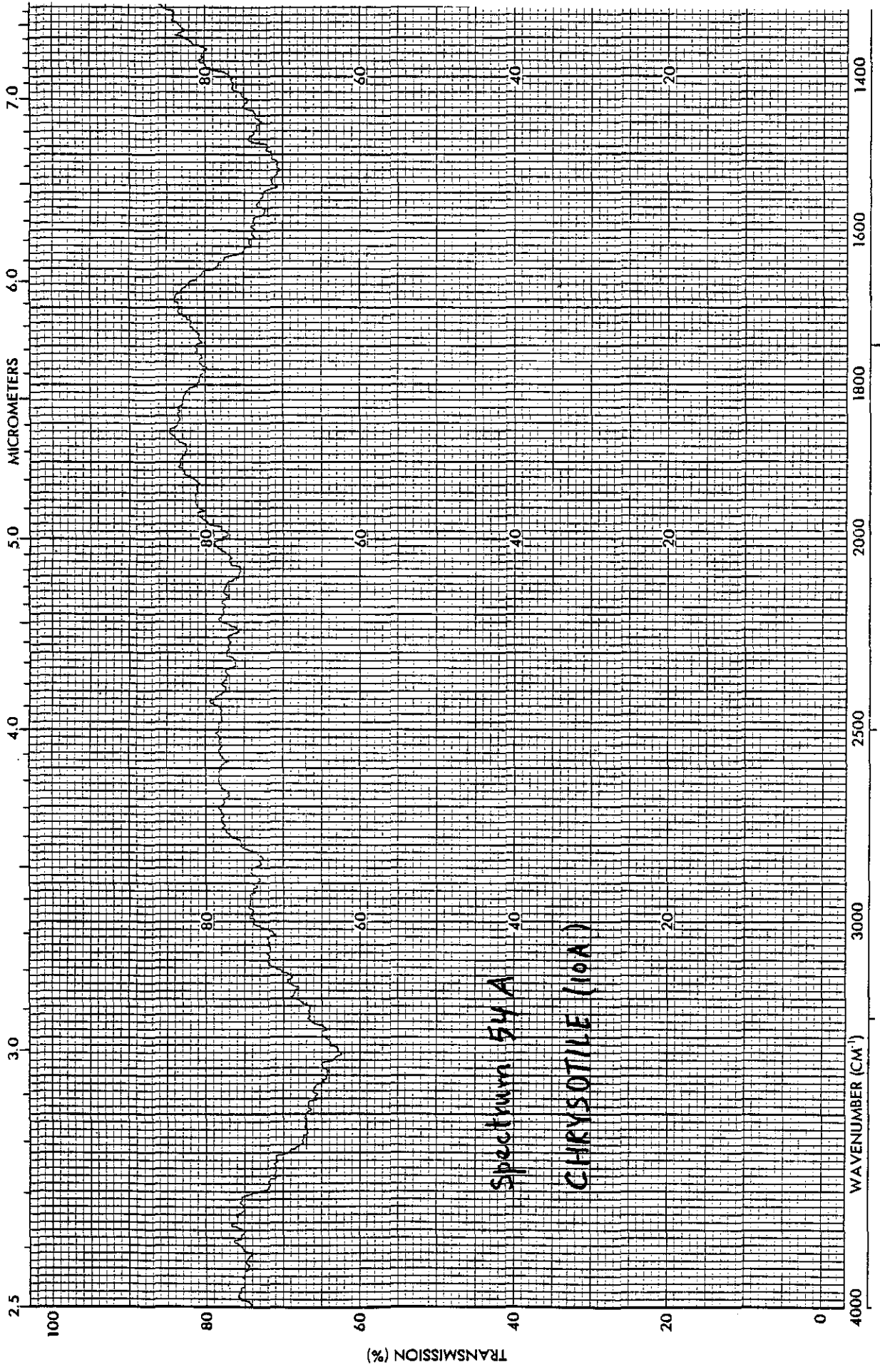
CHRYSOPILE (JM-4M05, demo plate)



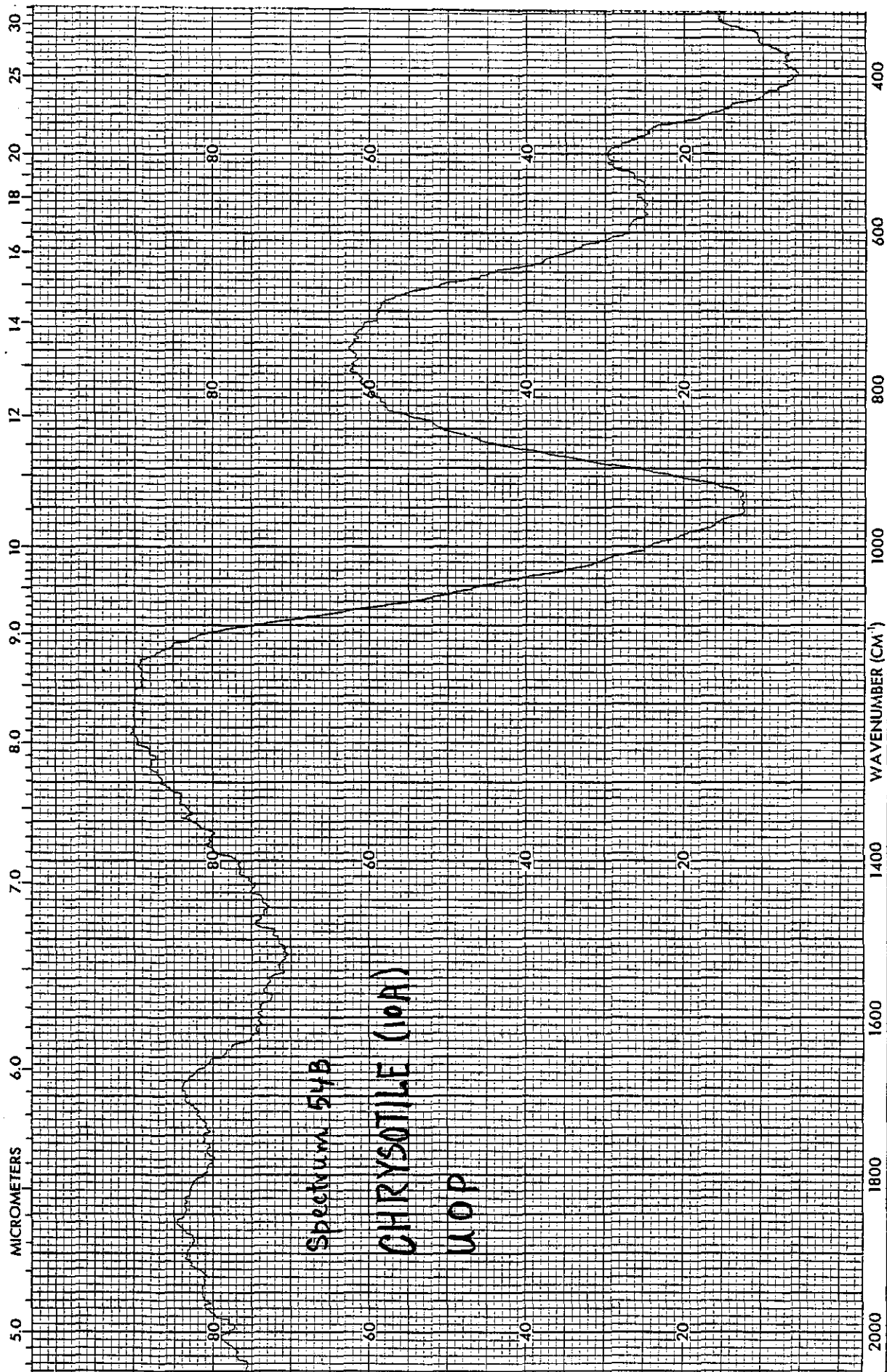
Spectrum 53A

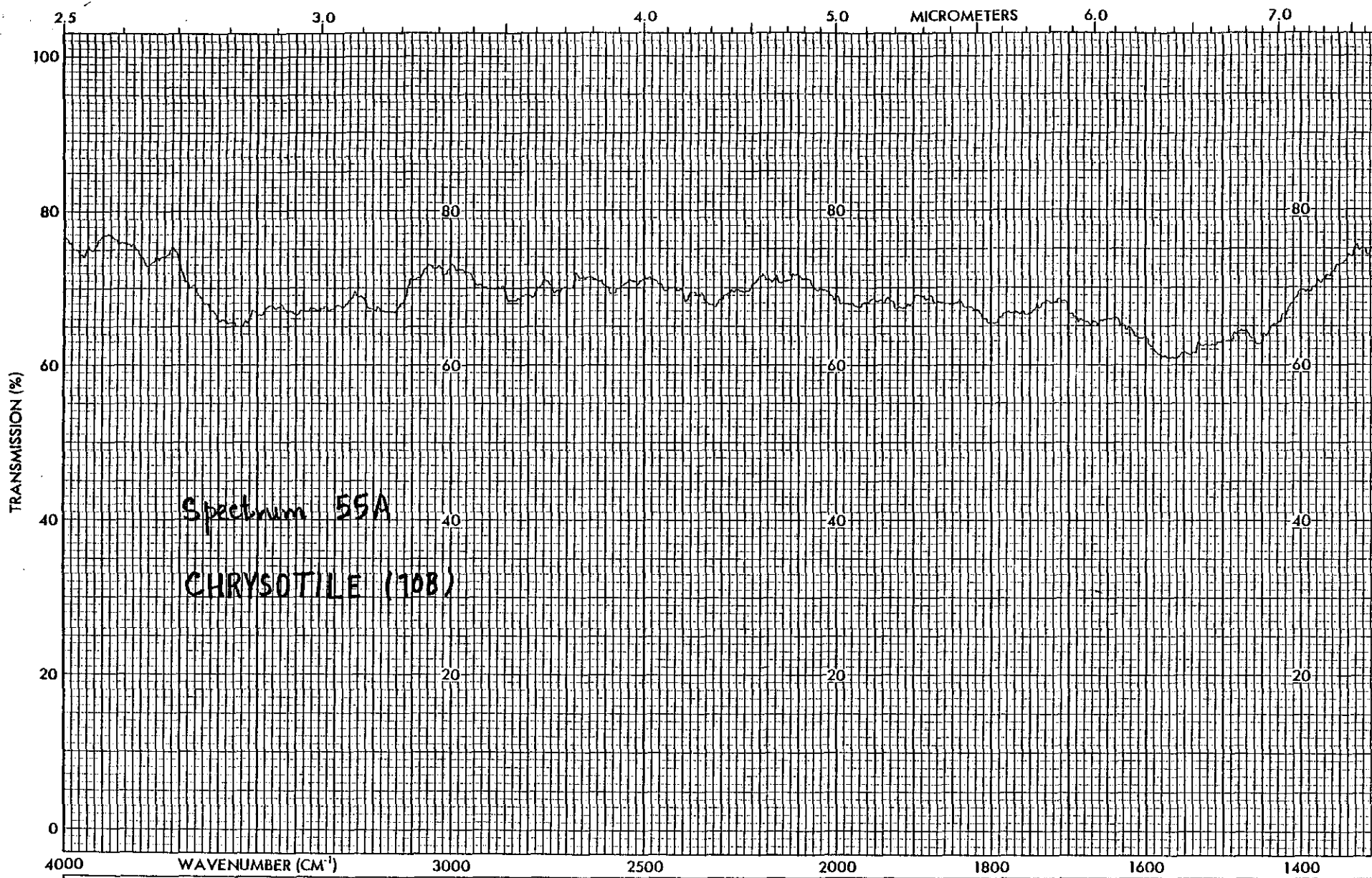
CHRYSOTILE (JM-7M05, sample 2)

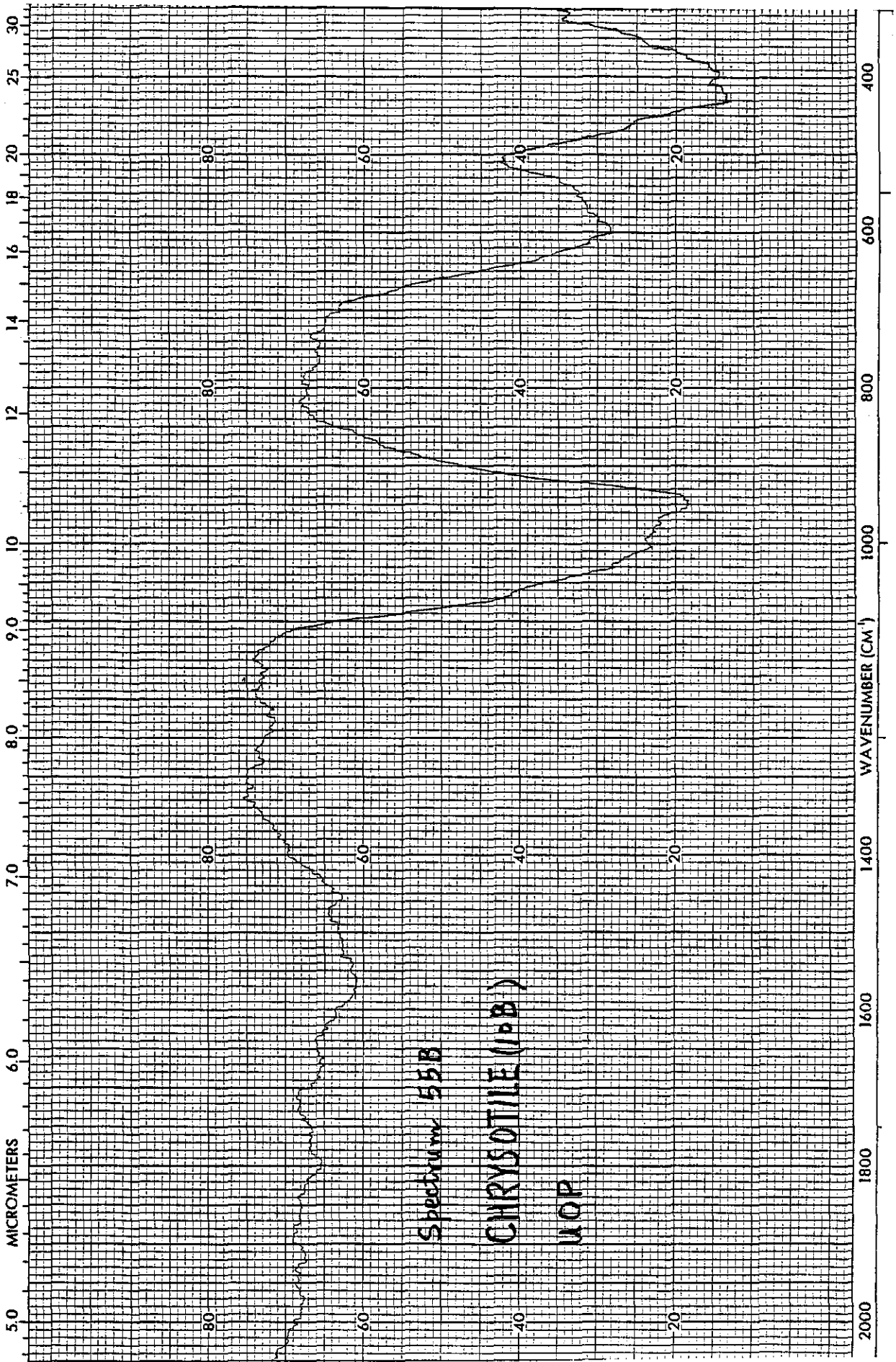


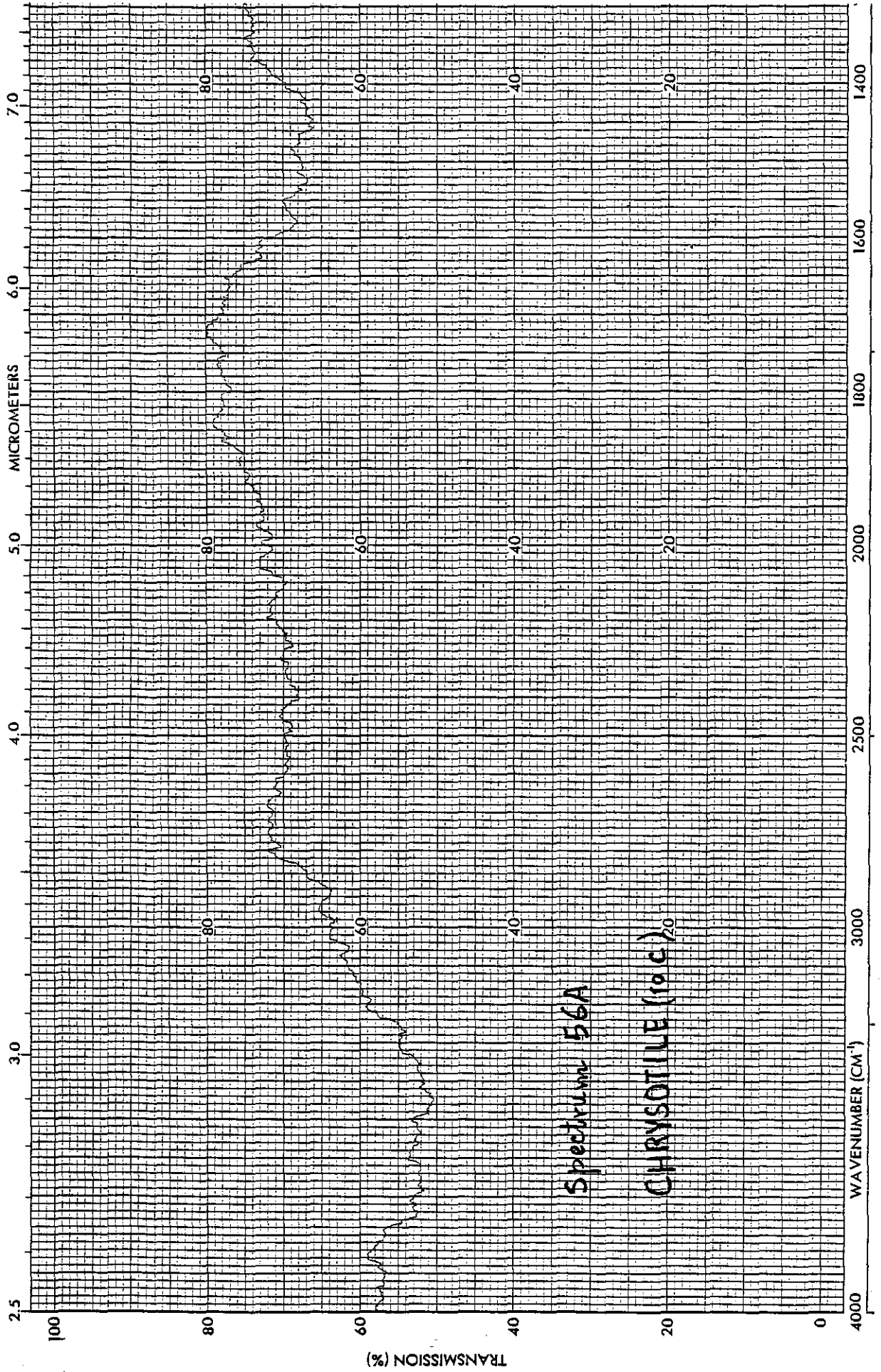


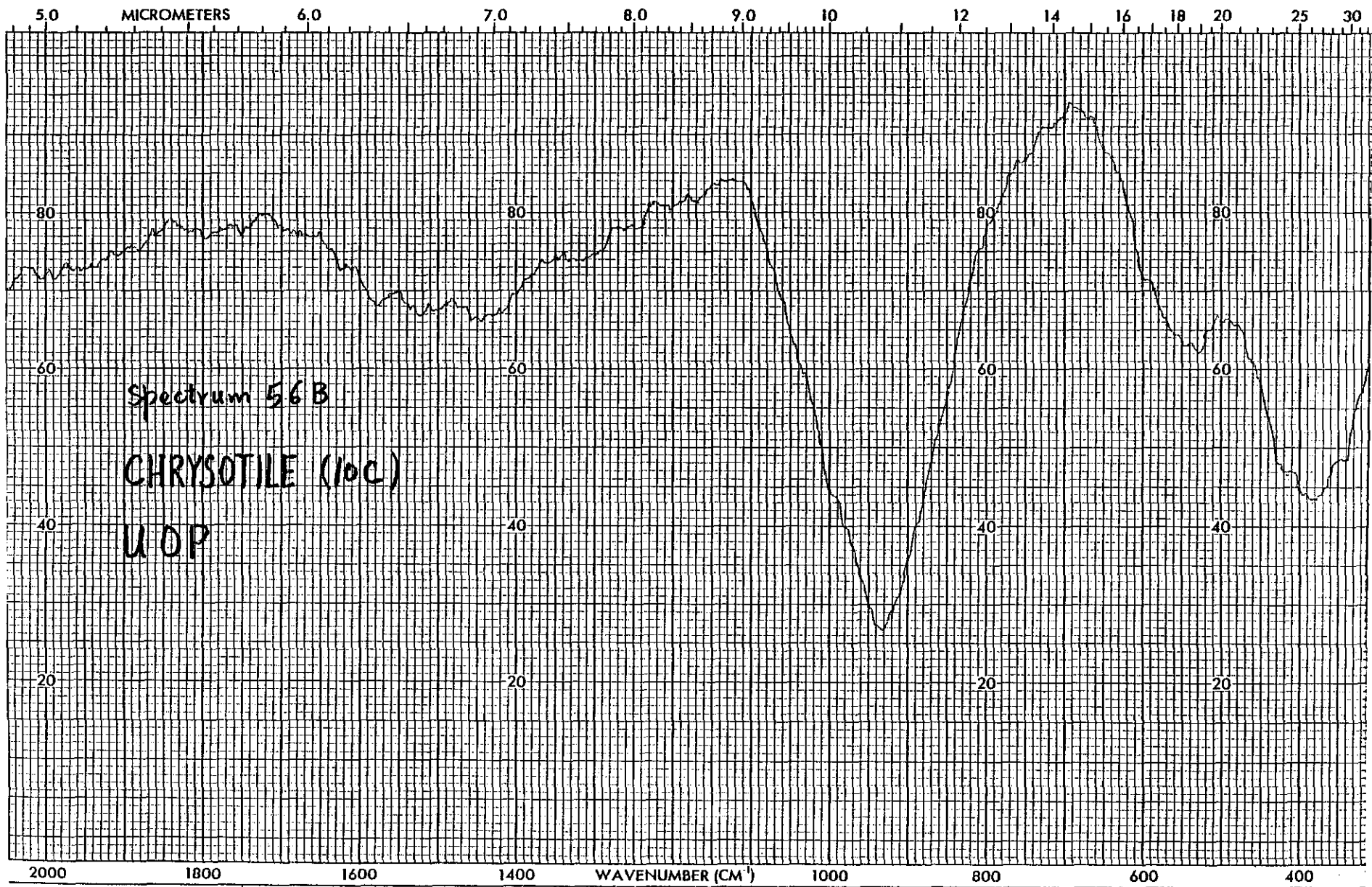
Spectrum 54A
CHRYSOTILE (10A)











APPENDIX B

Master Table of Spectral Positions of Attenuated Total Reflection Infrared Absorption Bands in Minerals

Mineral Name Wavenumber in cm^{-1}

	4000	3000	2000	1500	1000	800	600	400
KRS-5, reflector plate, IR	Transparent through this range							
KRS-5, ATR-IR	1025w							
CLAY MINERALS								
Kaolinite (Langley, SC)	3955w	3000w	1600-1500b,mp,w			760w	650m	453m
	3880w	2905w	1100m	1018s		742-35m		310w
	3720w	2798w			1000d,s		600m	
	3660w	2700w			930w		520s	
	3630w	2522-12w			901s,sh			
	3616w	2103w						
	3602w							
	3442w							
	3318-3260w							
	3127-20w							
Kaolinite (Bath, SC)	3918w	3000w	1615-1589b,mp,w			770w	650w	442w
	3770w	2782w	1099w	1022s		740-32w		412w
	3660w	2580w			1000d,s		600w	400w
	3630w	2100w			932w		518s	315w
	3608w				903s			
	3520-3492w							
	3400w							
	3350w							
	3278w							
	3160w							
	3130w							
Kaolinite (DCG, Unk)	3900w	3000w	1611-1580b,mp,w			766w	650w	448w
	3808w	2982w	1098m	1019s		750-32b,w		415w
	3724w	2950w			1009s		600w	315w
	3662w	2808w			928w		525s	
	3632w	2712-2690w			906s			
	3620w	2602w						
	3540w	2555w						
	3415w	2460w						
	3360w	2345w						
	3278w							
Kaolinite (UOP, Unk)	3850w	3020w	2060w		1010s	760w	660w	422w
	3810w	2890w	1602-1560b,mp,w				600w	415s
	3634w	2806w					518m	
	3476w	2778w						
	3403w	2600w						
	3300w	2355-14w						
		2240-00w						

Master Table [continued]

	4000	3000	2000	1500	1000	800	600	400
Bentonite								
(Rock River, WY)	3720w	2920w	2005w	1570w	1000s	790w	682-68w	
	3630-10w		1620-1478b,w		998s	780w	600w	435w
	3500w	2780w				770w	505-495m	
	3160w	2630w						420s
	3072w	2540-24w						
		2360w						
Bentonite								
(Osage, WY)	3840w	2740w	1620-1590b,mp,w			880m	675w	410-00m,
	3800w	2560-20w		1450w	1010s	790w	600w	mp
	3690-50w				1000s	780w	510w	330w
	3468-3378w				953m	770w		
	3180-30w				910m	749w		
		2410-2280w				719w		
Halloysite								
(Eureka, UT)	3540-3310w		1786w	1590-50b,w		882w	642w	450m
		2740-24w		1510w	1032s	868w	600w	438w
		2476-62w			1012s	740w	560m	414w
		2250-2178w			992s		529-19m	
			1770-64mp,w		928w		515w	392w
					904m			355w
								335w
Halloysite								
(Bedford, IN)	3580-3455w		1858w	1508w	1010d,s		669w	448-38
	3380-3260w		1812w	1235w	900m	770w	600w	d,w
		2920-2740w		1160-50mp,w		745w	580w	360w
		2440-2280w				738w	520m	330w
			1806w					
			1772w					
			1750w					
			1657w					
			1600-1570b,w					
Bauxite								
(Dominican), SRM # 697	3900w			1150w	1046m	790w	655w	462w
	3366-40w				1034s	732-26w		450-10
	3200w				1005s	700w	600w	mp,w
					1000s		558w	340w
					990s		504w	
					930s			
					910w			
Bauxite								
(Jamaican), SRM # 698	3900w			1150w	1078w	790w	600w	496w
	3366-40w				1046m	732-24w		478w
					1014m		570w	460w
					1005s			448w
					990m			330w
					930w			
					910w			
					900w			

Master Table [continued]

	4000	3000	2000	1500	1000	800	600	400
Sodium Feldspar, SRM # 99a	3860w	2900w	1748w	1588-1395b,mp,w			630w	412-345
	3790w	2830-18w		1131m	1080m	720w	560w	b,w
	3736-3310b,mp,w				1008s		531m	318w
	3284-3250w				995s			
		2470w			950m			
		2280w						
Potassium Feldspar, SRM # 70a	3860vw	2910w	1728w	1150m	1035s	775w	655w	410m
	3815w	2860-2552d,w			1010s	717m	637w	360w
	3690-3120b,mp,w				1002s		570m	315w
		2390-2815w			998s		530m	
					982s			
Potassium Feldspar, SRM # 607	3810w	3084w		1390w	1018s	750w	660w	400m
	3780w	3000-2980w		1275w	1010s	708m	628w	358-00
	3735w	2900w			998s		560m	mp,w
	3664w	2415w			985s		520m	
	3585w							
	3440-3310w							
	3200w							
Talc (Low-Vis) (John K. Bice Company)	3910-3870w		1618-1426b,mp,w			742-35w		438s
	3690w	2980w			1003s		658m	
	3645-15w						600w	
	3530w	2900w					516m	
	3495w	2750w						
	3474w	2640-257-w						
	3355w	2500w						
	3260w	2400-2374w						
Talc (DCG, Unk)	3938w	3048-38w			1003-970mp,s		660s	404-00s
	3848-20d,w		1612-1430b,mp,w			885m		335-20w
	3600-3320b,w					780-60w		
	3180-50w							
		2715w						
		2515w						
Talc (UOPC, Unk)	3960w	3020-2965w		1150w	1000-970mp,s		655s	416-09s
	3920-3860w		1613-1438b,mp,w			851m	648s	
	3845-3795w				901m			
	3558w							
	3438-3150w							
HIGH SILICA MATERIALS								
Glass Sand (High Iron), SRM # 81a	3480-3010b,w			1580-1470b,mp,w			678-68w	
					991-40m,mp			440-08w
					759w			350w

Master Table [continued]

	4000	3000	2000	1500	1000	800	600	400
Phosphate	3600w	2920-2800b,mp,w			1012s,sh		660w	497w
Rock,	3480w		1775w	1455-20b,m		875w	600m	450m
SRM # 120b	3378w		1750w			860w	560m	420w
	3150-20w							322s
								308s
								290-80s
CHRYSOTILE								
Serpentine			1640-1430b,mp,w			875w	620-08w	
(DCG, Unk)			1283w	1075w		769w	550w	440-14
			1265w	1006s			534w	m,mp
				955m				370w
								345-30w
Asbestos (SWC)	3535-3482w		1667-1380b,mp,w			888m	600w	422-00w
	3380-20w		1150w	1046w			520-00w	
				1028w				342w
				943m				
				933m				
				915m				
Asbestos,	3418w		1450w	990m			542-13w	
Remping Fiber	3220w		1395w	929s				400-388m
(UOPC, Unk)	3160w		1165-40w					
Chrysotile, 4K	3650w		1600-1405b,mp,w			740w	600m	440s
(UOPC, Unk)	3600w						540m	395m
	3530w							
	3400w							
	3300w							
	3160w							
Chrysotile, 4T	3680-3500b,w		1738-1450b,mp,w				555-18m	
(UOPC, Unk)		2870w				1008s		460m
		2586w				970s		398s
						950-25s		
Chrysotile,	3680w		1600-1396b,mp,w			730w	600-52m	
4T-2 (UOPC,	3600w		1260-20mp,w					420w
Unk)	3460w		1140w	990-80s				390-65s
	3360w			972s				
	3220w			958s				
				946-30mp,s				
Chrysotile,	3820w	2640w	1550-1490mp,w				600-530mp,w	
5RNS (PAC)	3740w							418-395s
	3700w							348m
	3660w							320w
	3620w							
	3490w							
	3320w							
	3110w							

Master Table [continued]

	4000	3000	2000	1500	1000	800	600	400
Chrysotile, 6DN (PAC)	3650w 3625w 3240w 3220w 3175w 3130w	2960w 2880w 2620w 2480w 2400w			950-20mp,s		600m 530m	430m 410-370m 345m
Chrysotile, 7EK-3, Sample 1 (PAC)	3790w 3760w 3460-3060b,mp,w	2900w	1950-1800b,mp,w	1490w 1410w	930-890m		600-345b,mp,w	
Chrysotile, 7EK-3, Sample 2 (PAC)	3580w 3555w 3400w 3370-20w 3270w	2990w 2850w 2780w	1690-65mp,w	1560-1400b,m,mp 1138w	950m		578m	465w 416-360 mp,w
		2760w 2650w 2635w 2320w 2150w						
Chrysotile, 7EX-3, Sample 1 (SWC)	3680-3260b,mp,w 3150w 3130w 3100w	3050w 2880w 2760w		1580-1450b,mp,w	993s 979s 950-37s	770w	525m	600-545m,mp 430-384s 350m
		2660w 2580w 2320w						
Chrysotile, 7EX-3, Sample 2 (UOPC, Unk)	3684w 3530w 3380w 3340w	2620w 2570w	1630-1390b,mp,w	1250w 1230w 1204w 1150w	1010s 1000s 950s	796w 756-09mp,w	650m 630m	416-375s 352m 595-36m,mp
Chrysotile, 7EX-3A (UOPC, Unk)	3880w 3855w 3810w 3790w 3640-20w 3505w 3490w 3482w	2520w 2360-00w	1675-1500b,mp,w	1336w 1111w	1059w 980-74w	855m 823m 950-28mp,s 740w	560-20mp,w	430-370 m,mp
Chrysotile, 7MS-1 (CC)	3836-25w 3635w 3580w 3460-3120b,mp,w	2490-2390w		1550-1395b,m,mp	990s 968s 948-34s	725-20w	590-39m,mp	430-330 m,mp
Chrysotile, KB-753 (UOPC, Unk)	3520w 3192w 3100w	2120w	1810-1700b,mp,w	1640-05mp,w	937-06s		605w 590-88w 560w 538w	470w 460w 400w 370w

Master Table [continued]

	4000	3000	2000	1500	1000	800	600	400
Chrysotile, JM-7M02 (UOPC, Unk)	3648w 3595w 3536w 3240w 3180w 3100w	2965w	1610-1378b,mp,w		980s 944s 940-30s		644w 600m 580-40m,mp	427-380 mp,s
Chrysotile, JM-7M05, Sample 1, (UOPC, Unk)	3665-20w 3586w 3306w 3280w	2980w 2900w 2292w	1750w 1648w 1615w	1580-42mp,w 1450w	998s 992s 970s 960-40s 928s 915s	750-38w	593-50m,mp 370m 350m	412-38m,mp
Chrysotile, JM-7M05, Sample 2, (UOPC, Unk)	3800w 3720w 3688w 3520-3400b,w 3180w	2910w 2840-18w 2710w 2620-2540w 2515-2470w	1900w 1830w 1800w	1529w 1460-48w 1420w 1195w 1160-36mp,w	992s 942-30s 910s	710w	590m 540m 505m 370m 355m 348m	468m 416s 390-80s 370m 355m 348m 322w
Chrysotile, 10A (UOPC, Unk)	3800w 3690w 3580w 3345w 3280w 3176w 3142w 2240w	3040w 2895w 2850w 2840w 2680-70w 2580w 2400w	1800-1730b,mp,w 1620-1430mp,w 1365w 1340w				600m 580-35m,mp 370s 350s 319m	400s
Chrysotile, 10B (UOPC, Unk)	3780w 3690w 3680w 3600-3120b,mp,w 1800w	2855-2785w 2735-2684w 2584-76w		1580-60mp,w 1450w 1240-12mp,w	1030s		612s 600s 577-40m,mp 401-394s 382s 318m	460m 430-12s
Chrysotile, 10C, (UOPC, Unk)	3800w 3750-3250-3240b,mp,w 3000w 2980w 2900w 2400w	3050w 1750w 1625w	1800w 1505w 1458w 1448w 1420w 1200w 1170w	1580w 1525w	1034m 992m 930s	890m 805m	600m 545m 530m	415s 396-70s 340m

National Bureau of Standards Certificate of Analysis

Standard Reference Material 697

Bauxite (Dominican)

(In Cooperation with the American Society for Testing and Materials)

(All analyses are based on samples dried 2 hours at 140 °C)

This material is in the form of fine powder (<0.08 mm) for use in checking chemical and instrumental methods of analyses.

Constituent	Certified Value ¹ Percent, by weight	Estimated Uncertainty ²
Al ₂ O ₃	45.8	0.2
Fe ₂ O ₃	20.0	.2
SiO ₂	6.81	.07
TiO ₂	2.52	.05
ZrO ₂	0.065	.007
P ₂ O ₅	.97	.06
V ₂ O ₅	.063	.005
Cr ₂ O ₃	.100	.005
CaO	.71	.03
MgO	.18	.02
MnO	.41	.03
ZnO	.037	.003
K ₂ O	.062	.007
SO ₃	.13	.03
Loss on Ignition ³	22.1	.2

¹The certified value listed for a constituent is the *present best estimate* of the "true" value.

²The estimated uncertainty listed for a constituent is based on judgment and represents an evaluation of the combined effects of method imprecision, possible systematic errors among methods, and material variability for samples 1.0 g or more. (No attempt was made to derive exact statistical measures of imprecision because several methods were involved in the determination of most constituents.)

³Determined by igniting to constant weight at 1050 °C.

Washington, D.C. 20234
August 24, 1979

George A. Uriano, Chief
Office of Standard Reference Materials

(over)

ADDITIONAL INFORMATION ON THE COMPOSITION

Elements other than those certified may be present in this material as indicated below. These are not certified but are given as additional information on the composition.

<u>Constituent</u>	<u>Concentration, Percent by weight</u>	<u>Constituent</u>	<u>Concentration, Percent by weight</u>
BaO	(0.015)	Co	(0.0013)
Na ₂ O	(0.036)	Hf	(0.0014)
Ce	(0.069)	Sc	(0.0058)

The mineralogical composition of SRM 697 was determined by x-ray diffraction studies at the Geological Survey, U.S. Department of the Interior, Reston, Va., (J.W. Hosterman) to be 15% kaolinite, 50% gibbsite, 10% boehmite, 20% hematite, and 5% anatase. These results are semiquantitative (to the nearest 5%).

PLANNING, PREPARATION, TESTING, ANALYSIS:

The material for this SRM was mined in the Dominican Republic and was provided by the Aluminum Company of America, Alcoa Technical Center, Pittsburgh, Pa., through the courtesy of H. B. Hartman. It was processed (crushed, ground, sieved, and mixed) at the Colorado School of Mines Research Institute under a contract with the National Bureau of Standards.

Homogeneity testing was performed at NBS by J.S. Maples and T.E. Gills.

Cooperative analyses for certification were performed in the following laboratories:

- Aluminum Company of America, Alcoa Center, Pa., R. C. Obbink.
- Aluminum Company of Canada, Ltd., Arvida Research Center, Arvida, Quebec, Canada, L. Girolami.
- Andrew S. McCreath & Son, Inc., Harrisburg, Pa., F. A. Pennington, Jr., R. F. Eakin, and S. L. Miller.
- General Refractories Co., U.S. Refractories Division, Research Center, Baltimore, Md., S. Banerjee.
- Geological Survey, U.S. Department of the Interior, Reston, Va., H. J. Rose, Jr., and J. W. Hosterman.
- Kaiser Aluminum and Chemical Corp., Center for Technology, Pleasanton, Calif., H. J. Seim, A. E. McLaughlin, D. F. G. Marten, A. Kermaninejad, R. C. Kinne, J. R. Skarset, J. Boruk, and U. Vogel.
- National Bureau of Standards, Washington, D.C., R. K. Bell, ASTM-NBS Assistant Research Associate.
- National-Southwire Aluminum Co., Hawesville, Ky., N. Robinson and E. Gotzy.
- Ormet Corp., Burnside, La., W. L. Brown and A. D. Lafleur.
- Reynolds Aluminum Co., Alumina Research Division, Bauxite, Ark., J. B. Ezell, Jr.
- University of Kentucky, Institute for Mining and Minerals Research, Center for Energy Research Laboratory, Lexington, Ky., T. V. Rebagay.

The overall coordination of the technical measurements leading to certification were performed under the direction of J. I. Shultz, Research Associate, ASTM-NBS Research Associate Program.

The technical and support aspects involved in the preparation, certification, and issuance of this Standard Reference Material were coordinated through the Office of Standard Reference Materials by R. E. Michaelis and R. Alvarez.

National Bureau of Standards

Certificate of Analysis

Standard Reference Material 698

Bauxite (Jamaican)

(In Cooperation with the American Society for Testing and Materials)

(All analyses are based on samples dried 2 hours at 140 °C)

This material is in the form of fine powder (<0.08 mm) for use in checking chemical and instrumental methods of analyses.

Constituent	Certified Value ¹ Percent, by weight	Estimated Uncertainty ²
Al ₂ O ₃	48.2	0.4
Fe ₂ O ₃	19.6	.2
SiO ₂	0.69	.03
TiO ₂	2.38	.07
ZrO ₂	0.061	.009
P ₂ O ₅	.37	.01
V ₂ O ₅	.064	.005
Cr ₂ O ₃	.080	.006
CaO	.62	.02
MgO	.058	.008
MnO	.38	.03
ZnO	.029	.002
K ₂ O	.010	.002
SO ₃	.22	.03
Loss on Ignition ³	27.3	.2

¹The certified value listed for a constituent is the *present best estimate* of the "true" value.

²The estimated uncertainty listed for a constituent is based on judgment and represents an evaluation of the combined effects of method imprecision, possible systematic errors among methods, and material variability for samples 1.0 g or more. (No attempt was made to derive exact statistical measures of imprecision because several methods were involved in the determination of most constituents.)

³Determined by igniting to constant weight at 1050 °C.

Washington, D.C. 20234
August 24, 1979

George A. Uriano, Chief
Office of Standard Reference Materials

(over)

ADDITIONAL INFORMATION ON THE COMPOSITION

Elements other than those certified may be present in this material as indicated below. These are not certified but are given as additional information on the composition.

<u>Constituent</u>	<u>Concentration, Percent by weight</u>	<u>Constituent</u>	<u>Concentration, Percent by weight</u>
BaO	(0.008)	Co	(0.0045)
Na ₂ O	(0.015)	Hf	(0.0015)
Ce	(0.030)	Sc	(0.0051)

The mineralogical composition of SRM 698 was determined by x-ray diffraction studies at the Geological Survey, U.S. Department of the Interior, Reston, Va., (J.W. Hosterman) to be 75% gibbsite, 20% hematite, and 5% anatase. These results are semiquantitative (to the nearest 5%).

PLANNING, PREPARATION, TESTING, ANALYSIS:

The material for this SRM was mined in Jamaica, and was provided by the Reynolds Metals Company, Bauxite, Arkansas, through the courtesy of J. B. Ezell, Jr. It was processed (crushed, ground, sieved, and mixed) at the Colorado School of Mines Research Institute under a contract with the National Bureau of Standards.

Homogeneity testing was performed at NBS by J.S. Maples and T.E. Gills.

Cooperative analyses for certification were performed in the following laboratories:

Aluminum Company of America, Alcoa Center, Pa., R. C. Obbink.

Aluminum Company of Canada, Ltd., Arvida Research Center, Arvida, Quebec, Canada, L. Girolami.

Andrew S. McCreath & Son, Inc., Harrisburg, Pa., F. A. Pennington, Jr., R. F. Eakin, and S. L. Miller.

General Refractories Co., U.S. Refractories Division, Research Center, Baltimore, Md., S. Banerjee.

Geological Survey, U.S. Department of the Interior, Reston, Va., H. J. Rose, Jr., and J. W. Hosterman.

Kaiser Aluminum and Chemical Corp., Center for Technology, Pleasanton, Calif., H. J. Seim, A. E. McLaughlin, D. F. G. Marten, A. Kermaninejad, R. C. Kinne, J. R. Skarset, J. Boruk, and U. Vogel.

National Bureau of Standards, Washington, D.C., R. K. Bell, ASTM-NBS Assistant Research Associate.

National-Southwire Aluminum Co., Hawesville, Ky., N. Robinson and E. Gotzy.

Ormet Corp., Burnside, La., W. L. Brown and A. D. Lafleur.

Reynolds Aluminum Co., Alumina Research Division, Bauxite, Ark., J. B. Ezell, Jr.

University of Kentucky, Institute for Mining and Minerals Research, Center for Energy Research Laboratory, Lexington, Ky., T. V. Rebagay.

The overall coordination of the technical measurements leading to certification were performed under the direction of J. I. Shultz, Research Associate, ASTM-NBS Research Associate Program.

The technical and support aspects involved in the preparation, certification, and issuance of this Standard Reference Material were coordinated through the Office of Standard Reference Materials by R. E. Michaelis and R. Alvarez.

National Bureau of Standards

Certificate of Analysis

Standard Reference Material 69b

Bauxite (Arkansas)

(In Cooperation with the American Society for Testing and Materials)

(All analyses are based on samples dried 2 hours at 140 °C)

This material is in the form of fine powder (<0.08 mm) for use in checking chemical and instrumental methods of analyses.

Constituent	Certified Value ¹ Percent, by weight	Estimated Uncertainty ²
Al ₂ O ₃	48.8	0.2
Fe ₂ O ₃	7.14	.12
SiO ₂	13.43	.10
TiO ₂	1.90	.05
ZrO ₂	0.29	.07
P ₂ O ₅	.118	.004
V ₂ O ₅	.028	.003
Cr ₂ O ₃	.011	.002
CaO	.13	.02
MgO	.085	.008
MnO	.110	.005
ZnO	.0035	.0005
K ₂ O	.068	.009
SO ₃	.63	.02
Loss on Ignition ³	27.2	.2

¹The certified value listed for a constituent is the *present best estimate* of the "true" value.

²The estimated uncertainty listed for a constituent is based on judgment and represents an evaluation of the combined effects of method imprecision, possible systematic errors among methods, and material variability for samples 1.0 g or more. (No attempt was made to derive exact statistical measures of imprecision because several methods were involved in the determination of most constituents.)

³Determined by igniting to constant weight at 1050 °C.

Washington, D.C. 20234
August 24, 1979

George A. Uriano, Chief
Office of Standard Reference Materials

(over)

ADDITIONAL INFORMATION ON THE COMPOSITION

Elements other than those certified may be present in this material as indicated below. These are not certified but are given as additional information on the composition.

<u>Constituent</u>	<u>Concentration, Percent by weight</u>	<u>Constituent</u>	<u>Concentration, Percent by weight</u>
BaO	(0.008)	Co	(0.0001)
Na ₂ O	(0.025)	Hf	(0.0063)
Ce	(0.024)	Sc	(0.0008)

The mineralogical composition of SRM 69b was determined by x-ray diffraction studies at the Geological Survey, U.S. Department of the Interior, Reston, Va., (J.W. Hosterman) to be 30% kaolinite, 60% gibbsite, and 10% siderite. These results are semiquantitative (to the nearest 5%).

PLANNING, PREPARATION, TESTING, ANALYSIS:

The mine run material for this SRM was provided by the Aluminum Company of America, Bauxite, Arkansas, through the courtesy of T.J. Forbes and by the Alcoa Technical Center, Pittsburgh, Pa., courtesy of H.B. Hartman. It was processed (crushed, ground, sieved, and mixed) at the Colorado School of Mines Research Institute under a contract with the National Bureau of Standards.

Homogeneity testing was performed at NBS by J.S. Maples and T.E. Gills.

Cooperative analyses for certification were performed in the following laboratories:

Aluminum Company of America, Alcoa Center, Pa., R. C. Obbink.

Aluminum Company of Canada, Ltd., Arvida Research Center, Arvida, Quebec, Canada, L. Girolami.

Andrew S. McCreath & Son, Inc., Harrisburg, Pa., F. A. Pennington, Jr., R. F. Eakin, and S. L. Miller.

General Refractories Co., U.S. Refractories Division, Research Center, Baltimore, Md., S. Banerjee.

Geological Survey, U.S. Department of the Interior, Reston, Va., H. J. Rose, Jr., and J. W. Hosterman.

Kaiser Aluminum and Chemical Corp., Center for Technology, Pleasanton, Calif., H. J. Seim, A. E. McLaughlin, D. F. G. Marten, A. Kermaninejad, R. C. Kinne, J. R. Skarset, J. Boruk, and U. Vogel.

National Bureau of Standards, Washington, D.C., R. K. Bell, ASTM-NBS Assistant Research Associate.

National-Southwire Aluminum Co., Hawesville, Ky., N. Robinson and E. Gotzy.

Ormet Corp., Burnside, La., W. L. Brown and A. D. Lafleur.

Reynolds Aluminum Co., Alumina Research Division, Bauxite, Ark., J. B. Ezell, Jr.

University of Kentucky, Institute for Mining and Minerals Research, Center for Energy Research Laboratory, Lexington, Ky., T. V. Rebagay.

The overall coordination of the technical measurements leading to certification were performed under the direction of J. I. Shultz, Research Associate, ASTM-NBS Research Associate Program.

The technical and support aspects involved in the preparation, certification, and issuance of this Standard Reference Material were coordinated through the Office of Standard Reference Materials by R. E. Michaelis and R. Alvarez.

National Bureau of Standards

Certificate of Analysis

Standard Reference Material 696

Bauxite (Surinam)

(In Cooperation with the American Society for Testing and Materials)

(All analyses are based on samples dried 2 hours at 140 °C)

This material is in the form of fine powder (<0.08 mm) for use in checking chemical and instrumental methods of analyses.

Constituent	Certified Value ¹ Percent, by weight	Estimated Uncertainty ²
Al ₂ O ₃	54.5	0.3
Fe ₂ O ₃	8.70	.10
SiO ₂	3.79	.10
TiO ₂	2.64	.05
ZrO ₂	0.14	.02
P ₂ O ₅	.050	.006
V ₂ O ₅	.072	.006
Cr ₂ O ₃	.047	.003
CaO	.018	.002
MgO	.012	.003
MnO	.004	.001
ZnO	.0014	.0007
K ₂ O	.009	.003
SO ₃	.21	.03
Loss on Ignition ³	29.9	.2

¹The certified value listed for a constituent is the *present best estimate* of the "true" value.

²The estimated uncertainty listed for a constituent is based on judgment and represents an evaluation of the combined effects of method imprecision, possible systematic errors among methods, and material variability for samples 1.0 g or more. (No attempt was made to derive exact statistical measures of imprecision because several methods were involved in the determination of most constituents.)

³Determined by igniting to constant weight at 1050 °C.

Washington, D.C. 20234
August 24, 1979

George A. Uriano, Chief
Office of Standard Reference Materials

(over)

ADDITIONAL INFORMATION ON THE COMPOSITION

Elements other than those certified may be present in this material as indicated below. These are not certified but are given as additional information on the composition.

<u>Constituent</u>	<u>Concentration, Percent by weight</u>	<u>Constituent</u>	<u>Concentration, Percent by weight</u>
BaO	(0.004)	Co	(0.00009)
Na ₂ O	(0.007)	Hf	(0.0032)
Ce	(0.0041)	Sc	(0.0008)

The mineralogical composition of SRM 696 was determined by x-ray diffraction studies at the Geological Survey, U.S. Department of the Interior, Reston, Va., (J.W. Hosterman) to be 5% kaolinite, 80% gibbsite, 10% pyrite, and 5% anatase. These results are semiquantitative (to the nearest 5%).

PLANNING, PREPARATION, TESTING, ANALYSIS:

The material for this SRM was mined in Surinam, South America, and was provided by the Aluminum Company of America, Alcoa Technical Center, Pittsburgh, Pa., through the courtesy of H. B. Hartman. It was processed (crushed, ground, sieved, and mixed) at the Colorado School of Mines Research Institute under a contract with the National Bureau of Standards.

Homogeneity testing was performed at NBS by J.S. Maples and T.E. Gills.

Cooperative analyses for certification were performed in the following laboratories:

Aluminum Company of America, Alcoa Center, Pa., R. C. Obbink.

Aluminum Company of Canada, Ltd., Arvida Research Center, Arvida, Quebec, Canada, L. Girolami.

Andrew S. McCreath & Son, Inc., Harrisburg, Pa., F. A. Pennington, Jr., R. F. Eakin, and S. L. Miller.

General Refractories Co., U.S. Refractories Division, Research Center, Baltimore, Md., S. Banerjee.

Geological Survey, U.S. Department of the Interior, Reston, Va., H. J. Rose, Jr., and J. W. Hosterman.

Kaiser Aluminum and Chemical Corp., Center for Technology, Pleasanton, Calif., H. J. Seim, A. E. McLaughlin, D. F. G. Marten, A. Kermaninejad, R. C. Kinne, J. R. Skarset, J. Boruk, and U. Vogel.

National Bureau of Standards, Washington, D.C., R. K. Bell, ASTM-NBS Assistant Research Associate.

National-Southwire Aluminum Co., Hawesville, Ky., N. Robinson and E. Gotzy.

Ormet Corp., Burnside, La., W. L. Brown and A. D. Lafleur.

Reynolds Aluminum Co., Alumina Research Division, Bauxite, Ark., J. B. Ezell, Jr.

University of Kentucky, Institute for Mining and Minerals Research, Center for Energy Research Laboratory, Lexington, Ky., T. V. Rebagay.

The overall coordination of the technical measurements leading to certification were performed under the direction of J. I. Shultz, Research Associate, ASTM-NBS Research Associate Program.

The technical and support aspects involved in the preparation, certification, and issuance of this Standard Reference Material were coordinated through the Office of Standard Reference Materials by R. E. Michaelis and R. Alvarez.

Certificate of Analysis

STANDARD REFERENCE MATERIAL 97 a

Flint Clay

(Results based on sample dried for two hours at 140 °C)

Analyst	SiO ₂	Al ₂ O ₃	Fe ₂ O ₃	TiO ₂	P ₂ O ₅	K ₂ O	Na ₂ O	Li ₂ O	ZrO ₂	BaO	MgO	CaO	SrO	Cr ₂ O ₃	Loss on Ignition
1 ⁽¹⁾	43.74	38.65	{0.45 ^a .46 ^b }	{1.88 ^c 1.89 ^d }	0.34	0.53 ^e	0.033 ^e	0.12 ^e	0.063 ^f	0.078 ^e	0.16 ^g	0.11 ^g	0.17 ^g	0.028 ^h	13.32
2 ⁽²⁾	43.68	38.95	.45	1.95	.35	.51 ^e	.041 ^e	.10 ^g	-----	.07	.14 ^g	.11 ^g	.18 ^g	.03	13.31
3.....	43.60	38.79	.43 ^a	1.87 ^d	.38 ⁱ	.46 ^e	-----	-----	-----	-----	-----	-----	-----	-----	-----
Average..	43.67	38.79	0.45	1.90	0.36	0.50	0.037	0.11	-----	0.07 ₅	0.15	0.11	0.18	0.03	13.32

References: [1] G.E.F. Lundell and J.I. Hoffman, NBS J. Res. 1, 91 (1928) RP5.
 [2] L. C. Peck, Geological Survey Bulletin 1170, (1964).

^ao-phenanthroline photometric method.
^bIron reduced with SnCl₂ and titrated with standard potassium dichromate solution.
^cCupferron gravimetric method.
^dH₂O₂ photometric method.

^eFlame emission spectrometric method.
^fPyrocatechol violet photometric method.
^gAtomic absorption method.
^hDiphenylcarbazide photometric method.
ⁱMolybdenum-blue photometric method.

List of Analysts

1. R. K. Bell, B. B. Bendigo, T. C. Rains, T. A. Rush, E. R. Deardorff, J. R. Baldwin, R. A. Paulson, W. P. Schmidt, and S. D. Rasberry, Analytical Chemistry Division, Institute for Materials Research, National Bureau of Standards.

2. L. C. Peck, United States Geological Survey, Denver, Colorado.
 3. L. M. Melnick, J. D. Selvaggio, and D. G. Cunningham, Applied Research Laboratory, United States Steel Corporation, Pittsburgh, Pennsylvania

The material for the preparation of this standard was provided by the A. P. Green Fire Brick Company, Mexico, Missouri.

The overall direction and coordination of the technical measurements leading to certification were performed under the chairmanships of O. Menis and J. I. Shultz.

The technical and support aspects involved in the preparation, certification and issuance of this Standard Reference Material were coordinated through the Office of Standard Reference Materials by J. L. Hague.

Certificate of Analysis

STANDARD REFERENCE MATERIAL 98^a

Plastic Clay

(Results based on sample dried for two hours at 140 °C)

Analyst	SiO ₂	Al ₂ O ₃	Fe ₂ O ₃	TiO ₂	P ₂ O ₅	K ₂ O	Na ₂ O	Li ₂ O	ZrO ₂	BaO	MgO	CaO	SrO	Cr ₂ O ₃	Loss on Ignition
1 ^[1]	48.98	33.13	{1.34 ^a 1.37 ^b }	{1.56 ^c 1.63 ^d }	0.11	1.07 ^e	0.080 ^e	0.075 ^e	0.042 ^f	0.031 ^e	0.42 ^g	0.31 ^g	0.041 ^g	0.030 ^h	12.40
2 ^[2]	48.91	33.31	1.35	1.64	.10	1.08 ^e	.083 ^e	.064 ^g03	.43 ^g	.31 ^g	.037 ^g	.04	12.49
3.....	33.12	1.28 ^a	1.61 ^d	.11 ⁱ	0.98 ^e
Average..	48.94	33.19	1.34	1.61	0.11	1.04	0.082	0.070	0.03	0.42	0.31	0.039	0.03	12.44

References: [1] G.E.F. Lundell and J.I. Hoffman, NBS J. Res. 1, 91 (1928) RP5.
 [2] L.C. Peck, Geological Survey Bulletin 1170, (1964).

^ao-phenanthroline photometric method.
^bIron reduced with SnCl₂ and titrated with standard potassium dichromate solution.
^cCupferron gravimetric method.
^dH₂O₂ photometric method.

^eFlame emission spectrometric method.
^fPyrocatechol violet photometric method.
^gAtomic absorption method.
^hDiphenylcarbazide photometric method.
ⁱMolybdenum-blue photometric method.

List of Analysts

- R. K. Bell, B. B. Bendigo, T. C. Rains, T. A. Rush, E. R. Deardorff, J. R. Baldwin, R. A. Paulson, W. P. Schmidt, and S. D. Raspberry, Analytical Chemistry Division, Institute for Materials Research, National Bureau of Standards.
- L. C. Peck, United States Geological Survey, Denver, Colorado.
- L. M. Melnick, J. D. Selvaggio, and D. G. Cunningham, Applied Research Laboratory, United States Steel Corporation, Pittsburgh, Pennsylvania.

The material for the preparation of this standard was provided by the A. P. Green Fire Brick Company Mexico, Missouri.

The overall direction and coordination of the technical measurements leading to certification were performed under the chairmanship of O. Menis and J. I. Shultz.

The technical and support aspects involved in the preparation, certification and issuance of this Standard Reference Material were coordinated through the Office of Standard Reference Materials by J. L. Hague.

Washington, D. C. 20234
 October 8, 1969

J. Paul Cali, Acting Chief
 Office of Standard Reference Materials

APPENDIX I

Certificate of Analysis
Standard Reference Material 99a
Feldspar

(All Analyses are Based on Samples Dried 2 hours at 105 °C)

	<i>Percent</i>
Silica (SiO ₂) -----	65.2
Alumina (Al ₂ O ₃) -----	20.5
Iron (as Fe ₂ O ₃) -----	0.06 _s
Titania (TiO ₂) -----	.007
Calcium (as CaO) -----	2.14
Barium (as BaO) -----	0.26
Magnesium (as MgO) -----	.02
Sodium (as Na ₂ O) -----	6.2
Potassium (as K ₂ O) -----	5.2
Phosphorus (as P ₂ O ₅) -----	0.02
Loss on Ignition -----	0.26

APPENDIX J

Certificate of Analysis

Standard Reference Material 70a

Feldspar

(All Analyses are Based on Samples Dried 2 hours at 105 °C)

	<i>Percent</i>
Silica (SiO ₂) -----	67.1
Alumina (Al ₂ O ₃) -----	17.9
Iron (as Fe ₂ O ₃) -----	0.07 _s
Titania (TiO ₂) -----	.01
Calcium (as CaO) -----	.11
Barium (as BaO) -----	.02
Sodium (as Na ₂ O) -----	2.5 _s
Potassium (as K ₂ O) -----	11.8
Rubidium (as Rb ₂ O) -----	0.06
Loss on Ignition -----	.40

National Bureau of Standards
Certificate of Analysis
Standard Reference Material 607
Potassium Feldspar
Trace Rubidium and Strontium

This material consists of a carefully sieved fraction (+200, -325) of SRM 70a, Potassium Feldspar. It is intended for use as a standard for the determination of Rb and Sr and Sr isotopic ratios as originally suggested by Compston, et al. [1].

<u>Element</u>	<u>Concentration ($\mu\text{g/g}$)</u>
Rubidium	523.90 \pm 1.01 ^a
Strontium	65.485 \pm 0.320

^a All error limits are reported as the 95 percent limit of error for a single analysis, calculated from the results of single subsamples from ten different bottles, and thus include a term for sample heterogeneity.

<u>Isotopic Ratio</u>	<u>Value</u>
$^{87}\text{Sr}/^{86}\text{Sr}$	1.20039 \pm 0.00020 ^b

^bNormalized to $^{86}\text{Sr}/^{88}\text{Sr} = 0.1194$.

Samples should be dried before use by heating at 105 °C for two to four hours and then cooled in a desiccator.

Material homogeneity was determined using approximately 0.1g samples. The rubidium concentration was determined using SRM 984, Rubidium Chloride, as a comparative standard and the strontium concentration and isotopic ratios were determined using SRM 988, Strontium-84 spike, and SRM 987, Strontium Carbonate, as comparative standards

The analytical work was performed in the NBS Analytical Chemistry Division by J. R. Moody, L. J. Moore and I. L. Barnes under the direction of W. R. Shields.

The technical aspects leading to the preparation, certification, and issuance of this material were coordinated through the Office of Standard Reference Materials by W. P. Reed.

[1] Compston, W., Chappell, B. W., Arriens, P. A., and Vernon, M. J., Geochim. et Cosmochim. Acta, 33, 753-757 (1969).

Analysis

Carbon dioxide in this Standard Reference Material was determined by comparison with a secondary standard that had previously been intercompared with a set of gravimetric primary standards. The imprecision of intercomparison is less than 0.3 percent of the concentration of carbon dioxide. The method of intercomparison was gas chromatography using thermal conductivity determination of carbon dioxide. The gravimetric standards against which the secondary standard was analyzed were prepared at such concentrations and in such numbers that non-linearity of the thermal conductivity detection was minimized. The limits of inaccuracy represent the uncertainty in the concentration of carbon dioxide in the gravimetric primary standards.

Stability

The stability of these mixtures is considered to be excellent. No loss of carbon dioxide has been observed in either the standards or the Standard Reference Material. Periodic reanalyses of representative samples from this batch will be performed, and if any change in concentration is observed the purchasers of other samples from this batch will be notified.

The Standard Reference Material should be stored at room temperature and should not be allowed to experience either high or low ambient temperatures.

National Bureau of Standards Certificate of Analysis Standard Reference Material 81a Glass Sand

(In Cooperation with the American Society for Testing and Materials)

This SRM is issued in the form of a ground powder (95% less than 106 μm) blended to ensure homogeneity. It should be dried for 2 hours at 105 °C before use.

<u>Constituent</u>	<u>Recommended Value</u>		<u>s</u>
	<u>Percent by Weight</u>	<u>Range</u>	
Al ₂ O ₃	0.66	0.62 - 0.69	0.011
Fe ₂ O ₃	.082	.075 - .089	.0024
TiO ₂	.12	.10 - .14	.0064
ZrO ₂	.034	.025 - .042	.0026
Cr ₂ O ₃	46 $\mu\text{g/g}$	33 - 58	3.9

Certification - The recommended value listed for each oxide is the best estimate of the true value based on the analytical data from both cooperators and NBS. The range of values listed is the tolerance interval, constructed such that it will cover at least 95% of the population with a probability of 0.99. It is computed as $X \pm Ks$: where s is the standard deviation, K is a factor that depends on n (the number of samples measured), p , the proportion of the total sample covered (95%), and γ , the probability level (99%). In all cases none of the n values used exceeded the range specified. Thus, it includes variability between laboratories and between samples.

The overall direction and coordination of the round-robin analysis leading to certification were performed by Paul Close, Chairman of ASTM Subcommittee C-14.02 on Chemical Analysis of Glass and Glass Products.

The technical and support aspects involved in the preparation, certification, and issuance of this Standard Reference Material were coordinated through the Office of Standard Reference Materials by W. P. Reed.

Washington, D.C. 20234
January, 1978

J. Paul Cali, Chief
Office of Standard Reference Materials

(over)

Chemical analyses for certification were performed in the following laboratories:

Anchor Hocking Corp., Lancaster, Ohio, R. E. Carr
Brockway Glass Co., Inc., Brockway, Pa., E. L. McKinley.
Corning Glass Works, Corning, N.Y., Y. S. Su.
Ford Motor Co., Lincoln Park, Mich., T. O. LaFramboise.
National Bureau of Standards, Analytical Chemistry Division, E. J. Maienthal, J. D. Messman and T. C.
Rains.
Kimble Div. Owens-Illinois, Vineland, N. J., H. S. Moser.
Owens-Illinois, Inc., Toledo, Ohio, P. Close.
Penn State Univ., University Park, Pa., J. B. Bodkin.

National Bureau of Standards
Certificate of Analysis
Standard Reference Material 165a
Glass Sand

(In Cooperation with the American Society for Testing and Materials)

This SRM has been blended to ensure homogeneity. It should be dried for 2 hours at 105 °C before use.

<u>Constituent</u>	<u>Percent by Weight</u>	<u>Range</u>	<u>s</u>
Al ₂ O ₃	0.059	.051 - 0.066	.0024
Fe ₂ O ₃	.012	.007 - .017	.0018
TiO ₂	.011	.0065 - .015	.0016
ZrO ₂	.006	.0005 - .012	.002

Certification - The value listed for each oxide is the best estimate of the "true" value based on the analytical data from both cooperators and NBS. The range of values listed is the tolerance interval, constructed such that it will cover at least 95% of the population with a probability of 0.99. It is computed as $X \pm Ks$: where s is the standard deviation, K is a factor that depends on n (the number of samples measured), p , the proportion of the total covered (95%), and γ , the probability level (99%). In all cases none of the n values used exceeded the range specified. Thus, it includes variability between laboratories and samples.

The overall direction and coordination of the round-robin analysis leading to certification were performed by Paul Close, Chairman of ASTM Subcommittee C-14.02 on Chemical Analysis of Glass and Glass Products.

The technical and support aspects involved in the preparation, certification, and issuance of this Standard Reference Material were coordinated through the Office of Standard Reference Materials by W. P. Reed.

Washington, D.C. 20234
October 16, 1978

J. Paul Cali, Chief
Office of Standard Reference Materials

(over)

Additional Information

A content of 1 $\mu\text{g/g}$ for Cr_2O_3 is not certified but rather is provided for information only.

Chemical analyses for certification were performed in the following laboratories:

Anchor Hocking Corp., Lancaster, Ohio, R. E. Carr.

Brockway Glass Co., Inc., Brockway, Pa., E. L. McKinley.

Corning Glass Works, Corning, N.Y., Y. S. Su.

Ford Motor Co., Lincoln Park, Mich., T. L. LaFramboise.

National Bureau of Standards, Analytical Chemistry Division, E. J. Maienthal, J. D. Messman and T. C. Rains.

Kimble Div. Owens-Illinois, Vineland, N.J., H. S. Moser.

Owens-Illinois, Inc., Toledo, Ohio, P. Close.

Penn State Univ., University Park, Pa., J. B. Bodkin.

Certificate of Analysis
STANDARD REFERENCE MATERIALS
181, 182, and 183
Lithium Ores

	<u>S.S. 181</u> (Spodumene) %	<u>S.S. 182</u> (Petalite) %	<u>S.S. 183</u> (Lepidolite) %
Li ₂ O	6.39	4.34	4.12

The following values are approximate, and are listed only for information.
Certified values for these elements will be made available later.

Na ₂ O	0.8	.4	0.2
K ₂ O	.3	.1	8.
Rb ₂ O		.03	3.5
Cs ₂ O		--	.3

Washington, D. C. 20234
February 24, 1958
(Reprinted August 20, 1970)

Edward Wichers, Chief
Division of Chemistry



National Bureau of Standards

Certificate of Analysis

Standard Reference Material 120b

Phosphate Rock

(Florida)

This standard is a finely powdered material intended for use in checking chemical methods of analysis and in calibration with optical emission and x-ray spectrometric methods of analysis.

See ADDENDUM* (Over) for Uranium (Radium and Thorium)
(All results are based on samples dried for 1 hour at 105 °C.)

Percent by Weight

ANALYST*	P ₂ O ₅	CaO	SiO ₂	F	Soluble Fe ₂ O ₃	Soluble Al ₂ O ₃	MgO	Na ₂ O	MnO	K ₂ O		TiO ₂	CO ₂	CdO
1	34.51 ^a	49.42 ^b	4.70 ^c	3.82 ^d	1.10 ^e	1.09 ^{f,g}	0.29 ^h	0.33 ⁱ	0.032 ^j	0.12 ^{f,j}	..	0.15 ^k	..	0.002 ^l
2	34.51 ^m	49.35 ^m	4.73 ⁿ	3.79 ^m	1.10 ^h	1.07 ^h	.28 ^h	.36 ^h	.031 ^h	.12 ^j	0.09 ^o	..	2.76 ^p	.002 ^h
3	34.66 ⁿ	49.38 ^m	4.67 ^q	3.83	1.09 ^h	1.07 ^h	.30	.36 ^h	.032 ^h	.12 ^j	.098 ^o	.15	2.79	.002 ^h
4	34.67 ^r	49.47 ^m	4.69 ^q	3.81 ^s	1.13 ^h	1.04 ^h	.28 ^h	.35 ^h	.032 ^h	..	.087 ^o	.15 ^k	2.78 ^p	.003 ^h
5	34.57	49.32 ^m	4.63 ^q	3.86	1.06 ^h	1.05 ^h	.25 ^h	.34 ^h085 ^o	..	2.83	..
6	34.48 ^m	49.45 ^m	..	3.92 ^s	1.14 ^m	1.07 ^t
Average	34.57	49.40	4.68	3.84	1.10	1.06	0.28	0.35	0.032	0.12	0.090	0.15	2.79	0.002

^a Phosphorus precipitated with magnesia mixture, ignited and weighed as Mg₂P₂O₇.

^b Calcium precipitated as oxalate, ignited and weighed as CaO.

^c Sample fused with Na₂CO₃, silica precipitated with ZnO and dehydrated with HCl. Traces of SiO₂ recovered by H₂SO₄ dehydration.

^d Fluorine distilled into NaOH solution and precipitated as lead chlorofluoride. Chloride is precipitated with excess AgNO₃ and excess AgNO₃ is titrated with standard KCNS solution.

^e SnCl₂ reduction - K₂Cr₂O₇ titration.

^f Flame emission spectrometry with repetitive optical scanning.

^g A value of 1.13 percent was obtained for total Al₂O₃ by gravimetry.

^h Atomic absorption spectrometry.

ⁱ KIO₄ spectrophotometric method.

^j Sample digested with mixed acids for 1 hour. Determination completed by atomic absorption spectrometry.

^k H₂O₂ spectrophotometric method.

^l Polarographic method.

^m Volumetric method.

ⁿ Gravimetric method.

^o Sample digested with dilute HCl or aqua regia for 15 minutes. Determination completed by atomic absorption spectrometry.

^p CO₂ absorbed and weighed.

^q Dehydration with HClO₄ in presence of boric acid.

^r Molybdovanadophosphate spectrophotometric method.

^s Distillation - titration with standard thorium nitrate solution.

^t Aluminum precipitated with 8 hydroxyquinoline and weighed.

Washington, D.C. 20234
July 31, 1972
ADDENDUM* (Over)
July 31, 1979

The overall direction and coordination of the technical measurements leading to certification were performed under the chairmanship of O. Menis and J. I. Shultz.

The technical and support aspects involved in the preparation, certification, and issuance of this Standard Reference Material were coordinated through the Office of Standard Reference Materials by R. E. Michaelis and C. L. Stanley.

PREPARATION, TESTING, AND ANALYSIS: The material for this standard was prepared by the American Cyanamid Company. Eighty five percent of the lot was made to pass 200 mesh sieve and some blending was done at the plant. Final sieving and blending operations were accomplished at NBS.

Homogeneity testing was performed by S. D. Rasberry, C. E. Fiori, and J. McKay with x-ray fluorescence analysis. Calcium and phosphorus determinations were made on 14 samples representative of the top and the bottom of seven containers. The size of the samples taken for analysis was approximately 35 mg. The maximum variations in concentration among samples were within 0.09 percent for CaO and 0.12 percent for P₂O₅.

The laboratories and analysts cooperating in the analytical program for certification were:

1. R. K. Bell, E. R. Deardorff, E. J. Maienthal, T. C. Rains, T. A. Rush, and S. A. Wicks, Analytical Chemistry Division, Institute for Materials Research, National Bureau of Standards.
2. J. Padar, Agrico Chemical Co., Division of Continental Oil Company, Pierce, Florida.
3. D. B. Underhill, Borden Chemical Co., Plant City, Florida.
4. C. C. Thornton, Thornton Laboratories, Inc., Tampa, Florida.
5. W. W. Harwood, R. M. Lynch and H. N. Gomez, International Minerals and Chemical Corp., Bartow, Florida.
6. J. A. Sielski, American Cyanamid Co., Brewster Plant, Bradley, Florida.

*ADDENDUM

Uranium has been determined at NBS by thermal ionization mass spectrometry, E. L. Garner and L. A. Machlan, and the following certification is made:

	Value, $\mu\text{g/g}$	Estimated Uncertainty ^a
Uranium	128.4	± 0.5

^aThe estimated uncertainty is based on judgment and represents an evaluation of method imprecision and material variability.

(NOTE: On similar phosphate rock materials, a value of 127 $\mu\text{g/g}$ for uranium was reported in Ref. 1; additionally, values of 17 $\mu\text{g/g}$ for thorium and 43 pCi ²²⁵Ra/g for radium also were reported.)

Ref. 1 Agr. Food Chem., 16, No. 2, 1968 (p232)

APPENDIX P

LIST OF ABBREVIATIONS

AES	Augur electron spectroscopy
ATR	Attenuated total reflection
ATR-IR	Attenuated total reflection infrared
CC	Carey Company
Co	Company
Corp	Corporation
DCG	Delta College Geology Department
DTA	Differential thermal analysis
DTG	Differential thermogravimetry
EGA	Evolved gas analysis
EPMA	Electron probe microanalysis
Eq	Equation
ESCA	Electron spectroscopy for chemical analysis
Fig	Figure
IN	Indiana, USA
IR	Infrared
IRE	Internal reflection element
IRS	Internal reflection spectroscopy
LEED	Low energy electron diffraction
NBS	National bureau of Standards
PAC	Pacific Asbestos Corporation
SC	South Carolina, USA
SEM	Scanning electron microscopy
SRM	Standard Reference Material
SWC	S. W. Corner Company
TG	Thermogravimetry
UOP	University of the Pacific Geology Department
UOPC	University of the Pacific Chemistry Department
Unk	Unknown source
UT	Utah, USA
WY	Wyoming, USA

APPENDIX Q

NAMES AND FORMULAS OF VARIOUS MINERALS

Name	Formula
Allophane	$\text{Al}_4\text{Si}_4\text{O}_{10}(\text{OH})_8 \cdot 4\text{H}_2\text{O}$
Anauxite	$\text{Al}_2\text{O}_3 \cdot 3\text{SiO}_2 \cdot 2\text{H}_2\text{O}$
Argillaceous limestone	CaCO_3
Bauxite	$\text{Al}_2\text{O}_3 \cdot 2\text{H}_2\text{O}$
Beidellite	$\text{Al}_{2.17}(\text{Al}_{0.33})(\text{Na}_{0.33})(\text{Si}_{3.17})\text{O}_{10}(\text{OH})_2$
Biotite	$(\text{H}, \text{K})_2(\text{Mg}, \text{Fe})\text{Al}_2(\text{SiO}_4)_3$
Boehmite	$\text{Al}_2\text{O}_3 \cdot \text{H}_2\text{O}$
Bravaisite	$\text{K}_{0.50}(\text{Al}_{1.65}\text{Fe(III)}_{0.15}\text{Mg}_{0.30})(\text{Al}_{0.50}\text{Si}_{3.50})\text{O}_{10}(\text{OH})_2$
Chrysotile	$3\text{MgO} \cdot 2\text{SiO}_2 \cdot 2\text{H}_2\text{O}$
Cliachite	$\text{Al}_2\text{O}_3 \cdot \text{H}_2\text{O}$
Diaspore	$\text{Al}_2\text{O}_3 \cdot \text{H}_2\text{O}$
Dickite	$\text{Al}_2\text{O}_3 \cdot 2\text{SiO}_2 \cdot 2\text{H}_2\text{O}$
Dolomitic limestone	$\text{CaMg}(\text{CO}_3)_2$
Endellite	$\text{Al}_4\text{Si}_4\text{O}_{10}(\text{OH})_8 \cdot 4\text{H}_2\text{O}$
Gibbsite	$\text{Al}_2\text{O}_3 \cdot 3\text{H}_2\text{O}$
Halloysite	$\text{Al}_2\text{Si}_2\text{O}_5(\text{OH})_4$
Hectorite	$(\text{Mg}_{2.67}\text{Li}_{0.33})\text{Na}_{0.33}\text{Si}_4\text{O}_{10}(\text{OH})_2$
Illite	$2\text{K}_2\text{O} \cdot 3\text{MO} \cdot 8\text{R}_2\text{O}_3 \cdot 24\text{SiO}_2 \cdot 12\text{H}_2\text{O}$, where M = Mg(II), Fe(II), etc.; and R = Fe(III), Al(III), etc.
Kaolinite	$\text{Al}_2\text{O}_3 \cdot 2\text{SiO}_2 \cdot 2\text{H}_2\text{O}$
Lepidolite	$4[\text{K}(\text{Li}, \text{Al})_3(\text{Si}, \text{Al})_4\text{O}_{10}(\text{OH}, \text{F})_2]$
Metahalloysite	$\text{Al}_4\text{Si}_4\text{O}_{10}(\text{OH})_8 \cdot 2\text{H}_2\text{O}$
Montmorillonite	$\text{Al}_{1.67}\text{Mg}_{0.33}(\text{Na}_{0.33})\text{Si}_4\text{O}_{10}(\text{OH})_2$
Muscovite	$4[\text{KAl}_3\text{Si}_3\text{O}_{10}(\text{OH})_{12}]$
Nacrite	$\text{Al}_2\text{O}_3 \cdot 2\text{SiO}_2 \cdot 2\text{H}_2\text{O}$
Nontronite	$\text{Fe(III)}_{2.00}(\text{Al}_{0.33}(\text{Na}_{0.33})\text{Si}_{3.67})\text{O}_{10}(\text{OH})_2$
Parakaolinite	$1.01 \text{Al}_2\text{O}_3 \cdot 2\text{SiO}_2 \cdot 2.09 \text{H}_2\text{O}$
Petalite	$4[\text{LiAlSi}_4\text{O}_{10}]$
Potassium feldspar (Microcline)	KAlSi_3O_8
Ptilolite	$(\text{Ca}, \text{K}, \text{Na})\text{O} \cdot \text{Al}_2\text{O}_3 \cdot 10\text{SiO}_2 \cdot 7\text{H}_2\text{O}$
Pyrophyllite	$\text{Si}_8\text{Al}_4\text{O}_{20}(\text{OH})_4$
Saponite	$\text{Mg}_{3.00}(\text{Al}_{0.33}(\text{Na}_{0.33})\text{Si}_{3.67})\text{O}_{20}(\text{OH})_2$
Sodium feldspar:	
Albite	$\text{NaAlSi}_3\text{O}_8$
Nepheline	NaAlSiO_4
Oligoclase	$[\text{Na}_2, \text{Ca}]\text{O} \cdot \text{Al}_2\text{O}_3 \cdot 5\text{SiO}_2$
Spodumene	$4[\text{LiAl}(\text{SiO}_3)_2]$
Sporogelite	$\text{Al}_2\text{O}_3 \cdot \text{H}_2\text{O}$
Talc	$\text{Si}_8\text{Mg}_6\text{O}_{20}(\text{OH})_4$